THE MECHANISMS UNDERLYING SIGH GENERATION IN THE PREBÖTZINGER COMPLEX ARE DEPENDENT ON NEUROGLIAL INTERACTIONS

Liza J. Severs

A dissertation

submitted in partial fulfillment of the

requirements for the degree of

Doctor of Philosophy

University of Washington

2021

Reading Committee:

Jan-Marino Ramirez, Chair

Jane M. Sullivan

Steve I. Perlmutter

Program authorized to offer degree:

Physiology and Biophysics

University of Washington

Abstract

The Mechanisms Underlying Sigh Generation in the PreBötzinger Complex are Dependent on Neuroglial Interactions

Liza J. Severs

Chair of the Supervisory Committee:
Dr. Jan-Marino Ramirez

Rhythm generation is a vital component of life. Rhythmic activity regulates the circadian clock, which controls hormonal cycles, sleep wake states, blood pressure, body temperature, and reaction times. Rhythmogenesis underlies breathing and produces several behaviors -such as eupnea, sighs, and gasps- that are critical to everyday life. Moreover, rhythmic oscillations have emerged throughout the brain that link these coordinated activities together. Gaining a better understanding of rhythm generation and the underlying cell activities that make up these behaviors can help to provide a better understanding of many diseases which originate from the disruption of these cycles. The breathing networks in the medulla are a fantastic model system for studying rhythm generation. These areas maintain their intrinsic rhythm generating properties *in vitro* for extended periods of time, providing valuable insight into how individual cells and ion channels contribute to producing complex breathing behaviors. The preBötzinger Complex (preBötC) in the ventral-lateral medulla is one of these rhythmogenic circuits. Within this circuit, three behaviors necessary for normal breathing arise- normal breathing ‘eupnea’, sighing, and gasping. This thesis primarily focuses on the generation of the sigh rhythm.

Sighing is a critical element of normal breathing that has vital physiological functions. Sighs are deep augmented breaths that are critical for survival as they prevent collapse of the lungs, clinically referred to as atelectasis, by re-inflating collapsed alveoli. Furthermore, during

sleep, sighs trigger arousal to hypoxic conditions and are more common during REM sleep and transitions between different sleep states. Indeed, reduced sighing has been reported in infants who have died from sudden infant death syndrome (SIDS). Sighing is also linked to higher-order brain function and emotions such as love, stress, exasperation, and is clinically tied to several anxiety disorders. These 'augmented breaths' occur at a rate of ~12 per hour in adults and much more frequently in infants. Sighs often occur as a superimposed burst overlaying the ongoing eupneic burst, giving the sigh its characteristic biphasic shape. Eupnea consists of three primary phases: inspiration, postinspiration, and active expiration, each hypothesized to be generated by an excitatory rhythmogenic microcircuit in the ventral lateral medulla. Evidence suggests that eupneic inspiration, gasping, and sighing are generated by the same breathing circuit, the preBötC. ***Yet, how the same neural circuit gives rise to two distinct rhythmic activities with separate timing characteristics remains unknown. The primary directive of this thesis is to provide a novel hypothesis for sigh generation.***

TABLE OF CONTENTS

ACKNOWLEDGEMENTS

First and foremost, thank you to the mice that went toward my graduate training. I have great appreciation for animal research, and it has been an enormous privilege to be able to conduct these experiments. Secondly, I want to thank everyone in my life who has paved the way for my success:

To my advisor, Dr. Nino Ramirez, I am grateful for being able to train with such an exceptional scientist and have learned many valuable lessons from your grantsmanship and scientific expertise. The wonderfully diverse environment you helped to create has fostered many collaborations and friendships that will outlast my graduate training. Thank you also to Erika, for being so welcoming and supportive.

To my committee members, Drs. Jane Sullivan, Steve Perlmutter, Andre Berndt, and Douglas Fowler, thank you for providing such valuable counsel, mentorship, and support throughout graduate school.

To my colleagues, Ibis Agosto, Nathan Baertsch, Sanja Ramirez, Lely Quina, Keira Ramirez, Elke Vlemincx, Tatiana Anderson, Marlusa Amarante, Luiz Oliveira, Aguan Wei, Senta Furman, Alyssa Huff, Nicholas Bush, Nicholas Burgraff, Maria José (Coté), Jia-Der Ju Wang, Chelsea Pagan, Hema Bhagavan, Hendrik Backhaus, Roberta Guimaraes-Backhaus, Albrecht Stroh, and Andy Shih, thank you for all your mentorship, friendship, and time.

To the undergraduate students I have had the pleasure of mentoring, Colleen Shikany, Kate Guion, Jackson Axtell, Skyler Hidalgo-Andrade, Christy Yu, and Ishira Parikh, thank you for your support, hard work, and for helping me grow as a mentor.

To all of the scientists I have worked with, I am so appreciative of your collaboration and support - Jule Gust, Susan Ferguson, Jonathan Lautz, Jonathan Skibo, Christopher Woods, Franck Kalume, Marge Sedensky, Philip Morgan, Stephen Smith, Emily Brown, and Stephanie Zuchowski. Special thanks to Elizabeth Crummy and Timothy O'Neal for being such supportive coffee companions.

To my incredibly skilled group of friends, I am so grateful for your positivity, advice, dinners, running, climbing, backpacking- you are the best and I am so lucky! Special thanks to Susan Morgensztern for introductions, mentorship, life guidance, and friendship, and to Felipe Guzman, who is responsible for steering me in the right direction.

To my family, for generating and fostering an endless amount of love and support, to my Dad and sister for getting me stuck on science, and my Mom for teaching me all the canning, cooking, and gardening skills that have kept me sane. To my in-laws and sister-in-law, thank you for accepting me as one of your own and providing so much love and encouragement.

To my husband, Matt, for being so supportive, a source of tough love, advice, and encouragement. I will always look up to your achievements, dedication, and skill in everything. You have helped me to progress as a person in so many ways and helped me to grow. I love you.

CHAPTER 1 - INTRODUCTION

Anatomical organization of the respiratory networks in the brainstem

Respiratory pattern generation is controlled by separate sets of muscles, which includes one set controlling thoracic pressure, and another controlling airway resistance. Motoneurons that control thoracic pressure are located in the spinal cord, while the nerves that drive muscle activity in the upper airway project out of the brainstem. The brainstem controls the airway muscles via several cranial nerves- primarily the V (trigeminal), IX (glossopharyngeal), X (Vagus), and XII (hypoglossal). These efferent fibers originate within the medulla from neural circuitry that is critical in generating the neural correlate of breathing behaviors.

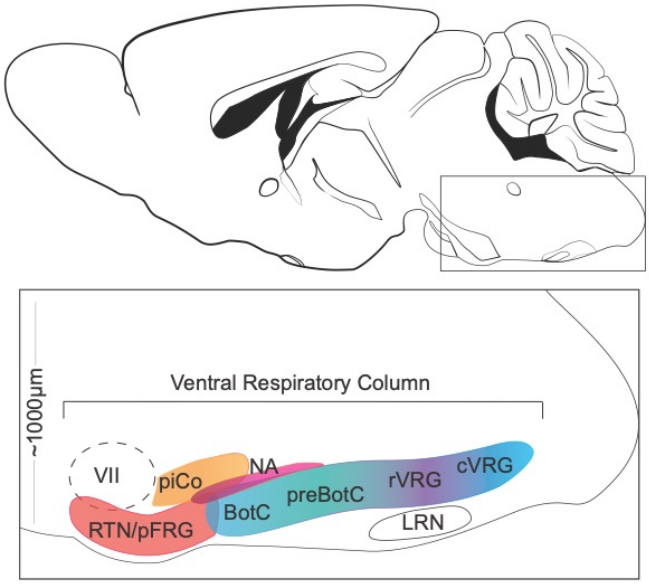

Figure 1. Organization of the ventral respiratory column (VRC). Top shows sagittal section of mouse brain, with inset depicting the areas comprising the VRC. Rostral to caudal, the VRC includes the retrotrapezoid nucleus/parafacial respiratory group (RTN/pFRG) overlayed with the facial nucleus (VII), the postinspiratory complex (PiCo), the nucleus ambiguus (NA), Bötzinger Complex (BötC), preBötzinger Complex (preBötC), and rostral (rVRG) and caudal ventral respiratory groups (cVRG) located dorsal to the lateral ventricular nucleus (LRN). Modified from Anderson et al. 2016 and Baertsch and Ramirez 2018 (1, 2).

There are several areas within the medulla that have been identified as vital rhythmogenic control centers for breathing. The function, neuronal makeup, and organization of each of these areas has been under intense scrutiny for many years. The ventrolateral medulla is the core of these regions and can be further separated into the ventral respiratory groups (VRG). These areas have recently been proposed to be organized in a columnar fashion (3) but historically are compartmentalized based on the firing patterns of the neurons within– the post-inspiratory complex (PiCo), the Bötzinger Complex (BötC), the preBötC, the rostral ventral respiratory group (rVRG) and caudal ventral respiratory groups (cVRG) (Fig. 1). While borders of these areas and neural subtype/organization/function are still debated, the defining characteristics of the BötC are that it purportedly contains a large proportion of inhibitory expiratory neurons with projections spanning to respiratory neurons in the medulla and spinal cord (4-7). PiCo was very recently discovered (1), and is characterized by a population of neurons that co-express vesicular glutamate transporter 2 (Vglut2) and Choline acetyltransferase (ChAt). Neurons within PiCo are

rhythmically active and discharge phasically following inspiratory activity from the preBötC. The preBötzinger complex (preBötC) is a critical area that is located in the more caudal portion of the brainstem. This region was first discovered in 1991 (8); because of its functional relevance, it has been considered as the 'noeud vitale' for respiratory rhythmogenesis. This small area of the brainstem has been implicated in the generation of normal breathing, or 'eupnea', sighing, and gasping behaviors (9, 10). Neurons in the preBötC are derived from neural progenitor cells that express the transcription factor developmental homeobox protein 1, or Dbx1, during specific developmental time points (11, 12). Ablation of this population of neurons results in cessation of breathing as well as a gradual reduction in hypoglossal motor output corresponding to the number of ablated neurons (13). Dbx1 delineated at this same developmental time point also labels a significant number of astrocytes in the preBötC, the importance of which has yet to be determined (Ch. 8). Along with Dbx1, neurons in the preBötC express receptors for neurokinin 1 (NK1R) and somatostatin (SST). The rostral and caudal ventral respiratory groups (cVRG and rVRG, respectively) contain a large portion of respiratory pre-motoneurons that are thought to be involved in generating the motor pattern.

Other areas within and outside of the medulla also play important functions in the control of breathing. The pons, located rostral of the medulla, plays an important role in the adaptive control of breathing and functions to modulate muscles that control downstream breathing circuits and airflow to the lungs, and has been thought to contribute to the gain switch for breathing (14). The pons includes other nuclei such as the Kölliker-Fuse (KF, thought to regulate the inspiratory-expiratory phase transition and to contribute to the control of the upper airways; neurons in KF express Foxp2), the intertrigeminal region (ITR, which may mediate apnea), the locus coeruleus (LC, a major noradrenergic nucleus which has important implications for breathing, cardiorespiratory coupling, and arousal), and the pedunclopontine tegmental nuclei. Another region with significance to breathing is the noradrenergic A5 area located at the junction between the medulla and pons (mediates cardiovascular and respiratory functions) (15).

The RTN and pFRG are sometimes referenced as functionally separate regions, but this concept as well as the function of both of these areas is readily debated. The RTN is located strategically near the ventral medullary surface, is defined by a population of neurons expressing the transcription factor Phox2b, which is implicated in congenital central hypoventilation syndrome (16), and is purportedly involved in active expiration as well as chemoreception due to the expression of pH-sensitive TASK channels (17-24). The RTN projects directly to the pFRG, which is located slightly lateral to the RTN and also contains Phox2b expressing cells. These projections relay chemoreceptive inputs to the preBötC and their activation increases respiratory frequency. This area also projects to the cVRG to drive the augmenting phase of expiration and abdominal activity during late expiration, generating the phase called "active expiration" (21, 25-27).

Another important area for breathing pattern generation is the Nucleus tractus solitarius (NTS), which contains the dorsal respiratory group (DRG). This area is primarily associated with integrating sensory information from peripheral chemoreceptors and is thought to be involved in recruiting neural pathways to appropriately alter the cardiorespiratory responses (28). The nucleus ambiguus (NA) is located in the ventral medulla, containing a large motor neuron pool which innervates the soft palate, pharynx, and larynx to control swallowing and speech. The NA also contains cholinergic preganglionic parasympathetic neurons of the heart, which provides inhibition to the heart and contributes to fast blood pressure changes (29).

Methods used to study respiratory circuits

The critical breathing networks are not easily accessible, as they are dorsally covered by the cerebellum, and are anatomically located underneath the trachea, esophagus, thick laryngeal muscles, and bone on the ventral aspect. Moreover, these networks are not characterized by discrete anatomical landmarks. Thus, studying these networks has been difficult. Several methods that were utilized throughout this thesis have allowed for the study of these areas in precise detail. The 'pacemaker-like' ability of these networks to intrinsically and spontaneously generate rhythmic activity allows them to be isolated from the rest of the brain while preserving critical rhythmic properties, up to a certain postnatal age (30). These slice preparations can be isolated from embryonic to early postnatal mice (typically up to postnatal day 13) and maintained for hours or even up to a full day in artificial cerebrospinal fluid (ACSF) when continuously perfused with carbogen gas mixture (95% O_2/5% CO_2). In these preparations, genetic and pharmacological manipulations allow the study of discrete networks in isolation. Although these *in vitro* approaches have several obvious drawbacks, the benefit is that they become amenable to a rigorous study of the cellular basis of rhythmic respiratory activity in the brainstem in the absence of inputs from the cortex, the pons, and sensory and peripheral chemoreceptor afferents. As mentioned earlier, the most commonly used preparation isolates the preBötC in a ~570-610 μm transverse slice, (Fig. 2) (9). Furthermore, this slice can be isolated into a 'wedge' preparation, only containing the core of preBötC neurons, without perturbing eupnea, sighs, and gasps (31). The ventral aspect of the respiratory column can also be isolated in an ~800 μm horizontal slice preparation (Fig. 2), which is the basis for the column hypothesis of rhythm generation (3) as well as the identification of PiCo (1). In this preparation, the same rhythmic activity is reported, with variation in the robustness of the eupneic rhythm and a reduction in the frequency of sighs (3).

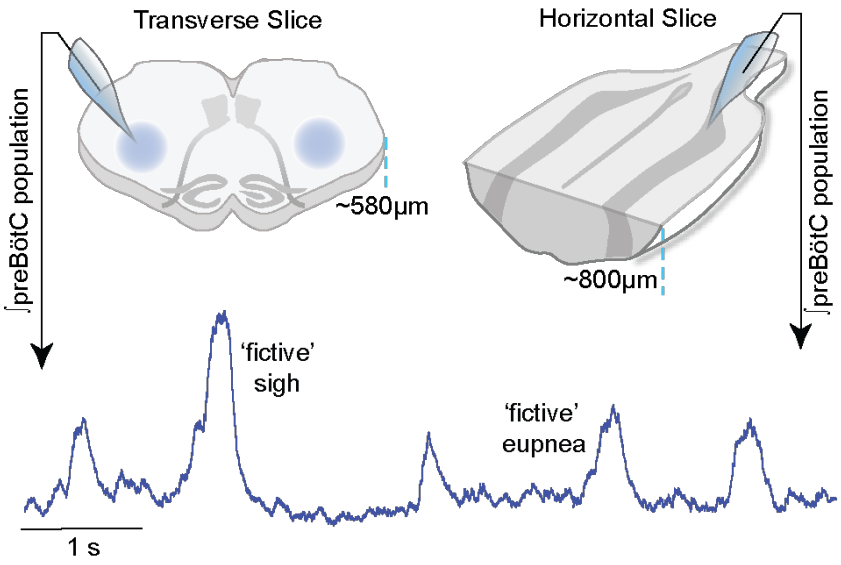

Figure 2. In vitro slice preparations of the preBötC. Transverse slice (left) isolates the preBötC in a ~580um slice, while the horizontal slice preparation preserves the entire ventral column allowing for simultaneous recordings of preBötC and piCo (right). Amplified population activity recorded from the slice surface is filtered and integrated.

The *in vivo* anesthetized preparation offers an additional method for studying breathing in the intact mouse (Fig. 3). In this preparation, urethane anesthesia is utilized, as most other volatile anesthetics depress breathing significantly. In this preparation, the animal is tracheostomized, and spontaneously breathes either room air or 100% oxygen. To record respiratory output, bipolar electrodes are placed in the diaphragm muscle, located lateral to midline. The esophagus, trachea, and sternohyoid muscle are dissected out, and the bone covering the medulla is cut away, revealing the basilar artery and anterior inferior cerebellar artery. The pia and dura are removed. Bilaterally and just caudal from the junction of the anterior inferior cerebellar artery with the basilar artery is the approximate location of the preBötC. The XII and X nerves run parallel to the brainstem, along the carotid arteries. Rostral of the preBötC, the hypoglossal nerve is isolated and severed just below the bifurcation, and a suction electrode is used to record XII nerve activity. These signals are then amplified, filtered, rectified, and acquired in a A/D converter connected to a computer running commercially available software (pClamp).

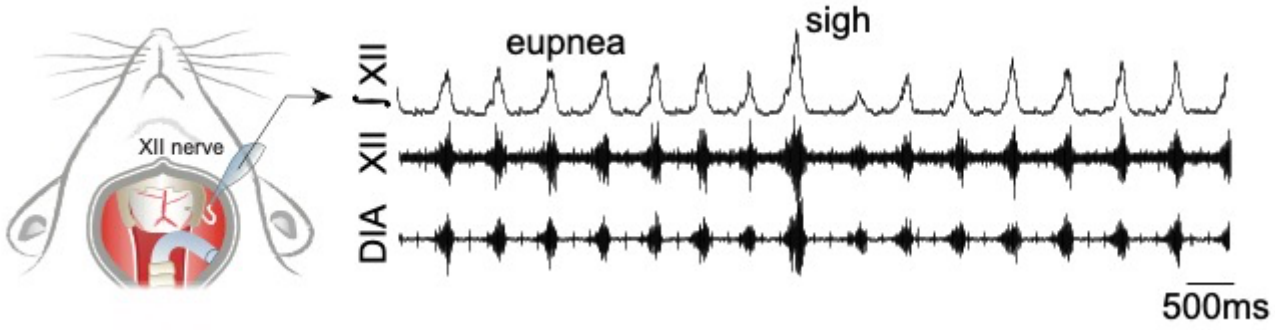

Figure 3. Intact mouse anesthetized preparation. Ventral surface of the medulla is exposed, and XII nerve is used to record preBötC activity. Amplified signal (XII) is filtered and integrated (∫XII). Bipolar diaphragm (DIA) electrodes placed lateral to the midline record respiratory behaviors and EKG activity. Figure modified from Baertsch et al. 2019 (3).

Triple oscillator hypothesis and the column theory

The three primary rhythm generating networks in the medulla are the RTN/pFRG, the preBötC, and the piCo. In the last several years, experiments from the Ramirez lab have provided an alternate depiction of how the respiratory networks are functionally organized in the ventrolateral medulla (Fig. 1), pdrimarily concerning the separation of the preBötC and the BötC. The data behind this reorganization focuses on several recent lines of evidence. The first of these refutes the idea that the BötC is a separate entity from the preBötC and harbors a larger proportion inhibitory neurons than other regions in the medulla. Secondly, isolating the respiratory networks in a different slice preparation- horizontally, as opposed to the historically utilized transverse preparation- allowed for the study of this population of respiratory neurons as an entire, fully connected network. Recent studies utilizing this preparation showed that inspiratory preBötC activity stretches well into, and beyond the BötC, generating the concept of the preBötC and BötC as a combined column that stretches further rostral (3) and borders a second region- PiCo (1). PiCo is a recent discovery and is located rostral and medial of the BötC (figure 1). PiCo generates auto-rhythmic bursts that occur immediately following preBötC bursting behavior. This area may be involved in swallowing, coughing, and vocalizations, and can be modulated independently from the preBötC (1). Interestingly, neurons in PiCo co-express vesicular glutamate transporter 2 ($Vglut_2$) and choline acetyltransferase (ChAT), a trait observed in few other brain regions (32). The RTN/pFRG is an area that is famously known for its chemosensitive neurons and astrocytes; this population of cells expresses the transcription factor Phox2b. The RTN and pFRG are often grouped together; however, these areas have separate functions and project to different regions of the brainstem to modulate breathing.

This column functions to generate the three primary phases of breathing: inspiration (I), postinspiration (post-I), and active expiration (composed of passive vs. active expiration). Each of these phases is generated by three anatomically distinct regions- the preBötC, PiCo, and the pFRG (33). The respiratory column is dynamic and shaped by the control of excitatory glutamatergic neurons by GABAergic and glycinergic inhibitory neurons distributed throughout. This new organizational theory supports the necessary function of the breathing networks in being reliable, stable, and flexible to meet metabolic demand. This concept is derived primarily from experiments showing that expression of Dbx1 neurons with inspiratory-related activity extends beyond the limits of the preBötC and BötC (Ch. 6). Furthermore, this concept is consistent with the inability to eliminate all respiratory drive when lesioning the preBötC. To demonstrate these activity patterns, the transverse slice preparation containing the preBötC was compared with activity within the horizontal slice preparation, which is instead cut along the rostro-caudal axis of the medulla and preserves the entire ventral aspect. These slices maintained similar rhythmic properties, with small differences including a larger irregularity and slower rhythm in horizontal slice preparations. Patching experiments also support a more distributed theory of network organization,

where inspiratory and expiratory neurons did not appear to be segregated within this region. Moreover, application of glycinergic and GABAergic antagonists revealed that excitatory activity along the VRC increases drastically (3, 34).

Role of breathing during hypoxia and hypercapnia

A critical aspect of breathing is the control of gas homeostasis. Given that breathing needs to be controlled in a very dynamic manner to meet the needs of a constantly changing metabolic demand, this is, at least in part, controlled within the medullary respiratory circuits. The carotid bodies located at the bifurcation of the carotid artery play a large role in this function. However, several areas in the VRG have been described to contribute to the central component of the hypoxic ventilatory response. The RTN/pFRG is the most studied site within the VRG which contributes to gas homeostasis. Here, the Phox2b expressing neurons, as well as an undefined population of astrocytes, can detect changes in pH and CO_2 and directly alter respiratory frequency (17, 18, 24, 26). Although neurons were initially identified as being the pH detecting cells in this area, recent evidence focuses on the role of astrocytes in detecting these changes (35), and consequently altering neuronal output (20, 36, 37).

Conversely, the preBötC is sensitive to changes in hypoxia. During a hypoxic episode, the respiratory frequency increases, termed the ‘augmenting phase’. This is accompanied by several sighs, followed by a reduction in respiratory frequency, gasping, and eventual cessation of inspiratory activity (38). This secondary phase, corresponding to a decrease in respiratory frequency, has been shown to be mediated in part by the release of ATP from astrocytes (38-40). Unlike the RTN/pFRG, outside of this overt response to severe hypoxia, there is little evidence to say the preBötC is also stimulated by CO_2 (41-43). Beltrán-Castillo et al. found that D-serine is released, synthesized, and stored within astrocytes in several brainstem centers including the VRC and results in CO_2 induced increases in respiratory frequency in mice (43). More so, a recent study has added to this small group of work and shows that preBötC astrocytes contribute to CO_2 detection. Experiments by Sheikhbahaei and colleagues found that disrupting vesicular release from astrocytes had several strong effects on breathing. First, the respiratory frequency was significantly reduced at rest, corresponding to a reduction in the number of sighs. Secondly, since inspiratory activity must increase with increasing oxygen demand, they next hypothesized that blocking vesicular release would alter the exercise capacity in unanesthetized rats. Indeed, exercise capacity (as measured by kJ of energy output) was significantly reduced in these animals (44).

Together, these studies suggest that chemoreception in the brainstem is a very complex function, and not likely controlled by one region alone, as has been suggested as to RTN/pFRG regions; more support for the ‘distributed central chemosensitivity’ hypothesis is gaining traction with further development of how astrocytes provide a significant contribution to chemoreception (42, 45, 46).

Sighing and its importance to normal breathing

Sighing is a component of normal breathing, occurring at a rate of approximately 12 per hour in adults and noticeably more frequent in infants (47-52). Sighs occur superimposed on normal breaths (Fig. 2/3) and have been suggested to play a role in 'resetting' the breathing rhythm; this idea is due to several observations about sighs: they are immediately followed by a large apneic period and coincide with a decrease in rhythm variability (10).

The sigh has several vital physiological functions. First, sighs function to prevent collapse of the lungs, or what is clinically termed atelectasis. Small fluid filled sacs at the end of the bronchioles in the lungs, called alveoli, are responsible for the transfer of CO_2 and O_2 in the lungs- the oxygen that is inspired travels through the bronchi into the alveoli; here CO_2 and O_2 can pass through the thin lining of the alveoli and reoxygenate blood in the small surrounding capillaries (53, 54). During the course of the normal respiratory cycle, alveoli gradually deflate (Fig 4). The body is able to overcome this potential problem by generating a large, augmented breath, or what is more commonly termed a sigh. The sigh is, essentially, a deep breath which generates enough pressure to re-inflate these alveoli. Atelectasis can occur for several reasons, including a blocking of the airways, incomplete lung development in infants, emphysema, smoking, sleep apnea, and obesity. It can also occur following some surgeries, as ventilators can under or over distend the alveoli and cause injury (55). The importance of sighing has been well depicted in genetic knockout models of the P/Q type calcium channel ($Ca_v2.1$). Mice without P/Q-type channel expression exhibited a complete cessation of sighing and succumbed to pneumonia and atelectasis shortly after birth *(56)*. In a clinical setting, sighs are included in artificial ventilation paradigms and are necessary for adequate oxygenation and prevention of ventilator-associated lung injury (57-59). Furthermore, artificial airway occlusion leading to atelectasis is able to induce sighs (60). Thus, ventilators must include sighing as part of artificial breathing paradigms to properly mimic normal breathing (61).

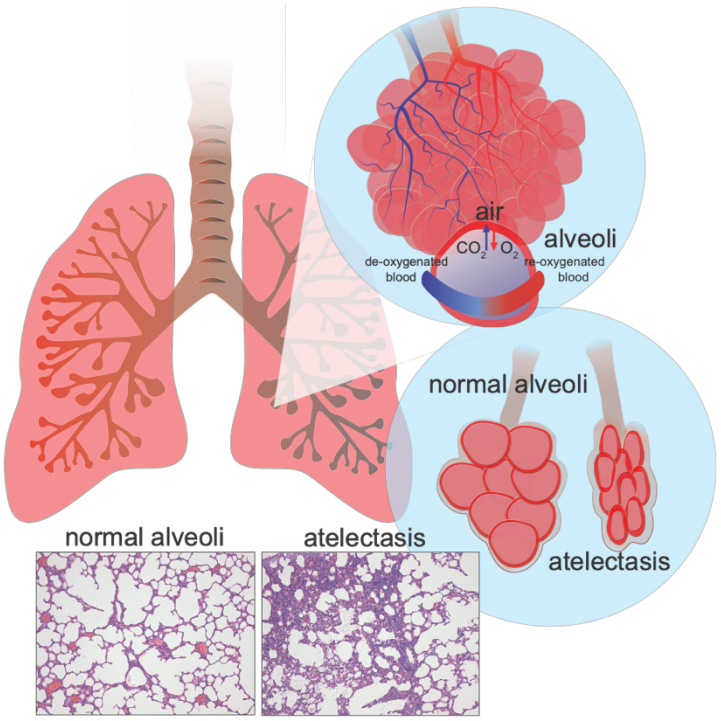

Figure 4. Anatomical depiction of alveoli. Gas exchange occurs in the alveoli; when sighs are not present during normal breathing, the alveoli deflate over time and can result in lung collapse, or atelectasis, if not mediated in a normal manner by sigh activity. Lower panels are histological sections from the lungs of P/Q type knockout mice, which do not sigh and die of atelectasis. Left are normal alveoli, right are alveoli in P/Q knockout mice with atelectasis. Adapted from Koch et al. 2013 (56).

As briefly discussed, sighing is produced in a region of the medulla that is responsible for generating inspiratory breathing activity, the preBötC. When isolated from the rest of the network in small slices, the preBötC continues to produce this breathing rhythm- including sighs. It is reported that patients who receive heart-lung transplants that do not transmit sensory signals from the lungs still are able to generate sighs in a rhythmic manner (62). Thus, it appears that sighs can be generated within the brainstem areas in the absence of afferent input. However, it would be misleading to imply that this is the normal physiological situation. In addition to the medullary areas, inputs from other brain regions and lung mechanoreceptors which provide feedback to the brainstem to regulate breathing during changing metabolic demand also contribute to the generation of sighs. Both mechanoreceptors and chemoreceptors located in the pulmonary tissue detect changes in transmural pressure and communicate collapse of alveoli back to the brainstem via the X cranial nerve to stimulate sighing. Sighs stimulate these mechanoreceptors, or receptors that are sensitive to ‘stretch’ (60).

Opioid-induced respiratory depression (OIRD) is a result of μ-opioid receptors expressed in several critical brainstem areas. Although a complete understanding is lacking as to expression patterns within the respiratory networks, the preBötC and, more recently, the KF nucleus are implicated (63-65). Sighing is also very sensitive to opioids (66). This phenomenon has been observed in patients undergoing postoperative analgesia (67, 68), but the reason for the reduction and its potential contribution to OIRD remains unclear. In animal studies, morphine was given at a low dose to avoid having significant depressing effects on the normal respiratory rhythm. Although at this dose animals still sigh, it was effective at significantly reducing the frequency. Furthermore, the opioid antagonist naloxone was not able to rescue this reduction, suggesting that sighs are reduced by morphine from other

downstream effects of morphine binding. Moreover, sighs were still induced during the hypoxic response at this low dose.

Given the consequential role of sighing in hypoxia, and thus arousal, it is important to discuss how sighing is linked to cardiorespiratory coupling. In addition to its control by peripheral mechano- and chemo- receptors, the sigh, like all inspiratory activity, is also very tightly coupled to heart rate (69, 70). Heart rate and breathing are tightly coupled through the respiratory sinus arrythmia (RSA). This synergy is critical to maintaining proper autonomic function and mediating the fight or flight response. When looking at an electrocardiogram (ECG), the RSA can be described as a shortening of the R-R interval (time between R-waves of the QRS signal on the ECG) during inspiratory activity and extension during expiratory activity (71). The role of the RSA in normal breathing is thought of as an improvement in efficiency for pulmonary gas exchange (71, 72). Studies have clearly demonstrated that sighing is linked to changes in heart rate, and it is somewhat understood that sighs regulate the normal respiratory rhythm at the cellular level; however, the specific mechanisms that link this coordinated physiologic activity are unknown (70, 73). Sighs are known to reset the respiratory rhythm, and from a psychological perspective, sighs occur during a variety of emotions; emotions that also induce changes in heart rate frequency (74).

Accordingly, sighs have been suggested as a link between the medulla and the rest of the brain. This theory is best illustrated by the psychological aspects of sighing. Sighs occur not only physiologically to prevent atelectasis, but they also occur voluntarily and during exasperation, frustration, love, and other emotions. Some anxiety disorders also present with uncontrollable sighing, or a failure to satisfy the need to deeply breath, as in sigh dyspnea (75-77). The link between sighing and arousal certainly- given the connection to C1 neurons, cardiovagal neurons in the NA, and multiple pathways from other breathing centers that control sighing (bombesin peptides, noradrenergic inputs, etc.) indicates that the function of the sigh is critically important to the rest of the brain circuitry (10, 78).

The role that sighs appear to play in the arousal response, along with the observation that they are observed at a higher frequency in infants and the integral role of sighs in the hypoxic response, also provides evidence for the concept that the sigh may be affected in SIDS (79). It follows that a reduction in sighs has been linked to SIDS (80) and that glial apoptosis has been reported in SIDS victims (81).

A mechanistic understanding of the circuitry that generates sighs could lead to significant progress towards understanding the pathogenesis of respiratory-related diseases including SIDS. Furthermore, understanding how sighs are generated could provide more knowledge on when to induce sighs during artificial breathing paradigms in patients who cannot breathe on their own. Moreover, understanding sighs from the psychological perspective could provide more insight into many types of anxiety and stress disorders.

Theories of sigh generation

A recent model of sigh rhythmogenesis has suggested that sighs are generated by a network of neuromedin B (Nmb) and Gastrin releasing peptide (Grp) containing neurons within the pFRG/RTN that project to the preBötC (82). Yet, there are several important observations that are inconsistent with this model. First, although modulation by rostral areas is likely, it is unlikely that sigh rhythmogenesis is initiated in the pFRG/RTN because it has been repeatedly shown that the isolated preBötC maintains both normal inspiratory activity and sigh rhythmogenesis (31, 83-85). Furthermore, sighing is a critical component of the hypoxic response since the onset of hypoxia triggers more sighs (10). Yet, hypoxia silences these rostral areas (86). Lastly, lesioning Nmb neurons does not eliminate sighs (87). Interestingly, the same circuit has been linked to 'emotional' sighs, as mice placed in claustrophobic conditions experienced 'emotional sighs' which are also linked to Nmb release from the same rostral area (88), perhaps indicating the role of bombesin-like peptides stimulates sighs initiated in the cortex, while other mechanisms drive sighing locally within the preBötC.

A second hypothesis posits that a subset of 'sigh only' neurons drive sighing activity. As described by their name, this population of neurons has activity patterns that coincide with fictive sigh bursts, but not eupneic activity (31). It is understood that the same population of inspiratory neurons is activated during both eupnea and sighing activities; however, this doesn't explain the mechanistic underpinnings of how bursts with different properties can be driven on two separate time scales (9, 31). Therefore, the identification of this small subset of sigh specific neurons drove the hypothesis that this separate rhythm could be driven by a small group of autorhythmic cells, in a similar manner to the pacemaker generation theory of rhythmogenesis (9, 89-91). Some of these pacemaker neurons in synaptic isolation are able to generate two different types of pacemaker activities with separate characteristics- a faster frequency pacemaker with low amplitude bursting and a large amplitude burst with slower frequency (31). Interestingly, the muscarinic agonist oxotremorine can modulate these states separately. While increasing the larger, low amplitude bursts, oxotremorine significantly reduces, often eliminates, the lower amplitude, fast frequency bursts. While this idea conceptually makes sense, it is unlikely that such a small population (<~5% of inspiratory neurons) of these unique cells would be capable of driving this core rhythm. Furthermore, when synaptically isolated from the network, sigh only 'pacemakers' are not able to continue bursting without synaptic input, like true pacemakers that play a role in driving inspiratory behaviors (31). Additionally, a modeled network proposed that sighs could be generated based on a balance of slow intracellular Ca^{2+} oscillations (31, 92). This proposed computational model requires inhibitory input (93), which may be the case in the embryo and early postnatal mice (9), but it is not the case in older mice

Astrocyte function in the brain

Astrocytes are only beginning to be recognized as an important player in brain regulation. The existence of glia has been known for over a century. The group of cells termed 'neuroglia' were described initially by Rudolf Virchow in 1846 (94), who initially described them as being a type of 'cement' between cells. Ramon y Cajal further characterized these 'non-excitable' cells and provided important hypotheses on the role of astrocytes in brain function. He theorized astrocytes to be involved in sleep, wakefulness, and attention- and only in the recent decade has significant work gone into understanding their involvement in brain science (94). Astrocytes were initially considered a hindrance to brain function, given that the most famous depictions of them are in forming the 'glial scar'- a barrier to stymy the entry of peripheral dangers into the CNS- following traumatic brain and spinal cord injuries, and preventing the regrowth of severed axons (95-97). Astrocytes are now understood to play significant roles in the pathophysiology of many brain diseases, such as Alzheimer's, Huntington's, Parkinson's, and ALS (98-101). Later, newer understanding of their function led to the discovery that astrocytes also tightly control glutamate levels in the brain- uptake and recycling glutamate to prevent glutamate toxicity in neurons (102). Most recently, the work of Ben Barres and colleagues began to define astrocytes as a diverse group of cells, perhaps as diverse as neurons, with a wide array of functions that not only support neural activity, but can also drive some behaviors (103, 104).

Now, astrocytes are understood to be much more active players in normal brain activity (105) (106). They express many overlapping receptor subtypes with neurons, can drive brain activity states, play many roles during injury and neurological disease, develop into tumors, sense changes in oxygen, manipulate blood vessel dilation, are able to divide and differentiate into adulthood, all in addition to supporting the cellular milieu (38, 40, 100, 103, 105).

Astrocyte signaling mechanisms – purinergic signaling and gap junctions

Astrocytes communicate by autocrine signaling and with other cell types through many different means- they express ion channels, GPCRs, and gap junctions (107). Although our knowledge about how astrocytes communicate with other cell types is still lacking in comparison with our understanding of neurons, purinergic signaling has emerged as a ubiquitous method for functional cell-cell communication, and we focus on this signaling mechanism for its specific role in the following thesis research (108-112). Purinergic signaling refers to extracellular communication by means of purines and their metabolites, i.e., ATP (adenosine triphosphate), ADP (adenosine diphosphate), and adenosine (ADO) (109, 112). ATP was originally discovered for its release from synaptic terminals and has been established since the 70's for this role; more recently it was established that ATP could also be co-released alongside other neurotransmitters from neurons (109, 113, 114). Moreover, it is now understood that many cell types in the CNS release ATP and is widely accepted as a broad communication mechanism for astrocytes (109). ATP binds both purinergic P2Y and P2X receptors, of which there are many subtypes (115, 116). The

degradation of ATP into ADP results in activation of P2Y receptors, and finally ADO, which activates P1 or adenosine receptors (117). P2Y receptors are coupled with GPCRs, and activate cAMP and inositol trisphosphate second messengers downstream, while P2X receptors are ionotropic, gated by ATP and selective for Na^+, K^+, and Ca^{2+} (117). In the last ~20 years, purinergic signaling among astrocytes and neurons of the breathing networks has become a popular topic, especially with the discoveries surrounding how astrocytes in these areas contribute to breathing (38, 40, 118-120).

ATP is generally understood to be released from astrocytes in response to increases in intracellular Ca^{2+} (121). Original hypotheses suggested that these calcium 'waves' propagated in astrocytes through gap junctions; however, evidence has suggested the idea that the spread of Ca^{2+} can also propagate by purinergic signaling mechanisms alone (122, 123). Yet, purinergic signaling also has been shown to mediate opening of these hemichannels, further propagating the Ca^{2+} spread (117). While it is true that Ca^{2+} waves can also be propagated by other mechanisms, such as glutamate, evidence supports purinergic signaling as the primary mediator of this type of astroglial communication (121). Since ATP, ADP, and ADO can also activate neurons directly in the respiratory networks, it becomes difficult to tease out the exact mechanisms by which astrocytes specifically modulate breathing through ATP release and subsequent breakdown and binding of ATP. These experiments are further complicated by the abundance of ectonucleotidases present in tissue that rapidly break down ATP.

Gap junctions are intercellular channels that allow the passage of ions and small molecules and are expressed by many cell types throughout the CNS (124, 125). Gap junctions expressed in vertebrate systems are primarily connexins or pannexins, of which there are many different types (124-126). Interestingly, gap junctions have variable gating kinetics, allowing the passage of different types of ions and molecules such as varying sensitivity to phosphorylation, pH, or Ca^{2+} (125, 127). Gap junctions also exist as 'hemichannel' forms, occurring when they ae not connected to a neighboring channel (124-126). Hemichannels purportedly can have different functions than their coupled counterparts and may release larger molecules into the extracellular space. Astrocytes famously utilize gap junctions to communicate with neurons and with neighboring astrocytes; until the discovery of purinergic signaling in astrocytes, it was more generally believed that information was spread in astrocytes through gap junctions. One of the most commonly described functions of gap junctions in these cells is that they are used to disperse potassium taken up by astrocytes after bursts of action potentials (128). However, gap junctions are also important for buffering glutamate, allow for propagation of calcium waves, and can even affect synaptic plasticity (124, 129-131). Indeed, it is suggested that astrocytes form distributed networks linked by gap junction channels. Few studies have determined the precise role of gap junctions in the respiratory networks; however, evidence suggests that they are expressed throughout many brainstem areas such as in the LC and VRC (127, 132, 133).

Tools for studying astrocytes

Most of the 'tools' we use today in the field of neuroscience were developed as a means to interrogate neuronal function. Over time, as the interest in glial cells grew, scientists found that these tools could also be used to study astrocyte function, albeit often in less physiological ways, leading to questions concerning the development of astrocyte specific tools, or how the current tools mechanistically altered astrocytic function and signaling processes. Here, we provide a brief overview of some of these techniques utilized through this thesis, as well as some that have recently come into light for the use within astrocytes specifically.

Transgenic mice

There are many different types of transgenic mice - mice which have been genetically altered to express different proteins to allow the study of specific cell populations- many of which have utilized a technique discovered and isolated from P1 bacteriophage. This is called the 'cre-lox' system, and utilizes an enzyme derived from this bacteriophage, which functions to catalyze the recombination event between two 34 base pair consensus sequences of DNA which are termed 'loxP' sites; the cre-mediated recombination event occurs between these two loxP sites and results in excision of the DNA sequence centered between. Cre expressing animals are then bred to animals with loxP sites to delete specific target sequences (134). Most applicable to the methods used in this thesis, loxP sites are used to delete a STOP codon, which results in the expression of a transgene (such as channelrhodopsin or a fluorescent protein) in cells expressing Cre. This system also provides a method for expressing many other proteins, such as fluorescent proteins, calcium indicators, opsins, Designer Receptors Exclusively Activated by Designer Drugs (DREADDs), tracing experiments with cre-dependent viruses, and the ability to knock out or reduce expression in proteins of interest.

While an extensive number of transgenic mice have been developed to study different neuronal subtypes, there are only two primary mouse strains that have been developed to study astrocytes. Both strains have the expression of Cre driven by an astrocyte specific promoter- either Aldehyde dehydrogenase Type I (Aldh1l1) (135, 136) or Glial fibrillary acidic protein (GFAP). Given that many neural progenitors are derived from glia (136), it has since been understood that both of these promoters have some overlap with adult stem cell populations and other glial cell types in some brain regions, further hindering precise study of these populations.

Opsins

Optogenetics, the idea of controlling cell populations with light, was pioneered by Richard Tsien and Ed Boyden in the early 2000's (137). Channelrhodopsins (Chr2) are non-specific light-gated ion channels derived from algae, which allow for cell movement based on light conditions (138). These proteins have since been isolated and developed for use in mammalian cells and tissues, allowing the

possibility of studying the effects of specific subpopulations of neuronal subtypes throughout the brain. These proteins now exist in many engineered forms, which endow the protein with different gating kinetics and light sensitivities (139-141). The 'original' forms of ChR2 allowed the transport of all ions across the surface of the cell when opened by a specific wavelength of light- activating neuronal firing by allowing the passage of Na^+ ions. Now, newer tools also allow passage of Cl^-, providing a tool with which to inhibit specific neuronal populations (137). While ChR2 was developed with neuron-specific manipulation in mind, similar tools have not yet been developed for the study of other non-excitable cell populations. While astrocytes, or glia in general, are not considered electrically excitable cells, they do express a large variety of transmembrane ion channels, gap junctions, G-protein coupled receptors, and ion exchangers which drive their activity patterns (142). Studies in the last ~10 years have started to experiment with the use of optogenetics in astrocytes, and until most recently, the mechanisms for how these proteins were able to activate 'non-excitable' cells were unknown. Since ChR2 allows for non-selective passage of ions, it was initially thought that activating ChR2 in astrocytes increased intracellular Ca^{2+} levels, known to initiate the start of many pathways of activation in astrocytes. Recent experiments suggest that ChR2 induces intracellular Ca^{2+} release, mediating reversal of a Na^+/K^+ exchanger following the influx of Na^+ through open channels (143).

Ca^{2+} indicators

Ca^{2+} is one of the most ubiquitous signaling molecules in the CNS and has impacts on nearly every aspect of life (144-147). Given this, the development of tools that can detect minute changes in Ca^{2+} concentration and the ability to associate these concentration changes with physiologic activity was a very important discovery the last several decades. Of the tools utilized for studying astrocytes, the most broadly used is the category of Ca^{2+} genetically encoded indicators (GECI) or organic dyes. Each indicator can be selected for several parameters, including cell organelle compartment, Ca^{2+} binding affinity, sensitivity, cell type, and wavelength. Even though Ca^{2+} indicators are a more recent discovery (i.e., in the last 30 years (148)), there are now hundreds. First, there are chemically produced indicator dyes, which can be split into two primary types: ratiometric or single wavelength. Ratiometric dyes present a shift in wavelength when binding Ca^{2+} (e.g. Oregon Green Bapta-1, Fura-2 dyes, and Fluo-1/2, and Indo dyes), while the single wavelength dyes have Ca^{2+} dependent changes in fluorescent intensity when binding Ca^{2+}, without changing excitation/emission spectra (e.g., Fluo-4, Rhod dyes) (149, 150).

Secondly, there are GECI's. Here we will primarily discuss two different types of GECI's, the most relevant to this thesis- GCaMP6f (151), and R26 Lck Gcamp6f (136, 152), modified versions of the original GCaMP (148). In short, GCaMPs were modified from original green fluorescent proteins (GFP) to be circularly permuted and capitalizes on the mechanisms of Ca^{2+}-calmodulin/myosin light chain kinase binding kinetics. The pore of GCaMP quenches the GFP fluorescent protein until Ca^{2+} binds to calmodulin, allowing for a conformational change, leading to opening of the pore and increasing GFP

fluorescence (153). The Ca^{2+}-calmodulin domain is concentration dependent, thereby allowing for fine precision analysis of Ca^{2+} signals and for single action potentials to be detected. Various screening methods have led to the development of GCaMP proteins with varying fluorophores and on/off kinetics (153). Perhaps the most widely used version of GCaMP today is GCaMP6f. It is most likely the best that exists to date, (with the exception of the newest releases GCaMP7/8 (154)) providing extremely high sensitivity, a high signal to noise ratio, and fast response kinetics. Due to these advancements, GCaMP6f is readily used to image both individual and population Ca^{2+} activity in the soma of cells. Lck-GCaMP6f utilizes the same Ca^{2+} binding protein, however, is localized to the plasma membrane of fine processes and membranes of cells (136, 152). This may be of particular importance to Ca^{2+} imaging in astrocytes, given that a large amount of information transmitted by astrocytes occurs in these specializations; astrocytes make many contacts with other cells and blood vessels through specialized processes termed astrocytic endfeet. Thus imaging with a traditional cell-body labeled GCaMP may likely miss a large amount of signaling information (152).

References

1. Anderson, T.M., et al., *A novel excitatory network for the control of breathing.* Nature, 2016. **536**(7614): p. 76-80.
2. Ramirez, J.M. and N.A. Baertsch, *The Dynamic Basis of Respiratory Rhythm Generation: One Breath at a Time.* Annu Rev Neurosci, 2018. **41**: p. 475-499.
3. Baertsch, N.A., et al., *A spatially dynamic network underlies the generation of inspiratory behaviors.* Proc Natl Acad Sci U S A, 2019. **116**(15): p. 7493-7502.
4. Song, G., Q. Li, and M. Lu, *Roles of the Botzinger complex in the formation of respiratory rhythm.* Adv Exp Med Biol, 2001. **499**: p. 153-7.
5. Otake, K., et al., *Morphology of expiratory neurons of the Botzinger complex: an HRP study in the cat.* J Comp Neurol, 1987. **258**(4): p. 565-79.
6. Otake, K., et al., *Axonal projections from Botzinger expiratory neurons to contralateral ventral and dorsal respiratory groups in the cat.* Exp Brain Res, 1988. **72**(1): p. 167-77.
7. Shen, L., Y.M. Li, and J. Duffin, *Inhibitory connections among rostral medullary expiratory neurones detected with cross-correlation in the decerebrate rat.* Pflugers Arch, 2003. **446**(3): p. 365-72.
8. Smith, J.C., et al., *Pre-Bötzinger Complex: A Brainstem Region That May Generate Respiratory Rhythm in Mammals.* Science, 1991. **254**(5032): p. 726-729.
9. Lieske, S., et al., *Reconfiguration of the neural network controlling multiple breathing patterns: eupnea, sighs and gasps.* Nature Neuroscience, 2000. **3**: p. 600-607.
10. Ramirez, J.M., *The integrative role of the sigh in psychology, physiology, pathology, and neurobiology.* Prog Brain Res, 2014. **209**: p. 91-129.
11. Revill, A.L., et al., *Dbx1 precursor cells are a source of inspiratory XII premotoneurons.* Elife, 2015. **4**.
12. Kottick, A., C.A. Martin, and C.A. Del Negro, *Fate mapping neurons and glia derived from Dbx1-expressing progenitors in mouse preBotzinger complex.* Physiol Rep, 2017. **5**(11).
13. Wang, X., et al., *Laser ablation of Dbx1 neurons in the pre-Bötzinger complex stops inspiratory rhythm and impairs output in neonatal mice.* Elife, 2014. **3**: p. e03427.
14. Molkov, Y.I., et al., *Control of breathing by interacting pontine and pulmonary feedback loops.* Front Neural Circuits, 2013. **7**: p. 16.
15. Dutschmann, M. and T.E. Dick, *Pontine mechanisms of respiratory control.* Compr Physiol, 2012. **2**(4): p. 2443-69.
16. Amiel, J., et al., *Polyalanine expansion and frameshift mutations of the paired-like homeobox gene PHOX2B in congenital central hypoventilation syndrome.* Nature Genetics, 2003. **33**(4): p. 459-461.

17. Wang, S., et al., *Phox2b-Expressing Retrotrapezoid Neurons Are Intrinsically Responsive to H+ and CO2.* The Journal of Neuroscience, 2013. **33**(18): p. 7756-7761.
18. Lazarenko, R., et al., *Acid sensitivity and ultrastructure of the retrotrazezoid nucleus in Phox2b-EGFP mice.* J Comp Neurol, 2009. **517**(1): p. 69-86.
19. Ruffault, P., et al., *The retrotrapezoid nucleus neurons expressing Atoh1 and Phox2b are essential for the respiratory response to CO2.* Elife, 2015. **4**.
20. Czeisler, C.M., et al., *The role of PHOX2B-derived astrocytes in chemosensory control of breathing and sleep homeostasis.* J Physiol, 2019. **597**(8): p. 2225-2251.
21. Takakura, A.C., et al., *Peripheral chemoreceptor inputs to retrotrapezoid nucleus (RTN) CO2-sensitive neurons in rats.* J Physiol, 2006. **572**(Pt 2): p. 503-23.
22. Stornetta, R.L., et al., *Expression of Phox2b by brainstem neurons involved in chemosensory integration in the adult rat.* J Neurosci, 2006. **26**(40): p. 10305-14.
23. Kanbar, R., et al., *Photostimulation of Phox2b medullary neurons activates cardiorespiratory function in conscious rats.* Am J Respir Crit Care Med, 2010. **182**(9): p. 1184-94.
24. Onimaru, H., K. Ikeda, and K. Kawakami, *Phox2b, RTN/pFRG neurons and respiratory rhythmogenesis.* Respir Physiol Neurobiol, 2009. **168**(1-2): p. 13-8.
25. Guyenet, P.G. and D.K. Mulkey, *Retrotrapezoid nucleus and parafacial respiratory group.* Respir Physiol Neurobiol, 2010. **173**(3): p. 244-55.
26. Abbott, S.B., et al., *Phox2b-expressing neurons of the parafacial region regulate breathing rate, inspiration, and expiration in conscious rats.* J Neurosci, 2011. **31**(45): p. 16410-22.
27. Gallego, J. and S. Dauger, *PHOX2B mutations and ventilatory control.* Respir Physiol Neurobiol, 2008. **164**(1-2): p. 49-54.
28. Zoccal, D.B., et al., *The nucleus of the solitary tract and the coordination of respiratory and sympathetic activities.* Front Physiol, 2014. **5**: p. 238.
29. Petko, B. and P. Tadi, *Neuroanatomy, Nucleus Ambiguus*, in *StatPearls*. 2021: Treasure Island (FL).
30. Ramirez, J.M., et al., *Respiratory rhythm generation: converging concepts from in vitro and in vivo approaches?* Respir Physiol Neurobiol, 2002. **131**(1-2): p. 43-56.
31. Tryba, A.K., et al., *Differential modulation of neural network and pacemaker activity underlying eupnea and sigh-breathing activities.* J Neurophysiol, 2008. **99**(5): p. 2114-25.
32. Nasirova, N., et al., *Dual recombinase fate mapping reveals a transient cholinergic phenotype in multiple populations of developing glutamatergic neurons.* J Comp Neurol, 2020. **528**(2): p. 283-307.
33. Anderson, T. and J. Ramirez, *Respiratory rhythm generation: triple oscillator hypothesis.* F1000Res, 2017. **6**(139).

34. Baertsch, N.A., H.C. Baertsch, and J.M. Ramirez, *The interdependence of excitation and inhibition for the control of dynamic breathing rhythms.* Nat Commun, 2018. **9**(1): p. 843.
35. Mulkey, D.K. and I.C. Wenker, *Astrocyte chemoreceptors: mechanisms of H+ sensing by astrocytes in the retrotrapezoid nucleus and their possible contribution to respiratory drive.* Experimental Physiology, 2011. **96**(4): p. 400-406.
36. Funk, G.D., *The 'connexin' between astrocytes, ATP and central respiratory chemoreception.* J Physiol, 2010. **588**(Pt 22): p. 4335-7.
37. Turovsky, E., et al., *Mechanisms of CO2/H+ Sensitivity of Astrocytes.* J Neurosci, 2016. **36**(42): p. 10750-10758.
38. Rajani, V., et al., *Release of ATP by preBotzinger complex astrocytes contributes to the hypoxic ventilatory response via a Ca2+ -dependent P2Y1 receptor mechanism.* J Physiol, 2017.
39. Rajani, V., et al., *The role of P2Y1 receptor signaling in central respiratory control.* Respiratory Physiology and Neurobiology, 2016. **226**: p. 3-10.
40. Funk, G.D., et al., *Neuroglia and their roles in central respiratory control; an overview.* Comparative Biochemistry and Physiology, Part A, 2015. **186**: p. 83-95.
41. Nattie, G. and A. Li, *Multiple central chemoreceptor sites: cell types and function in vivo.* Adv Exp Med Biol, 2008. **605**: p. 343-7.
42. Nattie, E. and A. Li, *Central chemoreception is a complex system function that involves multiple brain stem sites.* J Appl Physiol (1985), 2009. **106**(4): p. 1464-6.
43. Beltrán-Castillo, S., et al., *D-serine released by astrocyte in brainstem regulates breathing response to CO2 levels.* Nature Communications, 2017. **8**(838).
44. Sheikhbahaei, S., et al., *Astrocytes modulate brainstem respiratory rhythm-generating circuits and determine exercise capacity.* Nat Commun, 2018. **9**(1): p. 370.
45. Dean, J.B. and E.E. Nattie, *Central CO2 chemoreception in cardiorespiratory control.* J Appl Physiol (1985), 2010. **108**(4): p. 976-8.
46. Nattie, E.E. and A. Li, *Central chemoreception in the region of the ventral respiratory group in the rat.* J Appl Physiol (1985), 1996. **81**(5): p. 1987-95.
47. Hoch, B., M. Bernhard, and A. Hinsch, *Different patterns of sighs in neonates and young infants.* Biol Neonate, 1998. **74**(1): p. 16-21.
48. Alvarez, J.E., et al., *Sighs and their relationship to apnea in the newborn infant.* Biol Neonate, 1993. **63**(3): p. 139-46.
49. Thach, B.T. and H.W. Taeusch, Jr., *Sighing in newborn human infants: role of inflation-augmenting reflex.* J Appl Physiol, 1976. **41**(4): p. 502-7.
50. Thoby-Brisson, M., *Neural mechanisms for sigh generation during prenatal development.* J Neurophysiol, 2018. **120**(3): p. 1162-1172.

51. Baldwin, D.N., et al., *Effect of sighs on breathing memory and dynamics in healthy infants.* J Appl Physiol (1985), 2004. **97**(5): p. 1830-9.
52. Perez-Padilla, R., P. West, and M.H. Kryger, *Sighs during sleep in adult humans.* Sleep, 1983. **6**(3): p. 234-43.
53. Treacher, D.F. and R.M. Leach, *Oxygen transport-1. Basic principles.* BMJ, 1998. **317**(7168): p. 1302-6.
54. Leach, R.M. and D.F. Treacher, *Oxygen transport-2. Tissue hypoxia.* BMJ, 1998. **317**(7169): p. 1370-3.
55. National Heart, L., and Blood Institute *Atelectasis*. Available from: https://www.nhlbi.nih.gov/health-topics/atelectasis.
56. Koch, H., et al., *Stable respiratory activity requires both P/Q-type and N-type voltage-gated calcium channels.* Journal of neuroscience, 2013. **33**(8): p. 3633-3645.
57. Mauri, T., et al., *Pressure support ventilation + sigh in acute hypoxemic respiratory failure patients: study protocol for a pilot randomized controlled trial, the PROTECTION trial.* Trials, 2018. **19**(1): p. 460.
58. Moraes, D.J., B.H. Machado, and J.F. Paton, *Specific respiratory neuron types have increased excitability that drive presympathetic neurones in neurogenic hypertension.* Hypertension, 2014. **63**(6): p. 1309-18.
59. Naik, B.I. and C.G. Durbin, Jr., *Variability in Mechanical Ventilation: What's All the Noise About?* Respir Care, 2016. **61**(1): p. 125.
60. Li, P. and K. Yackle, *Sighing.* Curr Biol, 2017. **27**(3): p. R88-R89.
61. Housley, E., N. Louzada, and M.R. Becklake, *To sigh or not to sigh.* Am Rev Respir Dis, 1970. **101**(4): p. 611-4.
62. Shea, S.A., et al., *The effect of human heart-lung transplantation upon breathing at rest and during sleep.* Respir Physiol, 1988. **72**(2): p. 131-49.
63. Varga, A.G., et al., *Differential impact of two critical respiratory centres in opioid-induced respiratory depression in awake mice.* J Physiol, 2020. **598**(1): p. 189-205.
64. Lalley, P.M., et al., *CrossTalk opposing view: The pre-Botzinger complex is not essential for respiratory depression following systemic administration of opioid analgesics.* J Physiol, 2014. **592**(6): p. 1163-6.
65. Bachmutsky, I., et al., *Opioids depress breathing through two small brainstem sites.* Elife, 2020. **9**.
66. Bell, H.J., E. Azubike, and P. Haouzi, *The "other" respiratory effect of opioids: suppression of spontaneous augmented ("sigh") breaths.* J Appl Physiol, 2011. **111**(5): p. 1296-303.
67. Egbert, L.D. and H.H. Bendixen, *Effect of Morphine on Breathing Pattern. A Possible Factor in Atelectasis.* JAMA, 1964. **188**: p. 485-8.

68. Nozaki-Taguchi, N. and T. Nishino, *Depression of sighing in the first three postoperative days with epidural morphine analgesia.* J Anesth, 1994. **8**(4): p. 415-419.
69. Anrep, G., F. Pascual, and R. Rossler, *Respiratory Variations of the Heart Rate. II. The Central Mechanism of Respiratory Arrhythmia and the Inter-Relations between the Central and Reflex Mechanisms.* Proceedings of the Royal Society, 1936. **119**: p. 218-230.
70. Garcia, A.J., 3rd, et al., *Cardiorespiratory Coupling in Health and Disease.* Autonomic Neuroscience, 2013. **175**(0): p. 26-37.
71. Yasuma, F. and J. Hayano, *Respiratory sinus arrhythmia: why does the heartbeat synchronize with respiratory rhythm?* Chest, 2004. **125**(2): p. 683-90.
72. Hayano, J., et al., *Respiratory sinus arrhythmia. A phenomenon improving pulmonary gas exchange and circulatory efficiency.* Circulation, 1996. **94**(4): p. 842-7.
73. Vaschillo, E.G., et al., *The effects of sighing on the cardiovascular system.* Biol Psychol, 2015. **106**: p. 86-95.
74. Vlemincx, E., I. Van Diest, and O. Van den Bergh, *A sigh of relief or a sigh to relieve: The psychological and physiological relief effect of deep breaths.* Physiol Behav, 2016. **165**: p. 127-35.
75. Sody, A.N., et al., *Sigh syndrome: is it a sign of trouble?* J Fam Pract, 2008. **57**(1): p. E1-5.
76. Vlemincx, E., et al., *Respiratory variability and sighing: a psychophysiological reset model.* Biol Psychol, 2013. **93**(1): p. 24-32.
77. Guyon, A., et al., *Respiratory Variability, Sighing, Anxiety, and Breathing Symptoms in Low- and High-Anxious Music Students Before and After Performing.* Front Psychol, 2020. **11**: p. 303.
78. Ramirez, J., et al., *Central and peripheral factors contributing to obstructive sleep apneas.* Respiratory Physiology and Neurobiology, 2013. **189**(2): p. 344-353.
79. Biondo, B., et al., *Glial and neuronal alterations in the nucleus tractus solitarii of sudden infant death syndrome victims.* Acta Neuropathol, 2004. **108**(4): p. 309-18.
80. Kahn, A., et al., *Polysomnographic studies of infants who subsequently died of sudden infant death syndrome.* Pediatrics, 1988. **82**(5): p. 721-7.
81. Sawaguchi, T., et al., *Apnea, glial apoptosis and neuronal plasticity in the arousal pathway of victims of SIDS.* Forensic Sci Int, 2005. **149**(2-3): p. 205-17.
82. Li, P., et al., *The peptidergic control circuit for sighing.* Nature, 2016. **530**(7590): p. 293-297.
83. Johnson, S.M., N. Koshiya, and J.C. Smith, *Isolation of the kernel for respiratory rhythm generation in a novel preparation: the pre-Botzinger complex "island".* J Neurophysiol, 2001. **85**(4): p. 1772-6.
84. Doi, A. and J.M. Ramirez, *State-dependent interactions between excitatory neuromodulators in the neuronal control of breathing.* J Neurosci, 2010. **30**(24): p. 8251-62.

85. Peña, F., et al., *Differential contribution of pacemaker properties to the generation of respiratory rhythms during normoxia and hypoxia.* Neuron, 2004. **43**(1): p. 105-17.
86. Basting, T.M., et al., *Hypoxia silences retrotrapezoid nucleus respiratory chemoreceptors via alkalosis.* J Neurosci, 2015. **35**(2): p. 527-43.
87. Souza, G., et al., *Breathing regulation and blood gas homeostasis after near complete lesions of the retrotrapezoid nucleus in adult rats.* J Physiol, 2018. **596**(13): p. 2521-2545.
88. Li, P., et al., *Brain Circuit of Claustrophobia-like Behavior in Mice Identified by Upstream Tracing of Sighing.* Cell Rep, 2020. **31**(11): p. 107779.
89. Thoby-Brisson, M. and J.M. Ramirez, *Role of inspiratory pacemaker neurons in mediating the hypoxic response of the respiratory network in vitro.* J Neurosci, 2000. **20**(15): p. 5858-66.
90. Ramirez, J.M., A.K. Tryba, and F. Pena, *Pacemaker neurons and neuronal networks: an integrative view.* Curr Opin Neurobiol, 2004. **14**(6): p. 665-74.
91. Ramirez, J.M., et al., *The role of spiking and bursting pacemakers in the neuronal control of breathing.* J Biol Phys, 2011. **37**(3): p. 241-61.
92. Chapuis, C., et al., *Emergence of sigh rhythmogenesis in the embryonic mouse.* J Physiol, 2014. **592**(10): p. 2169-81.
93. Toporikova, N., M. Chevalier, and M. Thoby-Brisson, *Sigh and Eupnea Rhythmogenesis Involve Distinct Interconnected Subpopulations: A Combined Computational and Experimental Study(1,2,3).* eNeuro, 2015. **2**(2).
94. Garcia-Marin, V., P. Garcia-Lopez, and M. Freire, *Cajal's contributions to glia research.* Trends Neurosci, 2007. **30**(9): p. 479-87.
95. Faulkner, J.R., et al., *Reactive astrocytes protect tissue and preserve function after spinal cord injury.* J Neurosci, 2004. **24**(9): p. 2143-55.
96. Liddelow, S.A. and B.A. Barres, *Regeneration: Not everything is scary about a glial scar.* Nature, 2016. **532**(7598): p. 182-3.
97. Liddelow, S.A. and B.A. Barres, *Reactive Astrocytes: Production, Function, and Therapeutic Potential.* Immunity, 2017. **46**(6): p. 957-967.
98. Matias, I., J. Morgado, and F.C.A. Gomes, *Astrocyte Heterogeneity: Impact to Brain Aging and Disease.* Front Aging Neurosci, 2019. **11**: p. 59.
99. Sofroniew, M.V., *Reactive astrocytes in neural repair and protection.* Neuroscientist, 2005. **11**(5): p. 400-7.
100. Liddelow, S. and B. Barres, *SnapShot: Astrocytes in Health and Disease.* Cell, 2015. **162**(5): p. 1170-1170 e1.
101. Khakh, B.S. and M.V. Sofroniew, *Diversity of astrocyte functions and phenotypes in neural circuits.* Nat Neurosci, 2015. **18**(7): p. 942-52.

102. Anderson, C.M. and R.A. Swanson, *Astrocyte glutamate transport: review of properties, regulation, and physiological functions.* Glia, 2000. **32**(1): p. 1-14.
103. Zhang, Y. and B.A. Barres, *Astrocyte heterogeneity: an underappreciated topic in neurobiology.* Curr Opin Neurobiol, 2010. **20**(5): p. 588-94.
104. Emery, B. and B.A. Barres, *Unlocking CNS cell type heterogeneity.* Cell, 2008. **135**(4): p. 596-8.
105. Allen, N.J. and B.A. Barres, *Neuroscience: Glia - more than just brain glue.* Nature, 2009. **457**(7230): p. 675-7.
106. Barres, B.A., *The mystery and magic of glia: a perspective on their roles in health and disease.* Neuron, 2008. **60**(3): p. 430-40.
107. McNeill, J., et al., *Ion Channels and Electrophysiological Properties of Astrocytes: Implications for Emergent Stimulation Technologies.* Front Cell Neurosci, 2021. **15**: p. 644126.
108. Shen, W., et al., *An autocrine purinergic signaling controls astrocyte-induced neuronal excitation.* Sci Rep, 2017. **7**(1): p. 11280.
109. Burnstock, G., *Introduction to Purinergic Signaling*, in *Purinergic Signaling: Methods and Protocols*, P. Pelegrin, Editor. 2020, Springer Nature
110. Funk, G.D., *Neuromodulation: purinergic signaling in respiratory control.* Compr Physiol, 2013. **3**(1): p. 331-63.
111. Pascual, O., et al., *Astrocytic Purinergic Signaling Coordinates Synaptic Networks.* Science, 2005. **310**: p. 113-116.
112. Burnstock, G., *Purinergic Signaling.* British Journal of Pharmacology, 2009. **147**(S1): p. S172-S181.
113. Svensson, E., et al., *General Principles of Neuronal Co-transmission: Insights From Multiple Model Systems.* Front Neural Circuits, 2018. **12**: p. 117.
114. Burnstock, G., *Do some nerve cells release more than one transmitter?* Neuroscience, 1976. **1**(4): p. 239-48.
115. Burnstock, G., *Purine and purinergic receptors.* Brain Neurosci Adv, 2018. **2**: p. 2398212818817494.
116. Harden, T.K., J.L. Boyer, and R.A. Nicholas, *P2-purinergic receptors: subtype-associated signaling responses and structure.* Annu Rev Pharmacol Toxicol, 1995. **35**: p. 541-79.
117. Baroja-Mazo, A., M. Barbera-Cremades, and P. Pelegrin, *The participation of plasma membrane hemichannels to purinergic signaling.* Biochim Biophys Acta, 2013. **1828**(1): p. 79-93.
118. Erlichman, J.S., J.C. Leiter, and A.V. Gourine, *ATP, glia and central respiratory control.* Respir Physiol Neurobiol, 2010. **173**(3): p. 305-11.
119. Marina, N., et al., *Astrocytes and Brain Hypoxia.* Adv Exp Med Biol, 2016. **903**: p. 201-7.
120. Gourine, A.V., et al., *Astrocytes control breathing through pH-dependent release of ATP.* Science, 2010. **329**(5991): p. 571-5.

121. Guthrie, P., et al., *ATP Released from Astrocytes Mediates Glial Calcium Waves.* The Journal of Neuroscience, 1999. **19**(2): p. 520-528.
122. Hassinger, T.D., et al., *An extracellular signaling component in propagation of astrocytic calcium waves.* Proc Natl Acad Sci U S A, 1996. **93**(23): p. 13268-73.
123. Naus, C.C., et al., *Altered gap junctional communication, intercellular signaling, and growth in cultured astrocytes deficient in connexin43.* J Neurosci Res, 1997. **49**(5): p. 528-40.
124. Bruzzone, R. and C. Ressot, *Connexins, gap junctions and cell-cell signalling in the nervous system.* Eur J Neurosci, 1997. **9**(1): p. 1-6.
125. Goodenough, D.A. and D.L. Paul, *Gap junctions.* Cold Spring Harb Perspect Biol, 2009. **1**(1): p. a002576.
126. Nicholson, S.M. and R. Bruzzone, *Gap junctions: getting the message through.* Curr Biol, 1997. **7**(6): p. R340-4.
127. Dean, J.B., et al., *Role of gap junctions in CO(2) chemoreception and respiratory control.* Am J Physiol Lung Cell Mol Physiol, 2002. **283**(4): p. L665-70.
128. Fields, R.D. and G. Burnstock, *Purinergic signalling in neuron-glia interactions.* Nat Rev Neurosci, 2006. **7**(6): p. 423-36.
129. Lapato, A.S. and S.K. Tiwari-Woodruff, *Connexins and pannexins: At the junction of neuro-glial homeostasis & disease.* J Neurosci Res, 2018. **96**(1): p. 31-44.
130. Bennett, M.V., et al., *New roles for astrocytes: gap junction hemichannels have something to communicate.* Trends Neurosci, 2003. **26**(11): p. 610-7.
131. Li, T., C. Giaume, and L. Xiao, *Connexins-mediated glia networking impacts myelination and remyelination in the central nervous system.* Mol Neurobiol, 2014. **49**(3): p. 1460-71.
132. Huckstepp, R.T., et al., *CO2-dependent opening of connexin 26 and related β connexins.* Journal of Physiology, 2010. **588**(20): p. 3921-3931.
133. Solomon, I.C. and J.B. Dean, *Gap junctions in CO(2)-chemoreception and respiratory control.* Respir Physiol Neurobiol, 2002. **131**(3): p. 155-73.
134. Sofroniew, M.V., *Transgenic techniques for cell ablation or molecular deletion to investigate functions of astrocytes and other GFAP-expressing cell types.* Methods Mol Biol, 2012. **814**: p. 531-44.
135. Tien, A.C., et al., *Regulated temporal-spatial astrocyte precursor cell proliferation involves BRAF signalling in mammalian spinal cord.* Development, 2012. **139**(14): p. 2477-87.
136. Srinivasan, R., et al., *New Transgenic Mouse Lines for Selectively Targeting Astrocytes and Studying Calcium Signals in Astrocyte Processes In Situ and In Vivo.* Neuron, 2016. **92**(6): p. 1181-1195.
137. Boyden, E.S., *A history of optogenetics: the development of tools for controlling brain circuits with light.* F1000 Biol Rep, 2011. **3**: p. 11.

138. Schneider, F., C. Grimm, and P. Hegemann, *Biophysics of Channelrhodopsin.* Annu Rev Biophys, 2015. **44**: p. 167-86.
139. Lin, J.Y., et al., *Characterization of engineered channelrhodopsin variants with improved properties and kinetics.* Biophys J, 2009. **96**(5): p. 1803-14.
140. Lin, J.Y., *Optogenetic excitation of neurons with channelrhodopsins: light instrumentation, expression systems, and channelrhodopsin variants.* Prog Brain Res, 2012. **196**: p. 29-47.
141. Lin, J.Y., *A user's guide to channelrhodopsin variants: features, limitations and future developments.* Exp Physiol, 2011. **96**(1): p. 19-25.
142. Matyash, V. and H. Kettenmann, *Heterogeneity in astrocyte morphology and physiology.* Brain Res Rev, 2010. **63**(1-2): p. 2-10.
143. Yang, J., et al., *Na(+)-Ca(2)(+) exchanger mediates ChR2-induced [Ca(2)(+)]i elevation in astrocytes.* Cell Calcium, 2015. **58**(3): p. 307-16.
144. Verkhratsky, A., *Astroglial Calcium Signaling in Aging and Alzheimer's Disease.* Cold Spring Harb Perspect Biol, 2019. **11**(7).
145. Kawamoto, E.M., C. Vivar, and S. Camandola, *Physiology and pathology of calcium signaling in the brain.* Front Pharmacol, 2012. **3**: p. 61.
146. Catterall, W.A., *Voltage-gated calcium channels.* Cold Spring Harb Perspect Biol, 2011. **3**(8): p. a003947.
147. Giorgi, C., et al., *Calcium Dynamics as a Machine for Decoding Signals.* Trends Cell Biol, 2018. **28**(4): p. 258-273.
148. Nagai, T., et al., *Circularly permuted green fluorescent proteins engineered to sense Ca2+.* Proc Natl Acad Sci U S A, 2001. **98**(6): p. 3197-202.
149. Paredes, R.M., et al., *Chemical calcium indicators.* Methods, 2008. **46**(3): p. 143-51.
150. Russell, J.T., *Imaging calcium signals in vivo: a powerful tool in physiology and pharmacology.* Br J Pharmacol, 2011. **163**(8): p. 1605-25.
151. Chen, T.W., et al., *Ultrasensitive fluorescent proteins for imaging neuronal activity.* Nature, 2013. **499**(7458): p. 295-300.
152. Shigetomi, E., et al., *A genetically targeted optical sensor to monitor calcium signals in astrocyte processes.* Nat Neurosci, 2010. **13**(6): p. 759-66.
153. Miyawaki, A., et al., *Fluorescent indicators for Ca2+ based on green fluorescent proteins and calmodulin.* Nature, 1997. **388**(6645): p. 882-7.
154. Dana, H., et al., *High-performance calcium sensors for imaging activity in neuronal populations and microcompartments.* Nat Methods, 2019. **16**(7): p. 649-657.

CHAPTER 2

Advances in Cellular and Integrative Control of Oxygen Homeostasis within the Central Nervous System

Jan-Marino Ramirez[1,2]*, Liza Severs*[2], Sanja C. Ramirez[1], Ibis M. Agosto-Marlin[1]

[1]Center for Integrative Brain Research, Seattle Children's Research Institute, Department of Neurological Surgery, University of Washington School of Medicine, Seattle, WA 98101, USA
[2]Department of Physiology and Biophysics, The University of Washington, Seattle, WA 98101, USA
* *Both authors contributed equally to this article*

Published in the Journal of Physiology, May 2018
Find the article here.

Abstract

Mammals must continuously regulate the levels of O_2 and CO_2, which is particularly important for the brain. Failure to maintain adequate O_2/CO_2 homeostasis has been associated with numerous disorders including sleep apnea, Rett syndrome, and sudden infant death syndrome (SIDS). But, O_2/CO_2 homeostasis poses major regulatory challenges, even in the healthy brain. Neuronal activities change in a differentiated, spatially and temporally complex manner, which is reflected in equally complex changes in O_2 demand. This raises important questions: Is oxygen sensing an emergent property, locally generated within all active neuronal networks, and/or the property of specialized O_2-sensitive CNS regions? Increasing evidence suggests that the regulation of the brain's redox state involves properties that are intrinsic to many networks, but that specialized regions in the brainstem orchestrate the integrated control of respiratory and cardiovascular functions. Although the levels of O_2 in arterial blood and the CNS are very different, neuro-glial interactions and purinergic signaling are critical for both peripheral and CNS chemosensation. Indeed, the specificity of neuroglial interactions seems to determine the differential responses to O_2, CO_2, and the changes in pH.

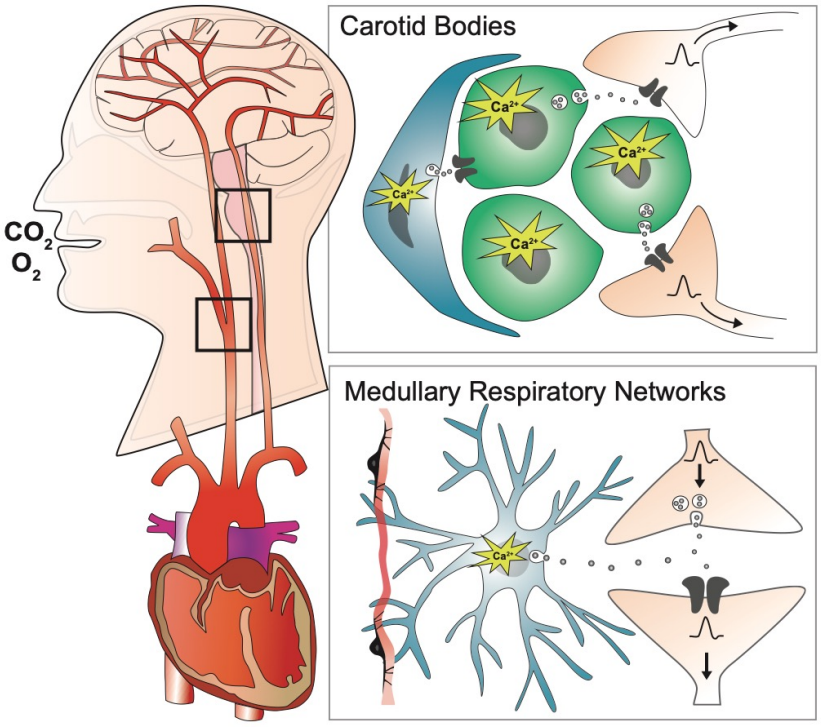

Key Words (3-6): preBötzinger Complex, retrotrapezoid nucleus, carotid body, glomus cells, astrocytes, cardiorespiratory coupling

Introduction

Endothermy gave mammals and birds distinct evolutionary advantages. It allowed them to move quickly and over long distances irrespective of their surrounding environmental temperatures. This enabled them to conquer novel ecological niches. However, endothermy came with a substantially higher metabolic demand (1). This demand is best met by aerobic metabolism, since oxygen releases substantial energy per electron transfer (2). Aerobic metabolism is particularly important to maintain the brain's state of persistent activity (3-5).

The dependency on aerobic metabolism is challenging because of two important reasons: Firstly, O_2 cannot effectively be stored; consequently mammals and birds cannot survive a prolonged cessation of breathing and heartbeat. Secondly, the dependency on the molecule with the largest energy release per electron transfer poses major regulatory challenges because too little oxygen is as detrimental as too much oxygen, a topic of great clinical significance (6-11). Indeed, the PO_2 within the CNS is maintained within a narrow range of approximately 1-4% O_2 (12). This suggests that neuronal microcircuits in the brain must maintain persistent activity in an oxidative microenvironment that is only slightly higher than the threshold for aerobic metabolism which lies around 1% O_2 (13, 14). Thus, maintaining a stable redox state requires precise and dynamic O_2 sensing and response mechanisms, which is achieved through neurovascular coupling involving neurons, smooth muscle cells, astrocytes (15-19), and possibly oligodendrocytes (20).

The neuronal responses to hypoxia are differentiated, and involve various mechanisms (21-23). In general, acute exposure to hypoxia leads to a rapid decrease in neuronal activity and synaptic depression in many regions of the brain (24-26). While this may be protective, it also leads to the loss of synaptic plasticity (27) and learning deficits (28). During anoxia this homeostatic response breaks down as neurons depolarize within minutes until they lose their ionic gradients across the membranes (29-31). Interestingly, diving mammals have developed specialized neuroglial adaptations to withstand prolonged periods of anoxia (31-34).

The neuronal responses to hyperoxia are as differentiated (24, 25). The reactive oxygen species (ROS) superoxide anion and H_2O_2 serve neuromodulatory functions. In midbrain dopaminergic neurons, H_2O_2 activates KATP channels to reduce neuronal excitability (35). At the neuromuscular junction, H_2O_2 differentially modulates presynaptic Ca^{2+} entry (36). The superoxide anion facilitates phrenic and hypoglossal motor outputs (37, 38), and can induce plasticity (37, 39). Similar modulatory effects have been described for the carotid body (CB) (40, 41).

The response to changes in oxygen is of critical importance in areas that are responsible for controlling O_2 supply. The preBötzinger complex (preBötC) is a microcircuit critical for different forms of inspiration that range from normal breathing to sighing and gasping (42-45). This network is located within the medulla (42, 46), and is essential for breathing (47-49) (Figure 1). Neuronal and glial functions within this network are responsive to hypoxia even when the network is isolated in a slice preparation

(14, 50-59). Hypoxia evokes a biphasic response: a rapid augmentation with the generation of sighs is followed by a respiratory depression (43, 60-65) (Figure 2). This hypoxic sensitivity of the preBötC neurons was also demonstrated *in vivo* (66). Hypoxia also evokes increased activity in hypoglossal (XII) neurons (62, 67-70) and in pre-sympathetic neurons of the rostral ventrolateral medulla (RVLM) (71, 72), while hypoxia hyperpolarizes the dorsal vagal motor nucleus (73-76). The central responses to hypoxia within the preBötC, XII, presympathetic, and parasympathetic neurons will likely contribute to an increased respiratory and sympathetic drive and a decreased parasympathetic drive (77). These examples of sensitivity to hypoxia within brainstem respiratory circuits illustrates that central oxygen sensitive mechanisms exist and locally regulate the activity of microcircuits in an adaptive manner.

This raises the important question: are these neuronal responses controlled by discrete central oxygen sensors, such as the specialized cellular interactions within the CB (78-82), or do these responses emerge from multiple oxygen sensitivities intrinsic to the networks themselves? Here we propose that the hypoxic response involves both emergent network properties as well as specialized chemosensitive neuroglial interactions. From the functional perspective the responses to changes in O_2, CO_2 and pH must be different. Indeed, there is increasing evidence that different networks seem to specialize in sensing primarily e.g. hypoxia or hypercapnia. Yet, the strikingly different network responses seem to rely on neuroglial interactions in which astrocytes are instrumental in differentiating chemosensory responses into specific O_2 as well as CO_2 sensitivities. Thus, although this review focuses on oxygen homeostasis and the hypoxic response of the CNS, we will consider the differential O_2 and CO_2 sensitivities when discussing the neuroglial interactions. Ultimately, the organism needs to respond to changes in both blood gases in a synergistic and adaptive manner.

Unraveling the network mechanisms underlying peripheral and central O_2 sensing

To mount an effective response to changes in blood gases, O_2 sensing mechanisms within the CNS must be tightly coordinated with inputs derived from peripheral chemosensory mechanisms (83-85). Exactly how these peripheral mechanisms are integrated within the central neuronal networks in the brainstem is not fully understood, and is a source of controversy as reviewed in (86). At the organismal level, the hypoxic ventilatory response (HVR) is biphasic (87): an initial augmentation is followed by a ventilatory depression (88). The augmentation has been associated with an excitatory drive from the CB, the depression with central regulatory activity (89, 90). However, it is not quite this simple. Some experiments suggest that CB denervation eliminates the augmentation phase (14, 91-93), while others suggest that the initial augmentation during hypoxia is preserved in peripherally chemoreceptor denervated animals (94-96). Indeed elegant studies have convincingly demonstrated that specific CNS hypoxia stimulates ventilation during wakefulness and sleep (97-99). This is consistent with surgical CB denervation which does not lead to obvious catastrophic, physiological consequences. Thus, CB

denervation became a procedure performed on patients in instances of carotid sinus syndrome (CSS), asthma, or pulmonary disease. For more details on benefits and risks see (100-106).

Limitations and caveats associated with studying the hypoxic response

The discussion in the previous section is representative for the challenges faced when exploring oxygen homeostasis and the neuronal response: O_2 supply and delivery depend on experimental conditions that vary widely and any experimental manipulation can have complex ramifications that are difficult to control and often difficult to interpret. This is not only the case for in vivo studies, but also for studies that are performed in reduced preparations in which oxygen-depth profiles differ, e.g. in the working heart-brainstem preparation (107), the isolated brainstem spinal cord preparation (108, 109), as well as brain slices (12, 14, 25, 110). Oxygen profiles even differ within a given preparation, because oxygen levels depend on neuronal activity that varies between different regions of a slice (110). Brain slices are typically studied at cooler temperatures. By decreasing metabolic consumption tissue oxygenation increases within the core, but renders superficial layers hyperoxic. Thus, the neuronal networks will be exposed concurrently to hyperoxic and hypoxic conditions that will affect neuronal activity. Oxygenation is also influenced by the rate and method of superfusion, the exact composition of the artificial cerebrospinal fluid, as well as the ambient barometric pressure (12, 111, 112). Experimental conditions also depend on the research questions. Studying the postnatal development of a network will be complicated by the fact that mature and neonatal slices vary in their oxygenation profile (12, 14, 111) . Characterizing network interactions between different regions also require slices to be cut in different thicknesses (8, 14, 113-115).

Yet, to achieve a complete understanding of the central hypoxic response different preparations and approaches have to be combined. The introduction of modern transgenic, optogenetic, and molecular biological methods significantly increased the experimental repertoire and allows for more specific manipulations and characterizations of identified neuron classes in preparations that range from brain slices to alert and freely behaving animals (59, 90, 116-118).

Reconfiguration of the Respiratory Network during hypoxia

Much has been learned about the hypoxic response of the preBötC. The respiratory rhythm in this microcircuit depends on glutamatergic neurons that are primarily derived from progenitor cells characterized by the transcription factor Dbx1 (119-121), and inhibitory neurons that can be subdivided into glycinergic and GABAergic neurons (122-124). These neurons possess a variety of intrinsic membrane properties. Upon synaptic isolation respiratory neurons are either silent, tonically active, or they possess intrinsic bursting properties (125-127). These bursting properties are mediated by two principle inward currents: the persistent sodium current (I_{Nap}) and the calcium-dependent non-specific cation current (I_{CAN}), (51, 128-132). Early during hypoxia, I_{CAN} dependent bursting ceases but bursting

persists in neurons that depend on I_{Nap} (Figure 2). This differential sensitivity impacts the network's dependency on these two properties. Rhythmogenesis persists when I_{Nap} is blocked with riluzole in control, but it ceases when I_{Nap} is blocked during hypoxia (50). At the concentration used, riluzole specifically blocked bursting, but not action potential generation (50), suggesting that the "bursting property" is critical for rhythmogenesis in hypoxia. However, these pharmacological experiments cannot exclude that riluzole also altered other properties, such as synaptic transmission. Yet, modulators unrelated to riluzole had similar effects: blocking 5-HT2A or □2 adrenergic receptors blocked I_{Nap} and respiratory activity during hypoxia, but not in controls (52, 133). These data imply that the respiratory network changes from a "normoxic" state that depends on multiple, heterogeneous membrane properties to a "hypoxic (i.e. gasping)" state that is particularly sensitive to the blockade of I_{Nap} (51, 134). This hypoxic network state is characterized not only by an increased dependency on I_{Nap}, but also by weakened connectivity between respiratory neurons (53).

The selective dependency of the hypoxic state on the activation of the 5-HT2A receptor subtype is interesting in the context of SIDS. Children that died from SIDS breathe normally under normoxic conditions, but fail to gasp during hypoxia (135, 136). Various studies also demonstrated dysregulation of 5-HT in SIDS (137-142). Thus, infants with disturbed 5-HT mechanisms might be protected under normal oxygenated conditions, but become vulnerable to genetic mutations that affect serotonergic neurons when the network transitions into a hypoxic state (52, 136).

Importantly, the reconfiguration of the preBötC can only describe a small aspect of a wider network reconfiguration which will include additional microcircuits located rostral to the preBötC. This includes the RTN/pFRG, which is critical for the generation of active expiration (143-145), and the postinspiratory complex (PiCo), which is critical for generating postinspiration (146); since postinspiratory neurons lose their inhibitory input during the inspiratory phase, we suggest these neurons might synchronize with inspiratory activity (147-149). This synchronization of the network can be an acute endogenous survival response to extreme environmental changes, such as hypoxia (56, 150).

The effect of intermittent hypoxia on the Cardiorespiratory Network and implications for OSA

Hypoxic conditions are often experienced in form of intermittent hypoxia. It is a characteristic condition in patients suffering from obstructive sleep apnea (OSA), familial dysautonomia (151, 152), Rett Syndrome (153-156), Mitochondrial disease (157-159), epilepsy (160, 161), and many other disorders characterized as "dysautonomia". These disorders are often associated with breathing disturbances, increased heart rate, decreased heart rate variability and other forms of disturbed cardiorespiratory coupling.

Chronic exposure to intermittent hypoxia (CIH) results in increased levels of HIF1α and decreased HIF2, which causes an imbalance between the hypoxic and antioxidant system and a buildup of reactive oxygen species (162-164). CIH seems to act directly on the CB which then affects CNS

networks through the release of neurogenic ROS. This conclusion is based on the observation that CB lesioning abolishes many of the detrimental consequences associated with OSA (6, 165). CIH leads to an upregulation of heme-oxygenase 1 (166) and to an increased desynchronization of the inspiratory neurons within the preBötC (167, 168). Incompletely synchronized preBötC bursts fail to evoke a population burst within the XII motor nucleus (167), which could contribute to a pharyngeal collapse (169). The transmission failures from the preBötC to the XII can be prevented with ROS scavengers, suggesting that the CIH-induced changes involve a build-up of ROS and oxidative stress within the brainstem (Figure 3) (167). The CIH induced amplitude fluctuations in the preBötC are reminiscent of fluctuations also seen in an animal model of Rett Syndrome (Figure 4) (170). These mice and also human patients are characterized by increased oxidative stress (156, 171-176). It is therefore conceivable that the oxidative stress seen after CIH also contributes to the breathing disturbances in Rett Syndrome including the characteristic fluctuations in tidal volume (Figure 4) (153). However, CIH and ROS production affects not only the preBötC but also other CNS sites, including the nucleus tractus solitarius (NTS) (177), where CIH alters neurotransmission, neuromodulation (178-183), neuroprotection, and plasticity by altering proteins such as TrkB and BDNF (184, 185). CIH also enhances sympathetic drive and alters the baroreflex by acting differentially on central respiratory neurons (186-190). Indeed, these studies show the close interaction between the central respiratory and cardiovascular response. It seems that the changes in sympathetic discharge and the levels of arterial pressure are due to the changes in the central respiratory network (190). This interaction occurs via connections from the respiratory microcircuits to the brainstem neurons that control sympathetic, but also parasympathetic activity. How the recently discovered excitatory postinspiratory complex (146) contributes to the integration of the sympathetic nervous system is still an open question, but a recent study indicates that there are anatomical interactions between PiCo, preBötC, and the RVLM (191). For the preBötC it has been shown that it contributes to the activity of vagal neurons and parasympathetic control (192) involving GABAergic neurons(193).

It is important to emphasize that the degree and specific pattern of hypoxia determines whether the consequences are detrimental or beneficial (194, 195), as intermittent hypoxia can decrease (196) or increase long-term facilitation (LTF) (197, 198). Thus, under the right conditions, intermittent hypoxia has been successfully used to induce plasticity that is very beneficial during the rehabilitation following spinal cord injury (199-202).

These studies also revealed a close link to inflammation, which can suppress some aspects of the plasticity evoked by intermittent hypoxia (203-205), while other pathways that lead to facilitation are resistant to inflammation (206). How hypoxia and inflammation interact within the CNS is an interesting and emerging area of research, with important implications for the respiratory system and the clinic (55, 207-209). A commonly used approach to study inflammation is the use of lipopolysaccharide (LPS) (207, 209-211), which via the vagal nerve causes neuroinflammation (212-214). The relationship between

inflammation and CIH is particularly relevant for premature infants that are susceptible to lung injuries and have unstable periodic breathing (215). Both CIH and LPS-induced inflammation modulate CB development with long-lasting consequences (216) on the control of breathing, including attenuated hypoxic and hyperoxic responses (211, 217). Unraveling these interactions will be critical to understand the relationship between respiratory infections and the resulting changes in breathing that are characteristic of small infants (207, 210).

There is increasing evidence that astrocytes play a central role in the response to inflammation and hypoxia. These cells are intrinsically sensitive to hypoxic insults, and they have been implicated in the inflammatory response (218, 219), the control of the cardiorespiratory responses, and the modulation of sympathetic drive (59, 220-222). The hypoxic environment increases ATP and lactate release by astrocytes, which is thought to lead to over excitation of sympathetic circuits affecting cardiorespiratory control (221, 223). A recent review by Marina and colleagues has detailed how researchers have tackled the astrocyte hypothesis by blocking ATP-mediated signaling which leads to slow progression of cardiac remodeling in rats and reduced systemic blood pressure in hypertensive rats (224, 225). The role of glia and purinergic signaling will be discussed in more detail in the next section.

The role of purinergic signaling and neuroglia interaction in sensing O_2 and CO_2

There is an increasing consensus that neuroglial interactions play critical roles in sensing changes not only in PO_2 but also PCO_2/H^+. Indeed, it seems that specialized glia cells determine whether a given region, organ, or network is sensitive to PO_2 or PCO_2/H^+. These glial cells then communicate with neurons and other glia through transmitter release (57, 226); in particular, ATP (227), D-serine (228, 229), and glutamate (230) (Figure 6). The concept of specialized cell-to-cell interactions among neurons is emerging for astrocytes within the medulla, but also the cortex (222), and they may confer differential sensitivity to PO_2 and PCO_2/H^+ depending on location within the ventral respiratory column (VRC) (229, 231-233). Interestingly, the neuroglial interactions that seem to underlie $PO_2/PCO_2/H^+$ sensitivity in the central nervous system are strikingly similar to those that occur peripherally in the carotid bodies (Figure 5-6) (234).

Therefore, the CB could provide critical insights into our understanding of how the CNS responds to hypoxia and CO_2. The CB consists of two primary cell types: type I (glomus) and type II (sustentacular) cells. These cells are bundled tightly in groups, and located in close contact with capillary beds. Afferent sensory nerves leading to the carotid sinus nerve receive autonomic innervation from the petrosal ganglion, and connect to the NTS to control breathing (234-237). Type I cells are of neural origin (236, 238, 239), and there are proposed to be several subtypes (240-242). The responsiveness of type I cells to changes in $PO_2/PCO_2/H^+$ may therefore be representative of the heterogeneous hypoxic responses of central respiratory neurons (14, 50, 96, 229, 243, 244). In contrast, type II cells are glial-like

and are located in close proximity to groups of type I cells, where they ensheath type I cells with thin proccesses and are arranged into glomeruli (Figure 5) (234).

Both CB cell types possess distinct electrophysiological properties (238, 245), and there is significant crosstalk between them. ATP released from type I cells during hypoxia or hypercapnia leads to a rise in intracellular Ca^{2+} ($[Ca^{2+}]_i$), followed by a delayed, secondary $[Ca^{2+}]_i$ increase in proximal type II cells (246, 247). A depolarization of type I cells results in sensory output to the petrosal ganglion and on to the carotid sinus nerve, mediating the cardiorespiratory response in the NTS (235, 248). The primary transmitter ATP activates $P2X_{2/3}$ receptors on afferent nerve terminals (102, 247, 249), possibly through pannexin-1 channels, which release ATP after activation of $P2Y_2$ receptors (78, 246, 250, 251).

Mechanisms proposed to underlie chemoreception in the RTN/pFRG, Raphe Nucleus (RN), NTS, preBötC, and other areas of the respiratory network similarly rely on purinergic signaling involving astrocytes (57, 227) (105, 252-254). Much has been learned about the RTN/pFRG as an important site for PO_2 and PCO_2/H^+ sensing, but there are additional areas with varying sensitivity to hypoxia and hypercapnia in the VRC (255). Purinergic signaling also plays a critical role in the central control of the cardiovascular system (256-258).

In principle, the astrocytic response to local changes in $PO_2/PCO_2/H^+$ results in elevated levels of $[Ca^{2+}]_i$, which then leads to release of ATP, which further propagates the astrocytic Ca^{2+} signal in a feedforward manner. This in turn increases the activation of chemosensitive neuron populations that are directly activated by the release of ATP (Figure 6) (57, 259-261). Dependent on the microcircuits in which these neuroglial interactions occur, there will be different responses at the organismic level. For example, the RTN or preBötC will mount different aspects of the systems level responses to changes in CO_2 and O_2. The direct effect on astrocytes seems relatively clear, as blocking neuronal responses or injection of current does not alter the astrocytic Ca^{2+} response (57). Additionally, ATP antagonists diminished pH induced $[Ca^{2+}]_i$ signals (57). The Ca^{2+} spread is partially due to gap junctions (57), and is mediated by release of gliotransmitters (for review of Ca^{2+} spread in astrocytes, see (262). Interestingly, acidosis of the cortex and dorsal areas of the brainstem caused no change in the astrocytic $[Ca^{2+}]_i$ response, supporting the hypothesis that central chemoreception is localized to specific area(s) within the respiratory network (57, 254).

Precise mechanisms behind astrocytic chemosensitivity and the role of various P2X and P1/2Y receptors in modulating respiratory frequency have been partially revealed for the preBötC. (90, 263-266). These mechanisms are possibly similar for the RTN/pFRG. However, this is still debated as the sensitivity of the RTN/pFRG to ATP does not appear to be dependent on P2 related mechanisms (267-269) (Figure 6).

In slices, $P2Y_1$ receptor ($P2Y_1R$) activation in the preBötC by ATP creates a 2-4 fold increase in the frequency of fictive inspiratory burst activity (264). ATP released by astrocytes in the preBötC during the HVR also mediate an increase in inspiratory frequency and reduces the secondary depression phase

through activation of $P2Y_1Rs$ (90). Astrocytes in the preBötC sense changes in PO_2 and release $[Ca^{2+}]_i$, translating to ATP release (and possibly other gliotransmitters), and activation of $P2Y_1Rs$ on neurons (90). It is hypothesized that astrocytes detect changes in blood gas levels through mitochondria, relaying this information through a ROS and PIP_2-mediated cascade that leads to the commonly detected increase in $[Ca^{2+}]_i$ (59). As mentioned above, the effect of $P2Y_1R$ activation in the RTN/pFRG is somewhat unclear. Several experiments have shown that although $P2Y_1Rs$ are expressed in RTN/pFRG neurons, they may only play a partial role in modulating CO_2 (270) or pH driven excitation (267), as these responses show experimental cell to cell variablity in vitro versus in vivo. However, with local application of $P2Y_1R$ antagonists during hypercapnia, there is a resultant increase in amplitude and frequency of phrenic nerve output (256, 268). Further downstream effects of receptor activation occur to create changes in respiratory output. Breakdown of ATP results in neuroactive metabolites, such as ADP and ADO, which are agonists of P2YRs and P1YRs, respectively {Zimmermann, 2001 #1268, 271). Both of these biproducts have additional effects on respiratory frequency, as ADP is excitatory (264) while ADO may have an inhibitory effect in neonates (Figure 6) (272) (For review on $P2Y_1Rs$ in respiration, see Rajani et al 2016 (273)).

An emergent concept is that astrocytes form different functional subpopulations. This is best illustrated as astrocytes that exist in the RTN/pFRG and preBötC may perform different functions in modulating respiratory network activity (231-233, 274). Forsberg et al. recently produced novel evidence of two astrocyte subtypes within the RTN/pFRG and preBötC; a portion of which exhibited rhythmic calcium oscillations, and another group that maintained a state of inactivity. They also found sensitivity differences in regions of the VRC. Selective activation of astrocytes in the RTN/pFRG and preBötC increased oscillatory activity; but, RTN/pFRG astrocytes released PGE2 resulting in neural activation, whereas neurons in the preBötC had no response to an increase in calcium oscillations (233). However, as already discussed, the interpretation of findings like this needs to carefully consider experimental caveats. In normoxia, high levels of glutamate seem to be required to create astrocyte-neuron coupling. As hypothesized, these non-physiological levels of glutamate could potentially only occur during hypoxia or when blocking neuronal glutamate uptake (274). Regardless of these uncertainties, it appears that each respiratory microcircuit is sensitive to changes in $PO_2/PCO_2/H^+$ and that multiple astrocytic subtypes may have different support functions, which is reminiscent of the situation in the CBs (222). This concept has been raised for networks throughout the CNS, not only the respiratory network (275). Further support for the concept of astrocyte subtypes and differential sensitivity in the respiratory networks comes from evidence that astrocytes also respond to changes in CO_2 by releasing D-serine (229). It is thought that D-serine in the RN and VRC, but not NTS, increases respiratory frequency under control conditions and hypercapnia through NMDAR-dependent mechanisms (229, 276). Astrocytes appear to interact not only with neurons, but also with pericytes. Pericytes are responsive to lactate

which results in contraction and relaxation under normal and hypoxic conditions, respectively. Lactate has been shown to be released by astrocytes located in the respiratory groups (220, 277-281).

Astrocytes versus neurons as the primary target in oxygen sensing

As discussed above, there is support for the notion that astrocytes are directly targeted by changes in $PO_2/PCO_2/H^+$, while neurons are indirectly controlled by the astrocytes. Specifically, it is hypothesized that changes in blood gases are detected by astrocytes (59), which in turn elicit an increase in $[Ca^{2+}]_{i,}$ a subsequent release of gliotransmitters, and neuronal activation (259). However, most likely, this hypothesized mode of chemosensory transmission is much more complex, and there is still much to be learned when it comes to specific neuroglial interactions. Moreover, as discussed before, the responsiveness and mechanisms may vary for different regions.

However, can neurons be intrinsically sensitive to changes in O_2 or CO_2? In the preBötC, synaptically isolated pacemaker neurons respond to hypoxia with transient increases in rhythmicity, which is followed by cessation of the endogenous rhythm during extended exposure to hypoxia, indicating that pacemakers play a direct role in the hypoxic response (63). While these hypoxic responses persist after synaptic isolation, it is important to emphasize that this study does not exclude a possible involvement of glialtransmitter involving purinergic signaling. Thus, it will be necessary to demonstrate that the hypoxic responses are maintained when physically isolated, as has been shown for Raphe neurons and RVLM neurons for the CO_2 response (166, 282-284). For the preBötC and C1 region it has been shown that cells express heme-oxygenase (HO-1), but these cells were anatomically identified, and it is not clear whether they play a role in the hypoxic response (284, 285). Some neurons in the RTN/pFRG have also been reported to respond directly to changes in PCO_2/H^+ (117). These neurons are purported to detect PCO_2 via TASK-2 and GPR4 receptors (Figure 6) (117, 286-288). Yet, these neurons seem to obtain this information also from surrounding astrocytes and peripheral chemoreceptors (57). In this study, blocking activity of RTN/pFRG neurons had no effect on the astrocytic Ca^{2+} increase (57). It has also been reported that inward currents in preBötC astrocytes occurring in phase with rhythmic neuronal oscillations under normoxia are due to neuronal release of K^+ and glutamate (274).

Thus, while neurons may have intrinsic sensitivity to O_2 and CO_2, there seems to be more evidence to support the notion that astrocytes are the primary sensors for pH and hypoxic conditions. Moreover, astrocytes within the medulla are found to be in close proximity to blood vessels (57) and exhibit radial processes that are in contact with vessels (289). They have reversal potentials near K+ equilibrium potential (E_{K+}), and are blocked with Barium and desipramine, a blocker of Kir4.1 channels; this has led to later experiments that have helped to uncover specific channels that astrocytes use in sensing changes in oxygen or pH (289).

Ion channels and the mechanisms of O_2 and CO_2 sensing

These studies cohesively define the role of astrocytes within the ventrolateral medulla as chemosensitive units, but specific mechanisms underlying PO_2/PCO_2/H^+ sensing and what role each specific area of the respiratory network plays in chemosensitivy have yet to be completely uncovered. Our limited understanding is partly rooted in the aforementioned experimental challenges in isolating independent mechanisms in slices or in vivo. This is exemplified by the amount and variety of ion channels tied to the oxygen sensing abilities of astrocytes and neurons. Clearly, multiple ion channels are involved in chemoreception. However, which channels and what particular role they play is dependent on cell type, anatomic location, and experimental conditions (290). Gap junction channels facilitate Ca^{2+} spread (57), and several types of K^+ channels contribute to chemotransduction pathways within both astrocytes and neurons in the respiratory groups; especially within the RTN/pFRG (273, 278, 286, 291-294). K^+ channels such as the Kir4.1 inward rectifying channel have been implicated in regulation of the astrocyte resting membrane potential throughout the brain in several studies (295), and could explain astrocytic activation through voltage-dependent mechanisms (296)). Interestingly, the application of fluorocitrate had no effect on astrocytes when applied to the NTS nor raphe neurons (294). The possibility of TASK channels playing a role in chemoreception was proposed in 2001, as these channels are prominent in brainstem motor nuclei and exhibit high sensitivity to pH (291, 297). However, the situation may be more differentiated, since TASK1/3 knock-out mice seem to exhibit no signs of health issues (298), while the loss of TASK2 channels in the RTN/pFRG blunted the response to pH changes. Indeed, these 3 subunits are in different subgroups of the same family of K2P channels, thus the intrinsic sensitivities of TASK1/3 channels and TASK2 channels are different. Subunits 1/3 both exhibit a very tight range of pH sensitivity, while TASK2 has a much broader sensitivity to changes in alkalinity (297, 299). These subtle differences could underlie different mechanisms of chemosensitivity within networks of the VRC, and also explain why knockout and mutation studies did not show a severe detriment to respiratory activity. TASK-1 channels have similarly been suggested to have a role in controlling the background current in the carotid bodies, as mRNA and protein expression data show that they are expressed within the atrium and ventricles of heart tissue (300-302).

It has been well established in recent years that ATP plays a major role in astrocytic detection of changing PO_2/PCO_2/H^+ levels. However, it would be an oversimplification to imply that purinergic signaling is the only mechanism involved. Indeed, some studies indicate that sensing O_2 and CO_2/H^+ could involve entirely different pathways within astrocytes. Turovsky et al demonstrated that the Na^+/HCO_3^- cotransport (NBC) and the Na^+/Ca^{2+} exchanger (NCX) are required for increases in calcium fluctuations in astrocytes in response to changes in pH (Figure 6) (254). It will be interesting to learn whether mechanisms of mitochondrial activation and activation by NBC/NCX can occur in one astrocyte population, or if specialized subtypes exist that are specific to detecting O_2 and CO_2/H^+ changes.

As already mentioned, the mechanisms for sensing changes in $PO_2/PCO_2/H^+$ levels in both the carotid bodies and in the CNS are surprisingly similar. For the astrocytes in the RN and VRC it has been proposed that CO_2 evoked D-serine release is due to gap junction hemichannels, specifically pannexin1 (229), similar to type II cells in the CB (246). Moreover, NMDARs are expressed in CB glomus cells and CNS astrocytes. Thus, the role of D-serine in the VRC (303) may resemble those in the CB. Connexins, specifically connexin 26 respond to increases in CO_2 and mediate ATP release (58, 304), while connexin 36 and 43 are expressed in the carotid bodies and myenteric plexus in mice and are known to play a role in CO_2 detection (305, 306).

Taken together, there is accumulating evidence for a central chemosensory component to the HVR that acts through mechanisms not dissimilar from those proposed in the carotid bodies. With the understanding that the ventrolateral medulla plays a role in the HVR, we postulate that localized responsiveness to O_2 or CO_2/H^+ in the preBötC and RTN/pFRG, respectively, emerge through specialized neuroglial interactions. Each of these regions exhibits a high sensitivity to either O_2 or CO_2/H^+, that involves regionalized astrocytes with specialized sensitivity to either O_2 or CO_2/H^+. Thus, it seems that the differences between the RTN/pFRG and preBötC are a function of the proportion of each astrocyte subtype that exists in each location (Figure 6).

Summary

This review discussed the necessity and complexity involved in chemosensation in the CNS. We highlighted the evolutionary importance of aerobic metabolism and how our bodies have developed impeccable mechanisms to maintain homeostasis between O_2 and CO_2, which is particularly critical for normal brain function. Tightly regulated networks in the medulla that include the NTS, RN, RTN/pFRG, and preBötC are primarily responsible for the homeostatic response and the regulation of blood gases. The preBötC, involved in inspiration, responds to changes in O_2 in a biphasic manner by rapidly increasing neuronal activity followed by respiratory depression that leads to gasping. This biphasic response to O_2 is attributed to a dynamic reconfiguration involving changes in ionic channel dependencies, excitatory and inhibitory conductances and the synchronization of respiratory neurons. Abnormalities in this and other medullary networks lead to disorders that affect cardiorespiratory coupling and elicit inflammatory responses exacerbating these conditions. At the core of these central chemosensory network responses are highly differentiated neuroglial interactions involving purinergic signaling. Although the chemosensitive processes in RTN/pFRG and preBötC involve neuroglial interactions including several receptors and neuromodulators that are strikingly similar to those described for the CB, it is also important to emphasize their differences, as astrocytic subtypes imbue different regions with different response properties. Unraveling the differential roles of astrocytes as the primary target in O_2 and CO_2 sensing is a riveting concept, and is a departure from the ideas that (1) astrocytes are all similar and (2) neurons are the primary foci of study in the CNS. While this review emphasizes the

importance of chemosensitivity, we also wanted to highlight the need for more research that will be required to unravel how the body controls its most necessary function, respiration.

Acknowledgements

Work in this lab is supported by grants from the NIH (R01 HL126523, P01 HL 090554).

Competing Interests

The authors have no competing interests to declare.

Figures

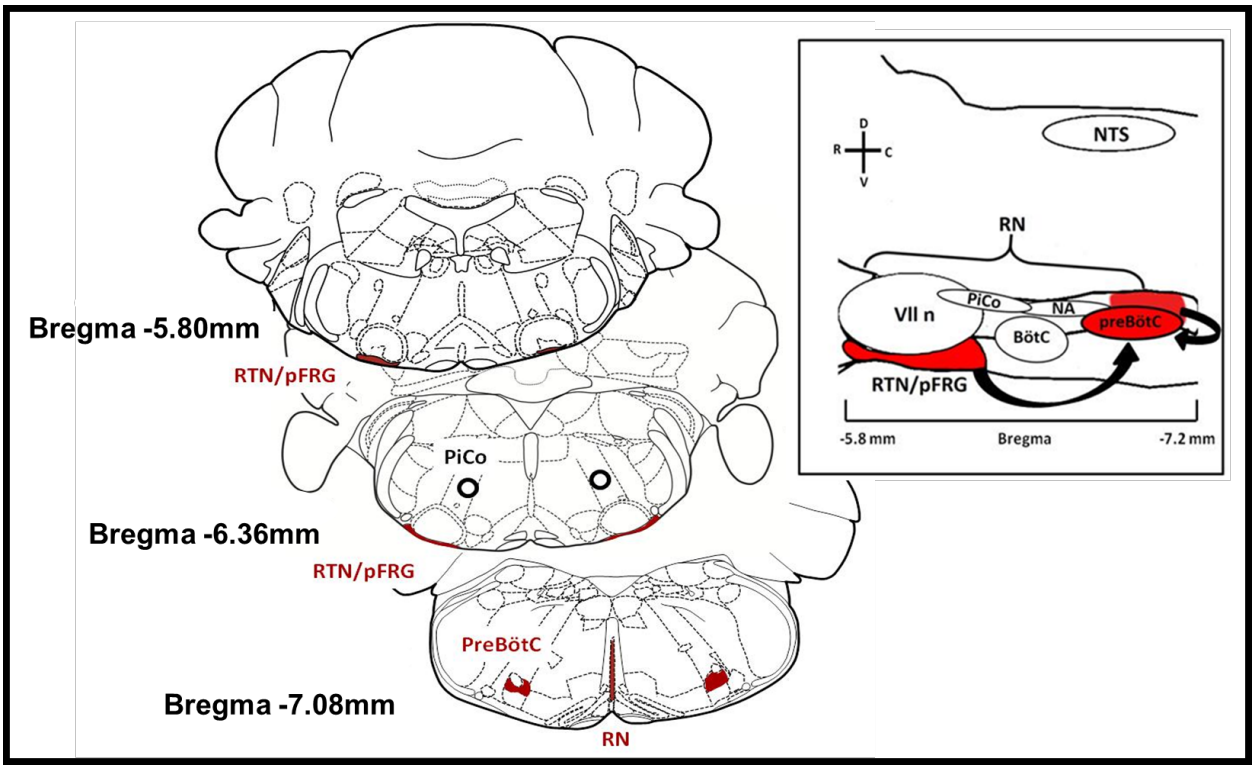

Figure 1. Anatomical schematic of medullary network involved in chemosensitivity. Sagittal view of ventral medullary respiratory group and the raphe nucleus (RN). The respiratory group consists of the retrotrapezoid nucleus (RTN)/parafacial respiratory group (pFRG) complex (RTN/pFRG),the Bötzinger complex (BötC), the postinspiratory complex (PiCo), and the pre-Bötzinger complex (preBötC). Structures in **RED** have been extensively studied and mentioned in this review contributing to chemosensitivity in the CNS. Black arrows suggest communication between medullary network, RTN/pFRG and RN signal the preBötC ultimately leading to changes in breathing. Adapted from Paxinos 2007 (Franklin & Paxinos, 2008).

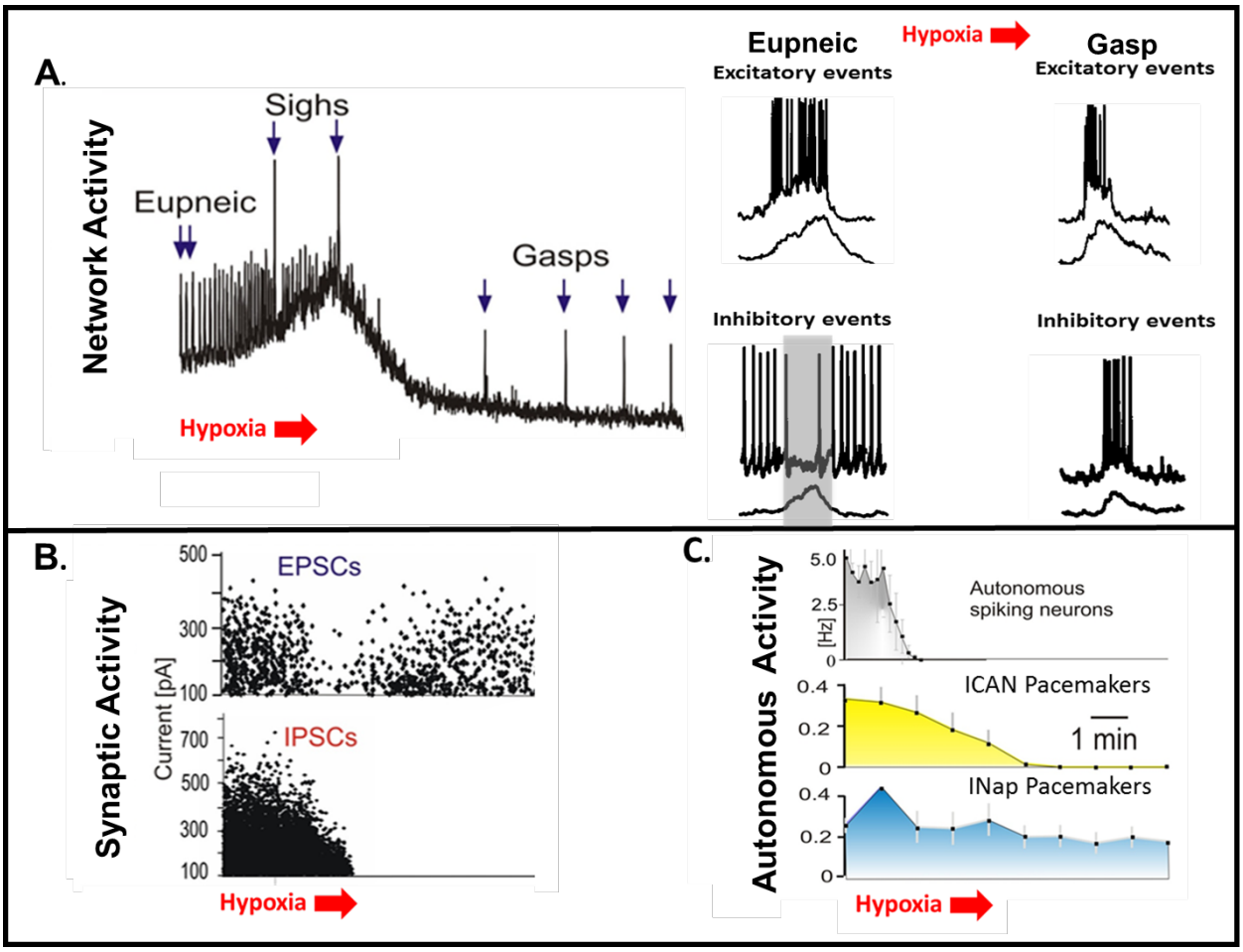

Figure 2. The effect of hypoxia on the preBötC. **A.** The respiratory network shows a biphasic response: An initial augmentation during which the respiratory frequency is enhanced and sighs are generated is followed by a depression during which the network reconfigures into gasping. **B.** Synaptic changes occur during the hypoxia-induced reconfiguration as exemplified by transient changes in synaptic excitation and a suppression of synaptic inhibition. **C.** Hypoxia alters bursting properties: it inhibits bursting properties that depend on the Ca^{2+}-activated nonspecific cation current (I_{CAN}), while bursting mechanisms that depend on the persistent sodium current (I_{Nap}) remain relatively unaffected.

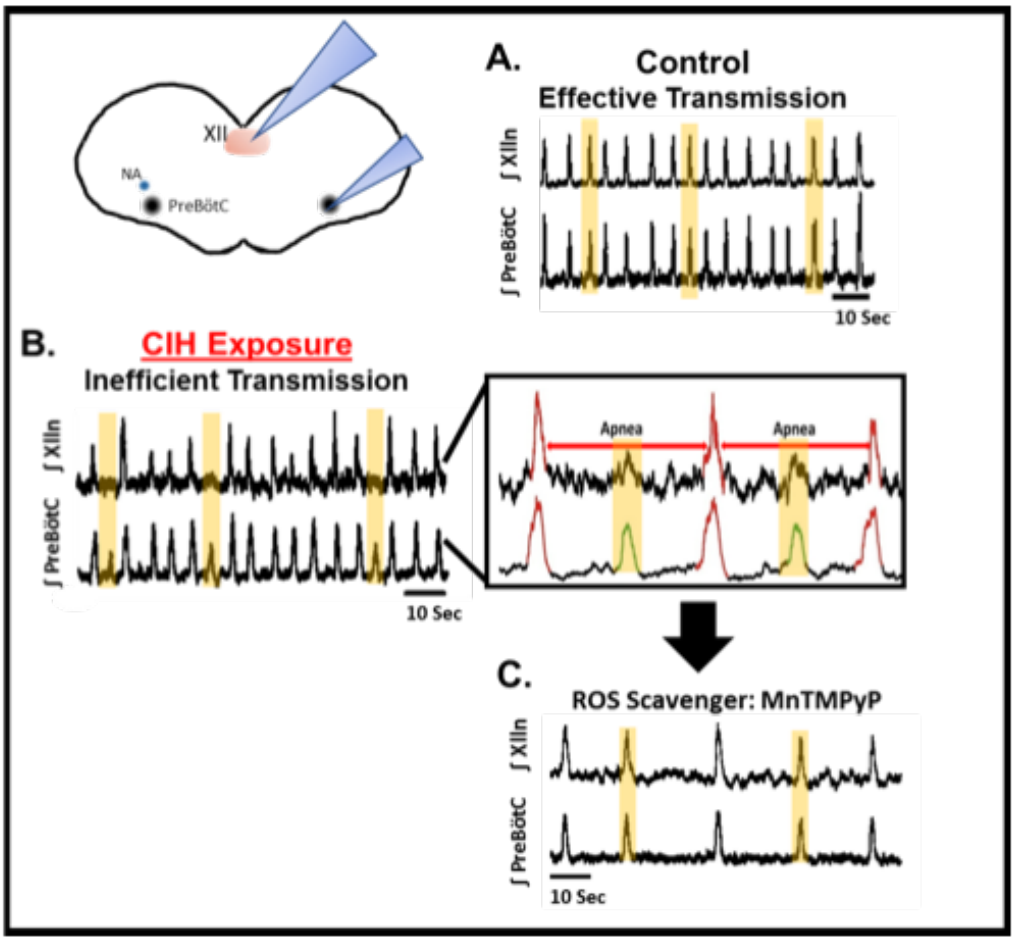

Figure 3. The effect of chronic intermittent hypoxia (CIH) on Respiratory Centers.

A and B. Integrated population recordings from the hypoglossal (XII, upper traces) and preBötC (lower traces) indicate that CIH exposure results in transmission failures reflected in the XII output. **C.** These transmission failures translate in “XII apneas” that are prevented by treatment with MnTMPyP.

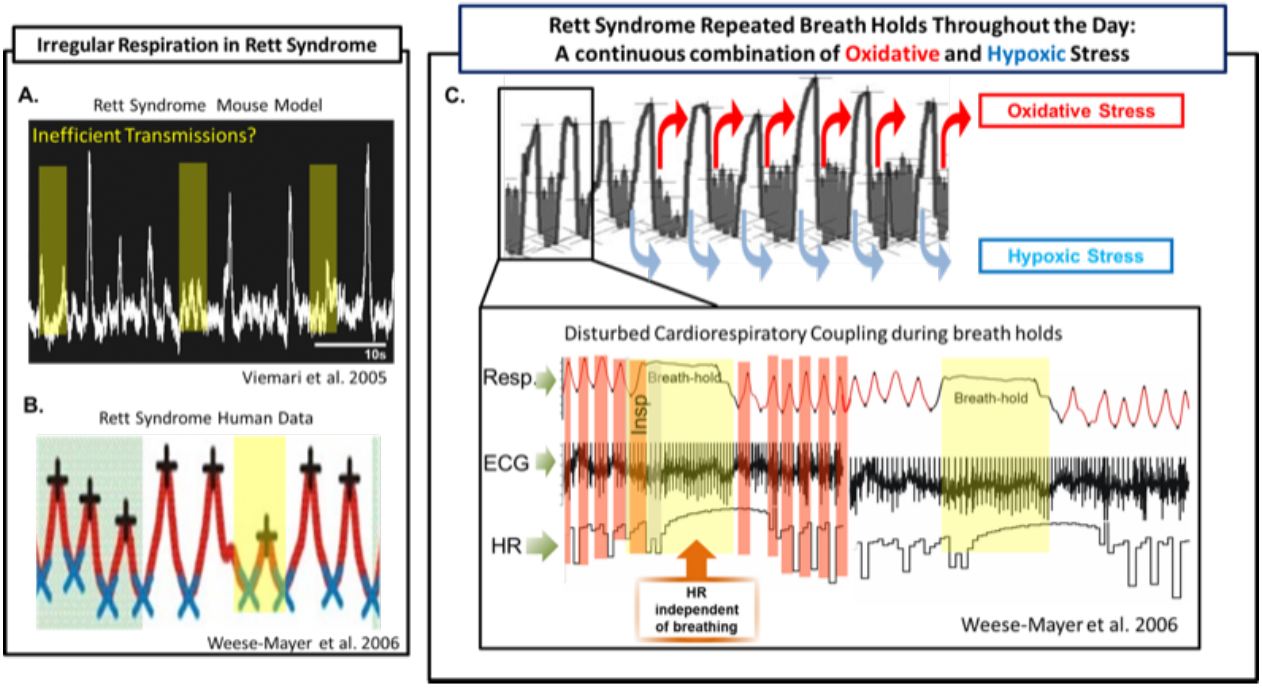

Figure 4. Respiratory Irregularities in Rett Syndrome. A. Slices obtained from a MeCP2 KO male mouse, a model for Rett Syndrome, show amplitude fluctuations in the integrated population recordings from the PreBötC that resemble those seen after CIH exposure. B. Human data from Rett Syndrome patients show large fluctuations in tidal volume. C. Breath holds during Rett Syndrome elicit oxidative and hypoxic stress. During these breath hold episodes cardiorespiratory coupling is compromised as the heart rate (HR) becomes independent from the breathing rhythm.

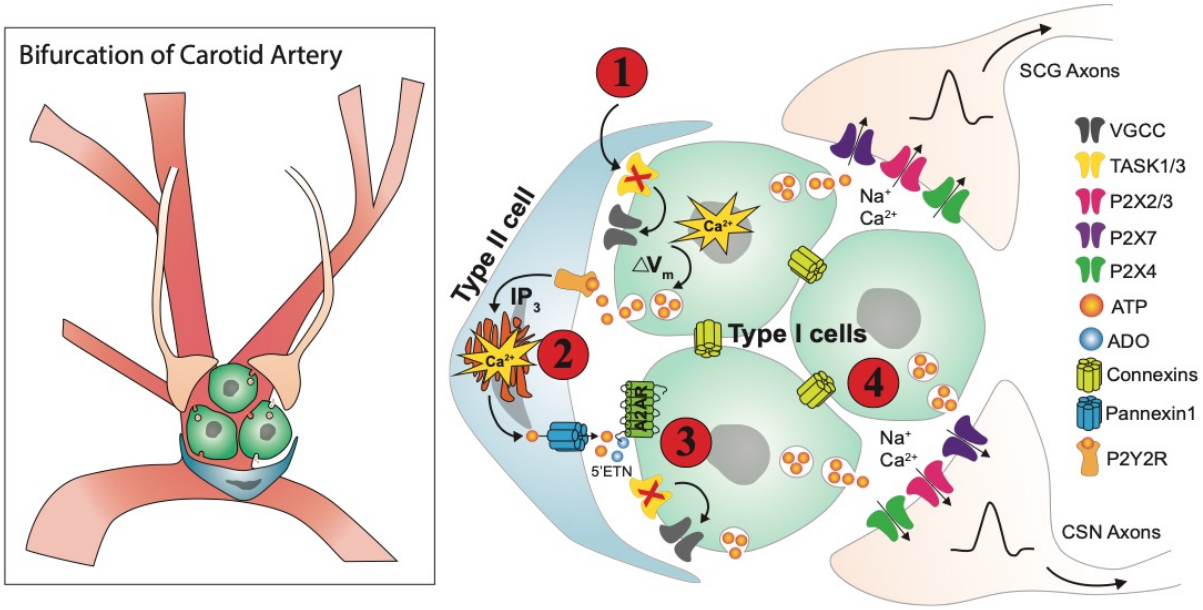

Figure 5. Illustration of the proposed mechanisms underlying chemosensitivity in the carotid bodies, located at the bifurcation of the aortic artery. Glomeruli are made up of Type I cells ensheathed by Type II cells, which relay changes in blood gas levels to the heart and brain through the petrosal ganglion and carotid sinus nerve. (1) Hypercapnia/H^+ or hypoxia trigger a rise in $[Ca^{2+}]_i$ in type I cells by inhibition of TASK1/3 K^+ channels, which is followed by a secondary increase in $[Ca^{2+}]_i$ in type II cells. (2) Type I cells depolarize, again creating an increase in $[Ca^{2+}]_i$ resulting in neuro/glial transmitter release, primarily ATP, binding to $P2Y_2R$ receptors in Type II cells and allowing ATP release through Pannexin-1 channels. ATP is broken down through 5'-endonucleotidase activity and converted to ADO, which (3) binds A2ARs on Type 1 cells. (4) This cascade creates a positive feedback loop, followed by Na^+/Ca^{2+} release from Type I cells that activates afferent/efferent axons through a variety of P2X channels. It has been hypothesized that the connexin family of gap junction channels may also play a role in facilitating electrical coupling (Murali *et al.*, 2014; Nurse, 2014; Murali & Nurse, 2016)

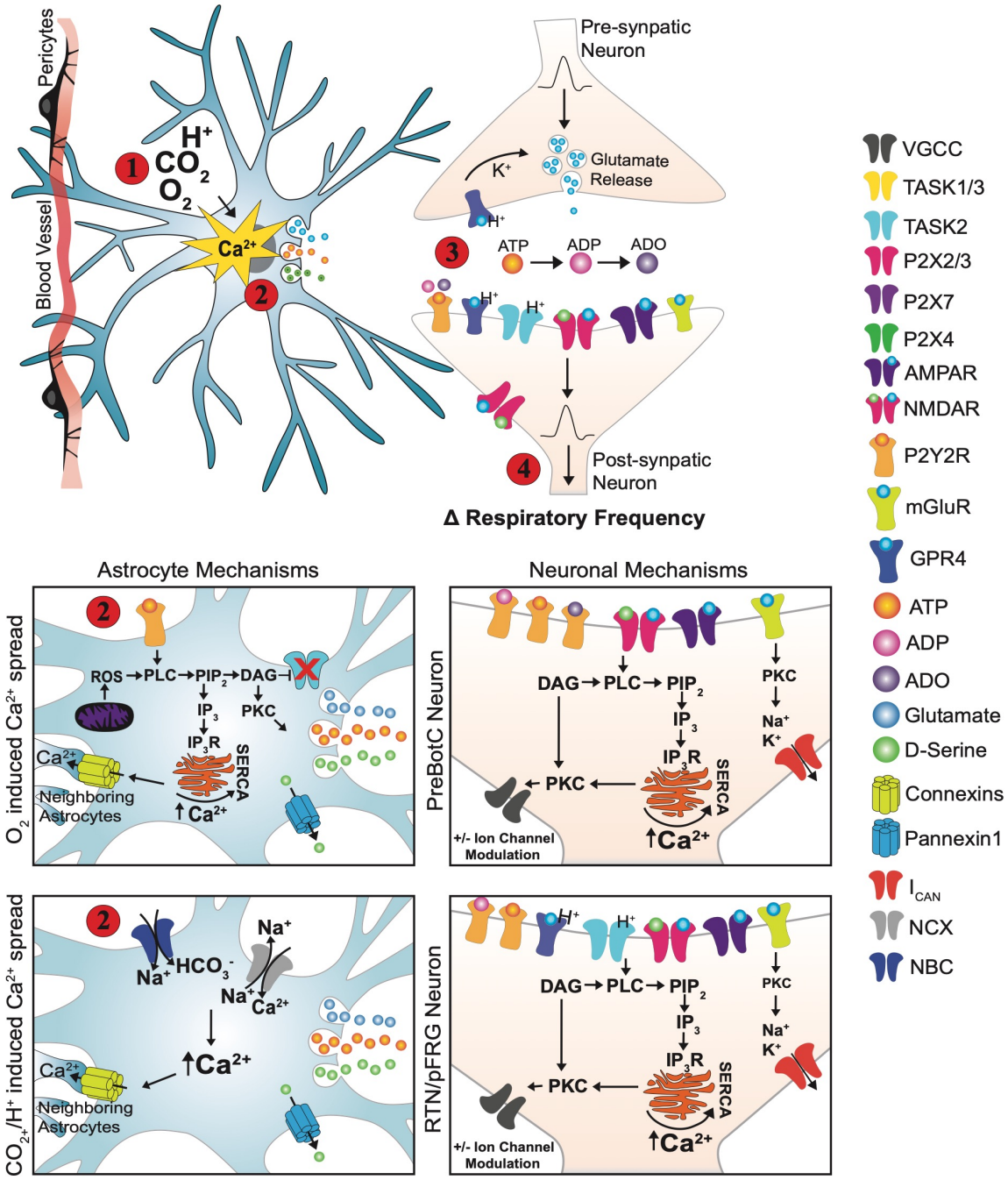

Figure 6. Illustration of the proposed mechanisms underlying sensitivity of the VRC to changes in blood gases. (1) Hypercapnia/H^+ or hypoxia triggers a cascade of events through which mitochondrial release of ROS or NBC/NCX transporters lead to a rise in $[Ca^{2+}]_i$ in astrocytes close to the ventral medullary surface near blood vessels (57, 59, 90, 254). (2) Increase in astrocytic $[Ca^{2+}]_i$ results in vesicular release of gliotransmitters, such as ATP (59, 227, 307), glutamate (252, 307), and D-serine (229). ATP release has been proposed to be facilitated by Connexin hemichannels (58, 304). (3) ATP and its derivatives (ADP and ADO (Zimmermann, 2001; Burnstock, 2006; Funk, 2013)), glutamate, and D-serine are released and bind to respective receptors on neurons (or ATP to P2YRs on other astrocytes, facilitating

$[Ca^{2+}]_i$ spread) (90, 229, 287). Different mechanisms have been proposed for responses of the preBötC and RTN/pFRG, where the RTN appears to respond to changes in astrocytic Ca^{2+} through $TASK_2$/P1YR activation (261, 267, 270, 286, 292) and preBötC neurons may respond by releasing glutamate that binds to NMDAR/AMPAR/mGluRs on the postsynaptic neuron or onto P2YRs on astrocytes. (4) Neuronal $[Ca^{2+}]_i$ release is then mediated by DAG/IP_3, further activating protein kinase C (PKC) to modulate ion channels, thereby altering respiratory frequency (263, 267).

References

1. Clarke, A. and H. Pörtner, *Temperature, metabolic power and the evolution of endothermy.* Biol Rev Camb Philos Soc, 2010. **85**(4): p. 703-727.
2. Ramirez, J., L.P. Folkow, and A. Blix, *Hypoxia Tolerance in Mammals and Birds: From the Wilderness to the Clinic.* Annual Reviews Physiology 2007. **69**: p. 113-143.
3. Raichle, M.E., et al., *A default mode of brain function* PNSA, 2001. **98**(2): p. 676-682.
4. Raichle, M.E., *The restless brain: how intrinsic activity organizes brain function* Philosophical Transactions of the Royal Society B, 2015. **370**(1668).
5. Mitra, A. and M. Raichle, *How networks communicate: propagation patterns in spontaneous brain activity.* Philos Trans R Soc Lond B Biol Sci, 2016. **371**(1705): p. pii: 20150546.
6. Semenza, G. and N. Prabhakar, *Neural regulation of hypoxia-inducible factors and redox state drives the pathogenesis of hypertension in a rodent model of sleep apnea.* J Appl Physiol, 1985. **119**(10): p. 1152-1156.
7. Haddad, G.G. and C. Jiang, *O2-Sensing Mechanisms in Excitable Cells: Role of Plpasma Membrane K+ Channels.* Annual Review of Physiology, 1997. **59**: p. 23-42.
8. D'Agostino, D.P., R.W. Putnam, and J.B. Dean, *Superoxide Production in CA1 Neurons of Rat Hippocampal Slices Exposed to Graded Levels of Oxygen* Journal of Neurophysiology, 2007. **98**: p. 1030-1041.
9. Huang, T., Y. Zou, and R. Corniola, *Oxidative stress and adult neurogenesis--effects of radiation and superoxide dismutase deficiency* Semin Cell Dev Biol, 2012. **23**(7): p. 738-744.
10. Popa-Wagner, A., et al., *ROS and brain disease: the good, the bad, and the ugly.* Oxid Med Cell Longev, 2013. **2013**(963520).
11. Igbal, M. and E. Eftekharpour, *Regulatory Role of Redox Balance in Determination of Neural Precursor Cell Fate.* Stem Cells Int, 2017. **2017**(9209127).
12. Mulkey, D.K., et al., *Oxygen measurements in brain stem slices exposed to normobaric hyperoxia and hyperbaric oxygen.* Journal of Applied Physiology, 2001. **90**(5): p. 1887-1899.
13. Clemens, S., et al., *A modulatory role for oxygen in shaping rhythmic motor output patterns of neuronal networks.* Respiration Physiology, 2001. **128**(3): p. 299-315.
14. Hill, A.A., et al., *Graded Reductions in Oxygenation Evoke Graded Reconfiguration of the Isolated Respiratory Network.* Journal of Neurophysiology, 2011. **105**(2): p. 625-639.
15. Filosa, J.A. and V.M. Blanco, *Neurovascular coupling in the mammalian brain.* Experimental Physiology, 2007. **92**(4): p. 641-646.
16. Ndunuizu, O. and J.C. LaManna, *Brain Tissue Oxygen Concentration Measurements.* Antioxidants and Redox Signaling, 2007. **9**(8): p. 1207-1219.
17. Kim, K., et al., *Vasculo-Neuronal Coupling: Retrograde Vascular Communication to Brain Neurons.* The Journal of Neuroscience, 2016. **36**(50): p. 12624-12639.

18. Iadecola, C., *The Neurovascular Unit Coming of Age: A Journey through Neurovascular Coupling in Health and Disease.* Neuron, 2017. **96**(1): p. 17-42.
19. Kisler, K., et al., *Cerebral blood flow regulation and neurovascular dysfunction in Alzheimer disease.* Nat Rev Neurosci, 2017. **18**(7): p. 419-434.
20. Roth, A. and M. Núñez, *Oligoendrocytes: Functioning in a Delicate Balance Between High Metabolic Requirements and Oxidative Damage.* Adv Exp Med Biol, 2016. **949**: p. 167-181.
21. Haddad, G. and C. Jiang, *Mechanisms of neuronal survival during hypoxia: ATP-sensitive K+ channels.* Biol Neonate, 1994. **65**(3-4): p. 160-165.
22. Björklund, O., et al., *Adenosine A1 and A3 receptors protect astrocytes from hypoxic damage.* Eur J Pharmacol, 2008. **596**(1-3): p. 6-13.
23. Bickler, P. and P. Donohoe, *Adaptive responses of vertebrate neurons to hypoxia.* J Exp Biol, 2002. **205**(pt 23): p. 3579-3586.
24. Garcia, A.J., 3rd, R.W. Putnam, and J.B. Dean, *Hyperoxic stimulation of synchronous orthodromic activity and induction of neural plasticity does not require changes in excitatory synaptic transmission.* J Appl Physiol (1985), 2010. **109**(3): p. 820-9.
25. Garcia, A.J., 3rd, R.W. Putnam, and J.B. Dean, *Hyperbaric hyperoxia and normobaric reoxygenation increase excitability and activate oxygen-induced potentiation in CA1 hippocampal neurons.* J Appl Physiol (1985), 2010. **109**(3): p. 804-19.
26. Mukandala, G., et al., *The Effects of Hypoxia and Inflammation on Synaptic Signaling in the CNS.* Brain Sci, 2016. **6**(1): p. pii: E6.
27. Lyubkin, M., D. Durand, and M. Haxhiu, *Interaction between tetanus long-term potentiation and hypoxia-induced potentiation in the rat hippocampus.* J Neurophysiol, 1997. **78**(5): p. 2475-2482.
28. Row, B., et al., *Intermittent hypoxia is associated with oxidative stress and spatial learning deficits in the rat.* Am J Respir Crit Care Med, 2003. **167**(11): p. 1548-1553.
29. Haddad, G. and C. Jiang, *Mechanisms of anoxia-induced depolarization in brainstem neurons: in vitro current and voltage clamp studies in the adult rat.* Brain Res, 1993. **625**(2): p. 261-268.
30. Fung, M. and G. Haddad, *Anoxia-induced depolarization in CA1 hippocampal neurons: role of Na+-dependent mechanisms.* Brain Res, 1997. **762**(1-2): p. 97-102.
31. Folklow, L., et al., *Remarkable neuronal hypoxia tolerance in the deep-diving adult hooded seal (Cystophora cristata).* Neurosci Lett, 2008. **446**(2-3): p. 147-150.
32. Mitz, S.A., et al., *When the brain goes diving: glial oxidative metabolism may confer hypoxia tolerance to the seal brain.* Neuroscience, 2009. **163**(2): p. 552-60.
33. Ramirez, J.M., et al., *Slow intrinsic oscillations in thick neocortical slices of hypoxia tolerant deep diving seals.* Neuroscience, 2011. **177**: p. 35-42.
34. Czech-Damal, N.U., et al., *The role of glycogen, glucose and lactate in neuronal activity during hypoxia in the hooded seal (Cystophora cristata) brain.* Neuroscience, 2014. **275**: p. 374-83.

35. Avshalumov, M.V., et al., *Endogenous hydrogen peroxide regulates the excitability of midbrain dopamine neurons via ATP-sensitive potassium channels.* J Neurosci, 2005. **25**(17): p. 4222-31.
36. Giniatullin, A.R. and R.A. Giniatullin, *Dual action of hydrogen peroxide on synaptic transmission at the frog neuromuscular junction.* J Physiol, 2003. **552**(Pt 1): p. 283-93.
37. MacFarlane, P.M. and G.S. Mitchell, *Respiratory long-term facilitation following intermittent hypoxia requires reactive oxygen species formation.* Neuroscience, 2008. **152**(1): p. 189-97.
38. MacFarlane, P.M., et al., *Reactive oxygen species and respiratory plasticity following intermittent hypoxia.* Respir Physiol Neurobiol, 2008. **164**(1-2): p. 263-71.
39. Kamsler, A. and M. Segal, *Hydrogen peroxide modulation of synaptic plasticity.* J Neurosci, 2003. **23**(1): p. 269-76.
40. Peng, Y.J., et al., *Induction of sensory long-term facilitation in the carotid body by intermittent hypoxia: implications for recurrent apneas.* Proc Natl Acad Sci U S A, 2003. **100**(17): p. 10073-8.
41. Peng, Y.J., et al., *NADPH oxidase is required for the sensory plasticity of the carotid body by chronic intermittent hypoxia.* J Neurosci, 2009. **29**(15): p. 4903-10.
42. Smith, J.C., et al., *Pre-Bötzinger Complex: A Brainstem Region That May Generate Respiratory Rhythm in Mammals.* Science 1991 **254**(5032): p. 726-729.
43. Lieske, S., et al., *Reconfiguration of the neural network controlling multiple breathing patterns: eupnea, sighs and gasps* Nature Neuroscience, 2000. **3**: p. 600-607.
44. Hayes, J.A., X. Wang, and C.A. Del Negro, *Cumulative lesioning of respiratory interneurons disrupts and precludes motor rhythms in vitro.* Proc Natl Acad Sci U S A, 2012. **109**(21): p. 8286-91.
45. Wang, X., et al., *Laser ablation of Dbx1 neurons in the pre-Bötzinger complex stops inspiratory rhythm and impairs output in neonatal mice.* Elife, 2014. **3**: p. e03427.
46. Schwarzacher, S.W., U. Rub, and T. Deller, *Neuroanatomical characteristics of the human pre-Botzinger complex and its involvement in neurodegenerative brainstem diseases.* Brain, 2011. **134**(Pt 1): p. 24-35.
47. Ramirez, J.M., *Reconfiguration of the respiratory network at the onset of locust flight.* J Neurophysiol, 1998. **80**(6): p. 3137-47.
48. Gray, P., et al., *Normal breathing requires preBötzinger complex neurokinin-1 receptor-expressing neurons.* Nature Neuroscience, 2001. **4**(9): p. 927-930.
49. Tan, W., et al., *Silencing preBötzinger complex somatostatin-expressing neurons induces persistent apnea in awake rat.* Nature Neuroscience, 2008. **11**(5): p. 538-540.
50. Peña, F., et al., *Differential contribution of pacemaker properties to the generation of respiratory rhythms during normoxia and hypoxia.* Neuron, 2004. **43**(1): p. 105-17.
51. Peña, F. and J.M. Ramirez, *Substance P-mediated modulation of pacemaker properties in the mammalian respiratory network.* J Neurosci, 2004. **24**(34): p. 7549-56.

52. Tryba, A.K., F. Peña, and J.-M. Ramirez, *Gasping Activity In Vitro: A Rhythm Dependent on 5-HT2A Receptors.* The Journal of Neuroscience, 2006. **26**(10): p. 2623-2634.
53. Nieto-Posadas, A., et al., *Change in network connectivity during fictive-gasping generation in hypoxia: prevention by a metabolic intermediate.* Front Physiol, 2014. **5**: p. 265.
54. Rivera-Angula, A. and F. Peña-Ortega, *Isocitrate supplementation promotes breathing generation, gasping, and autoresuscitation in neonatal mice.* J Neurosci Res, 2014. **92**(3): p. 375-388.
55. Lorea-Hernandez, J.J., et al., *Microglia modulate respiratory rhythm generation and autoresuscitation.* Glia, 2016. **64**(4): p. 603-19.
56. Peña-Ortega, F., *Neural Network Reconfigurations: Changes of the Respiratory Network by Hypoxia as an Example.* Adv Exp Med Biol, 2017. **1015**: p. 217-237.
57. Gourine, A.V., et al., *Astrocytes control breathing through pH-dependent release of ATP.* Science, 2010. **329**(5991): p. 571-5.
58. Huckstepp, R.T., et al., *CO2-dependent opening of connexin 26 and related β connexins.* Journal of Physiology, 2010. **588**(20): p. 3921-3931.
59. Angelova, P.R., et al., *Functional Oxygen Sensitivity of Astrocytes.* J Neurosci, 2015. **35**(29): p. 10460-73.
60. Ramirez, J.M., et al., *Selective lesioning of the cat pre-Botzinger complex in vivo eliminates breathing but not gasping.* J Physiol, 1998b. **507 (Pt 3)**: p. 895-907.
61. Wilken, B., et al., *Creatine protects the central respiratory network of mammals under anoxic conditions.* Pediatr Res, 1998. **43**(1): p. 8-14.
62. Telgkamp, P. and J.M. Ramirez, *Differential responses of respiratory nuclei to anoxia in rhythmic brain stem slices of mice.* J Neurophysiol, 1999. **82**(5): p. 2163-70.
63. Thoby-Brisson, M. and J.M. Ramirez, *Role of inspiratory pacemaker neurons in mediating the hypoxic response of the respiratory network in vitro.* J Neurosci, 2000. **20**(15): p. 5858-66.
64. Telgkamp, P., et al., *Long-term deprivation of substance P in PPT-A mutant mice alters the anoxic response of the isolated respiratory network.* J Neurophysiol, 2002. **88**(1): p. 206-13.
65. Peña, F. and J.M. Ramirez, *Hypoxia-induced changes in neuronal network properties.* Mol Neurobiol, 2005. **32**(3): p. 251-83.
66. Solomon, I.C., N.H. Edelman, and J.A. Neubauer, *Pre-Bötzinger Complex Functions as a Central Hypoxia Chemosensor for Respiration In Vivo.* Journal of Neurophysiology, 2000. **83**(5): p. 2854-2868.
67. Jiang, C. and G. Haddad, *A direct mechanism fo rsensing low oxygen levels by central neurons.* Proc Natl Acad Sci U S A, 1994. **91**(15): p. 7198-7201.

68. Donnelly, D., C. Jiang, and G. Haddad, *Comparative Responses of Brain Stem and Hippocampal Neurons to O2 Deprivation: In Vitro Intracellular Studies.* American Journal of Physiology 1992. **262**(5): p. L549-L554.
69. Jiang, C., S. Agulian, and G. Haddad, *Cl- and Na+ homeostasis during anoxia in rat hypoglossal neurons: intracellular and extracellular in vitro studies.* Journal of Physiology, 1992. **448**: p. 697-708.
70. Donnelly, D.F., et al., *Time course of alterations in pre- and post-synaptic chemoreceptor function during developmental hyperoxia.* Respir Physiol Neurobiol, 2009. **168**(3): p. 189-97.
71. Sun, M.K., I.T. Jeske, and D.J. Reis, *Cyanide excites medullary sympathoexcitatory neurons in rats.* American Journal of Physiology, 1992. **262**(2): p. R182-R189.
72. Sun, M.K. and D.J. Reis, *Dopamine or transmitter release from rat carotid body may not be essential to hypoxic chemoreception* American Journal of Physiology, 1994. **267**(6 pt 2): p. R1632-9.
73. Trapp, S. and K. Ballanyi, *KATP channel mediation of anoxia-induced outward current in rat dorsal vagal neurons in vitro.* Journal of Physiology, 1995. **15**(487): p. 37-50.
74. Kulik, A., et al., *Chemical anoxia activates ATP-sensitive and blocks Ca(2+) dependent K(+) channels in rat dorsal vagal neurons in situ.* Neuroscience, 2002. **110**(3): p. 541-554.
75. Ballanyi, K., *Protective role of neuronal KATP channels in brain hypoxia.* Journal of Experimental Biology 2004. **207**(Pt 18): p. 3201-3212.
76. Balfour, R. and S. Trapp, *Ionic currents underlying the response of rat dorsal vagal neurons to hypoglycaemia and chemical anoxia.* Journal of Physiology, 2007. **15**(579): p. 691-702.
77. Dyavanapalli, J., et al., *Chronic intermittent hypoxia-hypercapnia blunts heart rate responses and alters neurotransmission to cardiac vagal neurons.* Journal of Physiology, 2014. **592**(13).
78. Prabhakhar, N.R., *Sensing hypoxia: physiology, genetics and epigenetics.* Journal of Physiology, 2013. **591**(9): p. 2245-2257.
79. Nurse, C., *Synaptic and paracrine mechanisms at carotid body arterial chemoreceptors.* 592, 2014. **16**(3419-3426).
80. Nanduri, J., et al., *Hypoxia-inducible factors and hypertension: lessons from sleep apnea syndrome.* J Mol Med (Berl), 2015. **93**(5): p. 473-80.
81. Prabhakhar, N.R. and Y.J. Peng, *Oxygen Sensing by the Carotid Body: Past and Present.* Adv Exp Med Biol, 2017. **977**: p. 3-8.
82. Rakoczy, R. and C. Wyatt, *Acute oxygen sensing by the carotid body: a rattlebag of molecular mechanisms* Journal of Physiology, 2017.
83. Basting, T., et al., *Is plasticity within the retrotrapezoid nucleus responsible of the PCO2 set-point after carotid body denervation in rats? .* Journal of Physiology, 2016. **594**(12): p. 3371-3390.

84. Wilson, R. and L. Teppema, *Integration of Central and Peripheral Respiratory Chemoreflexes.* Compr Physiol, 2016. **6**(2): p. 1005-10041.
85. Guyenet, P., et al., *Interdependent feedback regulation of breathing by the carotid bodies and the retrotrapezoid nucleus.* Journal of Physiology, 2017.
86. Smith, C., et al., *An interdependent model of central/peripheral chemoreception: evidence and implications for ventilatory control.* 173, 2010. **3**(288-297).
87. Bissonnette, J.M., *Mechanisms regulating hypoxic respiratory depression during fetal and postnatal life.* American Journal of Regulatory Integrative Comparative Physiology, 2000. **278**(6): p. R1391-R1400.
88. Moss, I.R., *Respiratory responses to single and episodic hypoxia during development: mechanisms of adaption.* Respiration Physiology, 2000. **121**: p. 185-197.
89. Teppema, L.J. and A. Dahan, *The Ventilatory Response to Hypoxia in Mammals: Mechanisms, Measurement, and Analysis* Physiological Reviews, 2010. **90**(2): p. 675-754.
90. Rajani, V., et al., *Release of ATP by preBotzinger complex astrocytes contributes to the hypoxic ventilatory response via a Ca2+ -dependent P2Y1 receptor mechanism.* J Physiol, 2017.
91. Bureau, M.A., et al., *Postnatal maturation of respiration in intact and carotid body-demodenervated lambs.* Journal of Applied Physiology, 1985. **59**(3): p. 869-874.
92. Wang, W., et al., *Characterizations and comparisons of eupnoea and gasping in neonatal rats.* The Journal of Physiology, 1996. **490**(1): p. 277-292.
93. Izumizaki, M., M. Pokorski, and I. Homma, *Role of the carotid bodies in chemosensory ventilatory responses in the anesthetized mouse.* Journal of Applied Physiology, 2004. **97**(4): p. 1401-1407.
94. Moyer, C. and H. Beecher, *Effects of Barbiturate Anesthesia (Evipal and Penthothal Sodium) upon the Integration of Respiratory Control Mechanisms. A Study Directed Toward Improvement of Methods for the Preclinical Evaluation of Anesthetic Agents.* Journal of Clinical Investigation 1942. **21**(4): p. 429-445.
95. Miller, M. and S. Tenney, *Hypoxia-induced tachypnea in carotid-deafferented cats.* Respiration Physiology, 1975. **23**(1): p. 31-39.
96. Richter, D.W., et al., *Response of the medullary respiratory network of the cat to hypoxia.* J Physiol, 1991. **443**: p. 231-56.
97. Engwall, M., et al., *Ventilatory afterdischarge and central respiratory drive interactions in the awake goat.* Journal of Applied Physiology, 1985. **76**(1): p. 416-423.
98. Smith, C., et al., *Effects of specific carotid body and brain hypoxia on respiratory muscle control in the awake goat.* Journal of Physiology, 1993. **460**: p. 623-640.
99. Curran, A., et al., *Ventilatory resonses to specific CNS hypoxia in sleeping dogs.* Journal of Applied Physiology, 2000. **88**(5): p. 1840-1852.

100. Holton, P. and J.B. Wood, *The Effects of Bilateral Removal of the Carotid Bodies and Denervation of the Carotid Sinuses in Two Human Subjects.* Journal of Physiology, 1965. **553 (pt 1)**: p. 3-11.
101. Marschke, G., G.N. Beall, and E.W. Stern, *Carotid-Body Removal in Asthma.* JAMA 1965. **191**(5).
102. Wood, J.B., A.W. Frankland, and H.H. Eastcott, *Bilateral removal of carotid bodies for asthma.* Thorax, 1965. **20**(6): p. 570-573.
103. Toorop, R.J., et al., *Clinical Results of Carotid Denervation by Adventitial Stripping in Carotid Sinus Syndrome.* Eurpeon Journal of Vascular Endovascular Surgery, 2010. **39**(2): p. 146-152.
104. Fitzgerald, R., *Carotid body: a new target for rescuing neural control of cardiorespiratory balance in disease.* Frontiers in Physiology, 2014. **5**(304).
105. Gourine, A.V. and G.D. Funk, *On the existence of a central respiratory oxygen sensor.* Journal of Applied Physiology, 2017. **123**(5): p. 1344-1349.
106. Iturriaga, R., *Translating carotid body function into clinical medicine.* J Physiol, 2017.
107. Wilson, R., J. Remmers, and J. Paton, *Brain stem PO(2) and pH of the working heart-brain stem preparation during vascular perfusion with aqueous medium* American Journal of Regulatory, Integrative, and Comparative Physiology 2001. **281**(2): p. R528-R538.
108. Brockhaus, J., et al., *Microenvironment of respiratory neurons in the in vitro brainstem-spinal cord of neonatal rats.* Journal of Physiology, 1993. **462**: p. 421-445.
109. Okada, Y., K. Mückenhoff, and P. Scheid, *Hypercapnia and medullary neurons in the isolated brain stem-spinal cord of the rat.* Respiration Physiology, 1993. **93**(3): p. 327-336.
110. Bingmann, D. and G. Kolde, *PO2-profiles in hippocampal slices of the guinea pig.* Experimental Brain Research 1982. **48**(1): p. 89-96.
111. Jiang, C., S. Agulian, and G. Haddad, *O2 tension in adult and neonatal brain slices under several experimental conditions.* Brain Research 1991. **568**(1-2): p. 159-164.
112. Fong, A., et al., *Respiratory rhythm of brainstem-spinal cord preparations: Effects of maturation, age, mass and oxygenation.* Respiration Physiology Neurobiology 2008. **164**(3): p. 429-440.
113. Gourevitch, B. and N. Mellen, *The preBotzinger complex as a hub for network activity along the ventral respiratory column in the neonate rat.* Neuroimage, 2014. **98**: p. 460-74.
114. Anderson, T.M. and J.M. Ramirez, *Respiratory rhythm generation: triple oscillator hypothesis.* F1000Res, 2017. **6**: p. 139.
115. Ballanyi, K. and A. Ruangkittisakul, *Structure-function analysis of rhythmogenic inspiratory pre-Botzinger complex networks in "calibrated" newborn rat brainstem slices.* Respir Physiol Neurobiol, 2009. **168**(1-2): p. 158-78.
116. Burke, P., et al., *State-dependent control of breathing by the retrotrapezoid nucleus.* Journal of Physiology, 2015. **593**(13): p. 2909-2026.

117. Guyenet, P.G. and D.A. Bayliss, *Neural control of breathing and CO2 homeostasis.* Neuron, 2015. **87**(5): p. 946-961.
118. Guyenet, P., et al., *Proton detection and breathing regulation by the retrotrapezoid nucleus.* Journal of Physiology, 2016. **594**(6): p. 1529-1551.
119. Bouvier, J., et al., *Hindbrain interneurons and axon guidance signaling critical for breathing.* Nat Neurosci, 2010. **13**(9): p. 1066-74.
120. Gray, P.A., et al., *Developmental origin of preBotzinger complex respiratory neurons.* J Neurosci, 2010. **30**(44): p. 14883-95.
121. Cui, Y., et al., *Defining preBotzinger Complex Rhythm- and Pattern-Generating Neural Microcircuits In Vivo.* Neuron, 2016. **91**(3): p. 602-14.
122. Ramirez, J.M., U.J. Quellmalz, and B. Wilken, *Developmental changes in the hypoxic response of the hypoglossus respiratory motor output in vitro.* J Neurophysiol, 1997. **78**(1): p. 383-92.
123. Janczewski, W.A., et al., *Role of inhibition in respiratory pattern generation.* J Neurosci, 2013. **33**(13): p. 5454-65.
124. Sherman, D., et al., *Optogenetic perturbation of preBötzinger complex inhibitory neurons modulates respiratory pattern.* Nature Neuroscience, 2015. **18**(3): p. 408-414.
125. Viemari, J.-C. and J.-M. Ramirez, *Norepinheprine differentially modulates different types of respiratory pacemaker and nonpacemaker neurons.* Journal of Neurophysiology, 2006. **95**: p. 2070-2082.
126. Morgado-Valle, C., S.M. Baca, and J.L. Feldman, *Glycinergic pacemaker neurons in preBotzinger complex of neonatal mouse.* J Neurosci, 2010. **30**(10): p. 3634-9.
127. Carroll, J.L. and A. Agarwal, *Development of ventilatory control in infants.* Paediatr Respir Rev, 2010. **11**(4): p. 199-207.
128. Thoby-Brisson, M. and J.M. Ramirez, *Identification of two types of inspiratory pacemaker neurons in the isolated respiratory neural network of mice.* J Neurophysiol, 2001. **86**(1): p. 104-12.
129. Crowder, E., et al., *Phosphatidylinositol 4,5-bisphosphate regulates inspiratory burst activity in the neonatal mouse preBötzinger complex.* Journal of Physiology, 2007. **582**(pt 3): p. 1047-1058.
130. Rubin, J.E., et al., *Calcium-activated nonspecific cation current and synaptic depression promote network-dependent burst oscillations.* Proc Natl Acad Sci U S A, 2009. **106**(8): p. 2939-44.
131. Del Negro, C.A., J.A. Hayes, and J.C. Rekling, *Dendritic calcium activity precedes inspiratory bursts in preBotzinger complex neurons.* J Neurosci, 2011. **31**(3): p. 1017-22.
132. Dunmyre, J.R., C.A. Del Negro, and J.E. Rubin, *Interactions of persistent sodium and calcium-activated nonspecific cationic currents yield dynamically distinct bursting regimes in a model of respiratory neurons.* J Comput Neurosci, 2011. **31**(2): p. 305-28.

133. Viemari, J.C., et al., *Activation of alpha-2 noradrenergic receptors is critical for the generation of fictive eupnea and fictive gasping inspiratory activities in mammals in vitro.* Eur J Neurosci, 2011. **33**(12): p. 2228-37.
134. Paton, J.F., et al., *Respiratory rhythm generation during gasping depends on persistent sodium current.* Nat Neurosci, 2006. **9**(3): p. 311-3.
135. Poets, C., et al., *Gasping and other cardiorespiratory patterns during sudden infant deaths.* Pediatr Res, 1999. **45**(3): p. 350-354.
136. Garcia, A.J., 3rd, J.E. Koschnitzky, and J.M. Ramirez, *The physiological determinants of Sudden Infant Death Syndrome.* Respiratory Physiology and Neurobiology, 2013. **189**(2): p. 288-300.
137. Broadbelt, K., et al., *Brainstem deficiency of the 14-3-3 regulator of serotonin synthesis: a proteomics analysis in the sudden infant death syndrome.* Mol Cell Proteomics, 2012. **11**(1): p. M111.009530.
138. Massey, C., et al., *Development of brainstem 5-HT1A receptor-binding sites in serotonin-deficient mice.* J Neurochem, 2013. **126**(6): p. 749-757.
139. Rognum, I., et al., *Serotonin metabolites in the cerebrospinal fluid in sudden infant death syndrome.* J Neuropathol Exp Neurol, 2014. **73**(2): p. 115-122.
140. Haynes, R., et al., *Serotonin Receptors in the Medulla Oblongata of the Human Fetus and Infant: The Analytic Approach of the International Safe Passage Study.* N Neuropathol Exp Neurol, 2016.
141. Haynes, R., et al., *High serum serotonin in sudden infant death syndrome.* Proc Natl Acad Sci U S A, 2017. **114**(29): p. 7695-7700.
142. Bright, F.M., et al., *Medullary Serotonin Neuron Abnormalities in an Australian Cohort of Sudden Infant Death Syndrome.* Journal of Neuropathology and Experimental Neurology, 2017. **76**(10): p. 864-873.
143. Janczewski, W. and J.L. Feldman, *Distinct rhythm generators for inspiration and expiration in the juvenile rat.* Journal of Physiology, 2006. **570**(pt 2): p. 407-420.
144. Pagliardini, S., et al., *Active expiration induced by excitation of ventral medulla in adult anesthetized rats.* J Neurosci, 2011. **31**(8): p. 2895-905.
145. Huckstepp, R.T., et al., *Interactions between respiratory oscillators in adult rats.* Elife, 2016. **5**.
146. Anderson, T.M., et al., *A novel excitatory network for the control of breathing.* Nature, 2016. **536**(7614): p. 76-80.
147. Ramirez, J.M., et al., *The hypoxic response of neurones within the in vitro mammalian respiratory network.* J Physiol, 1998a. **507 (Pt 2)**: p. 571-82.
148. Richter, D.W. and J.C. Smith, *Respiratory rhythm generation in vivo.* Physiology (Bethesda), 2014. **29**(1): p. 58-71.

149. Schmidt, C., M.C. Bellingham, and D.W. Richter, *Adenosinergic modulation of respiratory neurones and hypoxic responses in the anaesthetized cat.* J Physiol, 1995. **483 (Pt 3)**: p. 769-81.
150. Michiels, C., *Physiological and pathological responses to hypoxia.* Am J Pathol, 2004. **164**(6): p. 1875-82.
151. Weese-Mayer, D.E., et al., *Familial dysautonomia: frequent, prolonged and severe hypoxemia during wakefulness and sleep.* Pediatr Pulmonol, 2008. **43**(3): p. 251-60.
152. Carroll, M.S., et al., *Respiratory and cardiovascular indicators of autonomic nervous system dysregulation in familial dysautonomia.* Pediatr Pulmonol, 2012. **47**(7): p. 682-91.
153. Weese-Mayer, D.E., et al., *Autonomic nervous system dysregulation: breathing and heart rate perturbation during wakefulness in young girls with Rett syndrome.* Pediatr Res, 2006. **60**(4): p. 443-9.
154. Weese-Mayer, D., et al., *Autonomic dysregulation in young girls with Rett Syndrome during nighttime in-home recordings.* Pediatr Pulmonol, 2008. **43**(11): p. 1045-1060.
155. Schüle, B., et al., *Severe congenital encephalopathy caused by MECP2 null mutations in males: central hypoxia and reduced neuronal dendritic structure.* Clin Genet, 2008. **74**(2): p. 116-126.
156. Janc, O., et al., *Systemic Radical Scavenger Treatment of a Mouse Model of Rett Syndrome: Merits and Limitations of the Vitamin E Derivative Trolox.* Front Cell Neurosci, 2016. **10**(266).
157. Brown, G. and M. Squier, *Neuropathology and pathogenesis of mitochondrial diseases.* J Inherit Metab Dis, 1996. **19**(4): p. 553-572.
158. Quintana, A., et al., *Fatal breathing dysfunction in a mouse model of Leigh syndrome.* J Clin Invest, 2012. **122**(7): p. 2359-68.
159. Herst, P., et al., *Functional Mitochondria in Health and Disease.* Front Endocrinol (Lausanne), 2017. **8**(296).
160. Cohen-Gadol, A., M. DiLuna, and D. Spencer, *Partial epilepsy presenting as episodic dyspnea: a specific network involved in limbic seizure propagation. Case report.* J Neurosurg, 2004. **100**(3): p. 565-567.
161. Farrell, J., et al., *Postictal behavioural impairments are due to a severe prolonged hypoperfusion/hypoxia event that is COX-2 dependent.* Elife, 2016. **5**.
162. Semenza, G. and N.R. Prabhakar, *HIF-1-dependent respiratory, cardiovascular, and redox responses to chronic intermittent hypoxia.* Antioxidants and Redox Signaling, 2007. **9**(9): p. 1391-1396.
163. Nanduri, J., et al., *Transcriptional Responses to Intermittent Hypoxia.* Respiratory Physiology and Neurobiology, 2008. **164**(0): p. 277-281.
164. Nanduri, J., et al., *HIF-1 α Activation by Intermittent Hypoxia Requires NADPH Oxidase Stimulation by Xanthine Oxidase.* PLoS One 2015. **10**(3): p. 1-12.

165. Prabhakhar, N.R. and G.L. Semenza, *Regulation of carotid body oxygen sensing by hypoxia-inducible factors.* Pflugers Arch, 2016. **468**(1): p. 71-5.
166. Sunderram, J., et al., *Heme oxygenase-1-dependent central cardiorespiratory adaptations to chronic intermittent hypoxia in mice.* J Appl Physiol (1985), 2016. **121**(4): p. 944-952.
167. Garcia, A.J., 3rd, et al., *Chronic Intermittent Hypoxia Alters Local Respiratory Circuit Function at the Level of the preBotzinger Complex.* Front Neurosci, 2016. **10**: p. 4.
168. Garcia, A.J., 3rd, et al., *Chronic Intermittent Hypoxia Differentially Impacts Different States of Inspiratory Activity at the Level of the preBotzinger Complex.* Front Physiol, 2017. **8**: p. 571.
169. Ramirez, J., et al., *Central and peripheral factors contributing to obstructive sleep apneas.* Respiratory Physiology and Neurobiology, 2013. **189**(2): p. 344-353.
170. Viemari, J.-C., et al., *Mecp2 Deficiency Disrupts Norepinephrine and Respiratory Systems in Mice.* The Journal of Neuroscience, 2005. **25**(50): p. 11521-11530.
171. De Felice, C., et al., *Oxidative brain damage in Mecp2-mutant murine models of Rett syndrome.* Neurobiol Dis, 2014. **68**: p. 66-77.
172. De Felice, C., et al., *The role of oxidative stress in Rett syndrome: an overview.* Ann N Y Acad Sci, 2012. **1259**: p. 121-135.
173. Janc, O.A. and M. Muller, *The free radical scavenger Trolox dampens neuronal hyperexcitability, reinstates synaptic plasticity, and improves hypoxia tolerance in a mouse model of Rett syndrome.* Front Cell Neurosci, 2014. **8**: p. 56.
174. Ciccoli L, D.F.C., Leoncini S, Signorini C, Cortelazzo A, Zollo G, Pecorelli A, Rossi M, Hayek J., *Red blood cells in Rett syndrome: oxidative stress, morphological changes and altered membrane organization.* Biol Chem, 2015. **396**(11): p. 1233-1240.
175. Filosa, S., et al., *Exploring the possible link between MeCP2 and oxidative stress in Rett syndrome.* Free Radic Biol Med, 2015. **88**(pt A): p. 81-90.
176. Pecorelli, A., et al., *OxInflammation in Rett syndrome.* Int J Biochem Cell Biol, 2016. **81**(Pt B): p. 246-253.
177. Kline, D., *Chronic intermittent hypoxia affects integration of sensory input by neurons in the nucleus tractus solitarii.* Respir Physiol Neurobiol, 2010. **174**(1-2): p. 29-36.
178. de Paula, P., G. Tolstykh, and S. Mifflin, *Chronic intermittent hypoxia alters NMDA and AMPA-evoked currents in NTS neurons receiving carotid body chemoreceptor inputs.* Am J Physiol Regul Integr Comp Physiol, 2007. **292**(6): p. R2259-R2265.
179. Kline, D., A. Ramirez-Navarro, and D. Kunze, *Adaptive depression in synaptic transmission in the nucleus of the solitary tract after in vivo chronic intermittent hypoxia: evidence for homeostatic plasticity.* J Neurosci, 2007. **27**(17): p. 4663-4673.

180. Kline, D., et al., *Dopamine inhibits N-type channels in visceral afferents to reduce synaptic transmitter release under normoxic and chronic intermittent hypoxic conditions.* Journal of Neurophysiology, 2009. **101**(5): p. 2270-2278.
181. Zhang, W., et al., *Chronic sustained and intermittent hypoxia reduce function of ATP-sensitive potassium channels in nucleus of the solitary tract.* Am J Physiol Integr Comp Physiol, 2008. **295**(5): p. R1555-R1562.
182. Costa-Silva, J., D. Zoccal, and B. Machado, *Chronic intermittent hypoxia alters glutamatergic control of sympathetic and respiratory activities in the commissural NTS of rats.* Am J Physiol Regul Integr Comp Physiol, 2012. **302**(6): p. R785-793.
183. Shell, B., K. Faulk, and J.T. Cunningham, *Neural Control of Blood Pressure in Chronic Intermittent Hypoxia.* Curr Hypertens Rep, 2016. **18**(3): p. 19.
184. Almado, C., B. Machado, and R. Leão, *Chronic intermittent hypoxia depresses afferent neurotransmission in NTS neurons by a reduction in the number of active synapses.* The Journal of Neuroscience, 2012. **32**(47): p. 16736-16746.
185. Moreau, J. and J. Ciriello, *Chronic intermittent hypoxia induces chnages in expression of synaptic proteins in the nucleus of the solitary tract.* Brain Research, 2015. **1622**: p. 300-307.
186. Moraes, D., et al., *Respiratory Network Enhances the Sympathoinhibitory Component of Baroreflex of Rats Submitted to Chronic Intermittent Hypoxia.* Hypertension, 2016. **68**(4): p. 1021-1030.
187. Moraes, D., et al., *Electrophysiological properties of rostral ventrolateral medulla presympathetic neurons modulated by the respiratory network in rats.* The Journal of Neuroscience, 2013. **33**(49): p. 19223-19237.
188. Souza, G., et al., *Inspiratory modulation of sympathetic activity is increased in female rats exposed to chronic intermittent hypoxia.* Exp Physiol, 2016. **101**(11): p. 1345-1358.
189. Souza, G., et al., *Sex differences in the respiratory-sympathetic coupling in rats exposed to chronic intermittent hypoxia.* Respir Physiol Neurobiol, 2017.
190. Machado, B., D. Zoccal, and D. Moraes, *Neurogenic hypertension and the secrets of respiration.* Am J Physiol Regul Integr Comp Physiol, 2017. **312**(6): p. R864-R872.
191. Dempsey, B., et al., *Mapping and Analysis of the Connectome of Sympathetic Premotor Neurons in the Rostral Ventrolateral Medulla of the Rat Using a Volumetric Brain Atlas.* Front Neural Circuits, 2017. **11**: p. 9.
192. Dergacheva, O., et al., *Respiratory modulation of premotor cardiac vagal neurons in the brainstem.* Respiratory Physiology and Neurobiology, 2010. **174**(1-2): p. 102-110.
193. Frank, J.G. and D. Mendelowitz, *Synaptic and intrinsic activation of GABAergic neurons in the cardiorespiratory brainstem network.* PLoS One, 2012. **7**(5): p. e36459.

194. Navarrete-Opazo, A. and G. Mitchell, *Therapeutic potential of intermittent hypoxia: a matter of dose* Am J Physiol Regul Integr Comp Physiol, 2014. **307**(10): p. R1181-R1197.
195. Wilkerson, J., M. Devinney, and G. Mitchell, *Intermittent but not sustained moderate hypoxia elicits long-term facilitation of hypoglossal motor output.* Respir Physiol Neurobiol, 2017. **pii: S1569-9048**(17): p. 30221-30225.
196. Edge, D. and K. O'Halloran, *Chronic Intermittent Hypoxia Blunts the Expression of Ventilatory Long Term Facilitation in Sleeping Rats.* Adv Exp Med Biol, 2015. **860**: p. 335-342.
197. Dougherty, B., et al., *Daily acute intermittent hypoxia improves breathing function with acute and chronic spinal injury via distinct mechanisms.* Respir Physiol Neurobiol, 2017. **pii: S1569-9048**(16).
198. Fuller, D. and G. Mitchell, *Respiratory neuroplasticity- Overview, significance and future directions.* Exp Neurol, 2017. **287**(pt 2): p. 144-152.
199. Dale, E., F. Ben Mabrouk, and G. Mitchell, *Unexpected benefits of intermittent hypoxia: enhanced respiratory and nonrespiratory motor function.* Physiology (Bethesda), 2014. **29**(1): p. 39-48.
200. Fields, D. and G. Mitchell, *Spinal metaplasticity in respiratory motor control.* Front Neural Circuits, 2015. **9**(2).
201. Gonzalez-Rothi, E., et al., *Intermittent hypoxia and neurorehabilitation.* J Appl Physiol, 2015. **119**(12): p. 1455-1465.
202. Trumbower, R.D., et al., *Exposure to acute intermittent hypoxia augments somatic motor function in humans with incomplete spinal cord injury.* Neurorehabil Neural Repair, 2012. **26**(2): p. 163-72.
203. Vinit, S., J. Windelborn, and G. Mitchell, *Lipopolysaccharide attenuates phrenic long-term facilitation following acute intermittent hypoxia.* Respir Physiol Neurobiol, 2011. **176**(3): p. 130-135.
204. Huxtable, A., et al., *Intermittent Hypoxia-Induced Spinal Inflammation Impairs Respiratory Motor Plasticity by a Spinal p38 MAP Kinase-Dependent Mechanism.* J Neurosci, 2015. **35**(17): p. 6871-6880.
205. Huxtable, A.G., et al., *Systemic LPS induces spinal inflammatory gene expression and impairs phrenic long-term facilitation following acute intermittent hypoxia.* J appl Physiol (1985), 2013. **114**(7): p. 879-887.
206. Agosto-Marlin, I., N. Nichols, and G. Mitchell, *Adenosine-dependent phrenic motor facilitation is inflammation resistant.* J Neurophysiol, 2017. **117**(2): p. 836-845.
207. Gresham, K., et al., *Airway inflammation and central respiratory control: results from in vivo and in vitro neonatal rat.* Respir Physiol Neurobiol, 2011. **178**(3): p. 414-421.
208. Jafri, A., et al., *Lung inflammation induces IL-1β expression in hypoglossal neurons in rat brainstem.* Respir Physiol Neurobiol, 2013. **188**(1): p. 21-28.

209. Ribeiro, A., et al., *Intratracheal LPS administration attenuates the acute hypoxic ventilatory response: Role of brainstem IL-1β receptors.* Respir Physiol Neurobiol, 2017. **242**: p. 45-51.
210. Balan, K.V., et al., *Intrapulmonary lipopolysaccharide exposure upregulates cytokine expression in the neonatal brainstem.* Acta Paediatr, 2012. **101**(5): p. 466-71.
211. Master, Z.R., et al., *Lipopolysaccharide exposure during the early postnatal period adversely affects the structure and function of the developing rat carotid body.* J Appl Physiol (1985), 2016. **121**(3): p. 816-827.
212. de La Serre, C.B., G. de Lartigue, and H.E. Raybould, *Chronic exposure to low dose bacterial lipopolysaccharide inhibits leptin signaling in vagal afferent neurons.* Physiol Behav, 2015. **139**: p. 188-94.
213. Le Maitre, E., et al., *Increased Recovery Time and Decreased LPS Administration to Study the Vagus Nerve Stimulation Mechanisms in Limited Inflammatory Responses.* J Vis Exp, 2017(121).
214. Balan, K.V., et al., *Vagal afferents modulate cytokine-mediated respiratory control at the neonatal medulla oblongata.* Respir Physiol Neurobiol, 2011. **178**(3): p. 458-64.
215. Di Fiore, J.M., R.J. Martin, and E.B. Gauda, *Apnea of prematurity--perfect storm.* Respir Physiol Neurobiol, 2013. **189**(2): p. 213-22.
216. Abbott, S.B., et al., *Phox2b-expressing neurons of the parafacial region regulate breathing rate, inspiration, and expiration in conscious rats.* J Neurosci, 2011. **31**(45): p. 16410-22.
217. Gauda, E.B., et al., *Inflammation in the carotid body during development and its contribution to apnea of prematurity.* Respir Physiol Neurobiol, 2013. **185**(1): p. 120-31.
218. Forster, D. and G. Reiser, *Nucleotides protect rat brain astrocytes against hydrogen peroxide toxicity and induce antioxidant defense via P2Y receptors.* Neurochem Int, 2016. **94**: p. 57-66.
219. Bellaver, B., et al., *Guanosine inhibits LPS-induced pro-inflammatory response and oxidative stress in hippocampal astrocytes through the heme oxygenase-1 pathway.* Purinergic Signal, 2015. **11**(4): p. 571-80.
220. Marina, N., et al., *Brainstem hypoxia contributes to the development of hypertension in the spontaneously hypertensive rat.* Hypertension, 2015. **65**(4): p. 775-83.
221. Marina, N., et al., *Astrocytes and Brain Hypoxia.* Adv Exp Med Biol, 2016. **903**: p. 201-7.
222. Kasymov, V., et al., *Differential Sensitivity of Brainstem versus Cortical Astrocytes to Changes in pH Reveals Functional Regional Specialization of Astroglia.* The Journal of Neuroscience, 2013. **33**(2): p. 435-441.
223. Marina, N., et al., *Glia, sympathetic activity and cardiovascular disease.* Exp Physiol, 2016. **101**(5): p. 565-76.
224. Marina, N., et al., *Brain metabolic sensing and metabolic signaling at the level of an astrocyte.* Glia, 2017.

225. Marina, N., et al., *Purinergic signalling in the rostral ventro-lateral medulla controls sympathetic drive and contributes to the progression of heart failure following myocardial infarction in rats.* Basic Res Cardiol, 2013. **108**(1): p. 317.
226. Pascual, O., et al., *Astrocytic Purinergic Signaling Coordinates Synaptic Networks.* Science, 2005. **310**: p. 113-116.
227. Guthrie, P., et al., *ATP Released from Astrocytes Mediates Glial Calcium Waves.* The Journal of Neuroscience, 1999. **19**(2): p. 520-528.
228. Schnell, M.J., M.E. Molliver, and S.H. Synder, *D-Serine, an endogenous synpatic modulator: Localization to astrocytes and glutamate-stimulated release.* Proc. Natl. Acad. Sci. , 1995. **92**.
229. Beltrán-Castillo, S., et al., *D-serine released by astrocyte in brainstem regulates breathing response to CO2 levels.* Nature Communications, 2017. **8**(838).
230. Parpura, V., et al., *Glutamate-mediated astrocyte-neuron signaling.* Nature Neuroscience, 1994. **369**: p. 744-747.
231. Grass, D., et al., *Diversity of Functional Astroglial Properties in the Respiratory Network.* The Journal of Neuroscience, 2004. **24**(6): p. 1358-1365.
232. Oku, Y., et al., *Respiratory calcium fluctuations in low-frequency oscillating astrocytes in the pre-Bötzinger complex.* Respiratory Physiology and Neurobiology, 2016. **226**: p. 11-17.
233. Forsberg, D., T. Ringstedt, and E. Herlenius, *Astrocytes release prostaglandin E2 to modify respiratory network activity* eLIFE, 2017. **6**(e29566).
234. Kumar, P. and N.R. Prabhakar, *Peripheral Chemoreceptros: Function and Plasticity of the Carotid Body.* Comarative Physiology, 2012. **2**(1): p. 141-219.
235. Housley, G.D., et al., *Brain stem projections of the glossopharyngeal nerve and its carotid sinus branch in the rat.* The Journal of Neuroscience, 1987. **22**: p. 237-250.
236. López-Barneo, J., et al., *Carotid body oxygen sensing.* Europeon Respiratory Journal 2008. **32**: p. 1386-1398.
237. Prabhakhar, N.R., et al., *Peripheral chemoreception and arterial pressure responses to intermittent hypoxia.* Compr Physiol, 2015. **5**(2): p. 561-77.
238. Duchen, M.R., et al., *Biophysical studies of the cellular elements of the rabbit carotid body.* Neuroscience, 1988. **26**(1): p. 291-311.
239. Pakkarato, S., et al., *Immunohistochemical analysis of sustentacular cells in the adrenal medulla, carotid body and sympathetic ganglion of mice using an antibody against brain-type fatty acid binding protein (B-FABP).* Journal of Anatomy, 2015. **226**: p. 348-353.
240. McDonald, D.M. and R.A. Mitchell, *The innervation of glomus cells, ganglion cells and blood vessels in the rat carotid body: A quantitative ultrastructural analysis.* Journal of Neurocytology, 1975. **4**(2): p. 177-230.

241. Chen, I. and R. Yates, *Two types of glomus cells in the rat carotid body as revealed by alpha-bungarotoxin binding.* J Neurocytol, 1984. **13**(2): p. 281-302.
242. Prabhakhar, N.R., G.K. Kumar, and Y.J. Peng, *Sympatho-adrenal activation by chronic intermittent hypoxia.* J Appl Physiol (1985), 2012. **113**(8): p. 1304-10.
243. St. John, W. and S. Wang, *Alteration from apneusis to more regular rhythmic respiration in decerebrate cats.* Respiration Physiology, 1977. **59**: p. 1201-1207.
244. Ballanyi, K., A. Volker, and D. Richter, *Anoxia induced functional inactivation of neonatal respiratory neurones in vitro* Neuroreport, 1994. **6**(1): p. 165-168.
245. Clarke, J.A. and M. de Burgh Daly, *Distribution of carotid body type I cells and other periadventitial type I cells in the carotid bifurcation regions of the rabbit.* Cell and Tissue Research, 1981. **216**(3): p. 603-614.
246. Murali, S., M. Zhang, and C.A. Nurse, *Angiotensin II mobilizes intracellular calcium and activates pannexin-1 channels in rat carotid body type II cells via AT1 receptors.* Journal of Physiology, 2014. **592**(21): p. 4747-4762.
247. Murali, S. and C.A. Nurse, *Purinergic signaling mediates bidirectional crosstalk between chemoreceptro type I and glial-like tyep II cells of the rat carotid body.* Journal of Physiology, 2016. **594**(2): p. 391-406.
248. Iturriaga, R. and J. Alcayaga, *Neuotransmission in the carotid body: transmitters and modulators between glomus cells and petrosal ganglion nerve terminals.* Brain Research Reviews, 2004. **47**(1-3): p. 46-53.
249. Prasad, M., et al., *Expression of P2X2 and P2X3 receptor subunits in rat carotid body afferent neurones: role in chemosensory signaling.* Journal of Physiology, 2001. **537 pt 3**(667-677).
250. Prabhakhar, N. and M. Joyner, *Tasting arterial blood: what do the carotid chemoreceptors sense? .* Frontiers in Physiology, 2015. **5**(524).
251. Prabhakhar, N.R. and G. Semenza, *Oxygen Sensing and Homeostasis* Physiology (Bethesda), 2015. **30**(5): p. 340-348.
252. Huxtable, A.G., et al., *Glia contribute to the purinergic modulation of inspiratory rhythm-generating networks.* J Neurosci, 2010. **30**(11): p. 3947-58.
253. Huda, R., et al., *Acid-sensing ion channels contribute to chemosensitivity of breathing-related neurons of the nucleus fo the solitary tract* Journal of Physiology, 2012. **590**(19): p. 4761-4775.
254. Turovsky, E., et al., *Mechanisms of CO2/H+ Sensitivity of Astrocytes.* J Neurosci, 2016. **36**(42): p. 10750-10758.
255. Gourine, A.V., et al., *ATP is a mediator of chemosensory transduction in the central nervous system.* Nature, 2005. **436**(7047): p. 108-11.
256. Burnstock, G., *Pruinergic Signalling.* British Journal of Pharmacology 2006. **147**(S172-181).

257. Nishimura, R.A., et al., *2017 AHA/ACC Focused Update of the 2014 AHA/ACC Guideline for the Management of Patients With Valvular Heart Disease: A Report of the American College of Cardiology/American Heart Association Task Force on Clinical Practice Guidelines.* J Am Coll Cardiol, 2017. **70**(2): p. 252-289.
258. Hawkins, V.E., et al., *Purinergic regulation of vascular tone in the retrotrapezoid nucleus is specialized to support the drive to breathe.* Elife, 2017. **6**.
259. Hartel, K., C. Schnell, and S. Hulsmann, *Astrocytic calcium signals induced by neuromodulators via functional metabotropic receptors in the ventral respiratory group of neonatal mice.* Glia, 2009. **57**(8): p. 815-27.
260. Okada, Y., et al., *Preinspiratory calcium rise in putative pre-Botzinger complex astrocytes* The Journal of Physiology 2012. **590**(19): p. 4933-4944.
261. Wang, S., et al., *Phox2b-Expressing Retrotrapezoid Neurons Are Intrinsically Responsive to H+ and CO2.* The Journal of Neuroscience, 2013. **33**(18): p. 7756-7761.
262. Chemes, E. and C. Ciaume, *Astrocyte Calcium Waves: What They Are and What They Do.* Glia, 2006. **54**(7): p. 716-725.
263. Lorier, A.R., et al., *ATP sensitivity of preBötzinger complex neurones in neonatal rat in vitro: mechanism underlying a P2 receptor-mediated increase in inspiratory frequency.* Journal of Physiology, 2008. **586**(5): p. 1429-1446.
264. Lorier, A.R., et al., *P2Y1 Receptor Modulation of the Pre-Bötzinger Complex Inspiratory Rhythm Generating Network In Vitro* The Journal of Neuroscience, 2007. **27**(5): p. 993-1005.
265. Huxtable, A.G., et al., *Tripartite Purinergic Modulation of Central Respiratory Networks during Perinatal Development: The Influence of ATP, Ectonucleotidases, and ATP Metabolites.* The Journal of Neuroscience, 2009. **29**(47): p. 14713-14725.
266. Zwicker, J., et al., *Purinergic modulation of preBötzinger complex inspiratory rhythm in rodents: the interaction between ATP and adenosine.* Journal of Physiology, 2011. **589**(pt18): p. 4583-4600.
267. Mulkey, D.K., et al., *Purinergic P2 receptors modulate excitability but do not mediate pH sensitivity of RTN respiratory chemoreceptors.* J Neurosci, 2006. **26**(27): p. 7230-3.
268. Wenker, I.C., et al., *Regulation of ventral surface CO2/H+-sensitive neurons by purinergic signaling.* Journal of Physiology, 2012. **590**(9): p. 2137-2150.
269. Wenker, I.C., et al., *P2Y1-receptors expressed by C1 neurons determine peripheral chemoreceptor modulation of breathing, sympathetic activity and blood pressure.* Hypertension, 2013. **62**(2): p. 263-273.
270. Mulkey, D.K., et al., *Respiratory control by ventral surface chemoreceptor neurons in rats.* Nature Neuroscience, 2004. **7**: p. 1360-1369.

271. Funk, G.D., *Neuromodulation: purinergic signaling in respiratory control.* Compr Physiol, 2013. **3**(1): p. 331-63.
272. Herlenius, E., *An inflammatory pathway to apnea and autonomic dysregulation.* Respir Physiol Neurobiol, 2011. **178**(3): p. 449-57.
273. Rajani, V., et al., *The role of P2Y1 receptor signaling in central respiratory control.* Respiratory Physiology and Neurobiology, 2016. **226**: p. 3-10.
274. Schnell, C., J. Fresemann, and S. Hulsmann, *Determinants of functional coupling between astrocytes and respiratory neurons in the pre-Botzinger complex.* PLoS One, 2011. **6**(10): p. e26309.
275. Ben Haim, L. and D.H. Rowitch, *Functional diversity of astrocytes in neural circuit regulation.* Nat Rev Neurosci, 2017. **18**(1): p. 31-41.
276. Papouin, T. and S.H. Oliet, *Organization, control and function of extrasynaptic NMDA receptors.* Philos Trans R Soc Lond B Biol Sci, 2014. **369**(1654): p. 20130601.
277. Erlichman, J.S., et al., *Inhibition of monocarboxylate transporter 2 in the retrotrapezoid nucleus in rats: a test of the astrocyte-neuron lactate-shuttle hypothesis.* J Neurosci, 2008. **28**(19): p. 4888-96.
278. Lazarenko, R., et al., *Acid sensitivity and ultrastructure of the retrotrazezoid nucleus in Phox2b-EGFP mice.* J Comp Neurol, 2009. **517**(1): p. 69-86.
279. Erlichman, J.S., J.C. Leiter, and A.V. Gourine, *ATP, glia and central respiratory control.* Respir Physiol Neurobiol, 2010. **173**(3): p. 305-11.
280. Erlichman, J.S. and J.C. Leiter, *Glia modulation of the extracellular milieu as a factor in central CO2 chemosensitivity and respiratory control.* J Appl Physiol (1985), 2010. **108**(6): p. 1803-11.
281. Funk, G.D., et al., *Neuroglia and their roles in central respiratory control; an overview.* Comparative Biochemistry and Physiology, Part A, 2015. **186**: p. 83-95.
282. Wang, W., J.H. Pizzonia, and G.B. Richerson, *Chemosensitivity of rat medullary raphe neurones in primary tissue culture.* J Physiology, 1998. **511**(pt 2): p. 433-450.
283. Wang, W. and G.B. Richerson, *Chemosensitivity of non-respiratory rat CNS neurons in tissue culture.* Brain Res, 2000. **860**(1-2): p. 119-29.
284. D'Agostino, D., E.J. Mazza, and J.A. Neubauer, *Heme oxygenase is necessary for the excitatory response of cultured neonatal rat rostral ventrolateral medulla neurons to hypoxia.* Am J Physiol Regul Integr Comp Physiol, 2009. **298**(1): p. R102-R118.
285. Mazza, E., et al., *Expression of heme oxygenase in the oxygen-sensing regions of the rostral ventrolateral medulla.* J Appl Physiol (1985), 2001. **91**(1): p. 379-85.
286. Gestreau, C., et al., *Task 2 potassium channels set central respiratory CO2 and O2 sensitivity* PNAS, 2009. **107**(5): p. 2325-2330

287. Kumar, N.N., et al., *Regulation of breathing CO2 requires the proton-activated receptor GPR4 in retrotrapezoid nucleus neurons.* Science, 2015. **348**(6240): p. 1255-1260.
288. Ruffault, P., et al., *The retrotrapezoid nucleus neurons expressing Atoh1 and Phox2b are essential for the respiratory response to CO2.* Elife, 2015. **4**.
289. Wenker, I., et al., *Astrocytes in the Retrotrapezoid Nucleus Sense H+ by Inhibition of a Kir4.1-Kir5.1-Like Current and May Contribute to Chemoreception by a Purinergic Mechanism.* Journal of Neurophysiology 2010. **104**: p. 3042-3052.
290. Lazarenko, R., et al., *Anesthetic activation of central respiratory chemoreceptor neurons involves inhibition of a THIK-1-like background K(+) current* The Journal of Neuroscience, 2010. **30**(27): p. 9324-9334.
291. Bayliss, D.A., et al., *TASK-1 is a highly modulated pH-sensitive 'leak' K+ channel expressed in brainstem respiratory neurons.* Respiration Physiology, 2001. **129**(1-2): p. 159-174.
292. Mulkey, D.K., et al., *TASK Channels Determine pH Sensitivity in Select Respiratory Neurons But Do Not Contribute to Central Respiratory Chemosensitivity.* The Journal of Neuroscience, 2007. **27**(51): p. 14049-14058.
293. Wang, S., et al., *TASK-2 Channels Contribute to pH Sensitivity of Retrotrapezoid Nucleus Chemoreceptor Neurons.* The Journal of Neuroscience, 2013. **33**(41): p. 16033-16044.
294. Sobrinho, C.R., et al., *Fluorocitrate-mediated depolarization of astrocytes in the retrotrapezoid nucleus stimulates breathing.* Journal of Neurophysiology, 2017. **In Press**.
295. Nwaobi, S.E., et al., *The role of glial-specific Kir4.1 in normal and pathological states of the CNS.* Acta Neuropathol, 2016. **132**(1): p. 1-21.
296. Olsen, M.L., et al., *New Insights on Astrocyte Ion Channels: Critical for Homeostasis and Neuron-Glia Signaling.* The Journal of Neuroscience, 2015. **35**(41): p. 13827-13835.
297. Bayliss, D.A., et al., *The role of pH-sensitive TASK channels in central respiratory chemoreception.* Pflugers Arch, 2014. **467**(5): p. 917-929.
298. Mulkey, D., et al., *Serotonergic neurons activate chemosensitive retrotrapezoid nucleus neurons by a pH-independent mechanism* The Journal of Neuroscience, 2007. **27**(51): p. 14128-14138.
299. Lesage, F. and J. Barhanin, *Molecular physiology of pH-sensitive background K2P channels.* Physiology (Bethesda), 2011. **26**: p. 424-437.
300. Jones, S.A., et al., *Expression of TASK-1, a pH-sensitivie twin-pore domain K+ channel, in rat myocutes.* American Journal of physiology 2002. **283**: p. H181.
301. O'Connell, A.D., M.J. Morton, and M. Hunter, *Two-pore domain K+ channels- molecular sensors.* Biochimica et Biophysica Acta 2002. **1566**: p. 152-161.
302. Buckler, K., *Two-pore domain k(+) channels and their role in chemoreception.* Adv Exp Med Biol, 2010. **661**: p. 15-30.

303. Liu, Y., et al., *Exposure to cyclic intermittent hypoxia increases expression of functional NMDA receptors in the rat carotid body* Journal of Applied Physiology, 2009. **106**(1): p. 259-267.
304. Huckstepp, R.T., et al., *Connexin hemichannel-mediated CO2-dependent release of ATP in the medulla oblongata contributes to central respiratory chemosensitivity* Journal of Physiology, 2010. **588**(20): p. 3901-3920.
305. Chen, J., et al., *Chronic hypoxia upregulates connexin43 expression in rat carotid body and petrosal ganglion.* Journal of Applied Physiology, 2001. **92**: p. 1480-1486.
306. Frinchi, M., et al., *Connexin36 (Cx36) expression and protein detection in the mouse carotid body and myenteric plexus.* Acta Histochemica, 2013. **115**(3): p. 252-256.
307. Holloway, B.B., et al., *The retrotrapezoid nucleus stimulates breathing by releasing glutamate in adult conscious mice.* Eur J Neurosci, 2015. **42**(6): p. 2271-2282.

CHAPTER 3

Neuron-astrocyte networking: Astrocytes orchestrate and respond to changes in neuronal network activity across brain states and behaviors

Marion R. Van Horn[1], Nicholas Benfey[1], Colleen Shikany[3], Liza J. Severs[3,4], Tara Deemyad[2]

[1]Department of Neurology and Neurosurgery, Montreal Neurological Institute, McGill University
[2]Department of Psychiatry, School of Medicine, University of Pittsburgh
[3]Center for Integrative Brain Research, Seattle Children's Research Institute
[4]Department of Physiology and Biophysics, The University of Washington

Published in *Journal of Neurophysiology, August 2021. Volume 126, issue 2.*
Find the article here.

ABSTRACT

Astrocytes are known to play many important roles in brain function. However, research underscoring the extent to which astrocytes modulate neuronal activity is still underway. Here we review the latest evidence regarding the contribution of astrocytes to neuronal oscillations across the brain, with a specific focus on how astrocytes respond to changes in brain state (e.g., sleep, arousal, stress). We then discuss the general mechanisms by which astrocytes signal to neurons to modulate neuronal activity, ultimately driving changes in behavior, followed by a discussion of how astrocytes contribute to respiratory rhythms in the medulla. Lastly, we contemplate the possibility that brainstem astrocytes could modulate brain-wide oscillations by communicating the status of oxygenation to higher cortical areas.

KEYWORDS: Astrocyte; brain state; neuronal network; behavioral state

INTRODUCTION

Rhythmic activity of billions of neurons is one of the critical drivers of our daily behaviors. Our attention, memory, perception, and basic physiological behaviors, such as breathing and sleeping, depend on coordinated oscillations of neuronal activity (1-3). Traditionally, different behaviors have been ascribed to an interface between patterns of connectivity (e.g., recurrent interactions between neurons), the existence of neuronal-autonomous mechanisms (e.g., intrinsic membrane properties), and synaptic transmission properties of neural networks. Recent evidence suggests that astrocytes also play an important role in regulating synchronized neuronal activities and responses (4-6). Astrocytic processes surround neurons, where they often interact directly at synapses and help in clearing the accumulation of neurotransmitters (e.g., glutamate) and ions (e.g., potassium) from synaptic spaces (7-9). Furthermore, astrocytes express many types of receptors for neurotransmitters and neuromodulators (e.g., neuropeptides, norepinephrine (NE), dopamine, serotonin, histamine, melatonin, GABA, endocannabinoids, and glutamate), release a number of gliotransmitters and other molecules, and are thus in a position to sense changes in the brain and influence neuronal excitability that underly network oscillations (6-8, 10-12). Although not electrically excitable, research over the last three decades has revealed that astrocytes display complex and dynamic intracellular calcium signaling, which has brought a spotlight on the important involvement of astrocytes in information processing in the brain (13, 14).

In this review, we focus on recent evidence demonstrating how astrocytes contribute to neuronal network activity across the brain and how astrocytic function is influenced by different behavioral states specifically within cortical, hippocampal, and brainstem circuits. Furthermore, we include an important discussion of how respiration may entrain brain-wide oscillations and facilitate transitions between behavioral states.

Astrocytes encode changes in cortical network activity

Macroscopic cortical rhythmic oscillations of neuronal activity, which arise within populations of neurons, are characteristic of the *in vivo* brain (15-18). Such rhythmic activity plays a role in shaping input gains, reducing reaction times, and enhancing information transfer between subsets of cortical neurons (19, 20). These neuronal oscillations can be classified according to their dominant rhythmic frequency, where specific oscillatory bands have been linked to different brain states: (1) activities between 0.5 and 4 Hz (delta, slow wave) occur during the deep stage of Non-REM sleep and play a critical role in memory consolidation, (2) 4–8 Hz (theta) oscillations are associated with active motor behavior as well as REM sleep, (3) 8–12 Hz (alpha) oscillations arise during relaxed wakefulness, (4) 12.5-25 Hz (beta) oscillations are linked to normal waking state of consciousness, and (5) frequencies at 25 -140 Hz (gamma) oscillations are related to large scale brain network activity and cognitive processing, such as when using working memory or shifting attention (Fig. 1) (4, 21).

There is accumulating evidence that astrocytes contribute to changes in oscillatory network activity, where transient increases in astrocytic Ca^{2+} signaling have been found to precede the onset of oscillatory activity (22). Several studies have shown that cortical astrocytes and neurons synchronously respond to sensory stimuli in a frequency-dependent fashion with elevations in Ca^{2+} signaling (23-25). Recently, Lines et al. provided the first "temporal" correlation of astrocytic Ca^{2+} signaling and cortical neuronal activity (24). Using recordings of cortical local field potentials and *in vivo* two photon Ca^{2+} imaging, this study revealed a significant influence of astrocytic Ca^{2+} signaling on the dynamic range of sensory evoked cortical rhythmic oscillations. The investigators showed that astrocytic Ca^{2+}, in both astrocytic soma and arbors, followed the synchronized neuronal responses to somatosensory stimuli in the gamma range (24). Importantly, using chemogenetic activation of astrocytes, as well as impairing astrocyte Ca^{2+} signaling (i.e., using $IP3R2^{-/-}$, mice), they showed that sensory-evoked astrocytic Ca^{2+} signaling directly regulates the dynamic range of cortical neuronal network excitability and diminished steady-state gamma oscillations in urethane anesthetized mice. Notably, although urethane is widely used in studies on brain waves, the use of anesthetics is known to directly affect cortical neuronal oscillations (26). Urethane increases delta band oscillations and decreases theta, beta, and gamma band oscillations without recovery of high-frequency oscillations (26). In other words, states that are generated under urethane anesthesia may not be identical to that of natural brain states. More importantly, urethane, like two other main anesthetic combinations, i.e., Ketamine/Xylazine and isoflurane, also suppresses neocortical astrocyte Ca^{2+} signaling in both soma and branches and reduces correlated spontaneous Ca^{2+} transients between astrocytes (27). Indeed, astrocytes may contribute to features of general anesthesia. Thus, the evoked astrocytic Ca^{2+} transients in Lines et al. study may not represent true astrocytic responses in an awake brain state (24, 28).

Additional studies evaluating awake animals will be required to better understand how astrocytes regulate synchronized cortical activity. To circumvent the use of anesthetics, several recent studies have measured astrocytic Ca^{2+} responses during natural brain states. For example, two independent research groups described astrocytic Ca^{2+} signaling across sleep-wake states and found that astrocyte Ca^{2+} activity, like that of neuronal Ca^{2+}, is greatly reduced across periods of sleep compared to wakefulness (29, 30). A detailed analysis of Ca^{2+} signaling across natural sleep revealed dynamic patterns of astrocytic Ca^{2+} corresponding to specific sleep phases. These studies revealed that astrocytes have increased Ca^{2+} activity during the transition from sleep to wakefulness. Bojarskaite et al. identified a specific increase in astrocytic Ca^{2+} 1-2s before the occurrence of other measured physiological changes. Interestingly, disrupting intracellular Ca^{2+} resulted in reduced slow wave sleep (SWS) and an increase in the number of microarousals and sleep spindles, providing further evidence that astrocytes are actively involved in the generation and maintenance of normal sleep patterns (29).

Astrocytes orchestrate rhythmic network activities by maintaining brain homeostasis

The regulation of brain homeostasis is one mechanism by which astrocytes are thought to contribute to neuronal oscillations (4). In the cortex, K^+ homeostasis is primarily controlled by the clearance and redistribution of extracellular K^+ by astrocytic Kir4.1 channels and Na^+/K^+-ATPase, which have been found to influence neuronal excitability and cortical network rhythmicity in all frequency ranges and states (Fig. 1) (7, 31). Bellot-Saez and colleagues have shown that a deficiency in astrocytic K^+ clearance results in hypersynchronous network activity by increasing the power of cortical oscillations in the beta and gamma range, which is followed by rise of power in theta and beta range during the period that K^+ is cleared from the extracellular space (7, 31). Thus, the "loss of function" defects of Kir4.1 in astrocytes can result in disruption of cortical rhythmic oscillations and early onset of seizures. Interestingly, it has been proposed that "gain-of-function" defects of astrocytic Kir4.1 channel, resulting from enhancing Kir4.1 membrane expression and current density or impediment of pH-dependent current inhibition, underlies increased susceptibility to epileptic neuronal network hypersynchrony in autistic individuals. In this scenario, activity of the $Na^+/HCO3^-$ cotransporter and extracellular pH is affected by increased Kir4.1 expression. Indeed, increased expression of Kir4.1 channels can result in membrane hyperpolarization, driving the membrane potential closer to equilibrium potential for K^+. Since the reversal potential for the $Na^+/HCO3^-$ cotransporter is negative to the equilibrium potential for K^+, the activity of this transporter will decrease with increased Kir4.1 expression resulting in decreased $HCO3^-$ influx, and small increasing in extracellular pH can consequently trigger seizures (32). Together, this highlights the importance of astrocytic Kir4.1 channels for regulating astrocyte-mediated K^+ buffering activity to maintain optimal K^+ concentrations, as well as pH level in the extracellular environment, and consequently contribute to the generation of rhythmic neuronal activity. Although the mechanisms regulating K^+ clearance processes are largely unknown, a recent study has found that the presence of neuromodulators can significantly impact K^+ clearance rates (33). In particular, serotonin and noradrenaline were found to mediate astrocytic spatial buffering via gap-junctions, and dopamine and histamine were found to affect the uptake mechanism via Kir channels.

Astrocytes are also known to regulate cortical rhythmicity by adjusting glutamate levels via astrocytic glutamate transporters and through glutamatergic gliotransmission (22, 34). Changes in extracellular glutamate levels mediated by astrocytes can induce cortical synchrony in the delta range (35) and extend the duration of gamma oscillations (22). Adding complexity, Mederos et al., recently showed that GABAergic signaling in astrocytes plays an important role in regulating low gamma oscillations, phase amplitude coupling between theta and gamma oscillation, and in turn goal-directed behaviors in the medial prefrontal cortex (36). The investigators found that astrocytes monitor local concentrations of GABA and release glutamate, which activates presynaptic group I metabotropic glutamate receptors in principal cells and facilitates inhibitory synaptic transmission. Taken together, it is likely that both glutamatergic and GABAergic signaling in astrocytes play critical roles in regulating cortical rhythmicity.

Astrocytes can also affect neuronal oscillations by releasing Ca^{2+} binding protein S100β, which can increase *in vivo* kainate-induced gamma oscillations in the hippocampus (37) and phase amplitude coupling between theta and gamma oscillations in the medial prefrontal cortex (Fig.1) (38).

Detection of intracranial pressure may be an additional way that astrocytes modulate neuronal oscillations. Piezo2, an ion channel sensitive to changes in pressure, could modulate synchronous activity throughout many brain regions by acting as a type of baroreceptor. Piezo2 has widespread but low expression patterns in neurons and is suggested to initiate pulsatile firing patterns coordinated with breathing and cardiorespiratory intracranial pressure changes (39). Piezo2 is also expressed in astrocytes (40); however, this study has yet to be validated through peer review (39), and the extent of Piezo2 expression specifically in astrocytes throughout the brain remains to be determined.

It is important to note that the efficiency and the contribution of astrocytes to cortical rhythmicity is likely to depend on underlying brain state. The physical proximity of astrocytic processes to neuronal synapses has been found to be extremely dynamic and physically reduced during sleep (41). Accordingly, K+, glutamate, and GABA clearance, and the delivery factors influencing neuronal oscillations, will inevitably vary depending on the proximity of the transporters and ion channels to neuronal synapses.

Behavioral state modulates astrocyte responsiveness and modulates neuronal activity

Emerging evidence suggests that astrocyte responsiveness is strongly influenced by the behavioral state of the animal. For example, increasing arousal, through locomotion on a treadmill, has been shown to greatly enhance visually evoked Ca^{2+} responses in astrocytes in the primary visual cortex in awake mice (42). Recently, these findings have been expanded in a study demonstrating that astrocytes in the primary visual cortex integrate both arousal state and local circuit activity through distinct mechanisms. Astrocytic Ca^{2+} activity induced by locomotion was found to be mediated by the release of NE, whereas visually evoked Ca^{2+} responses continued to occur following depletion of NE in the brain (Fig. 2) (43).

Considerable research has been devoted to understanding how NE, acting through astrocytes, can modulate neuronal activity and behavioural states. Of particular interest is the recent work by Mu et al. demonstrating that endogenous NE release in larval zebrafish acts through alpha-1 adrenergic receptors (α1-AR) on radial astrocytes to induce substantial and widespread increases in astrocyte Ca^{2+} levels that drive behavioural state switches. They showed that during fictive swimming, mismatches occurring between motor output and optical flow of the surrounding environment induced NE release in the motor system, which was detected and integrated by radial astrocytes. If enough swim failures occurred, and hence enough NE was released, radial astrocyte Ca^{2+} levels would exceed a threshold which would in turn lead to the activation of neighbouring inhibitory interneurons. Ultimately, the

activation of inhibitory circuitry by radial astrocytes prevented the fish from repeating futile swimming behavior (44), similar to the integrate and suppress algorithm that has been reported in mouse hippocampal slices (45). Despite the significant role of astrocytic NE in arousal and in modulating evoked Ca^{2+} responses throughout various brain regions, a mechanistic understanding of how astrocytes integrate NE signals and in turn influence neuronal activity in response noradrenergic still requires further development.

A more succinct understanding of the distinct second messenger responses that astrocytes exhibit *in vivo* in response to NE release during different arousal states has recently been found. Oe et al. show that mice respond to an air puff with a mild startle response, coinciding with a NE induced increase in Ca^{2+} levels in cortical astrocytes (likely through α1-AR), while prolonged states of high vigilance induced by a head-fixed fear conditioning paradigm induce both NE mediated increases in Ca^{2+} and cAMP (likely through simultaneous activation of α and β-ARs). These increases in cAMP were shown to lead to the breakdown of glycogen (46). Interestingly, another group has demonstrated that heightened arousal and NE signalling through β-ARs also causes the activity-dependent release of lactate from cortical astrocytes *in vivo* (47).

Both astrocyte-induced NE release and Ca^{2+} signalling has been observed to play a largely inhibitory role in the central nervous system. In accordance with this, in the hippocampus, Gaidin et al. have shown that NE induced activation of α2-ARs on astrocytes cause the release of GABA (48), and radial astrocytes in zebrafish recruit neighbouring inhibitory neurons to mediate behavioural effects (44); however, the mechanism by which this occurs has not been shown.

Interestingly, both optogenetic and NE induced Ca^{2+} increases in astrocytes have been linked to ATP release (49, 50). Despite channelrhodopsin acting as non-specific cation channels, their ability to readily pass substantial amounts of calcium is limited; as such, we believe it is important to highlight that optogenetic activation of calcium signaling in astrocytes likely relies on the conversion of sodium transients into calcium signals by electrogenic transporters such as the sodium-calcium exchangers (51). Using optogenetic activation of Ca^{2+} signalling in astrocytes in the hippocampus, Tan et al. discovered a mechanism which may provide insight into the events occurring between radial astrocyte activation and activation of inhibitory circuitry observed by Mu et al. which also has relevance for how NE induced Ca^{2+} increases in astrocytes may also modulate oscillatory rhythms in the brain (44). They showed that activation of astrocytes causes the release of ATP, decreases excitability of pyramidal neurons, and increases excitability of interneurons. Activation of astrocytes primarily enhanced the excitation of cholecystokinin-positive interneurons through a mechanism involving the activation of P2Y1 receptors and the inhibition of K2P potassium channels, and astrocyte-induced decreases in the excitability of pyramidal neurons occurred through activation of A1 receptors and the opening of GIRK channels. They conclude by showing that ATP released from astrocytes downregulates the power of *ex vivo* gamma oscillations occurring *in vitro*. Taken together, NE may act as a broad spectrum ‘astromodulator’,

enhancing astrocytic responses to local circuit activity as well as driving changes in interstitial space in a manner dependent upon the state of arousal. Activation of astrocytes by NE is likely to negatively regulate neuronal activity through the release of either GABA or ATP, enhancing inhibition, decreasing excitation, and fueling the surrounding neural circuitry through the activity-dependent release of lactate.

In addition to NE, there are a number of signaling peptides that act as global ‘astromodulators’. For instance, the firing rate of cholinergic neurons increases during states associated with gamma oscillations, such as active locomotion (52). Recently, Papouin et al. showed that cholinergic modulation of astrocytes plays an important role in gating neuronal activation across sleep-wake cycles. In particular, wakefulness was associated with increased activation of astrocytic α7-nicotinic acetylcholine receptors and resulted in increased levels of the NMDAR co-agonist D-serine (α7nAChR) (Fig 3) (53). Notably, D-serine and activation of NMDARs has been found to promote synaptic maturation and axonal stabilization in the developing visual system (54). Accordingly, it will be interesting to determine whether the increased availability of D-serine during wakefulness is also associated with daily fluctuations in synaptic strength and axonal motility.

The degree to which neurons and astrocytes interact is dynamic and changes significantly across the day and with changing behavioral states. For example, 2-photon imaging of astrocyte processes across sleep/wake cycles has shown that sleep is associated with a decrease in the astrocytic coverage of synapses compared to periods of wakefulness (Fig. 3) (41). A reduction in astrocyte coverage during sleep has also been associated with an increase in the brain's interstitial space, which has been hypothesized to facilitate the clearance of metabolic waste (55). Changes in synaptic coverage have been found to alter neuron-astrocyte interactions and consequently the ability of astrocytes to clear glutamate, GABA, and K^+ ions. Reduced synaptic coverage may result in an increase in glutamate spillover, as a result of decreased neuron-astrocyte interactions as well as a reduction in the proximity of transporters and ion channels, which could enhance neuronal synchronization during SWS. Furthermore, a retraction of astrocytic processes during lactation is associated with a decrease in the availability and delivery of gliotransmitters (56)(Fig 3).

Recent studies have also suggested that the decrease in astrocytic coverage during sleep could allow for microglia to more easily access synapses where they have been found to play an important role in synaptic pruning (57) (58, 59). In agreement with this hypothesis, studies have shown that NE, which is present at higher levels during wakefulness, inhibits microglial dynamics (60) (61).

Astrocyte morphology is altered by other physiological states. A recent study found that an acute period of stress was sufficient to alter astrocyte morphology in the cortex and impaired the ability of astrocytes to supply neurons with L-lactate (62). It will be interesting to determine what if the supply of other gliotransmitters like D-serine and ATP are also impaired during stress due to changes in astrocyte morphology.

Taken together, time of day, fluctuating brain states, and rhythmic activity modulates the proximity of astrocytic processes and the availability of neuromodulators in the brain milieu. These alterations thereby influence, or in some cases are driven by astrocyte signaling. These signaling cascades can ultimately alter the gating of neuronal activity and synaptic plasticity by delivering astrocyte-derived molecules that modulate neuronal excitability.

Astrocytes maintain homeostasis and modulate breathing within brainstem rhythm generating networks

In the brainstem, astrocytes have been found to play a role in altering the respiratory rhythm generating networks primarily by responding to changes in gas homeostasis (63-65) and coincidentally pH (66, 67). These changes are reportedly region specific, where in general, astrocytes in the preBötzinger Complex (preBötC) are sensitive to changes in hypoxia (64) while astrocytes within the Retrotrapezoid Nucleus (RTN) and parafacial region (pFRG) respond to changes in CO_2 and pH (67, 68).

The role of RTN astrocytes (and neurons) as central chemosensors is generally accepted. Although the precise mechanisms by which these astrocytes sense extrinsic CO_2/pH are still being uncovered (69), evidence suggests that an increase in astrocytic Ca^{2+} results in the consequent release of ATP, a direct increase in respiratory frequency (68), followed by vasoconstriction to further increase tissue CO_2/H^+ (70, 71). Most recently it has been suggested that this ATP-dependent response to CO_2/pH is a result of $P2Y_2$ expression on vascular smooth muscle cells and endothelial cells combined with the inhibition of pH-sensitive inward rectifying potassium channels (K_{ir}) expressed by RTN astrocytes (71). Although the functional role of pFRG/RTN astrocytes with chemosensitive properties is relatively established, there is some discussion on how ATP release alters breathing; ATP is rapidly degraded into ADO, which has been shown to blunt the effects of hypercapnia on respiratory frequency (72). Furthermore, the boundaries and function of the RTN/pfRG and chemosensitive properties of astrocytes and neurons within these regions are not clearly delineated (73). Other published mechanisms involved in altering respiratory frequency in these regions include the release of PGE2 from a subset of pFRG/RTN astrocytes, which have a blunting effect on the response to hypercapnia (74, 75). In addition to its role in cholinergic circuitry in the cortex as previously discussed, astrocyte derived D-serine has been identified to modulate breathing behaviors through NMDAR signaling. Specifically, injections of D-serine into the ventral respiratory column and raphe nucleus of caudal brainstem slices resulted in an increase in the basal respiratory frequency, reportedly through NMDAR coupling. Furthermore, it was shown that D-serine mediates the response to applied hypercapnic acidosis, decreasing the respiratory response to CO_2 (76).

Conversely, the effect of preBötC astrocyte activity on normal breathing (eupnea) is not agreed upon. Some studies have shown a direct link with astrocyte calcium fluctuations and respiratory activity, while other studies indicate this is only the case in non-physiological conditions. A report by Schnell et.

al. did not observe any fluctuations that coincided with the eupneic rhythm; Ca^{2+} activity in astrocytes was only observed with metabotropic glutamate receptor activation or when blocking uptake of glutamate in glia (77). However, several studies suggest that astrocytes within the preBötC are important for regulating breathing during the central hypoxic response, which consists of an initial increase in frequency followed by a respiratory depression. PreBötC astrocytes reportedly release ATP, functioning to attenuate the secondary depression through $P2Y_1$ receptor activation (64). A more recent study has shown that in the preBötC of alert rats, inhibiting astrocytic release of ATP by dnSNARE or TeLC reduces overall rhythmic breathing frequency and reduces breathing capacity during exercise (78). In the same study, expression of Gq coupled DREADDs in brainstem astrocytes increased respiratory frequency and the frequency of sighs (78).

A role for astrocytes in maintaining gas homeostasis in these areas can also be supported by their anatomical proximity to the vasculature. Indeed, astrocytes cover the ventral surface of the brainstem and astrocytic endfeet ensheath blood vessels throughout; furthermore, a structural comparison of astrocytes within different brain regions has revealed that complexity of astrocytic processes are much more extensive within brainstem networks (79). Indeed, astrocytes have emerged as a link between the vasculature and neuronal output in many areas throughout the brain. Although no direct link has been shown for astrocytes in the brainstem respiratory groups, it is an important consideration for future studies (65).

Respiratory-entrained oscillations synchronize brain-wide rhythms

In this review, we have discussed how astrocytes participate in modulating the neuronal activity that underlies brain waves. Neural oscillations are typically associated with higher order brain regions. However, respiratory entrained oscillations, previously believed to be underlying noise contamination in these network oscillations, are now recognized to be important in synchronizing brain-wide activity states and have been suggested to entrain a global brain rhythm (80-83). These breathing entrained oscillations are said to be initiated by nasal respiration, and synchronize activity beginning in the olfactory bulb and spanning regions of the cortex and hippocampus (80). Evidence points to these oscillations occurring in lower frequency delta and theta oscillations and could also modulate higher frequency oscillations in other parts of the brain (80, 81, 84). Importantly, astrocyte activity is known to span large network areas through Ca^{2+} waves and in different oscillatory bands (85, 86) (87), and thus could provide a functional link to anatomically distinct regions, perhaps initiated in the brainstem or olfactory bulb by nasal respiration, or a coordinated effort of both. Given that cardiorespiratory coupling and breathing behaviors are, at least in part, centered in the medulla (88, 89) (90), changes in O_2/CO_2/pH detected from these regions need to be communicated throughout the brain to support animal behavior.

Astrocyte function throughout brain regions is heterogeneous

Another important discussion point is the relatively new idea that astrocytes are highly heterogeneous and show specific encoded functions. It has been appreciated that there are subtypes of astrocytes, even within the same brain region, that are morphologically and genetically distinct, and respond differently to the same stimulus. For instance, Batiuk et al., by single-cell RNA sequencing, identified five transcriptomically distinct astrocyte subtypes in adult mouse cerebral cortex and hippocampus (91). Furthermore, , using a large-area spatial transcriptomic map method and by screening 46 candidate genes for astrocyte, the Rowitch lab recently identified distinct subtypes within layers 2–5 of cerebral cortex (92).One of the best examples of functional heterogenicity within the same region is presence of two subpopulations of astrocytes in dorsal striatum that each of them selectively respond to specific medium spiny neurons subtype activity and specifically regulate synapses belong to the either basal ganglia's direct or indirect pathways (93). Thus, the influence of heterogeneity in astrocytes should be considered in their contribution to regulation of neuronal network activity. For example, induction of an unusual retroaxonal barrage of firing in the gamma range in network of Neuropeptide Y interneurons has been proposed to be triggered by release of glutamate from subpopulation of astrocytes that specifically trigger distal axon of this subgroups of interneuron (45).

Conclusion

We have come a long way since neuron-astrocyte interactions were first so beautifully illustrated by Ramón y Cajal over one hundred years ago (94-96). While significant progress has been made in unraveling how astrocytes contribute to brain function, emerging evidence continues to expand on the dynamic and diverse nature of neuron-astrocyte interactions. Evolving experimental techniques have allowed us to visualize how astrocytes actively interact with neuronal processes, where they have been found to modulate neuronal network activity and drive and respond to changes in both arousal level and behavioral state. The recent findings discussed in this review make several important conclusions regarding brain state modulation by astrocytes: (1) the responsiveness of astrocytes, like neurons, is strongly affected by sensory stimuli, (2) astrocytes play a substantial part in regulating brain states (e.g. sleep-wake states, activity levels, and breathing frequency), (3) astrocytic coverage of the neuronal synapse is highly dependent on brain state and region, and (4) astrocyte activity levels are strongly altered with the use of anesthetics. Moreover, as mechanistic explanations evolve throughout the brain, consideration should be given to how astrocytic oscillations affect regional connectivity to adjust overall circuit activity and influence behavioral responses.

Figure legends

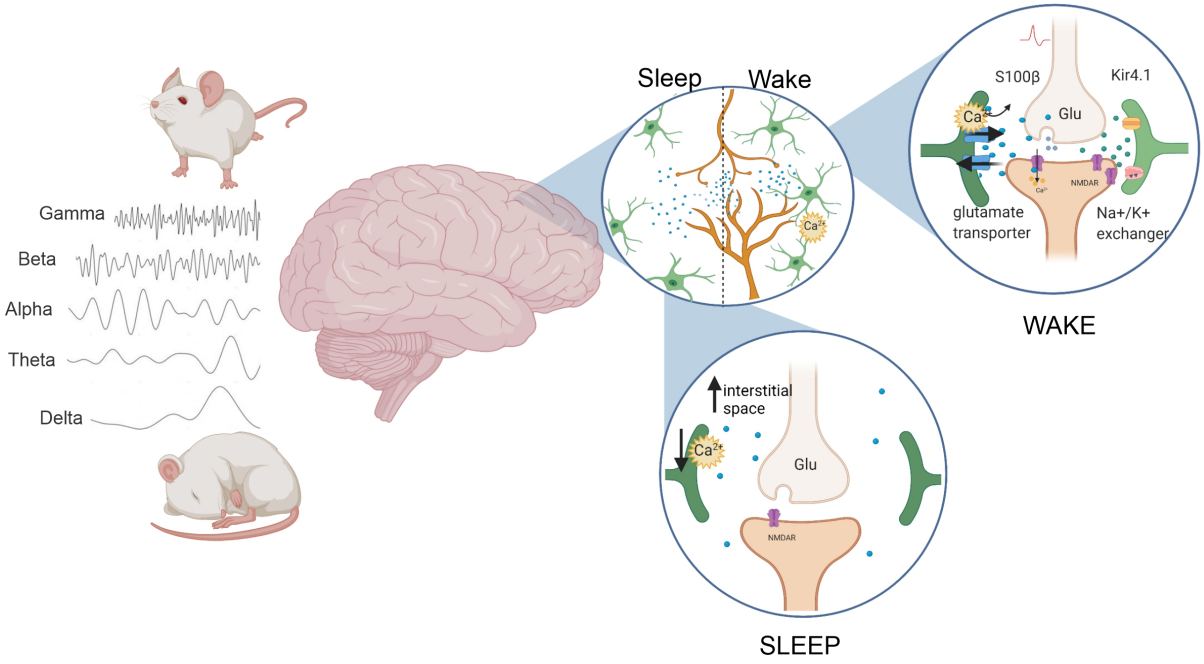

Figure 1. Astrocytes contribute to initiation of different neuronal synchronized activities. They participate in generation of brain waves with different frequencies appears at distinct brain states: gamma (wakeful attentional selection); beta (wakeful active mind); alpha (wakeful relaxation); theta (drowsiness) and delta (sleep/dreaming) (left). Astrocytes modulate neuronal excitability and synchronize their responses causing cortical rhythmic oscillations (middle top) by K^+ buffering, glutamate clearance and releasing S100β (right top). Astrocyte volume decreases during sleep, which may result in decreased clearance of neurotransmitters and ions by astrocytes.

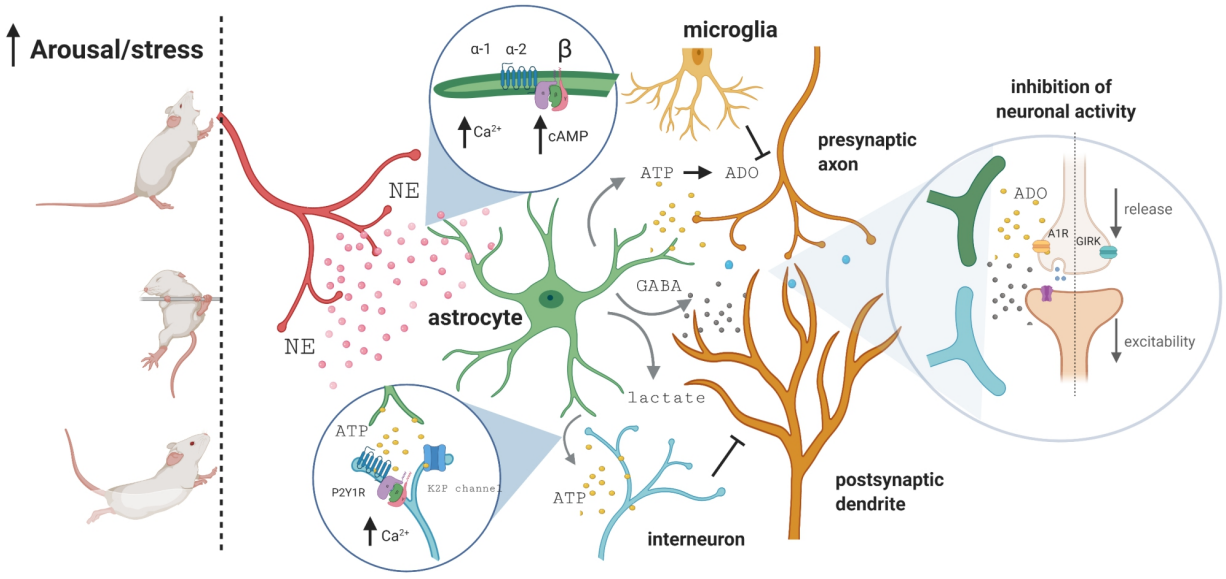

Figure 2. Astrocytes integrate noradrenergic signals and enhance local inhibition during states of heightened arousal. During periods of increased stress (left), noradrenergic axons projecting from the locus coeruleus release norepinephrine (NE) which activates astrocytes throughout the brain. Astrocytes respond to NE through both alpha- and beta-adrenergic receptors which induce elevations in astrocytic calcium and cyclic AMP levels respectively (middle top). In response to activation by NE, astrocytes have been shown to modulate neuronal activity through the release of ATP, GABA, and lactate into the extracellular space where microglia may further process ATP into adenosine (ADO). NE induced release of ATP from astrocytes reduces circuit activity through multiple parallel pathways. ADO acting on presynaptic A1 receptors (middle right) has been shown to decrease the release of glutamate, while ATP acting through P2Y1 receptors on interneurons (middle bottom, right) has been shown to increase the release of GABA, thereby decreasing postsynaptic excitability.

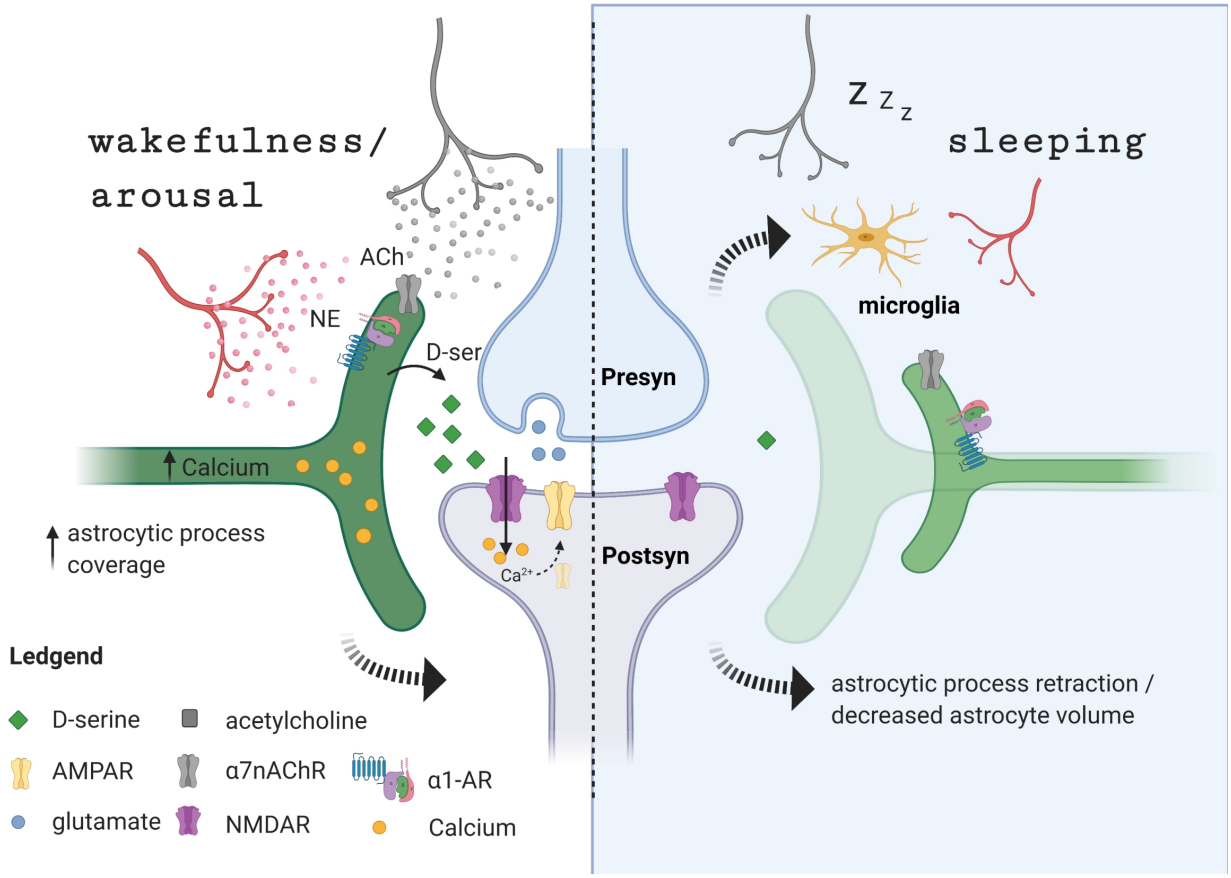

Figure 3. Astrocytic volume and proximity of processes to synapses changes across sleep-wake cycle. Wakefulness is associated with increased cholinergic tone which is sensed by α7nAChRs on astrocytes and leads to an increase in D-serine release. D-serine enhances NMDAR activity on nearby postsynaptic neurons. Astrocytic coverage of synapses is increased during periods of wakefulness (left) and decreased during periods of rest and during other physiological conditions (right). Lower levels of NE present during sleep facilitates microglial surveillance (right).

References

1. Brown, R.E., et al., *Control of sleep and wakefulness.* Physiol Rev, 2012. **92**(3): p. 1087-187.
2. Klimesch, W., *α-band oscillations, attention, and controlled access to stored information.* Trends Cogn Sci, 2012. **16**(12): p. 606-17.
3. Baertsch, N.A., H.C. Baertsch, and J.M. Ramirez, *The interdependence of excitation and inhibition for the control of dynamic breathing rhythms.* Nat Commun, 2018. **9**(1): p. 843.
4. Buskila, Y., A. Bellot-Saez, and J.W. Morley, *Generating Brain Waves, the Power of Astrocytes.* Front Neurosci, 2019. **13**: p. 1125.
5. Fields, R.D., et al., *Glial biology in learning and cognition.* Neuroscientist, 2014. **20**(5): p. 426-31.
6. Santello, M., N. Toni, and A. Volterra, *Astrocyte function from information processing to cognition and cognitive impairment.* Nat Neurosci, 2019. **22**(2): p. 154-166.
7. Bellot-Saez, A., et al., *Astrocytic modulation of cortical oscillations.* Sci Rep, 2018. **8**(1): p. 11565.
8. Khakh, B.S. and M.V. Sofroniew, *Diversity of astrocyte functions and phenotypes in neural circuits.* Nat Neurosci, 2015. **18**(7): p. 942-52.
9. Peterson, A.R. and D.K. Binder, *Astrocyte Glutamate Uptake and Signaling as Novel Targets for Antiepileptogenic Therapy.* Front Neurol, 2020. **11**: p. 1006.
10. Kofuji, P. and A. Araque, *Astrocytes and Behavior.* Annu Rev Neurosci, 2021.
11. Araque, A., et al., *Gliotransmitters travel in time and space.* Neuron, 2014. **81**(4): p. 728-39.
12. Perea, G., M. Navarrete, and A. Araque, *Tripartite synapses: astrocytes process and control synaptic information.* Trends Neurosci, 2009. **32**(8): p. 421-31.
13. Semyanov, A., C. Henneberger, and A. Agarwal, *Making sense of astrocytic calcium signals - from acquisition to interpretation.* Nat Rev Neurosci, 2020. **21**(10): p. 551-564.
14. Rusakov, D.A., *Disentangling calcium-driven astrocyte physiology.* Nat Rev Neurosci, 2015. **16**(4): p. 226-33.
15. Buzsáki, G. and A. Draguhn, *Neuronal oscillations in cortical networks.* Science, 2004. **304**(5679): p. 1926-9.
16. Trujillo, C.A., et al., *Complex Oscillatory Waves Emerging from Cortical Organoids Model Early Human Brain Network Development.* Cell Stem Cell, 2019. **25**(4): p. 558-569.e7.
17. Voytek, B., et al., *Oscillatory dynamics coordinating human frontal networks in support of goal maintenance.* Nat Neurosci, 2015. **18**(9): p. 1318-24.
18. Voytek, B. and R.T. Knight, *Dynamic network communication as a unifying neural basis for cognition, development, aging, and disease.* Biol Psychiatry, 2015. **77**(12): p. 1089-97.
19. Muller, L., et al., *Cortical travelling waves: mechanisms and computational principles.* Nat Rev Neurosci, 2018. **19**(5): p. 255-268.

20. Salinas, E. and T.J. Sejnowski, *Correlated neuronal activity and the flow of neural information.* Nat Rev Neurosci, 2001. **2**(8): p. 539-50.
21. Karakaş, S. and R.J. Barry, *A brief historical perspective on the advent of brain oscillations in the biological and psychological disciplines.* Neurosci Biobehav Rev, 2017. **75**: p. 335-347.
22. Lee, H.S., et al., *Astrocytes contribute to gamma oscillations and recognition memory.* Proc Natl Acad Sci U S A, 2014. **111**(32): p. E3343-52.
23. Gu, X., et al., *Synchronized Astrocytic Ca(2+) Responses in Neurovascular Coupling during Somatosensory Stimulation and for the Resting State.* Cell Rep, 2018. **23**(13): p. 3878-3890.
24. Lines, J., et al., *Astrocytes modulate sensory-evoked neuronal network activity.* Nat Commun, 2020. **11**(1): p. 3689.
25. Wang, X., et al., *Astrocytic Ca2+ signaling evoked by sensory stimulation in vivo.* Nat Neurosci, 2006. **9**(6): p. 816-23.
26. Li, A., et al., *Effects of different anesthetics on oscillations in the rat olfactory bulb.* J Am Assoc Lab Anim Sci, 2012. **51**(4): p. 458-63.
27. Thrane, A.S., et al., *General anesthesia selectively disrupts astrocyte calcium signaling in the awake mouse cortex.* Proc Natl Acad Sci U S A, 2012. **109**(46): p. 18974-9.
28. Mulkey, D.K., et al., *Putative roles of astrocytes in general anesthesia.* Curr Neuropharmacol, 2021.
29. Bojarskaite, L., et al., *Astrocytic Ca(2+) signaling is reduced during sleep and is involved in the regulation of slow wave sleep.* Nat Commun, 2020. **11**(1): p. 3240.
30. Ingiosi, A.M., et al., *A Role for Astroglial Calcium in Mammalian Sleep and Sleep Regulation.* Curr Biol, 2020. **30**(22): p. 4373-4383.e7.
31. Bellot-Saez, A., et al., *Astrocytic modulation of neuronal excitability through K.* Neurosci Biobehav Rev, 2017. **77**: p. 87-97.
32. Sicca, F., et al., *Gain-of-function defects of astrocytic Kir4.1 channels in children with autism spectrum disorders and epilepsy.* Sci Rep, 2016. **6**: p. 34325.
33. Bellot-Saez, A., et al., *Neuromodulation of Astrocytic K(+) Clearance.* Int J Mol Sci, 2021. **22**(5).
34. Fellin, T., et al., *Neuronal synchrony mediated by astrocytic glutamate through activation of extrasynaptic NMDA receptors.* Neuron, 2004. **43**(5): p. 729-43.
35. Poskanzer, K.E. and R. Yuste, *Astrocytes regulate cortical state switching in vivo.* Proc Natl Acad Sci U S A, 2016. **113**(19): p. E2675-84.
36. Mederos, S., et al., *GABAergic signaling to astrocytes in the prefrontal cortex sustains goal-directed behaviors.* Nat Neurosci, 2021. **24**(1): p. 82-92.
37. Sakatani, S., et al., *Neural-activity-dependent release of S100B from astrocytes enhances kainate-induced gamma oscillations in vivo.* J Neurosci, 2008. **28**(43): p. 10928-36.

38. Brockett, A.T., et al., *Evidence supporting a role for astrocytes in the regulation of cognitive flexibility and neuronal oscillations through the Ca2+ binding protein S100β.* PLoS One, 2018. **13**(4): p. e0195726.
39. Wang, J. and O.P. Hamill, *Piezo2, a pressure sensitive channel is expressed in select neurons of the mouse brain: a putative mechanism for synchronizing neural networks by transducing intracranial pressure pulses.* bioRxiv, 2020: p. 2020.03.24.006452.
40. Choi, H.J., D. Sun, and T.C. Jakobs, *Astrocytes in the optic nerve head express putative mechanosensitive channels.* Mol Vis, 2015. **21**: p. 749-66.
41. Bellesi, M., et al., *Effects of sleep and wake on astrocytes: clues from molecular and ultrastructural studies.* BMC Biol, 2015. **13**: p. 66.
42. Paukert, M., et al., *Norepinephrine controls astroglial responsiveness to local circuit activity.* Neuron, 2014. **82**(6): p. 1263-70.
43. Slezak, M., et al., *Distinct Mechanisms for Visual and Motor-Related Astrocyte Responses in Mouse Visual Cortex.* Curr Biol, 2019. **29**(18): p. 3120-3127 e5.
44. Mu, Y., et al., *Glia Accumulate Evidence that Actions Are Futile and Suppress Unsuccessful Behavior.* Cell, 2019. **178**(1): p. 27-43.e19.
45. Deemyad, T., J. Lüthi, and N. Spruston, *Astrocytes integrate and drive action potential firing in inhibitory subnetworks.* Nat Commun, 2018. **9**(1): p. 4336.
46. Oe, Y., et al., *Distinct temporal integration of noradrenaline signaling by astrocytic second messengers during vigilance.* Nat Commun, 2020. **11**(1): p. 471.
47. Li, Y., et al., *Activation of astrocytes in hippocampus decreases fear memory through adenosine A1 receptors.* Elife, 2020. **9**.
48. Gaidin, S.G., et al., *Activation of alpha-2 adrenergic receptors stimulates GABA release by astrocytes.* Glia, 2020. **68**(6): p. 1114-1130.
49. Chen, C., et al., *Astrocytes Amplify Neuronal Dendritic Volume Transmission Stimulated by Norepinephrine.* Cell Rep, 2019. **29**(13): p. 4349-4361 e4.
50. Tan, Z., et al., *Glia-derived ATP inversely regulates excitability of pyramidal and CCK-positive neurons.* Nat Commun, 2017. **8**: p. 13772.
51. Yang, J., et al., *Na(+)-Ca(2)(+) exchanger mediates ChR2-induced [Ca(2)(+)]i elevation in astrocytes.* Cell Calcium, 2015. **58**(3): p. 307-16.
52. Eggermann, E., et al., *Cholinergic signals in mouse barrel cortex during active whisker sensing.* Cell Rep, 2014. **9**(5): p. 1654-1660.
53. Papouin, T., et al., *Septal Cholinergic Neuromodulation Tunes the Astrocyte-Dependent Gating of Hippocampal NMDA Receptors to Wakefulness.* Neuron, 2017. **94**(4): p. 840-854 e7.
54. Van Horn, M.R., et al., *The Gliotransmitter d-Serine Promotes Synapse Maturation and Axonal Stabilization In Vivo.* J Neurosci, 2017. **37**(26): p. 6277-6288.

55. Xie, L., et al., *Sleep drives metabolite clearance from the adult brain.* Science, 2013. **342**(6156): p. 373-7.
56. Panatier, A., et al., *Glia-derived D-serine controls NMDA receptor activity and synaptic memory.* Cell, 2006. **125**(4): p. 775-84.
57. Parkhurst, C.N., et al., *Microglia promote learning-dependent synapse formation through brain-derived neurotrophic factor.* Cell, 2013. **155**(7): p. 1596-609.
58. Schafer, D.P., et al., *Microglia sculpt postnatal neural circuits in an activity and complement-dependent manner.* Neuron, 2012. **74**(4): p. 691-705.
59. Sipe, G.O., et al., *Microglial P2Y12 is necessary for synaptic plasticity in mouse visual cortex.* Nat Commun, 2016. **7**: p. 10905.
60. Stowell, R.D., et al., *Noradrenergic signaling in the wakeful state inhibits microglial surveillance and synaptic plasticity in the mouse visual cortex.* Nat Neurosci, 2019. **22**(11): p. 1782-1792.
61. Liu, Y.U., et al., *Neuronal network activity controls microglial process surveillance in awake mice via norepinephrine signaling.* Nat Neurosci, 2019. **22**(11): p. 1771-1781.
62. Murphy-Royal, C., et al., *Stress gates an astrocytic energy reservoir to impair synaptic plasticity.* Nat Commun, 2020. **11**(1): p. 2014.
63. Guyenet, P.G., et al., *The Retrotrapezoid Nucleus: Central Chemoreceptor and Regulator of Breathing Automaticity.* Trends Neurosci, 2019. **42**(11): p. 807-824.
64. Rajani, V., et al., *Release of ATP by preBotzinger complex astrocytes contributes to the hypoxic ventilatory response via a Ca2+ -dependent P2Y1 receptor mechanism.* J Physiol, 2017.
65. Funk, G.D., et al., *Neuroglia and their roles in central respiratory control; an overview.* Comparative Biochemistry and Physiology, Part A, 2015. **186**: p. 83-95.
66. Kasymov, V., et al., *Differential Sensitivity of Brainstem versus Cortical Astrocytes to Changes in pH Reveals Functional Regional Specialization of Astroglia.* The Journal of Neuroscience, 2013. **33**(2): p. 435-441.
67. Wenker, I.C., et al., *Regulation of ventral surface CO2/H+-sensitive neurons by purinergic signaling.* Journal of Physiology, 2012. **590**(9): p. 2137-2150.
68. Gourine, A.V., et al., *Astrocytes control breathing through pH-dependent release of ATP.* Science, 2010. **329**(5991): p. 571-5.
69. Turovsky, E., et al., *Mechanisms of CO2/H+ Sensitivity of Astrocytes.* J Neurosci, 2016. **36**(42): p. 10750-10758.
70. Cleary, C.M., et al., *Vascular control of the CO2/H(+)-dependent drive to breathe.* Elife, 2020. **9**.
71. Patterson, K.C., et al., *Kir 5.1-dependent CO2 /H(+) -sensitive currents contribute to astrocyte heterogeneity across brain regions.* Glia, 2021. **69**(2): p. 310-325.
72. Falquetto, B., et al., *Inhibition of the hypercapnic ventilatory response by adenosine in the retrotrapezoid nucleus in awake rats.* Neuropharmacology, 2018. **138**: p. 47-56.

73. Guyenet, P.G. and D.K. Mulkey, *Retrotrapezoid nucleus and parafacial respiratory group.* Respir Physiol Neurobiol, 2010. **173**(3): p. 244-55.
74. Forsberg, D., T. Ringstedt, and E. Herlenius, *Astrocytes release prostaglandin E2 to modify respiratory network activity.* eLIFE, 2017. **6**(e29566).
75. Forsberg, D., et al., *CO2-evoked release of PGE2 modulates sighs and inspiration as demonstrated in brainstem organotypic culture.* Elife, 2016. **5**.
76. Beltrán-Castillo, S., et al., *D-serine released by astrocyte in brainstem regulates breathing response to CO2 levels.* Nature Communications, 2017. **8**(838).
77. Schnell, C., J. Fresemann, and S. Hulsmann, *Determinants of functional coupling between astrocytes and respiratory neurons in the pre-Botzinger complex.* PLoS One, 2011. **6**(10): p. e26309.
78. Sheikhbahaei, S., et al., *Astrocytes modulate brainstem respiratory rhythm-generating circuits and determine exercise capacity.* Nat Commun, 2018. **9**(1): p. 370.
79. SheikhBahaei, S., et al., *Morphometric analysis of astrocytes in brainstem respiratory regions.* J Comp Neurol, 2018. **526**(13): p. 2032-2047.
80. Tort, A.B.L., J. Brankack, and A. Draguhn, *Respiration-Entrained Brain Rhythms Are Global but Often Overlooked.* Trends Neurosci, 2018. **41**(4): p. 186-197.
81. Tort, A.B.L., et al., *Parallel detection of theta and respiration-coupled oscillations throughout the mouse brain.* Sci Rep, 2018. **8**(1): p. 6432.
82. Corcoran, A.W., G. Pezzulo, and J. Hohwy, *Commentary: Respiration-Entrained Brain Rhythms Are Global but Often Overlooked.* Front Syst Neurosci, 2018. **12**: p. 25.
83. Heck, D.H., et al., *Breathing as a Fundamental Rhythm of Brain Function.* Front Neural Circuits, 2016. **10**: p. 115.
84. Zhong, W., et al., *Selective entrainment of gamma subbands by different slow network oscillations.* Proc Natl Acad Sci U S A, 2017. **114**(17): p. 4519-4524.
85. Chemes, E. and C. Ciaume, *Astrocyte Calcium Waves: What They Are and What They Do.* Glia, 2006. **54**(7): p. 716-725.
86. Cornell-Bell, A.H., et al., *Glutamate induces calcium waves in cultured astrocytes: long-range glial signaling.* Science, 1990. **247**(4941): p. 470-3.
87. Kuga, N., et al., *Large-scale calcium waves traveling through astrocytic networks in vivo.* J Neurosci, 2011. **31**(7): p. 2607-14.
88. Anderson, T.M., et al., *A novel excitatory network for the control of breathing.* Nature, 2016. **536**(7614): p. 76-80.
89. Smith, J.C., et al., *Pre-Bötzinger Complex: A Brainstem Region That May Generate Respiratory Rhythm in Mammals.* Science, 1991. **254**(5032): p. 726-729.

90. Spyer, K.M. and A.V. Gourine, *Chemosensory pathways in the brainstem controlling cardiorespiratory activity.* Philos Trans R Soc Lond B Biol Sci, 2009. **364**(1529): p. 2603-10.
91. Batiuk, M.Y., et al., *Identification of region-specific astrocyte subtypes at single cell resolution.* Nat Commun, 2020. **11**(1): p. 1220.
92. Bayraktar, O.A., et al., *Astrocyte layers in the mammalian cerebral cortex revealed by a single-cell in situ transcriptomic map.* Nat Neurosci, 2020. **23**(4): p. 500-509.
93. Martín, R., et al., *Circuit-specific signaling in astrocyte-neuron networks in basal ganglia pathways.* Science, 2015. **349**(6249): p. 730-4.
94. Navarrete, M. and A. Araque, *The Cajal school and the physiological role of astrocytes: a way of thinking.* Front Neuroanat, 2014. **8**: p. 33.
95. DeFelipe, J., *Cajal's Butterflies of the Soul: science and art*. 2010, New York, New York: Oxford University Press.
96. Swanson, L.W., et al., *The Beautiful Brain: The Drawings of Santiago Ramon y Cajal*. 2009: Abrams.

The psychophysiology of the sigh:
I: The sigh from the physiological perspective.

Liza Severs [3,4], Elke Vlemincx[1,2], & Jan-Marino Ramirez[3,4]

[1] Department of Health Sciences, Vrije Universiteit Amsterdam
de Boelelaan 1085, 1081HV, Amsterdam, Netherlands

[2] Health Psychology, KU Leuven
Tiensestraat 102, 3000 Leuven, Belgium

[3] Center for Integrative Brain Research, Seattle Children's Research Institute
1900 9th Avenue Seattle, WA 98101

[4] Department of Neurological Surgery, Department of Physiology and Biophysics, School of Medicine, University of Washington
1660 S. Columbian Way
Seattle, WA 98108

Severs, L.J.: Liza.severs@seattlechildrens.org
Ramirez, J.R.: Nino1@uw.edu
Vlemincx, E.: e.vlemincx@vu.nl

Under Review at Biological Psychology for a special issue review

Abstract

Breathing consists of several behaviors under autonomic and voluntary control and are bidirectionally regulated. One behavioral component is the sigh, which serves distinct physiological and psychological roles. In two accompanying reviews we will discuss these roles. The present review focuses on the physiological function, where sighs play a critical role in controlling lung compliance by preventing the collapse of alveoli. Implicated in the generation of sighs and normal breathing is the preBötzinger Complex, a rhythmogenic network in the medulla. Although sighs and normal inspiration are generated within the same network, they show distinct temporal characteristics. While sighs occur every few minutes, normal breathing is generated in the range of seconds. Both are differentiated by distinct modulatory and synaptic mechanisms, and recent evidence indicates that these mechanisms are regulated by inputs from different regions of the brain. An important modulator of sighs is hypoxia, implicating sighs in the arousal response.

Introduction

The ventilatory role of breathing is critical for homeostatic regulation of oxygen and carbon dioxide in the blood (1, 2). Yet, there is significantly more to breathing aside from the regulation of blood gases. Breathing is perhaps the most physiologically integrated behavior and is strongly adapted with metabolic, emotional, and cognitive state changes and behaviors (3-5). This state-dependency is bi-directional, since breathing also influences these same activity states. For example, breathing changes in response to pain, anxiety, panic, worry, joy, desire, and relief; conversely, breathing can be a driver of anxiety, panic, and relief, hyperventilation, and can sometimes even induce seizures (6-9). The ability of breathing to alter cognitive, emotional, and metabolic states offers important therapeutic opportunities as has long been recognized in Eastern Medicine (10). While breathing techniques have become very popular for stress management and relaxation purposes, only recently has research started to investigate the potential of breathing techniques as therapeutic add-ons to standard treatment in Western Medicine (11).

However, considering breathing as one behavior is too simplistic. Eupneic breathing ("normal breathing"), gasping, and sighing are distinct breathing behaviors with distinct physiological and psychological roles (12, 13). This raises an important question that may seem purely semantic: Do these different breathing activities constitute different behaviors or different patterns of the same behavior? Neurophysiologists have debated this question for more than a century, and based on lesion experiments, Lumsden postulated in the early 1900's that eupneic breathing and gasping are generated by separate centers located in different regions of the brain (14). He referred to the pneumotaxic center in the pons and the gasping center in the medulla as being the brainstem regions responsible for the generation of eupnea and gasping, respectively. *In vitro* approaches combined with contemporary transgenic and electrophysiological experiments *in vivo* provided an alternative explanation: that the same network can reconfigure to generate distinct motor behaviors (12). The more we learn about the underlying neurobiology, the more it becomes clear that there is no simple answer. Sighs, gasps, and eupnea are three separate motor behaviors that are distinct, yet mechanistically overlapping (12, 15-17).

In two back-to-back reviews we will focus specifically on one of these breathing behaviors, the sigh, which has long been recognized for its distinct physiological (Part 1) and psychological properties (Part 2).

The 'Sigh Reflex'

Sighs are considered a reflex; these deep breaths can be activated by sensory afferents such as lung stretch receptors (18) that respond to a decrease in lung compliance (19). Moreover, bilateral vagotomy abolishes sighs in rabbits and dogs (19, 20), suggesting that afferent input is required for the generation of sighs. Yet, this has not been confirmed by other studies; instead, it has been shown that sighs reappear post-vagotomy (21-23), and persist following lung transplantation in humans (24). Furthermore, sighs respond to chemosensory inputs as hypoxia increases sigh frequency (23, 25-28). This stimulatory effect depends in part on carotid body inputs, as has been demonstrated by carotid body (CB) denervation studies. However, these studies also show that CB input is not necessary for generating sighs, since sighs persist and continue to respond to hypoxia (29), and hypercapnia (27, 30) following denervation.

Still, these afferent inputs are functionally important. For example, combined mechano- and chemosensory inputs likely activate sighs in response to atelectasis (13, 31). The tidal volume of a sigh, more than two times larger than a normal "eupneic breath", allows sighs to reinflate the partially collapsed and under-ventilated regions of the lung, thereby increasing lung compliance (32, 33), and restoring the ventilation/perfusion ratio thereby maintaining normal lung function (23). Thus, sighs play a critical homeostatic role in maintaining the physiological partial pressure range for arterial O_2 and CO_2. In this functional context, the sigh serves as an important reflex that is activated by several relevant sensory inputs.

The origin of the sigh

The importance of the sigh as a reflex suggests that the generation of this large tidal volume is a result of mechanosensory inputs augmenting a normal breath. Indeed, this interpretation inspired the early vagotomy experiments as mentioned above, and this notion continues to persist as indicated by the somewhat misleading, synonymous use of the term "augmented breath" when referring to sighs. The fact that sighs are not simply breaths that are augmented by sensory inputs has clearly been demonstrated in brainstem slice preparations (12, 17). The generation of neuronal activity driving sigh activity persists even in small, isolated wedges of brain tissue containing one region of the medulla: the preBötzinger complex (preBötC) (Fig. 1) (17). This approach not only demonstrates that sighs constitute a centrally generated motor behavior but also that sighs possess physiological properties that differentiate them from normal breathing irrespective of the sensory inputs that clearly play a role *in vivo*.

Sighs are periodically generated within the preBötC and occur spontaneously and concurrently with the much faster respiratory drive for rhythmic eupneic activity which, like sigh activity, also persists in the absence of any sensory input. The periodic nature of the sigh is also seen in intact animals and humans. Furthermore, sighs occur more frequently in human infants where they occur every few minutes (34, 35), persisting into adulthood, albeit at a lower frequency (8, 36-38).

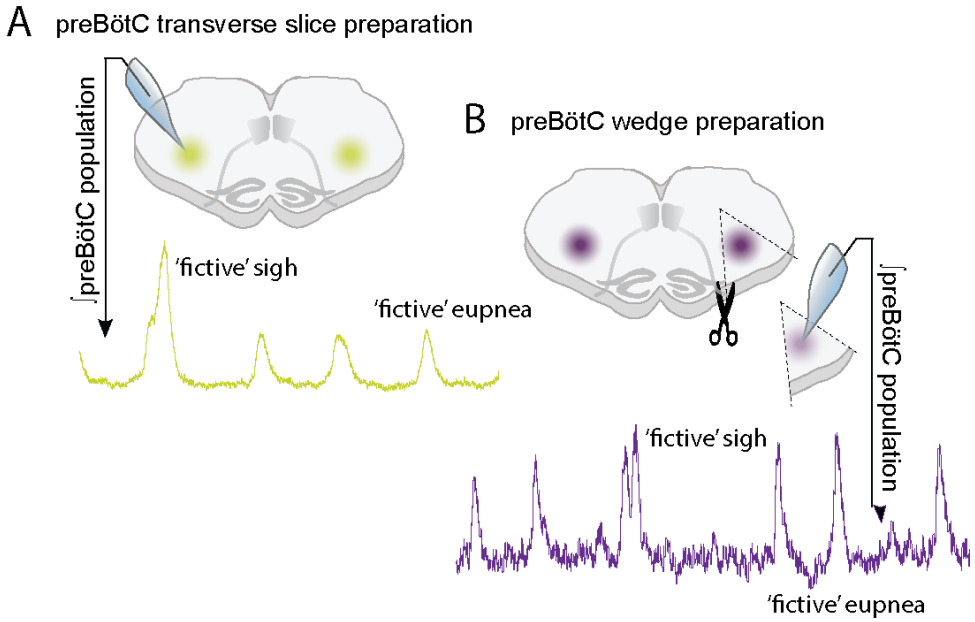

Figure 1. (A) The medullary brain slice transverse preparation containing the preBötzinger Complex (preBötC) generates both fictive eupnea and sigh activity. (B) Fictive eupnea and sigh activity can further be maintained in a small wedge isolated form the transverse preBötC slice. Figure is modified from Tryba et. al. 2006.

The possibility to preserve sighs *in vitro* enabled rigorous cellular investigations aimed at unraveling the neuronal mechanisms that differentiate sighs from normal breathing. Recordings obtained from the preBötC network indicated that the vast majority of rhythmic neurons are activated during both normal, “eupneic” and sigh respiratory activity. A small proportion of sigh-only neurons was identified within the preBötC, but these sigh-only neurons do not possess obvious pacemaker or other regenerative properties that would suggest that they “pace” the sigh rhythm (17). Thus, these insights remain puzzling: how can a shared neuronal network generate two motor activities with distinct temporal properties?

Several neuronal mechanisms distinguish sighs from eupneic activity. One of these is the dependence on the P/Q-type calcium current. Blocking this calcium channel subtype selectively

abolishes sighs, but not eupneic activity *in vitro* (15). The genetic knockout of P/Q-type calcium channels in mice confirmed this pharmacological evidence. These mutant mice survive initially, because of their continued ability to generate eupneic breathing, but they eventually succumb to pneumonia and atelectasis due to the failure to sigh (39). Sigh generation also depends on a specific metabotropic glutamate receptor (subtype 8, group III) suggesting that the synchronization giving rise to the large amplitude sigh burst depends on glutamatergic mechanisms that differ from those responsible for the eupneic burst (16).

Sighs also seem to depend on the persistent sodium current (INap) as suggested by pharmacological experiments, and the intriguing observation that certain INap- dependent pacemaker neurons can concurrently generate small amplitude, eupneic-like bursts occurring at a faster eupneic-like frequency, as well as sigh-like high-amplitude bursts occurring at a slower sigh-like frequency (40, 41). Even following pharmacological isolation, these two burst types are differentially modulated by muscarinic agonists in a manner that is consistent with the network response: oxotremorine inhibits eupnea while activating large amplitude sigh-like bursts (17). These experiments taken together indicate that distinct neuronal mechanisms contribute to the generation of sighs and eupnea. However, how these mechanisms work together to generate two rhythmic activities with very different temporal, modulatory (42-45), metabolic (29), and physiological properties (46) remains largely unknown.

More recent studies suggest that modulation from areas rostral of the preBötC, or slices that contain more rostral sections of the preBötC favor sigh generation (47, 48). Anatomically, preBötC slices that extend further rostral exhibit more sighs, whereas slices which retain more caudal sections reportedly do not (47). There are many possible explanations for this rostro-caudal gradient. Differential receptor subtype expression allowing sighs to be modulated in the preBötC could be eliminated in more caudal slice preparations, thereby potentially reducing the probability of the network to reconfigure to generate sigh bursts. Rostral structures such as the peptidergic circuit postulated to control sigh modulation will likely also facilitate the generation of sighs (48). These modulatory inputs, however, are not essential for rhythmogenesis, since sighs can still be generated in the isolated preBötC as discussed above (17).

There are a number of neuromodulators known to alter sigh frequency including metabotropic glutamate receptors, (16), substance P (SP) (47), norepinephrine (NE) (41), and acetylcholine (17). Thus, the notion that a singular neuromodulator is responsible for sigh generation is likely an oversimplification. Indeed, it is probable that these modulators act together to differentially orchestrate breathing and the generation of sighs, as well as function to

coordinate feedback with the rest of the brain. Some modulators will only activate sighs, as was described for norepinephrine acting on β-adrenergic receptors (41), the bombesin-like peptides neuromedin B (NMB) and gastrin releasing peptide (GRP) (48). Other neuromodulators will facilitate the generation of sigh and simultaneously inhibit eupneic breathing like oxotremorine acting on muscarinic acetylcholine receptors (17). Moreover, various neuromodulators activate both sighs and eupneic breathing synergistically like serotonin (42), noradrenergic modulation acting on alpha-receptors (49), or substance P via NK1 receptors (47). These synergistically acting modulators could target Dbx1 or Vglut2 populations within the preBötC, since optogenetic activation of these neurons evokes both eupnea and sighs. Somatostatin (SST) has inhibitory effects on both rhythms; however, it appears that SST has a more dramatic effect on sighs since this neuromodulator completely abolishes sighing while reducing eupneic frequency (50). An important question is how neurons located in different regions differentially modulate sighs within a behavioral context. It has been demonstrated that C1 neurons within the RTN activate arousal and sighs. Interestingly, selectively stimulating NMB neurons in this region failed to stimulate sighs (51), which is inconsistent with the hypothesis that NMB plays a critical role in the generation of sighs (48). Indeed, it is more likely that NMB neurons in the RTN are critical for the generation of sneezing, given that stimulating NMB neurons in this region evokes active expiration (51). NMB neurons also receive input from sneeze-evoking regions that are activated by irritants in the nose and these neurons project to the caudal VRG to activate the sneezing behavior (52).

During the normal eupneic cycle sighs typically occur every 5-30 minutes in slice preparations, but rarely occur more frequently without the application of certain modulators (e.g. norepinephrine, βAr1/2 agonist). Even with these neuromodulators, sighs do not occur sequentially. This suggests that the sigh has a refractoriness, similar to normal eupneic activity (53), an idea that remains relatively unexplored. The refractory period of the sigh rhythm could be tied to calcium overactivation in the network, and could also explain why a high amount of variability in the sigh rhythm is observed in transverse preBötC slices, analogous to altering the state of the eupneic network with varying concentrations of potassium (47, 54).

Differential inhibition has been suggested as a potential mechanism for how eupnea and sighs can both be generated simultaneously from within the preBötC. The emergence of sigh rhythmogenesis during late prenatal to early postnatal stages in the mouse were suggested to be, at least in part, due to the role of glycinergic inhibition (55, 56). However, further experimentation has indicated that inhibition during later postnatal stages and into adulthood

does not have any effect on the regulation or control of sighs (48, 57), a finding that may be due to developmental lineage changes that occur during these earlier time points (58).

The generation of sighs within the preBötC may be related to the stability of the respiratory rhythm as observed in different slice preparations. The horizontal slice preparation produces a much more stable network state with a reduction in the frequency of sighs. This could be a result of the network being more intact and includes a larger population of both excitatory and inhibitory neurons or could also indicate that other more dorsal areas contribute to sigh generation and are not included in this slice preparation. The horizontal slice preparation with slower rhythms and reduced sigh frequency, albeit complete lack of sighs in some cases, certainly is more similar to the *in vivo* anesthetized preparation (5).

There are several recent studies that suggest astrocytes could play a role in sigh modulation. Astrocytes have more recently been found to underly many of the functions of areas endowed with chemosensitive properties, such as the RTN/pFRG region (59-62). Here, astrocytes are known to express pH sensitive currents which are characteristic of Kir4.1-Kir5.1 channels (63, 64) and release different neuromodulators including some vasoactive substances which are able to alter breathing frequency (e.g., prostaglandin E2 (PGE2), ATP, and D-serine (60, 61, 65-70). Furthermore, astrocytes express many similar receptor subtypes as neurons, and therefore could modulate neuronal activity through different types of gliotransmitter release in response to activation by similar molecules. Astrocytes are further implicated in regulating breathing during metabolic changes, such as during physical exertion (60). Nevertheless, the direct role of astrocytes in modulating sighing is still under direct investigation.

Sighs and arousal

A clear indication that sighs are not only linked to the control of large lung volume comes from its association with arousal, indicating the role of largely unknown sigh circuitry in connecting to the rest of the brain (25). Sighs occur simultaneously with arousal (71), as well as during REM and NREM sleep states and the transition between these ‘state switches’ (71-73). Sighs often occur at the initiation of the arousal response, preceding apneas, following increased somatic activity, variable heart rate deceleration, and during sleep state transitions (74). In order to explore whether this arousal response may play a role in sudden infant death syndrome (SIDS), behavioral studies confirmed that in infants, arousal begins with the occurrence of a sigh (i.e., augmented breath), followed by thrashing, eye opening, and repositioning of the head (71, 75, 76). Indeed, there are reports indicating that some SIDS or

near-miss cases report with a reduction in the number of arousals from sleep (77-84). However, more studies are required in this area to determine if there is a concrete role for sighing in SIDS victims. As already mentioned, sighs are particularly sensitive to hypoxic challenge (12, 23, 27, 85-88); moreover, chemical sensitivity to hypoxia exists in the isolated brainstem slice preparation (Fig. 2) (12, 88). Further mechanistic insights into the association of sighs and arousal come from optogenetic experiments indicating that sighs and the associated cardiorespiratory response are activated by C1 noradrenergic neurons prior to arousal (51, 89-91). These catecholaminergic neurons could activate sighs via β-adrenergic receptors known to specifically activate sighs (41).

The sensitivity to hypoxia and hypercapnia in the context of arousal may be one of the mechanisms that awakens babies sleeping in the prone position. This position leads to a buildup of expired CO_2 and a decrease in inspired O_2 (92-95). The change in blood gases will likely activate C1 neurons and sighs which would contribute to the arousal of the sleeping infant (75, 76). Therefore, in addition to the important role in atelectasis, sighs seem to also play a central role in the events leading to the arousal response and replenishing inspired O_2 (75, 76, 96-101).

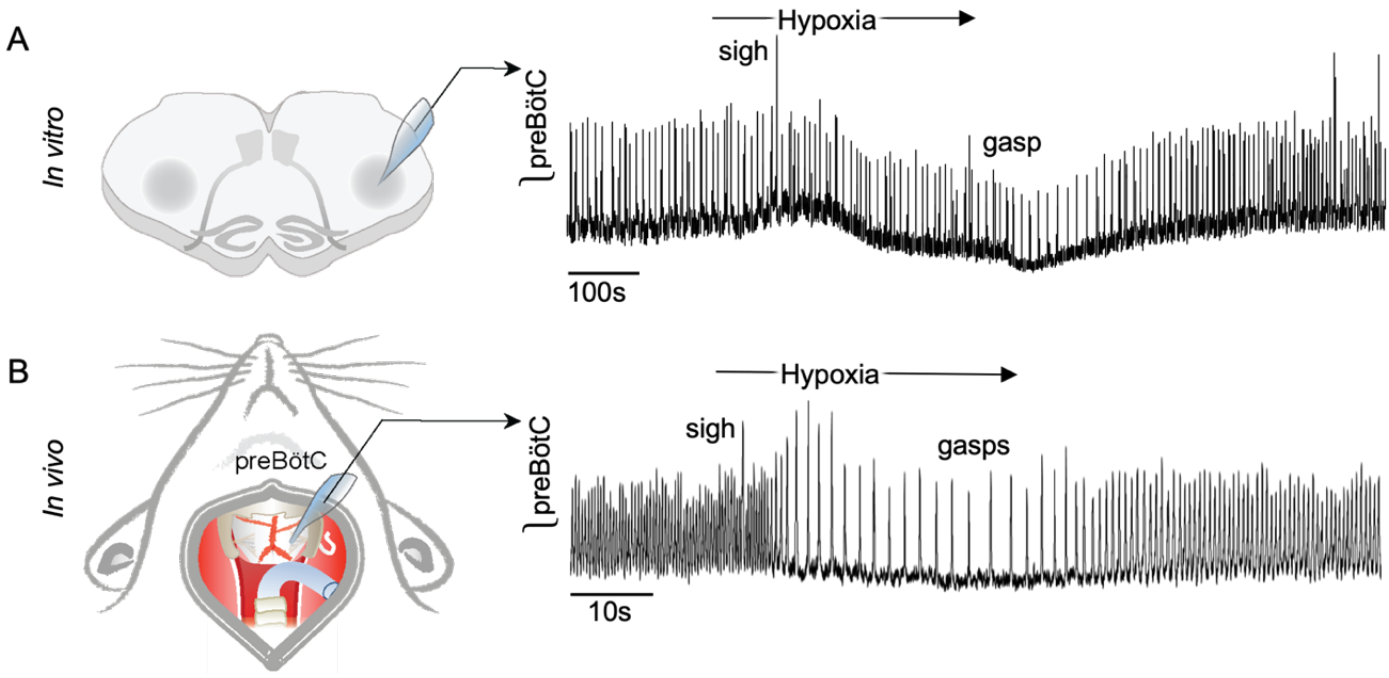

Figure 2. Hypoxic response in the *in vitro* preBötC transverse slice and in the *in vivo* anesthetized preparation. (A-B) The augmenting phase of the hypoxic response, onset of sighs, decrease in respiratory frequency, and onset of gasping occurs similarly in both *in vitro* and *in vivo* preparations. Hypoxia was ended after start of gasping in (A).

Sighing and the control of brain states

The link between C1 neurons and the sigh could provide a mechanistic explanation for the role of sighs in the regulation of different brain states. Sigh generation is facilitated during the transition from wakefulness to NREM sleep, or from sleep to arousal (46, 89, 102, 103). C1 neurons innervate the locus coeruleus (LC), potentially increasing brain-wide noradrenaline by activating populations of neurons in the LC and adrenergic neurons in the pons via glutamatergic drive (104, 105). These C1 neurons are also responsive to hypoxic stimuli (106). Direct connections between orexinergic neurons and C1 neurons in the rostral ventrolateral medulla (RVLM) provide further support for the role of this system in regulating sighing behavior at the level of the preBötC (51, 89, 105, 107). Orexin, which is released from hypothalamus, will likely contribute to the association between sighing and the regulation of brain states during sleep-wake transitions. This neuropeptide modulates the critical breathing regions, both through direct projections to the preBötC (108) and through secondary connections from the LC (109). Orexin modulates chemosensitivity during wakefulness (110), is further related to stress and anxiety (111), and plays a significant role in the modulation of circadian rhythms (112, 113). Furthermore, studies utilizing the orexin receptor antagonist, almorexant, show that inhibition of orexin signaling reduces the frequency of sighs, as well as reduces the post-sigh apnea (114, 115). The involvement or orexin in regulating the sigh is not straightforward, however. Studies in a mouse knockout model of Orexin A/B show that these mice present with a narcoleptic phenotype and have further disruptions in REM sleep. Interestingly, these mice had an increase in the number of central apneas during sleep states, with no difference in sighs or post-sigh apneas. However, the authors did report a reduction in the CO_2- mediated ventilatory response (109, 116).

It is relatively well established that the orexin/hypocretin system modulates brain state in part through the LC (117). Projections of orexinergic neurons are most dense in the LC, and Orexin A increases firing of noradrenergic neurons within this area (117). Hypocretin expressing neurons within the lateral hypothalamic area have also recently been identified to activate claustrophobia-related sighing in mice (118).

Breathing rhythms are understood to contribute to oscillations in other brain regions (119, 120). Respiratory ‘entrained’ oscillations may arise from nasal respiration, initiated in the olfactory bulb and spread to cortical regions and the hippocampus (120-122). These rhythms may play a part in synchronizing activity states in different frequency ranges and are suggested to entrain a global rhythm throughout the brain (120, 123, 124). Although there is little evidence

as to the functional role of respiratory oscillations, it is suggested that coordination with nasal respiration may be a means of ‘active sensing’ of the environment, thereby organizing the brain’s neural activity in a manner consistent with an organism’s environment (119). In lieu of this hypothesis, it is reasonable to suggest that the sensitivity of the sigh rhythm by hypoxia and hypercapnia is an important component of active sensing, particularly so during infancy. Moreover, as discussed later in detail, the sigh has very important psychological roles (see accompanying manuscript); sighs are implicated in several anxiety disorders and are an overt expression of many emotions such as frustration, stress, anxiety and fear, depression, joy, desire and relief (37, 125-128). Neural projections from the rostral medulla to the preBötC release the neuropeptides neuromedin B (NMB) and gastrin releasing peptide (GRP) to stimulate sighing (48). The same circuit has more recently been identified as an ‘emotional sigh circuit’, as mice placed in confinement conditions experienced ‘emotional sighs’ which are also linked to NMB release from the same rostral area (118), perhaps indicating the role of bombesin-like peptides stimulates sighs initiated in the cortex, while other mechanisms drive sighing locally at the level of the preBötC. Thus, respiratory entrained oscillations, and sighs specifically, have important implications both physiologically and emotionally. Indeed, breathing techniques, such as meditative breathing and slow breathing, have been used as a therapeutic technique for anxiety disorders for thousands of years and are incorporated into many different medical practices all over the world.

Acknowledgements:

This manuscript was supported by the following NIH grants: **HL151389, HL126523, HL090554, HL144801, HL149156-03**

THE PSYCHOPHYSIOLOGY OF THE SIGH:
II: THE SIGH FROM THE PSYCHOLOGICAL PERSPECTIVE

Elke Vlemincx[1,2], Liza Severs [3,4] & Jan-Marino Ramirez[3,4]

[1] Department of Health Sciences, Vrije Universiteit Amsterdam
de Boelelaan 1085, 1081HV, Amsterdam, Netherlands

[2] Health Psychology, KU Leuven
Tiensestraat 102, 3000 Leuven, Belgium

[3] Center for Integrative Brain Research, Seattle Children's Research Institute
1900 9th Avenue Seattle, WA 98101

[4] Department of Neurological Surgery, Department of Physiology and Biophysics, School of Medicine, University of Washington
1660 S. Columbian Way
Seattle, WA 98108

Severs, L.J.: Liza.severs@seattlechildrens.org
Ramirez, J.R.: Nino1@uw.edu
Vlemincx, E.: e.vlemincx@vu.nl

Under Review at Biological Psychology for a special issue review

Introduction

Breathing is undoubtedly one of the most complex psychophysiological behaviors. Respiration consists of a multitude of parameters that constitute the breathing pattern: inspiratory and expiratory volume, time and pauses, thoracic and abdominal breathing, nasal and mouth breathing. Moreover, respiration is both under autonomic and voluntary control. Autonomic regulation of breathing is controlled by a central pattern generator (CPG) in the medulla, the so called preBötzinger complex, which is particularly important for determining inspiratory activity in a breath-by-breath manner. This CPG is integrated with other neural networks to respond to biopsychosocial changes (129). In addition, voluntary control of breathing constitutes intricate bidirectional effects between breathing and biopsychosocial states, is used for vocalization, and allows breathing to control one's biopsychosocial state. One such breathing behavior which is generated autonomically, but also has an important voluntary component, is the sigh. In this review, we will summarize the functionality of a sigh from a psychological perspective, adjoining the physiological properties of a sigh outlined in Part I.

Sighing as a maladaptive behavior

Physiologically, complex breathing patterns serve to maintain blood gas levels consistent with metabolic need (130). Breathing patterns resulting in deviations from normoxia and normocapnia, may cause respiratory symptoms, but importantly, respiratory symptoms caused by dysfunctional breathing patterns can also occur in the presence of stable gas levels. For example, hyperventilation (i.e. increased ventilation in excess of metabolic need), both in the presence and absence of hypocapnia (i.e. low arterial carbon dioxide pressure, for example due to excessive exhalation), leads to dyspnea (131-134). While the term 'dysfunctional breathing' has been long used for a variety of maladaptive breathing patterns, recently, a classification system has been proposed to better understand and define dysfunctional breathing patterns. One type of dysfunctional breathing is defined as periodic sighing (135), also labeled as sigh syndrome, sighing dyspnea or sighing breathing (136-140), which consists of frequent sighing leading to hyperventilation-induced hypocapnia and associated respiratory symptoms.

Sighing more frequently than normal has been observed in persons with anxiety disorders (141-145), motion sickness (146), pain (e.g. in chronic low back pain (147, 148), rheumatoid arthritis (149), traumatic brain injury (150)), hyperventilation syndrome (151, 152), and respiratory disease (153, 154). Particularly the association between anxiety disorders and frequent sighing has been well established; persons with panic disorder, post-traumatic stress

disorder and chronic anxiety, sigh more frequently than (healthy) controls during quiet sitting and resting periods (141-145, 155-157). Furthermore, the frequent sighing in panic disorder patients has been associated with chronic hypocapnia (143) and respiratory dysregulation indicated by high respiratory irregularity (145, 158, 159), suggesting that panic disorder patients sigh 'excessively' (i.e. sigh in excess of metabolic need). Importantly, however, it should be noted that these findings were observed in experimental laboratory studies in which quiet sitting and resting baseline measurements may constitute anticipatory anxiety in persons with anxiety disorders, and panic disorder particularly. Excessive sighing in panic disorder has not been observed in ambulatory studies (160). In sum, it seems that frequent sighing is characteristic of anxiety disorders, and sighing may be common in psychopathological states in general.

This raises the important question why frequent sighing is a hallmark of psychopathology? We propose that the sigh is not only an important regulator of respiration (e.g., blood gases and lung compliance), but also an often overlooked contributor to the homeostatic regulation of psychological states. Disturbances in its homeostatic regulation will lead to a variety of maladaptive psychopathological states. As we will discuss in detail below, the role of a sigh is hypothesized to lie in its ability to periodically reset psychophysiological states. The periodicity of this resetting property is under homeostatic control (8, 161). Consciously or unconsciously generated changes in this autonomically controlled periodicity can lead to chronic deviations from homeostasis of both respiration and psychological states, thereby driving the organism into psychopathological states. As shown previously (143), frequent sighing may turn excessive, resulting in chronic hypocapnia, which may lead to widespread bodily symptoms (including autonomic, respiratory, cardiac, motor and emotional symptoms), overlapping with a broad range of psychopathological states. In turn, these bodily symptoms may further disrupt homeostasis, requiring more resetting and therefore evoking increased sighing. In addition, learning processes may reinforce sighing; the resetting of a sigh, either reflexively or voluntarily, may function as a reward value, enabling operant learning (162). Therefore, the resetting properties of a sigh may turn maladaptive when sighing becomes excessive, causing a vicious cycle of psychophysiological symptoms and sighing in a wide range of psychopathological states. Below, we will detail the ways in which sighs may function as resetters.

Sighing as an adaptive behavior

Under normal circumstances, sighs are considered to be adaptive responses controlling psychophysiological states. By means of a resetting mechanism, sighs contribute to homeostatic control of both physiological and psychological states, facilitating transitions from one state to the next, guaranteeing psychophysiological flexibility (53, 161). These transitions may involve anticipatory, activation or recovery responses. Next, we will describe three examples of this resetting mechanism of a sigh, detailing how a sigh resets respiration, arousal and psychological states.

The ”sigh reflex”: A sigh resets respiration

The physiological function of a sigh is to homeostatically control mechanical and metabolic properties of respiration (see accompanying manuscript). Both animal and human research have demonstrated that a sigh prevents atelectasis (i.e. alveolar collapse) and restores lung compliance (32, 33, 163-168). In addition, a sigh restores normoxia and efficient gas exchange when hypoxia or hypercapnia increase (23, 85, 87, 169). Sighs not only reset mechanical and metabolic deviations in respiration, but also related symptoms. For example, decreases in lung compliance can be associated with chest tightness, and deviations from normoxia go often hand in hand with dyspnea. Preliminary findings suggest that sighs may contribute to symptom management, as sighs have been shown to reduce feelings of respiratory tension and discomfort

and are related to relief of dyspnea (126, 170). Finally, a sigh also contributes to respiratory control by regulating variability of various breathing parameters. Disruptions in respiratory control can alter balanced variability in respiration, either reducing breathing variability below healthy levels or increasing breathing irregularity beyond healthy levels. Findings suggest that sighs are effective in temporarily restoring healthy breathing variability(161, 171-173), this way resetting respiratory control.

Sighs and arousal: A sigh resets physiological and behavioral arousal

Sighs do not only restore respiratory functions but have also been associated with physiological arousal. Because of the temporal association between sighs and physiological arousal, it has been hypothesized that sighs may facilitate transitions in arousal, either increases or decreases. For example, increased sigh rates have been found during transitions between wake and sleep, and between quiet and active sleep (74), both in the presence and absence of major changes in respiratory functions. The majority of sighs during sleep are

followed by increases in EEG arousal (174, 175). This increase in physiological arousal seems particularly functional during sleep in infants to stimulate behavioral arousal. Findings suggest that, when hypoxia increases during sleep (e.g. due of prone sleeping), sighs evoke an arousal response that leads to repositioning of the head during sleep, preventing sudden infant death syndrome (75, 76, 176, 177).

These findings are consistent with observations that a sigh in humans is consistently followed by a galvanic skin response. Anecdotally, asking persons to take a deep breath is a way to verify a valid skin conductance measurement in psychophysiological research.

Sighs and control of brain states: A sigh resets emotions

Sighs are implicated in the regulation of arousal and emotional states. Indeed, various studies, suggest a bidirectional relationship between sighs and emotions in which sighs are both the outcome and the cause of emotional changes. Sighs are associated with both high arousal or negative emotions. More specifically, sighs occur more frequently during unpleasant thoughts (178), high mental load or stress (7, 171, 172), fear, anxiety (7, 118, 179) and music anxiety specifically (180-182), aggression (183), and depression (7). However sighs also occur frequently during high arousal positive emotions, such as joy (7) and relief (including decreases in negative affect or disruptions of mental load) (37, 127, 170, 184-186). Sighs do not only occur more frequently during relief, but they may facilitate relief. Following a sigh, muscle tension decreases, particularly in persons with high anxiety sensitivity (126, 128). Thus, the acute relief effect of a sigh may function as a broader emotional and psychological resetting effect, acting as a response to cope with arousing or aversive psychological states. This interpretation is supported by preliminary findings that (non-excessive) sigh rates during stress are associated with resilience and physiological habituation to stress (187).

Important to note here, is that the above findings hold for spontaneous sighs. Studies have shown that the effects of instructed or imposed sighs (here defined as deep breaths on command), may be different. For example, following an instructed deep breath, no physiological relief effect was found (125) (128), nor a resetting of healthy breathing variability (128). This suggests that instructed deep breaths are at least physiologically different from actual spontaneous sighs.

Altogether, it seems that a sigh primarily serves an adaptive function, resetting psychophysiological states, including respiratory properties, arousal, and emotions. This resetting or regulatory nature of a sigh may originate from autonomic functioning related to

breathing. We hypothesize that the inspiratory component of the sigh may stimulate sympathetic arousal, whereas the expiratory component may enhance parasympathetic, vagal tone. This coupling is likely mediated via central, and possibly also peripheral, nervous system interactions between the areas controlling sighs and sympathetic and parasympathetic tone. As a result, a sigh may restore sympathovagal balance, by acutely increasing arousal, yet temporarily inducing calm, which may further support the hypothesis that sighs contribute to psychophysiological flexibility. However, more research is necessary to confirm this hypothesis.

Are sighs needed for psychophysiological control?

We have argued that sighs are resetters, enabling homeostatic control in constantly changing internal and external environments, ensuring psychophysiological flexibility and dynamic adaptability. From a regulation perspective, the question arises whether sighs are needed to achieve psychophysiological flexibility. One could argue that respiratory regulation by means of central and peripheral control mechanisms, resulting in basic breath-to-breath variability is sufficient to allow dynamic adaptive responding. Models in physics suggest this is not the case. Information theory predicts that nonlinear systems, such as the respiratory system, need considerable noise to provide the system sufficient information to ensure adaptive functioning. This phenomenon, stochastic resonance, is widely applicable to neuroscience and biopsychosocial models, and may also apply to the respiratory system (161). Stochastic resonance in the respiratory system would translate to the idea that considerable breathing variability is essential to ensure adaptive respiratory regulation. The use of breathing in the context of vocalization is one such example. Too little noise, i.e., too limited breathing variability, will over-stabilize the system, not allowing transitions from one state to the next. Extreme noise, i.e., excessive breathing variability, will dysregulate the system, transitioning from one state to the next in a random way. We hypothesize that sighs are noise elements in the respiratory system that ensure that breathing variability reaches the optimal level to allow resetting and flexible transitioning from one state to the next when necessary (161).

Figure 1 illustrates a biphasic model of two states, rest, and activation, in which the length of the horizontal lines represents respiratory volume. The variability in the horizontal lines characterizes breath-to-breath variability in volume. In the left graph, variability in respiratory volume is limited, allowing the system to function in the resting state, but variability is not sufficient to allow a transition to the activation state. In the right graph, variability in respiratory

volume is larger, e.g., due to sighs or deep breaths (bold lines), allowing the transition between rest and activation states.

While spontaneous sighs that contribute to optimal noise levels facilitate state changes, excessive sighs would result in extreme noise levels which would hinder both stability and adaptive state changes. The latter would model excessive sighing as a maladaptive behavior, as described above.

Altogether, this theorizing suggests that sighs, by contributing to optimal breathing variability, are essential elements in psychophysiological regulation to guarantee flexibility. Yet the same model explains how excessive sighing may lead to excessive breathing variability and psychophysiological dysregulation.

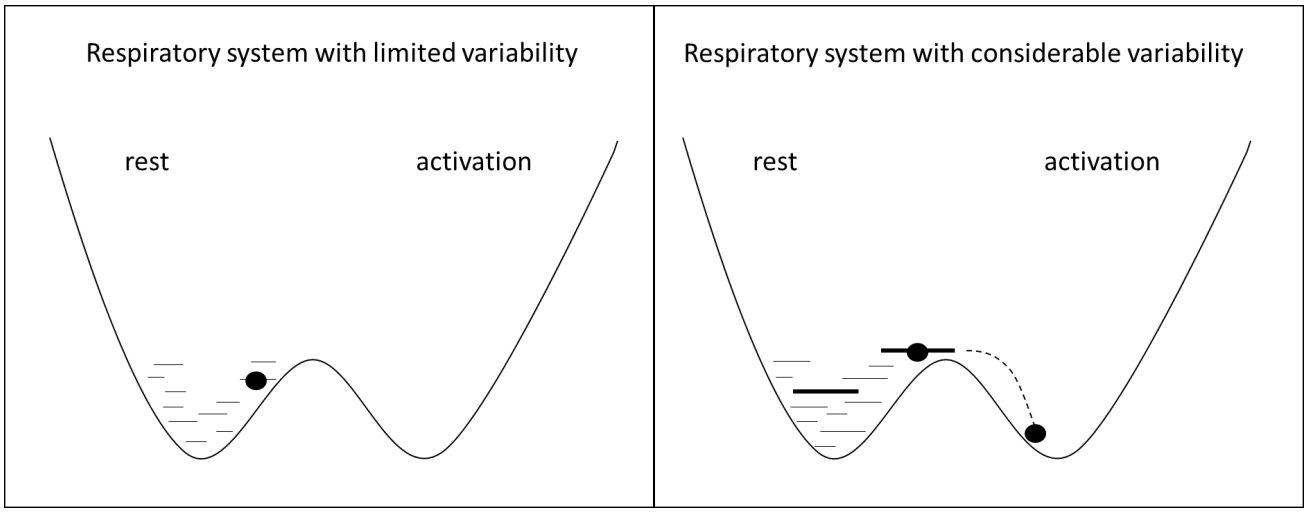

Figure 1.

A stochastic resonance model showing how considerable noise is essential to facilitate state changes, here between two basic states of rest and activation. Horizontal lines represent respiratory volume and variations in the length of these horizontal lines represents breath-to-breath variability in respiratory volume. Left, a respiratory system is depicted with limited variability, resulting in a stable resting state. Right, a respiratory system is shown with considerable variability due to occasional sighs (bold lines), resulting in the facilitation of state changes from rest to activation.

Sigh interventions

If sighs are not only temporarily but also causally associated with state changes as well as adaptive and maladaptive behaviors, can sighs be used in the context of therapeutic

interventions? Specifically, can increased sighing enhance resetting, and decreased sighing restore respiratory regulation?

Interventions to reduce sighing

Since excessive sighing and hypocapnia have been consistently found in panic disorder, capnometry biofeedback has been shown effective in reducing anxiety, and restoring healthy breathing in panic disorder patients (188). Aside from reducing respiratory frequency and increasing end-tidal carbon dioxide levels, capnometry biofeedback also includes the specific instruction to avoid sighs to reduce breathing irregularity and to reduce hypocapnia. In addition, capnometry biofeedback has been shown to reduce hypocapnia and asthma symptoms in asthma patients, more so than slow breathing alone (189, 190).

Other breathing techniques do not explicitly instruct to suppress sighing, but, by means of controlled breathing, may reduce sighs. Examples of these techniques are the Papworth method, the Buteyko technique or paced breathing, all shown to be effective in reducing asthma and respiratory symptoms in general (135).

Interventions to increase sighing

Despite the empirical findings that effects of instructed or imposed deep breaths are fundamentally different from the effects of spontaneous sighs, the instruction to “take a deep breath” is a popular one, and commonly recommended in a variety of stress management and relaxation techniques, such as yoga, Pilates, or meditation. If these effects of an intentional deep breath generalize to the occasional use of sighs in situations that require resetting, an instructed deep breath may be advantageous. However, if the effects of an intentional deep breath generalize to the excessive use of sighs, leading to respiratory dysregulation and associated symptoms, instructed deep breaths may do more harm than good. Therefore, more research is required to disentangle the effects of instructed or imposed sighing.

While instructed deep breaths may not have the same beneficial effects as a spontaneous sigh, and even more, may endanger sighing becoming excessive and maladaptive, paced sighing has been shown to train the cardiovascular system. Similarly to how slow breathing at 0.1 Hz seems to train the baroreflex (191), paced sighing at 0.066Hz seems to train vascular tone and arterial elasticity (192). This shows that stimulation of the cardiovascular system at specific frequencies by means of breathing, such as paced sighing, can train cardiovascular reflexes, and thus serve beneficial purposes when applied to train reflexes.

Another situation in which imposed sighing may be adaptive is during mechanical ventilation. Studies have shown that ventilation with a biologically variable pattern improves separation from the ventilator (193). Adding sigh breaths to the ventilation pattern to establish a biologically variable pattern improves respiratory parameters during and following mechanical ventilation by reducing atelectasis and increasing oxygenation (194-197).

One tool to engage adaptive sigh patterns specifically in targeted situations may be to engage learning processes. We have shown that sighs can be learned through reinforcement by relief of induced dyspnea (162). The technique of operant learning may therefore be promising to increase or decrease sighing in response to specific stimuli and contexts, by making persons aware of the immediate effects of a sigh, such as experiences of relief or hypocapnia to increase or decrease sighs, respectively.

Conclusion

Altogether, it seems that sighs serve important psychological functions that are supported by neurobiological mechanisms. While an increasing body of evidence suggests that a sigh may act as a psychophysiological resetter, more research is needed to show the resetting properties at a neurobiological and behavioral level. In addition, future research is required to better understand the tipping point where sighs may turn from adaptive to maladaptive behaviors, and the mechanisms underlying this shift.

References

1. Forster, H.V., P. Haouzi, and J.A. Dempsey, *Control of breathing during exercise.* Compr Physiol, 2012. **2**(1): p. 743-77.
2. Guyenet, P.G., et al., *The Retrotrapezoid Nucleus: Central Chemoreceptor and Regulator of Breathing Automaticity.* Trends Neurosci, 2019. **42**(11): p. 807-824.
3. Guyenet, P.G. and D.A. Bayliss, *Neural control of breathing and CO2 homeostasis.* Neuron, 2015. **87**(5): p. 946-961.
4. Ramirez, J.M. and N.A. Baertsch, *The Dynamic Basis of Respiratory Rhythm Generation: One Breath at a Time.* Annu Rev Neurosci, 2018. **41**: p. 475-499.
5. Baertsch, N.A., H.C. Baertsch, and J.M. Ramirez, *The interdependence of excitation and inhibition for the control of dynamic breathing rhythms.* Nat Commun, 2018. **9**(1): p. 843.
6. Indranada, A.M., et al., *The association of panic and hyperventilation with psychogenic non-epileptic seizures: A systematic review and meta-analysis.* Seizure, 2018. **59**: p. 108-115.
7. Vlemincx, E., I. Van Diest, and O. Van den Bergh, *Emotion, sighing, and respiratory variability.* Psychophysiology, 2015. **52**(5): p. 657-66.
8. Vlemincx, E., et al., *Respiratory variability and sighing: a psychophysiological reset model.* Biol Psychol, 2013. **93**(1): p. 24-32.
9. Grassmann, M., et al., *Respiratory Changes in Response to Cognitive Load: A Systematic Review.* Neural Plast, 2016. **2016**: p. 8146809.
10. Draeger-Muenke, R. and M. Muenke, *The Healing Energy of Breath in Traditional Chinese Medicine and Other Eastern Traditions*, in *Functional Respiratory Disorders*, A.R.D. (eds), Editor. 2012, Humana Press: Totowa, NJ. p. 301-323.
11. Russo, M.A., D.M. Santarelli, and D. O'Rourke, *The physiological effects of slow breathing in the healthy human.* Breathe (Sheff), 2017. **13**(4): p. 298-309.
12. Lieske, S., et al., *Reconfiguration of the neural network controlling multiple breathing patterns: eupnea, sighs and gasps.* Nature Neuroscience, 2000. **3**: p. 600-607.
13. Ramirez, J.M., *The integrative role of the sigh in psychology, physiology, pathology, and neurobiology.* Prog Brain Res, 2014. **209**: p. 91-129.
14. Lumsden, T., *Observations on the respiratory centres in the cat.* J Physiol, 1923. **57**(3-4): p. 153-60.
15. Lieske, S.P. and J.M. Ramirez, *Pattern-specific synaptic mechanisms in a multifunctional network. I. Effects of alterations in synapse strength.* J Neurophysiol, 2006. **95**(3): p. 1323-33.
16. Lieske, S. and J.M. Ramirez, *Pattern-specific synaptic mechanisms in a multifunctional network. II. Intrinsic modulation by metabotropic glutamate receptors.* Journal of Neurophysiology, 2006. **95**(3): p. 1334-1344.

17. Tryba, A.K., et al., *Differential modulation of neural network and pacemaker activity underlying eupnea and sigh-breathing activities.* J Neurophysiol, 2008. **99**(5): p. 2114-25.
18. Katagiri, H., et al., *Diaphragm function during sighs in awake dogs after laparotomy.* Am J Respir Crit Care Med, 1998. **157**(4 Pt 1): p. 1085-92.
19. Matsumoto, S., et al., *Effects of tachykinins on rapidly adapting pulmonary stretch receptors and total lung resistance in anesthetized, artificially ventilated rabbits.* J Pharmacol Exp Ther, 1997. **283**(3): p. 1026-31.
20. Bowes, G., et al., *Carotid chemoreceptor regulation of expiratory duration.* J Appl Physiol Respir Environ Exerc Physiol, 1983. **54**(5): p. 1195-201.
21. Galland, B.C., *The augmented Breath.* 1984.
22. Marshall, J.M. and J.D. Metcalfe, *Analysis of the cardiovascular changes induced in the rat by graded levels of systemic hypoxia.* J Physiol, 1988. **407**: p. 385-403.
23. Cherniack, N.S., et al., *Characteristics and rate of occurrence of spontaneous and provoked augmented breaths.* Acta Physiol Scand, 1981. **111**(3): p. 349-60.
24. Shea, S.A., et al., *The effect of human heart-lung transplantation upon breathing at rest and during sleep.* Respir Physiol, 1988. **72**(2): p. 131-49.
25. Glogowska, M., et al., *The role of the vagus nerves, peripheral chemoreceptors and other afferent pathways in the genesis of augmented breaths in cats and rabbits.* Respir Physiol, 1972. **16**(2): p. 179-96.
26. Widdicombe, J.G., *Pulmonary and respiratory tract receptors.* J Exp Biol, 1982. **100**: p. 41-57.
27. Schwenke, D.O. and P.A. Cragg, *Carotid bodies and the sigh reflex in the conscious and anaesthetised guinea-pig.* Adv Exp Med Biol, 2000. **475**: p. 801-13.
28. Marshall, J.M., *Analysis of cardiovascular responses evoked following changes in peripheral chemoreceptor activity in the rat.* J Physiol, 1987. **394**: p. 393-414.
29. Telgkamp, P. and J.M. Ramirez, *Differential responses of respiratory nuclei to anoxia in rhythmic brain stem slices of mice.* J Neurophysiol, 1999. **82**(5): p. 2163-70.
30. Galland, B.C. and P.A. Cragg, *Effect of carotid body denervation or vagotomy on the spontaneous and provoked sigh in the anaesthetised rat.* Proc. Univ. Otago Med. Sch, 1985. **63**: p. 17-18.
31. Li, P. and K. Yackle, *Sighing.* Curr Biol, 2017. **27**(3): p. R88-R89.
32. Caro, C.G., J. Butler, and A.B. Dubois, *Some effects of restriction of chest cage expansion on pulmonary function in man: an experimental study.* J Clin Invest, 1960. **39**: p. 573-83.
33. Ferris, B.G., Jr. and D.S. Pollard, *Effect of deep and quiet breathing on pulmonary compliance in man.* J Clin Invest, 1960. **39**: p. 143-9.
34. Fleming, P.J., et al., *The development of stability of respiration in human infants: changes in ventilatory responses to spontaneous sighs.* J Physiol, 1984. **347**: p. 1-16.

35. Hoch, B., M. Bernhard, and A. Hinsch, *Different patterns of sighs in neonates and young infants.* Biol Neonate, 1998. **74**(1): p. 16-21.
36. Bell, H.J., E. Azubike, and P. Haouzi, *The "other" respiratory effect of opioids: suppression of spontaneous augmented ("sigh") breaths.* J Appl Physiol, 2011. **111**(5): p. 1296-303.
37. Vlemincx, E., et al., *Why do you sigh? Sigh rate during induced stress and relief.* Psychophysiology, 2009. **46**(5): p. 1005-13.
38. Taelman, J., et al., *Instantaneous changes in heart rate regulation due to mental load in simulated office work.* Eur J Appl Physiol, 2011. **111**(7): p. 1497-505.
39. Koch, H., et al., *Stable respiratory activity requires both P/Q-type and N-type voltage-gated calcium channels.* Journal of neuroscience, 2013. **33**(8): p. 3633-3645.
40. Toporikova, N., M. Chevalier, and M. Thoby-Brisson, *Sigh and Eupnea Rhythmogenesis Involve Distinct Interconnected Subpopulations: A Combined Computational and Experimental Study(1,2,3).* eNeuro, 2015. **2**(2).
41. Viemari, J.-C., et al., *β-noradrenergic receptor activation specifically modulates the generation of sighs in vivo and in vitro.* Fontiers in Neural Circuits, 2013. **7**(179).
42. Peña, F. and J.-M. Ramirez, *Endogenous activation of serotonin-2A receptors is required for respiratory rhythm generation in vitro.* The Journal of Neuroscience, 2002. **22**(24): p. 11055-11064.
43. Peña, F. and J.M. Ramirez, *Substance P-mediated modulation of pacemaker properties in the mammalian respiratory network.* J Neurosci, 2004. **24**(34): p. 7549-56.
44. Doi, A. and J.M. Ramirez, *State-dependent interactions between excitatory neuromodulators in the neuronal control of breathing.* J Neurosci, 2010. **30**(24): p. 8251-62.
45. Reynolds, C.R., et al., *Disinhibition of the dorsomedial hypothalamus increases the frequency of augmented breaths in the anesthetized rat.* Adv Exp Med Biol, 2008. **605**: p. 274-8.
46. Orem, J. and R.H. Trotter, *Medullary respiratory neuronal activity during augmented breaths in intact unanesthetized cats.* J Appl Physiol, 1993. **74**(2): p. 761-9.
47. Ruangkittisakul, A., et al., *Generation of eupnea and sighs by a spatiochemically organized inspiratory network.* J Neurosci, 2008. **28**(10): p. 2447-58.
48. Li, P., et al., *The peptidergic control circuit for sighing.* Nature, 2016. **530**(7590): p. 293-297.
49. Viemari, J.C., et al., *Activation of alpha-2 noradrenergic receptors is critical for the generation of fictive eupnea and fictive gasping inspiratory activities in mammals in vitro.* Eur J Neurosci, 2011. **33**(12): p. 2228-37.
50. Ramirez-Jarquin, J.O., et al., *Somatostatin modulates generation of inspiratory rhythms and determines asphyxia survival.* Peptides, 2012. **34**(2): p. 360-72.
51. Souza, G., et al., *Differential Contribution of the Retrotrapezoid Nucleus and C1 Neurons to Active Expiration and Arousal in Rats.* J Neurosci, 2020. **40**(45): p. 8683-8697.

52. Li, F., et al., *Sneezing reflex is mediated by a peptidergic pathway from nose to brainstem.* Cell, 2021. **184**(14): p. 3762-3773 e10.
53. Baertsch, N.A., et al., *A spatially dynamic network underlies the generation of inspiratory behaviors.* Proc Natl Acad Sci U S A, 2019. **116**(15): p. 7493-7502.
54. Smith, J.C., et al., *Pre-Bötzinger Complex: A Brainstem Region That May Generate Respiratory Rhythm in Mammals.* Science, 1991. **254**(5032): p. 726-729.
55. Chapuis, C., et al., *Emergence of sigh rhythmogenesis in the embryonic mouse.* J Physiol, 2014. **592**(10): p. 2169-81.
56. Thoby-Brisson, M., *Neural mechanisms for sigh generation during prenatal development.* J Neurophysiol, 2018. **120**(3): p. 1162-1172.
57. Borrus, D.S., et al., *Role of Synaptic Inhibition in the Coupling of the Respiratory Rhythms that Underlie Eupnea and Sigh Behaviors.* eNeuro, 2020. **7**(3).
58. Thoby-Brisson, M. and J.J. Greer, *Anatomical and functional development of the pre-Botzinger complex in prenatal rodents.* J Appl Physiol (1985), 2008. **104**(4): p. 1213-9.
59. Funk, G.D., *The 'connexin' between astrocytes, ATP and central respiratory chemoreception.* J Physiol, 2010. **588**(Pt 22): p. 4335-7.
60. Sheikhbahaei, S., et al., *Astrocytes modulate brainstem respiratory rhythm-generating circuits and determine exercise capacity.* Nat Commun, 2018. **9**(1): p. 370.
61. Turovsky, E., et al., *Mechanisms of CO2/H+ Sensitivity of Astrocytes.* J Neurosci, 2016. **36**(42): p. 10750-10758.
62. Ramirez, J.M., et al., *Advances in cellular and integrative control of oxygen homeostasis within the central nervous system.* J Physiol, 2018.
63. Mulkey, D.K., I.C. Wenker, and O. Kréneisz, *Current ideas on central chemoreception by neurons and glial cells in the retrotrapezoid nucleus.* Journal of Applied Physiology, 2010. **108**: p. 1433-1439.
64. Wenker, I., et al., *Astrocytes in the Retrotrapezoid Nucleus Sense H+ by Inhibition of a Kir4.1-Kir5.1-Like Current and May Contribute to Chemoreception by a Purinergic Mechanism.* Journal of Neurophysiology, 2010. **104**: p. 3042-3052.
65. Forsberg, D., et al., *CO2-evoked release of PGE2 modulates sighs and inspiration as demonstrated in brainstem organotypic culture.* Elife, 2016. **5**.
66. Forsberg, D., T. Ringstedt, and E. Herlenius, *Astrocytes release prostaglandin E2 to modify respiratory network activity.* eLIFE, 2017. **6**(e29566).
67. Angelova, P.R., et al., *Functional Oxygen Sensitivity of Astrocytes.* J Neurosci, 2015. **35**(29): p. 10460-73.
68. Marina, N., et al., *Brain metabolic sensing and metabolic signaling at the level of an astrocyte.* Glia, 2017.

69. Eugenin Leon, J., M.J. Olivares, and S. Beltran-Castillo, *Role of Astrocytes in Central Respiratory Chemoreception.* Adv Exp Med Biol, 2016. **949**: p. 109-145.
70. Beltrán-Castillo, S., et al., *D-serine released by astrocyte in brainstem regulates breathing response to CO2 levels.* Nature Communications, 2017. **8**(838).
71. Thach, B.T. and A. Lijowska, *Arousals in infants.* Sleep, 1996. **19**(10 Suppl): p. S271-3.
72. Anderson, C.A., T.E. Dick, and J. Orem, *Respiratory responses to tracheobronchial stimulation during sleep and wakefulness in the adult cat.* Sleep, 1996. **19**(6): p. 472-8.
73. McNamara, F., A.S. Lijowska, and B.T. Thach, *Spontaneous arousal activity in infants during NREM and REM sleep.* J Physiol, 2002. **538**(Pt 1): p. 263-9.
74. McGinty, D.J., et al., *Sleep apnea in normal kittens.* Sleep, 1979. **1**(4): p. 393-412.
75. Lijowska, A., et al., *Sequential arousal and airway-defensive behavior of infants in asphyxial sleep environments.* Journal of Applied Physiology, 1997. **83**(1): p. 219-228.
76. McNamara, F., H. Wulbrand, and B. Thach, *Characteristics of the infant arousal response.* Journal of Applied Physiology, 1998. **85**(6): p. 2314-2321.
77. Schechtman, V.L., et al., *Sleep state organization in normal infants and victims of the sudden infant death syndrome.* Pediatrics, 1992. **89**(5 Pt 1): p. 865-70.
78. Dunne, K.P., et al., *Arousal responses in babies at risk of sudden infant death syndrome at different postnatal ages.* Ir Med J, 1992. **85**(1): p. 19-22.
79. Sawaguchi, T., et al., *Apnea, glial apoptosis and neuronal plasticity in the arousal pathway of victims of SIDS.* Forensic Sci Int, 2005. **149**(2-3): p. 205-17.
80. Kahn, A., et al., *Sleep and cardiorespiratory characteristics of infant victims of sudden death: a prospective case-control study.* Sleep, 1992. **15**(4): p. 287-92.
81. Kato, I., et al., *Spontaneous arousability in prone and supine position in healthy infants.* Sleep, 2006. **29**(6): p. 785-90.
82. McCulloch, K., et al., *Arousal responses in near-miss sudden infant death syndrome and in normal infants.* J Pediatr, 1982. **101**(6): p. 911-7.
83. Garcia, A.J., 3rd, J.E. Koschnitzky, and J.M. Ramirez, *The physiological determinants of Sudden Infant Death Syndrome.* Respiratory Physiology and Neurobiology, 2013. **189**(2): p. 288-300.
84. Ramirez, J.M., S.C. Ramirez, and T.M. Anderson, *Sudden Infant Death Syndrome, Sleep, and the Physiology and Pathophysiology of the Respiratory Network*, in *SIDS Sudden Infant and Early Childhood Death: The Past, the Present and the Future*, J.R. Duncan and R.W. Byard, Editors. 2018: Adelaide (AU).
85. Bartlett, D., Jr., *Origin and regulation of spontaneous deep breaths.* Respir Physiol, 1971. **12**(2): p. 230-8.

86. Bell, H.J. and P. Haouzi, *The hypoxia-induced facilitation of augmented breaths is suppressed by the common effect of carbonic anhydrase inhibition.* Respir Physiol Neurobiol, 2010. **171**(3): p. 201-11.
87. Bell, H.J., et al., *Hypocapnia increases the prevalence of hypoxia-induced augmented breaths.* Am J Physiol Regul Integr Comp Physiol, 2009. **296**(2): p. R334-44.
88. Hill, A.A., et al., *Graded Reductions in Oxygenation Evoke Graded Reconfiguration of the Isolated Respiratory Network.* Journal of Neurophysiology, 2011. **105**(2): p. 625-639.
89. Burke, P.G., et al., *Optogenetic stimulation of adrenergic C1 neurons causes sleep state-dependent cardiorespiratory stimulation and arousal with sighs in rats.* Am J Respir Crit Care Med, 2014. **190**(11): p. 1301-10.
90. Souza, G., et al., *Inspiratory modulation of sympathetic activity is increased in female rats exposed to chronic intermittent hypoxia.* Exp Physiol, 2016. **101**(11): p. 1345-1358.
91. Souza, G., et al., *Sex differences in the respiratory-sympathetic coupling in rats exposed to chronic intermittent hypoxia.* Respir Physiol Neurobiol, 2017.
92. Bolton, D.P., et al., *Rebreathing expired gases from bedding: a cause of cot death?* Arch Dis Child, 1993. **69**(2): p. 187-90.
93. Chiodini, B.A. and B.T. Thach, *Impaired ventilation in infants sleeping facedown: potential significance for sudden infant death syndrome.* J Pediatr, 1993. **123**(5): p. 686-92.
94. Kemp, J.S. and B.T. Thach, *Sudden death in infants sleeping on polystyrene-filled cushions.* N Engl J Med, 1991. **324**(26): p. 1858-64.
95. Kemp, J.S., et al., *Unintentional suffocation by rebreathing: a death scene and physiologic investigation of a possible cause of sudden infant death.* J Pediatr, 1993. **122**(6): p. 874-80.
96. Ayas, N.T., R. Brown, and S.A. Shea, *Hypercapnia can induce arousal from sleep in the absence of altered respiratory mechanoreception.* Am J Respir Crit Care Med, 2000. **162**(3 Pt 1): p. 1004-8.
97. Fewell, J.E., *Protective responses of the newborn to hypoxia.* Respir Physiol Neurobiol, 2005. **149**(1-3): p. 243-55.
98. Horne, R.S., P.M. Parslow, and R. Harding, *Postnatal development of ventilatory and arousal responses to hypoxia in human infants.* Respir Physiol Neurobiol, 2005. **149**(1-3): p. 257-71.
99. Masa, J.F., et al., *Assessment of thoracoabdominal bands to detect respiratory effort-related arousal.* Eur Respir J, 2003. **22**(4): p. 661-7.
100. Parslow, P.M., et al., *Ventilatory responses preceding hypoxia-induced arousal in infants: effects of sleep-state.* Respir Physiol Neurobiol, 2003. **136**(2-3): p. 235-47.
101. Thach, B.T. and H.W. Taeusch, Jr., *Sighing in newborn human infants: role of inflation-augmenting reflex.* J Appl Physiol, 1976. **41**(4): p. 502-7.

102. Burke, P.G., et al., *Selective optogenetic stimulation of the retrotrapezoid nucleus in sleeping rats activates breathing without changing blood pressure or causing arousal or sighs.* J Appl Physiol (1985), 2015. **118**(12): p. 1491-501.
103. Eckert, D.J., et al., *Central sleep apnea: Pathophysiology and treatment.* Chest, 2007. **131**(2): p. 595-607.
104. Abbott, S.B., et al., *C1 neurons excite locus coeruleus and A5 noradrenergic neurons along with sympathetic outflow in rats.* J Physiol, 2012. **590**(12): p. 2897-915.
105. Guyenet, P.G., et al., *C1 neurons: the body's EMTs.* Am J Physiol Regul Integr Comp Physiol, 2013. **305**(3): p. R187-204.
106. Silva, T.M., A.C. Takakura, and T.S. Moreira, *Acute hypoxia activates hypothalamic paraventricular nucleus-projecting catecholaminergic neurons in the C1 region.* Exp Neurol, 2016. **285**(Pt A): p. 1-11.
107. Bochorishvili, G., et al., *The orexinergic neurons receive synaptic input from C1 cells in rats.* J Comp Neurol, 2014. **522**(17): p. 3834-46.
108. Young, J.K., et al., *Orexin stimulates breathing via medullary and spinal pathways.* J Appl Physiol (1985), 2005. **98**(4): p. 1387-95.
109. Nattie, E. and A. Li, *Respiration and autonomic regulation and orexin.* Prog Brain Res, 2012. **198**: p. 25-46.
110. Gestreau, C., M. Bevengut, and M. Dutschmann, *The dual role of the orexin/hypocretin system in modulating wakefulness and respiratory drive.* Curr Opin Pulm Med, 2008. **14**(6): p. 512-8.
111. Johnson, P.L., et al., *Orexin, stress, and anxiety/panic states.* Prog Brain Res, 2012. **198**: p. 133-61.
112. Kantor, S., et al., *Orexin neurons are necessary for the circadian control of REM sleep.* Sleep, 2009. **32**(9): p. 1127-34.
113. Tsujino, N. and T. Sakurai, *[Circadian rhythm of leptin, orexin and ghrelin].* Nihon Rinsho, 2012. **70**(7): p. 1121-5.
114. Brisbare-Roch, C., et al., *Promotion of sleep by targeting the orexin system in rats, dogs and humans.* Nat Med, 2007. **13**(2): p. 150-5.
115. Li, A. and E. Nattie, *Antagonism of rat orexin receptors by almorexant attenuates central chemoreception in wakefulness in the active period of the diurnal cycle.* J Physiol, 2010. **588**(Pt 15): p. 2935-44.
116. Nakamura, A., et al., *Vigilance state-dependent attenuation of hypercapnic chemoreflex and exaggerated sleep apnea in orexin knockout mice.* J Appl Physiol (1985), 2007. **102**(1): p. 241-8.
117. Hagan, J.J., et al., *Orexin A activates locus coeruleus cell firing and increases arousal in the rat.* Proc Natl Acad Sci U S A, 1999. **96**(19): p. 10911-6.

118. Li, P., et al., *Brain Circuit of Claustrophobia-like Behavior in Mice Identified by Upstream Tracing of Sighing.* Cell Rep, 2020. **31**(11): p. 107779.
119. Corcoran, A.W., G. Pezzulo, and J. Hohwy, *Commentary: Respiration-Entrained Brain Rhythms Are Global but Often Overlooked.* Front Syst Neurosci, 2018. **12**: p. 25.
120. Tort, A.B.L., J. Brankack, and A. Draguhn, *Respiration-Entrained Brain Rhythms Are Global but Often Overlooked.* Trends Neurosci, 2018. **41**(4): p. 186-197.
121. Heck, D.H., et al., *Breathing as a Fundamental Rhythm of Brain Function.* Front Neural Circuits, 2016. **10**: p. 115.
122. Ito, J., et al., *Whisker barrel cortex delta oscillations and gamma power in the awake mouse are linked to respiration.* Nat Commun, 2014. **5**: p. 3572.
123. Tort, A.B.L., et al., *Parallel detection of theta and respiration-coupled oscillations throughout the mouse brain.* Sci Rep, 2018. **8**(1): p. 6432.
124. Zhong, W., et al., *Selective entrainment of gamma subbands by different slow network oscillations.* Proc Natl Acad Sci U S A, 2017. **114**(17): p. 4519-4524.
125. Vlemincx, E., M. Meulders, and O. Luminet, *A sigh of relief or a sigh of expected relief: Sigh rate in response to dyspnea relief.* Psychophysiology, 2018. **55**(2).
126. Vlemincx, E., I. Van Diest, and O. Van den Bergh, *A sigh of relief or a sigh to relieve: The psychological and physiological relief effect of deep breaths.* Physiol Behav, 2016. **165**: p. 127-35.
127. Vlemincx, E., M. Meulders, and J.L. Abelson, *Sigh rate during emotional transitions: More evidence for a sigh of relief.* Biol Psychol, 2017. **125**: p. 163-172.
128. Vlemincx, E., et al., *Take a deep breath: the relief effect of spontaneous and instructed sighs.* Physiol Behav, 2010. **101**(1): p. 67-73.
129. Ramirez, J.M. and N. Baertsch, *Defining the Rhythmogenic Elements of Mammalian Breathing.* Physiology (Bethesda), 2018. **33**(5): p. 302-316.
130. Ben-Tal, A. and M.H. Tawhai, *Integrative approaches for modeling regulation and function of the respiratory system.* Wiley Interdiscip Rev Syst Biol Med, 2013. **5**(6): p. 687-99.
131. Hornsveld, H. and B. Garssen, *Hyperventilation syndrome: an elegant but scientifically untenable concept.* Neth J Med, 1997. **50**(1): p. 13-20.
132. Hornsveld, H.K., et al., *Double-blind placebo-controlled study of the hyperventilation provocation test and the validity of the hyperventilation syndrome.* Lancet, 1996. **348**(9021): p. 154-8.
133. Vlemincx, E., I. Van Diest, and O. Van den Bergh, *Imposing respiratory variability patterns.* Appl Psychophysiol Biofeedback, 2012. **37**(3): p. 153-60.
134. Courtney, R. and M. Cohen, *Assessment of the measurement tools of dysfunctional breathing.* Int Osteopath Med, 2006. **9**(1): p. 34.

135. Boulding, R., et al., *Dysfunctional breathing: a review of the literature and proposal for classification.* Eur Respir Rev, 2016. **25**(141): p. 287-94.
136. Sody, A.N., et al., *Sigh syndrome: is it a sign of trouble?* J Fam Pract, 2008. **57**(1): p. E1-5.
137. Wong, K.S., et al., *Personality profiles and pulmonary function of children with sighing dyspnoea.* J Paediatr Child Health, 2007. **43**(4): p. 280-3.
138. Wong, K.S., et al., *Plethysmographic lung volumes in children with sighing dyspnea.* Pediatr Int, 2009. **51**(3): p. 405-8.
139. Hurvitz, M. and M. Weinberger, *Functional Respiratory Disorders in Children.* Pediatr Clin North Am, 2021. **68**(1): p. 223-237.
140. Aljadeff, G., et al., *Pattern of lung volumes in patients with sighing breathing.* Thorax, 1993. **48**(8): p. 809-11.
141. Tobin, M.J., et al., *Breathing patterns. 2. Diseased subjects.* Chest, 1983. **84**(3): p. 286-94.
142. Blechert, J., et al., *Autonomic and respiratory characteristics of posttraumatic stress disorder and panic disorder.* Psychosom Med, 2007. **69**(9): p. 935-43.
143. Wilhelm, F.H., W. Trabert, and W.T. Roth, *Characteristics of sighing in panic disorder.* Biol Psychiatry, 2001. **49**(7): p. 606-14.
144. Wilhelm, F.H., W. Trabert, and W.T. Roth, *Physiologic instability in panic disorder and generalized anxiety disorder.* Biol Psychiatry, 2001. **49**(7): p. 596-605.
145. Abelson, J.L., et al., *Persistent respiratory irregularity in patients with panic disorder.* Biol Psychiatry, 2001. **49**(7): p. 588-95.
146. Leung, A.K. and K.L. Hon, *Motion sickness: an overview.* Drugs Context, 2019. **8**.
147. Keefe, F.J. and R.W. Hill, *An objective approach to quantifying pain behavior and gait patterns in low back pain patients.* Pain, 1985. **21**(2): p. 153-161.
148. Keefe, F.J., R.H. Wilkins, and W.A. Cook, *Direct observation of pain behavior in low back pain patients during physical examination.* Pain, 1984. **20**(1): p. 59-68.
149. Robbins, M.L., et al., *Naturalistically observed sighing and depression in rheumatoid arthritis patients: a preliminary study.* Health Psychol, 2011. **30**(1): p. 129-33.
150. Nazari, R., et al., *Behavioral Pain Indicators in Patients with Traumatic Brain Injury Admitted to an Intensive Care Unit.* J Caring Sci, 2018. **7**(4): p. 197-203.
151. Han, J.N., et al., *Unsteadiness of breathing in patients with hyperventilation syndrome and anxiety disorders.* Eur Respir J, 1997. **10**(1): p. 167-76.
152. Hormbrey, J., et al., *CO2 response and pattern of breathing in patients with symptomatic hyperventilation, compared to asthmatic and normal subjects.* Eur Respir J, 1988. **1**(9): p. 846-51.
153. Prys-Picard, C.O., F. Kellett, and R.M. Niven, *Disproportionate breathlessness associated with deep sighing breathing in a patient presenting with difficult-to-treat asthma.* Chest, 2006. **130**(6): p. 1723-5.

154. Stevenson, I. and H.S. Ripley, *Variations in respiration and in respiratory symptoms during changes in emotion.* Psychosom Med, 1952. **14**(6): p. 476-90.
155. Abelson, J.L., S. Khan, and N. Giardino, *HPA axis, respiration and the airways in stress--a review in search of intersections.* Biol Psychol, 2010. **84**(1): p. 57-65.
156. Abelson, J.L., et al., *Respiratory irregularity and stress hormones in panic disorder: exploring potential linkages.* Depress Anxiety, 2008. **25**(10): p. 885-7.
157. Schwartz, G.E., et al., *Tidal volume of respiration and "sighing" as indicators of breathing irregularities in panic disorder patients.* Anxiety, 1996. **2**(3): p. 145-8.
158. Yeragani, V.K., et al., *Nonlinear measures of respiration: respiratory irregularity and increased chaos of respiration in patients with panic disorder.* Neuropsychobiology, 2002. **46**(3): p. 111-20.
159. Martinez, J.M., et al., *Respiratory variability in panic disorder.* Depress Anxiety, 2001. **14**(4): p. 232-7.
160. Pfaltz, M.C., et al., *Respiratory pathophysiology of panic disorder: an ambulatory monitoring study.* Psychosom Med, 2009. **71**(8): p. 869-76.
161. Vlemincx, E., et al., *Respiratory variability preceding and following sighs: a resetter hypothesis.* Biol Psychol, 2010. **84**(1): p. 82-7.
162. Vlemincx, E. and O. Luminet, *Sighs can become learned behaviors via operant learning.* Biol Psychol, 2020. **151**: p. 107850.
163. Davis, G.M. and J. Moscato, *Changes in lung mechanics following sighs in premature newborns without lung disease.* Pediatr Pulmonol, 1994. **17**(1): p. 26-30.
164. Golder, F.J., et al., *Augmented breath phase volume and timing relationships in the anesthetized rat.* Neurosci Lett, 2005. **373**(2): p. 89-93.
165. McIlroy, M., J. Butler, and T. Finley, *Effects of chest compression on reflex ventilatory drive and pulmonary function.* Journal of Applied Physiology, 1962. **117**(4): p. 6701-705.
166. Mead, J. and C. Collier, *Relation of volume history of lungs to respiratory mechanics in anesthetized dogs.* Journal of Applied Physiology, 1959. **14**(5): p. 669-678.
167. Bendixen, H.H., G.M. Smith, and J. Mead, *Pattern of Ventilation in Young Adults.* J Appl Physiol, 1964. **19**: p. 195-8.
168. Reynolds, L., *Characteristics of an inspiration-augmenting reflex in anesthetized cats.* Journal of Applied Physiology, 1962. **17**.
169. Bell, H.J. and P. Haouzi, *Acetazolamide suppresses the prevalence of augmented breaths during exposure to hypoxia.* Am J Physiol Regul Integr Comp Physiol, 2009. **297**(2): p. R370-81.
170. Hirose, S., *Restlessness of respiration as a manifestation of akathisia: five case reports of respiratory akathisia.* J Clin Psychiatry, 2000. **61**(10): p. 737-41.
171. Wuyts, R., et al., *Sigh rate and respiratory variability during normal breathing and the role of negative affectivity.* Int J Psychophysiol, 2011. **82**(2): p. 175-9.

172. Vlemincx, E., I. Van Diest, and O. Van den Bergh, *A sigh following sustained attention and mental stress: effects on respiratory variability.* Physiol Behav, 2012. **107**(1): p. 1-6.
173. Baldwin, D.N., et al., *Effect of sighs on breathing memory and dynamics in healthy infants.* J Appl Physiol (1985), 2004. **97**(5): p. 1830-9.
174. Della Marca, G., et al., *Periodic sighs.* Sleep Med, 2013. **14**(11): p. 1224-5.
175. Perez-Padilla, R., P. West, and M.H. Kryger, *Sighs during sleep in adult humans.* Sleep, 1983. **6**(3): p. 234-43.
176. Franco, P., et al., *Polysomnographic study of the autonomic nervous system in potential victims of sudden infant death syndrome.* Clin Auton Res, 1998. **8**(5): p. 243-9.
177. Thach, B.T., *Graded arousal responses in infants: advantages and disadvantages of a low threshold for arousal.* Sleep Med, 2002. **3 Suppl 2**: p. S37-40.
178. Finesinger, J., *The effect of pleasant and unpleasant ideas on the respiratory pattern (spirogram) in psychoneurotic patients.* American Journal of Psychiatry 1944. **100**(5): p. 659-667.
179. Carnevali, L., et al., *Different patterns of respiration in rat lines selectively bred for high or low anxiety.* PLoS One, 2013. **8**(5): p. e64519.
180. Guyon, A., et al., *Respiratory Variability, Sighing, Anxiety, and Breathing Symptoms in Low- and High-Anxious Music Students Before and After Performing.* Front Psychol, 2020. **11**: p. 303.
181. Studer, R.K., et al., *Psychophysiological activation during preparation, performance, and recovery in high- and low-anxious music students.* Appl Psychophysiol Biofeedback, 2014. **39**(1): p. 45-57.
182. Studer, R.K., et al., *Hyperventilation in anticipatory music performance anxiety.* Psychosom Med, 2012. **74**(7): p. 773-82.
183. Carnevali, L., E. Nalivaiko, and A. Sgoifo, *Respiratory patterns reflect different levels of aggressiveness and emotionality in Wild-type Groningen rats.* Respir Physiol Neurobiol, 2014. **204**: p. 28-35.
184. Soltysik, S. and P. Jelen, *In rats, sighs correlate with relief.* Physiol Behav, 2005. **85**(5): p. 598-602.
185. McClernon, F.J., E.C. Westman, and J.E. Rose, *The effects of controlled deep breathing on smoking withdrawal symptoms in dependent smokers.* Addict Behav, 2004. **29**(4): p. 765-72.
186. Teigen, K.H., *Is a sigh "just a sigh"? Sighs as emotional signals and responses to a difficult task.* Scand J Psychol, 2008. **49**(1): p. 49-57.
187. Walker, F.R., et al., *Habituation of the electrodermal response - A biological correlate of resilience?* PLoS One, 2019. **14**(1): p. e0210078.
188. Meuret, A.E., F.H. Wilhelm, and W.T. Roth, *Respiratory biofeedback-assisted therapy in panic disorder.* Behav Modif, 2001. **25**(4): p. 584-605.
189. Meuret, A.E. and T. Ritz, *Hyperventilation in panic disorder and asthma: empirical evidence and clinical strategies.* Int J Psychophysiol, 2010. **78**(1): p. 68-79.

190. Ritz, T., et al., *Controlling asthma by training of Capnometry-Assisted Hypoventilation (CATCH) vs slow breathing: a randomized controlled trial.* Chest, 2014. **146**(5): p. 1237-1247.
191. Lehrer, P.M., et al., *Heart rate variability biofeedback increases baroreflex gain and peak expiratory flow.* Psychosom Med, 2003. **65**(5): p. 796-805.
192. Vaschillo, E.G., et al., *The effects of sighing on the cardiovascular system.* Biol Psychol, 2015. **106**: p. 86-95.
193. Wysocki, M., et al., *Reduced breathing variability as a predictor of unsuccessful patient separation from mechanical ventilation.* Crit Care Med, 2006. **34**(8): p. 2076-83.
194. Tabuchi, A., et al., *Acute Lung Injury Causes Asynchronous Alveolar Ventilation That Can Be Corrected by Individual Sighs.* Am J Respir Crit Care Med, 2016. **193**(4): p. 396-406.
195. Cammarota, G., et al., *Influence of lung collapse distribution on the physiologic response to recruitment maneuvers during noninvasive continuous positive airway pressure.* Intensive Care Med, 2011. **37**(7): p. 1095-102.
196. Badet, M., et al., *Comparison of optimal positive end-expiratory pressure and recruitment maneuvers during lung-protective mechanical ventilation in patients with acute lung injury/acute respiratory distress syndrome.* Respir Care, 2009. **54**(7): p. 847-54.
197. Hess, D.R. and L.M. Bigatello, *Lung recruitment: the role of recruitment maneuvers.* Respir Care, 2002. **47**(3): p. 308-17; discussion 317-8.

CHAPTER 5

Purinergic signaling mediates neuroglial interactions to generate sighs

[1,2]Liza J. Severs*, [1]Nicholas E. Bush, [1]Lely A, Quina, [1]Nicholas J. Burgraff, [1]Tatiana Dashevskiy, [1,4]Nathan A. Baertsch, [1,2,3,4]Jan-Marino Ramirez*

[1]Center for Integrative Brain Research, Seattle Children's Research Institute
[2]Department of Physiology and Biophysics, The University of Washington
[3]Department of Neurological Surgery, The University of Washington School of Medicine
[4]Department of Pediatrics, The University of Washington School of Medicine
*corresponding authors

Corresponding Author and Lead Contacts:
Dr. Jan-Marino Ramirez (jan.ramirez@seattlechildrens.org)

Acknowledgements: This work was supported by the following National Institutes of Health Grants: R01 HL151389, R01 HL126523, and P01 HL090554. We would also like to thank Dr. Marlusa Karlen-Amarante for her overwhelming support overall and for guidance and training for *in vivo* procedures.

Author Contributions: Conceptualization: J.M.R, T.D., L.J.S., N.A.B.; Methodology: L.J.S., N.A.B., L.A.Q.; Investigation: L.J.S., N.J.B., N.E.B., N.A.B., L.A.Q., T.D.; Formal Analysis: L.S., N.E.B.; Writing-Original Draft: L.S., N.A.B., T.D., J.M.R.; Writing-Review & Editing: J.M.R., N.A.B., N.E.B.; Funding Acquisition: J.M.R, L.J.S., T.D.; Visualization: L.S., N.A.B; Supervision: J.M.R

Declaration of Interests: The authors declare no competing interests.

Under preparation for resubmission to Nature Publishing.
Find the article here.

Abstract

Sighs prevent the collapse of alveoli in the lungs, initiate arousal under hypoxic conditions, and even express sadness and relief. Sighs are periodically superimposed on normal breaths, known as eupnea. Implicated in the generation of these rhythmic behaviors is the preBötzinger complex (preBötC)(1). Yet how this small microcircuit can produce two rhythms with strikingly different periodicities remains unresolved. Our computational simulations predict that sighs are generated by the coincidence of two temporally distinct calcium oscillations and are in agreement with experimental evidence suggesting that astrocytes drive sigh behavior through slower, extrinsically driven calcium oscillations that link the eupnea and sigh rhythms. We found that purinergic signaling is necessary to generate spontaneous and hypoxia- induced sighs, and photo-activation of preBötC astrocytes is sufficient to elicit sigh activity. We conclude that sighs are an emergent property of the preBötC network generated by neuroglial interactions, where the distinct modulatory responses of neurons and glia allow for both rhythms to be independently regulated.

Keywords: preBötzinger Complex, breathing, sigh, astrocytes, glia, purinergic signaling neuroglial interactions, rhythm generator, hypoxic response

Main

A question that is fundamental to the understanding of respiratory physiology is how the activity of a single population of neurons can be reconfigured to produce multiple behaviors, as is observed with eupnea, sighs, and gasps (2). The sigh is a critical component of breathing, serving to periodically reinflate collapsed alveoli in the lungs. The precise mechanisms by which sighs are generated remain unclear. However, it is understood that sighs and eupnea can be modulated separately (3-7) and are characterized by distinct intrinsic (8) and synaptic mechanisms within the preBötC (9). Contrary to this idea, it has been suggested that the control of sighing is driven by peptidergic projections from the Retrotrapezoid Nucleus (RTN) to the preBötC (7). However, lesioning the RTN does not alter sigh frequency (10), and sighs are preserved in wedges that physically isolate the preBötC (5). These findings led us to combine computational and experimental approaches to revisit the question of how sighs can be generated locally.

Characterization of sighs: sighs are not generated through inhibitory mechanisms

Sighs vary in shape and not every large amplitude burst is a sigh. Thus, we analyzed characteristics that distinguish sighs from eupneic bursts generated by the preBötC in brainstem slices from neonatal mice. Under control conditions, sigh amplitude, burst duration, and post-burst interval were significantly greater than eupneic bursts, and occurred on a much slower time scale (Fig. 1a, b). Variation in sigh shape is a result of different degrees of connection to the eupneic rhythm; some sighs appeared as connected double bursts, with a large amplitude burst superimposed on a eupneic burst (‘biphasic’), whereas others occurred as a single large amplitude burst (‘monophasic’) (Extended Data Fig. 1a). Biphasic and monophasic sighs did not differ in burst amplitude, burst duration, or post burst interval. Under control conditions *in vitro*, we found that 78.5 ± 5.8% of total sighs were biphasic and 21.4 ± 5.8% were monophasic. The prevalence of each sigh shape was variable between slices, and faster eupneic rhythms tended to have more monophasic sighs (Extended Data Fig. 1b). Previous hypotheses suggested that sighs are generated through inhibitory mechanisms (11). We show that pharmacological blockade of GABAergic and glycinergic synaptic inhibition with strychnine and gabazine, referred to as “inhibition block”, did not eliminate sighs, change their frequency, or dissociate them from eupneic bursts (Fig. 1c)(12). Sigh amplitude, post-burst interval, duration, and shape were also unaffected by inhibition block. However, the amplitude of eupneic bursts increased relative to sighs (13), thereby decreasing the ratio of sigh to eupnea amplitude (Extended Data Fig. 1c). Moreover, sigh frequency could still be increased pharmacologically following inhibition block with the β-adrenergic agonist isoproterenol (Fig. 1c), a potent sigh modulator (6).

An excitatory preBötC model combines Ca^{2+} oscillations to generate sighs

Based on these results, we designed an *in silico* model of the preBötC network comprised of 300 excitatory model neurons. To test the feasibility of calcium oscillations to generate sigh-like network activity, the *in silico* excitatory preBötC network modifies an existing model (14) to include a current gated by intracellular calcium (Ca^{2+}_{in}; Extended data Fig. 1d). Ca^{2+}_{in} evolves on both fast and slow timescales (Fig. 1d-f, Table 1, 2). The fast calcium signal (Ca^{2+}_{fast}) is linked to inactivation of persistent sodium channels (Eq. 17) and activates during periods of burst firing (i.e. eupnea) (15). The slow calcium (Ca^{2+}_{slow}) follows a slow oscillatory pattern(15, 16) that is extrinsically driven and synchronized across all neurons. This slow Ca^{2+} oscillation occurs independently of neuronal activity in the network and follows previously described dynamics (16). Thus, the total Ca^{2+}_{in} of each neuron of the respiratory network is a superposition of calcium dynamics on these two timescales (Eq.17).

Model neurons were defined as intrinsically bursting, tonic, or quiescent (B, T, Q) based on each neuron's firing pattern in synaptic isolation (Fig. 1d, Extended Data Fig. 3). Simulations including Ca^{2+} gated channels did not produce sigh bursts in the absence of Ca^{2+} oscillations. Neither the addition of a fast, eupnea-linked Ca^{2+} oscillation, nor a slow, extrinsically driven Ca^{2+} oscillation was sufficient to produce sigh bursts on their own. However, model networks including both fast and slow oscillations reliably produced periodic sigh-like bursts similar to those observed *in vitro* (5) (Fig. 1d, e). Indeed, compared to eupneic bursts, sigh bursts in the computational model were larger in amplitude and exhibited prolonged burst durations and post-burst intervals (Extended Data Fig. 1e). Modelled sighs were also temporally linked to the eupneic rhythm often occurring as an augmented population burst superimposed on a normal eupneic burst. Consistent with experimental findings *in vitro*, inclusion of both slow and fast Ca^{2+} components produced sigh-like bursts in "bursting" neurons even when synaptically isolated from the network (Fig. 1d) (5). Furthermore, the model produced a small subpopulation of "sigh-only" neurons (18/300, 6%) that were active during sighs but not eupnea (Fig. 1e, f) (5). These neurons were not defined to be "sigh-only" *a priori*.

To further test the role of Ca^{2+} oscillations in producing the sigh rhythm, Ca^{2+} dynamics were manipulated in the model network. We altered the amplitude of the slow Ca^{2+} oscillation by modifying the parameter $k1$, the amplitude of the fast Ca^{2+} oscillation by modifying $k2$, and the frequency of the slow Ca^{2+} oscillation by modifying the intracellular calcium release parameter [IP3] (16). Increasing the amplitude of Ca^{2+}_{slow} increased the probability of sighs (Fig. 2a, b). When the amplitude of Ca^{2+}_{slow} was small, total Ca^{2+} exceeded the Ca^{2+} gated channels' threshold and only evoked a sigh when the Ca^{2+}_{slow} burst coincided with the eupnea linked Ca^{2+}_{fast} oscillation, thereby linking the timing of sigh bursts to the burst phase of the eupnea rhythm (Fig. 2c). Indeed, sighs rarely occurred when the Ca^{2+}_{slow} peak occurred early in eupneic phase (see Methods), that is, when the Ca^{2+}_{slow} transient immediately followed a eupneic burst (Fig. 2c, Extended Data Fig. 2a) (16, 17). Increasing Ca^{2+}_{slow} amplitude increased the probability of a given Ca^{2+}_{slow} oscillation evoking a sigh by lengthening the time-window within the eupneic cycle during which the total Ca^{2+}_{in} could exceed the threshold for Ca^{2+} gated channel activity

(Extended Data Fig. 2a). The morphology of modeled sighs also depended on the amplitude and eupneic phase of the Ca^{2+}_{slow} oscillation (Extended Data Fig. 2b, d). Biphasic sighs occurred more often at low Ca^{2+}_{slow} amplitudes and when the Ca^{2+}_{slow} oscillation coincided with or slightly preceded the onset of a eupneic burst. Conversely, monophasic sighs occurred more frequently when Ca^{2+}_{slow} amplitude was high, and when the Ca^{2+}_{slow} oscillation peaked between eupneic bursts. While holding the dynamics of the Ca^{2+}_{slow} oscillation fixed, sighs also emerged from the model preBötC network when the amplitude of Ca^{2+}_{fast} was increased; however, sighs were only generated within a small range of Ca^{2+}_{fast} amplitudes (Extended Data Fig. 3). Increasing the frequency of Ca^{2+}_{slow} while holding the Ca^{2+}_{slow} amplitude constant led to a corresponding increased sigh frequency from low to moderate Ca^{2+}_{slow} frequencies (Extended Data Fig. 3). At higher Ca^{2+}_{slow} frequencies sighs were eliminated, and eupnea was disrupted (Fig. 2d).

Ca^{2+} dynamics drive sigh behavior *in silico* and *in vitro*

Our *in silico* preBötC model network made three predictions for the role of an extrinsically driven calcium oscillation in generating sigh bursts. Increases in $[Ca^{2+}]_{in}$ should: 1) increase sigh occurrence, 2) decrease the prevalence of biphasic sigh bursts, and 3) abolish sighs above a certain critical concentration. To test these predictions experimentally, we used norepinephrine (NE), a neuromodulator known to increase sigh frequency (6, 18) and up-regulate Ca^{2+}_{in} concentration(19) through second messenger pathways via activation of adrenergic receptors (17). NE increased the frequency of sighs in a manner consistent with the simulated manipulation of Ca^{2+}_{slow} frequency (Fig. 2d, e). Furthermore, increasing [NE] *in vitro* and increasing slow Ca^{2+} oscillation amplitude *in silico* had similar effects on sigh shape, shifting sighs from mostly biphasic to mostly monophasic (Fig. 2e, f). Consistent with simulated population activity observed at high Ca^{2+}_{slow} frequencies (Fig. 2d), inter-sigh interval decreased with increasing [NE] until the concentration was too high and resulted in cessation of sighs, leaving only eupneic activity (Fig. 2e, g). Collectively, these experimental and computational manipulations of Ca^{2+} suggest sigh generation is driven by the presence of a slow, rhythmic signaling mechanism that causes synchronized increases in $[Ca^{2+}]_{in}$ among preBötC neurons.

Astrocytes modulate sighing through purinergic signaling

We hypothesized that glia could be the source of the Ca^{2+}_{slow} transients that are synchronized across the respiratory rhythm generating network. Astrocytes respond to metabolic changes in their extracellular environment by increasing intracellular Ca^{2+} (20) through G-protein coupled receptor cascades. In the respiratory networks (21, 22), and throughout the central nervous system (23, 24), astrocyte responses spread through gap junctions (25) and involve the release of ATP which modulates neural activity via purinergic mechanisms (26-28). Therefore, we tested the contribution of purinergic signaling to sigh generation *in vitro* by pharmacological manipulation of ADP and ATP receptors P2Y1 and P2X, respectively (Fig. 3a, b) (29). In rhythmic brainstem slices containing the preBötC, activation of

purinergic P2Y1 receptors ($P2Y1_R$) with MRS2365 significantly increased sigh frequency (Fig. 3a), and subsequent blockade of P2Y1 receptors (MRS2279), but not P2X receptors (TNP-ATP), abolished sighs. The $P2Y1_R$ antagonist also blocked sighs induced with the β-adrenergic agonist isoproterenol (Fig. 3b). These findings suggest that P2Y1- but not P2X-dependent purinergic signaling is important for the generation of spontaneous sighs.

To test if purinergic P2Y1 inhibition would also block sighs generated during the central hypoxic response *in vitro* (Fig. 3d), eupnea and sigh activity was recorded before and during an initial bout of severe hypoxia (SH). After a recovery period, MRS2279 was applied prior to a second hypoxic episode. Inhibition of P2Y1 signaling eliminated or reduced sighs in 8 of 9 slices. We performed immunohistochemistry to confirm $P2Y1_R$ expression in the brainstem (29, 30). We found that $P2Y1_R$ was widely expressed in the preBötC and appeared to colocalize with both neurons and astrocytes (Fig. 3c). Furthermore, inhibition of $P2Y1_R$ significantly reduced the augmentation of eupneic frequency characteristic of the initial phase of the hypoxic response (26). In control experiments where no drugs were applied, similar effects were not observed during the second exposure to severe hypoxia (Fig. 3d).

Astrocytes are sufficient for sigh generation within the preBötC network

To further test the potential role of astrocytes in sigh generation, we tested whether selective manipulation of astrocytes (31, 32) would be sufficient to produce sighs. In brainstem preBötC slices from *Aldh1l1*^{Cre};*Rosa26*$^{ChR2:EYFP}$ mice, we found that brief (200ms) light pulses evoked both eupnea and sigh bursts recorded from the contralateral preBötC (Fig. 4a,b). Our photostimulation parameters were able to reliably evoke bursts in 12/25 slice preparations. In the remaining slices, longer duration or higher intensity light pulses were effective in evoking eupnea and sigh bursts. Sighs evoked by photoactivation of *Aldh1l1*-expressing cells were indistinct from spontaneous sighs in burst amplitude and post burst interval (Fig. 4a). However, the duration of evoked sigh bursts was shorter relative to spontaneous sighs, consistent with a small increase in the proportion evoked monophasic sighs. These experiments suggest that *Aldh1l1* astrocytes are sufficient to initiate both sigh and eupneic bursts that are largely indistinguishable from spontaneously occurring activities.

Blocking P/Q-type calcium channels inhibits sighs (9), and P/Q type ($Ca_V2.1$) knockout mice do not generate sighs *in vitro* or *in vivo*, and ultimately die of atelectasis (8). The effect of P/Q-type channel can also be mimicked by the general Ca^{2+} channel blocker Cd^{2+} which selectively inhibits sighs at low concentrations (5, 33). Therefore, 4 μM Cd^{2+} was applied during optogenetic stimulation to test if astrocyte stimulation would continue to evoke sighs (Fig. 4b, Extended Data Fig. 4a). In Cd^{2+}, photostimulation failed to evoke sighs. However, we observed evoked double bursts and bursts that appeared to have slightly larger amplitudes than eupneic bursts. We refer to these bursts as ‘sigh attempts’. Sigh attempts were less likely to occur than sighs evoked under baseline conditions; 4.7% of stimulations evoked a sigh attempt in Cd^{2+}, compared to 24.1% in baseline. The amplitude of sigh

attempts in Cd^{2+} was significantly reduced from baseline sighs but remained slightly larger than evoked eupnea. The duration of sigh attempts in Cd^{2+} was statistically indistinct from eupnea duration. Moreover, sigh attempts in Cd^{2+} lacked an extended post burst interval ("post-sigh apnea") that is characteristic of normal sighs.

We also tested if the $P2Y1_R$ antagonist MRS2279 would affect the ability of astrocytes to drive sighing (Fig. 4b, Extended Data Fig. 4a). Following $P2Y1_R$ inhibition, sighs evoked during photostimulation of *Aldh1l1* astrocytes were completely blocked in all but one slice (n = 7). Consistent with evoked sigh attempts observed in Cd^{2+}, sigh attempts in MRS2279 were smaller in amplitude than baseline sighs and had burst durations similar to evoked eupnea. However, post-burst intervals after sigh attempts in MRS2279 remained longer than those after eupnea (Fig. 4b). Collectively, these data indicate that $P2Y1_R$ - and Ca^{2+}-dependent signaling are important mechanisms that allow astrocytes to drive sighing activity in the preBötC.

Next, we asked if light activation of astrocytes *in vivo* would have the same effect on sigh modulation (n = 9). Indeed, we found that there was a higher probability of evoking sighs *in vivo* than *in vitro* (Fig. 4c, Extended Data Fig. 4c), and in general, sigh characteristics similarly matched *in vitro* data. Evoked sighs *in vivo* could be unambiguously distinguished from eupnea by characterizing the diaphragm amplitude (Fig. 4d). Notably, evoked eupnea in simultaneous recordings of the hypoglossal nerve (XII) tended to be larger in amplitude than spontaneous eupnea, which made distinguishing sighs from eupnea more difficult based solely on XII recordings (Extended Data Fig. 4b).

Interestingly, MRS2279 bilaterally injected into the preBötC *in vivo* was less effective in completely blocking spontaneous or evoked sighs (n = 3/6, Extended Data Fig. 4c, d); contrary to the very reliable inhibitory effect observed *in vitro* (Fig. 4b). This may not be surprising given that numerous descending inputs that are present *in vivo* and endogenously modulate sighs(34) including bombesin-like peptides (7) and noradrenergic inputs (6) will likely reduce the ability to block sighs by purinergic mechanisms *in vivo*. Corresponding to this variability, we observed a higher probability of evoked burst failures altogether in the presence of MRS2279 (Extended Data Fig. 4c). This weaker stimulation corroborates the control of sighs from outside areas (7), which are eliminated from *in vitro* slice experiments. Our data indicate that sighs are an emergent property involving local neuroglial interactions mediated by purinergic signaling and modulatory inputs intrinsic and extrinsic to the preBötC.

Materials and Methods

Computational Model

The computational model for the present study incorporates a shared external source of Ca^{2+} oscillations to elicit global synchronization across the respiratory network. Equations were adopted from an original model of the respiratory network(14). The membrane potential of each compartment and gating variables are described in equations 5 - 16. A Ca^{2+} dependent current which has bell shaped Ca^{2+}

activation/inactivation was incorporated into each neuron. Based on the previous experimental observations indicating that the sigh frequency is independent from eupneic frequency (2) and that sighs are inhibited by Ca^{2+} channel blockers and absent in P/Q type Ca^{2+} channel knock-out mice(8), we modeled the dynamics of Ca^{2+} oscillations as a superposition of two independent components: 1) slow oscillations with dynamics governed by IP_3 channels in endoplasmic reticulum (ER) (16, 35) and 2) fast Ca^{2+} that are associated with eupneic activity and are regulated by the dynamics of the persistent sodium current (4, 35). The slow component is defined by:

$$\frac{dC}{dt} = f_i \cdot \left(J_{ER_{in}} - J_{ER_{out}}\right) \quad \text{Eq.1}$$

$$J_{ER_{in}} = \left(L + P\left(\frac{I \cdot C \cdot l}{(I+k_I)(C+k_a)}\right)^3\right)\left(\frac{C_t - C}{\sigma} - C\right) \quad \text{Eq.2}$$

$$J_{ER_{out}} = \left(\frac{V_e C^2}{k_e^2 + C^2}\right) \quad \text{Eq.3}$$

$$l' = A \cdot \left(k_d - l \cdot (C + k_d)\right) \quad \text{Eq.4}$$

where C is the shared external calcium signal, $J_{ER_{in}}$ and $J_{ER_{out}}$ are the fluxes of Ca^{2+} into and out of the ER, respectively, and l is the IP_3 channel gating variable. The parameter f_i is the ratio of bound to free [Ca^{2+}], L is the leak ER permeability, P is the maximum permeability of the IP_3 channels, I is the concentration of IP_3 channels, k_I is the dissociation constant of IP_3 receptor by IP_3, k_a is the dissociation constant of the IP_3 receptor for Ca^{2+}, C_t is the maximal [Ca^{2+}] in the external source, σ is the ratio of the volume of the ER to the volume of the cytosol, V_e is the maximal SERCA pump rate, k_e is the SERCA pump coefficient, A is a scaling factor, and k_d is the constant of IP_3 receptor inactivation by Ca^{2+}.
Each neuron is a single compartment neuron modeled by the following equations:

$$\frac{dV}{dt} = \frac{-1}{C_m}\left(I_{Na} + I_K + I_{NaP} + I_{leak} + I_{syn} + I_{Cas}\right) \quad \text{Eq.5}$$

The sodium, potassium, persistent sodium, leak, synaptic, and Calcium sensitive currents are, respectively:

$$I_{Na} = g_{Na} \cdot m_\infty(V)^3 \cdot \left(1 - n(V)\right) \cdot (V - E_{Na}) \quad \text{Eq.6}$$

$$I_K = g_K \cdot n(V)^4 \cdot (V - E_K) \quad \text{Eq.7}$$

$$I_{NaP} = g_{NaP} \cdot m_{p_\infty}(V) \cdot h(V) \cdot (V - E_{Na}) \quad \text{Eq.8}$$

$$I_{leak} = g_{leak} \cdot (V - E_{leak}) \quad \text{Eq.9}$$

$$I_{syn} = \sum_i^k g_{syn_i} \cdot \left(V - E_{syn}\right) \quad \text{Eq.10}$$

$$I_{Cas} = g_{Cas} \cdot m_{Cas}(Ca)^2 \cdot h_{Cas}(Ca) \cdot (V - E_{Cas}) \quad \text{Eq.11}$$

where g_x represents the maximal conductance of each current, E_x represents the reversal potential of the respective channel.

The dynamic activation (n, m_{Cas}) and inactivation (h, h_{Cas}) of the currents are governed by:

$$\frac{dx}{dt} = \frac{x_\infty - x}{\tau_x} \quad \text{Eq.12}$$

for $x = \{n, h, m_{Cas}h_{Cas}\}$. Time constants τ_x are

$$\tau_x = \frac{\overline{\tau_x}}{\cosh\left(\frac{V - V_x}{2\sigma_x}\right)} \text{ for: } x = \{n, h\} \quad \text{Eq.13}$$

and

$$\tau_x = \tau_{0_x} + \frac{\overline{\tau_x}}{1 + \exp\left(\xi_x([Ca]_{in} - [Ca]_x)\right)} \text{ for: } x = \{m_{Cas}, h_{Cas}\} \quad \text{Eq.14}$$

Steady state voltage dependent activation or inactivation, x_∞ is defined as:

$$x_\infty = \frac{1}{1 + \exp\left(\frac{V - V_x}{\sigma_x}\right)} \text{ for: } x = \{m, m_p, h, n\} \quad \text{Eq.15}$$

and

$$x_\infty = \frac{1}{1 + \exp\left(\theta_x([Ca]_{in} - [Ca]_x)\right)} \text{ for: } x = \{m_{Cas}, h_{Cas}\} \quad \text{Eq.16}$$

The values of $[Ca]_{m_{Cas}}$ and $[Ca]_{h_{Cas}}$ define the opening and closing (respectively) of the Ca^{2+} "activation window" (the range of $[Ca]_{in}$ values that open the Ca^{2+} sensitive channel), the values of $\xi_{m_{Cas}}, \xi_{h_{Cas}}$ define the kinetics of the Ca^{2+} sensitive channel activation and inactivation (respectively), and the values of $\theta_{m_{Cas}}, \theta_{h_{Cas}}$define the steepness of the sigmoidal activation/inactivation of the Ca^{2+} sensitive channel.

Intracellular calcium concentration dynamics are described as:

$$\frac{d[Ca]_{in}}{dt} = \frac{1}{\tau_{Ca}}\left(k_1 \cdot C + (k_2 \cdot m_{p_\infty} \cdot h) - [Ca]_{in}\right) \quad \text{Eq.17}$$

Where the first term describes the slow external calcium dynamics and the second term describes the fast, bursting driven internal dynamics. The variables l, C are those from the slow, external calcium

oscillation. k_1, k_2 govern the relative influence of the slow and fast calcium sources, respectively, on the total intracellular calcium levels: $[Ca]_{in}$.

Synapses from a source neuron (i) to a target neuron (j) were governed by the equations(36):

$$\frac{ds_i}{dt} = \frac{(1 - s_i)m_{\infty_{syn}}(V_i) - s_i}{\tau_{syn}} \quad \text{Eq.18}$$

$$m_{\infty_{syn}} = \frac{1}{1 + \exp\left(\frac{V_i - Q_s}{\sigma_{syn}}\right)} \quad \text{Eq.19}$$

$$g_{syn_i} = g_{syn_{max}} \cdot s_i \quad \text{Eq.20}$$

Networks were constructed of 300 neurons with randomly generated excitatory synaptic connections such that the average neuron had a total of 6 synaptic connections (incoming and outgoing inclusive). Eight unique network configurations (connectivity patterns) were generated to allow for multiple replicates in some experiments. Neurons were defined such that their activity without synaptic inputs could be clearly defined as bursting, tonic, or quiescent by varying their leak conductance g_{leak} (Fig. 2a). Parameters that are shared across all neurons are given in Table 1. Network and cell specific parameters are given in Table 2. Simulations were constructed using the Brian2 python package(37) using the Runge-Kutta 4th order method with a fixed timestep of 0.25ms. Networks were simulated for 1000s, unless otherwise stated. After 1000s, synaptic conductance (g_{syn}) was set to 0nS to observe isolated neuron behavior. Spike times were computed as the time at which the cell voltage crossed a -20mV threshold. Population rate was computed by first taking the sum of the number of spikes in each timestep, then smoothing with a boxcar filter with width of 10-100ms. Eupneic phase was defined as the time difference between the peak of the Ca^{2+}_{slow} signal and the peak of the previous eupneic burst, divided by the mean eupneic interval.

Animals

All experiments and animal procedures were approved by the Seattle Children's Research Institute's Animal Care and Use Committee and conducted in accordance with the National Institutes of Health guidelines. Male and female mice were selected randomly. Experiments were performed in brainstem slices obtained from CD1 or transgenic mice age postnatal day 4-12 and bred at Seattle Children's Research Institute. Aldh1l1^{cre} mice were obtained from Jackson Laboratories (FVB-Tg (Aldh1l1-cre) JD1884Htz/J, Jax stock No. 023748). Cre mice were crossed with homozygous mice containing a floxed STOP channelrhodopsin2 fused to an EYFP (Ai32) reporter sequence. All mice were group housed with access to food and water *ad libitum* in a temperature controlled (22 ± 1°C) facility with a 12hr light/dark cycle.

In vitro transverse brainstem slice preparation and population recordings

The following techniques used are described in detail in a series of publications by the Ramirez laboratory (4, 9, 38). PreBötC slice thickness varied between 590-610μM. Animals were quickly decapitated, and brainstems were rapidly dissected in cold artificial cerebrospinal fluid (ACSF). Serial transverse slices were made from the appearance facial nerve until reaching the level of the preBötC, where a 580-610uM slice was made. Slices were transferred into the recording chamber with circulating ACSF with osmolarity of 305-320 osm/L, pH 7.4 and containing (in mM) NaCl (118), KCl (3), $CaCl_2$ (1.5), $MgCl_2$ (1), $NaHCO_3$ (25), NaH_2PO_4 (1), and D-glucose (30). Temperature was maintained at 29-31°C and ACSF was bubbled with carbogen (95% O_2 / 5% CO_2). During extracellular population recordings the superfused ACSF was circulating and recycled at a flow rate of 10-13ml/min. Activity was recorded from the caudal side of the transverse slice. Some experiments were performed with two slices at the same time using two extracellular electrodes. Extracellular raw traces were filtered and integrated. The data obtained were analyzed using GraphPad Prism 7 and PCLAMP 10 software which is available online at http://www.moleculardevices.com/systems/conventional-patch-clamp/pclamp-10-software. For unknown reasons, some preBötC slices do not have periodic sighs within the baseline recording period, or they occur at intervals >20 mins. These slices were not used for experiments. PreBötC slices were not used across multiple drug experiments. When selecting bursts for doublet analysis, bursts occurring in quick succession were only characterized as doublets if the first burst did not reach baseline before onset of the second burst.

In Vivo Anesthetized Preparation

In vivo anesthetized experiments were performed as previously published(39). Briefly, adult mice were anesthetized with urethane (1.5 mg/kg, i.p.) and placed supine on a custom surgical table. Adequate depth of anesthesia was determined via heart rate, breathing frequency, and response to toe pinch. Bipolar stainless steel electrodes were implanted in the diaphragm muscles to perform electromyographic recordings of inspiratory motor activities (40). The trachea was exposed through a midline incision and cannulated caudal to the larynx with a curved (180 degree) tracheal tube (24 G). The trachea and esophagus were removed rostral to the tracheotomy, and underlying muscles were removed to expose the basal surface of the occipital bone. Mice were supplied with 100% O_2 throughout the remainder of the surgery and experimental protocol. The portion of the occipital bone and dura overlying the ventral medullary surface were removed and the brainstem surface was perfused with aCSF (36 °C) equilibrated with carbogen (95% O_2, 5% CO_2). The hypoglossal nerve (XII) was then isolated unilaterally and recorded from using a fire-polished pulled glass pipette filled with aCSF. XII electrical activity was amplified (10,000×), filtered (low pass 300 Hz, high pass 5 kHz), rectified, integrated, and digitized (Digidata 1550 A, Axon Instruments). In animals in which we observed baseline sighs, MRS2279 (500μM, 41.3nL) and Evan's Blue dye or red fluorospheres were co-injected bilaterally in 3 positions

around the preBötC using a NanoInject, as to avoid lesioning the preBötC core and altering the rhythm. In most instances, injections close to preBötC stimulated sighs immediately following placement of the cannula. Saline injected control animals did not have any alterations in baseline breathing, and we observed the same increase in sighs in most injections (n = 4/5). Similar to *in vitro* experiments, many animals *in vivo* did not have baseline sighs and therefore MRS2279 was not injected.

Optogenetics and Pharmacology

A glass fiber optic (200μm core, 0.24NA) connected to a blue (447nm) high-powered LED was positioned above the preBötC contralateral to the extracellular electrode or XII nerve and positioned for maximal response. Power was set to 0.5 mW/mm^2. Fifty continuous 20s sweeps were recorded for each stimulation experiment *in vitro*, and 20 sweeps for *in vivo* experiments. Laser power settings and pulse width were selected based on previous experiments (13, 41). In approximately 1/3 of Aldh1l1^{cre}/Ai32 preBötC slices, we had difficulty evoking any responses unless increasing the wavelength to a higher laser power (>0.5 mW/mm^{2-} 1 mW/mm^2). Despite having robust respiratory rhythms, we did not continue to perform stimulations in these slices. Control stimulations were performed in Aldh1l1$^{cre\ -/-}$/Ai32 littermates for *in vitro* (n = 2) and adults for *in vivo* (n = 3) experiments. There were no observed non-specific effects of light stimulation, even at maximum laser power.

Norepinephrine (1-40 μM, DL-Norepinephrine hydrochloride, cat. A7256), Isoproterenol (Isoprenaline hydrochloride, cat. I5627), Strychnine (1 μM, cat. S0532), and cadmium (4 μM cadmium chloride, cat. 20208) were purchased from Sigma. Gabazine (1 μM, SR 99531 hydrobromide, cat. 1262), MRS2279 (20μM, P2Y1$_R$ antagonist, cat. 2158,), MRS2365 (20 μM, P2Y1$_R$ agonist, cat. 2157) and TNP-ATP triethylammonium salt (20 μM, P2X receptor antagonist, cat. 2464) were obtained from Tocris. All drugs were diluted in water.

Histology

After experiments, animals were fixed by transcardial perfusion with cold ACSF followed by 4% PFA in phosphate buffer solution (PBS). Medullary and cortical tissue was carefully extracted and equilibrated in graded sucrose solutions to a final concentration of 30%, embedded in OCT solution, frozen at −80 C, and cryosectioned at 25 μm for imaging of immunofluorescence. Slides containing brainstem tissue slices were washed 3x10 min in PBS. Tissue slices were then permeabilized and blocked with 1% normal donkey serum in 0.5% Triton X-100/PBS for 1 h. Following blocking, tissue slices were incubated with the primary antibody for either NeuN (Millipore MAB377), P2Y1 (Abcam ab140859), or EGFP (Abcam ab6673) (1:500 in 1% normal donkey serum in 0.5% Triton X-100/PBS) overnight. After primary antibody incubation, tissue was washed 3x10 min. in phosphate buffer solution (PBS), followed by secondary antibody incubation for 30 min. (Alexa Fluor 488, 594, or 647). Lastly,

tissue was washed 3x10 min. in PBS and hard set mounted (VECTASHIELD hardset mounting media with DAPI). Immunofluorescence images were acquired using an Olympus VS120 Virtual Slide Microscope Scanner. The excitation/emission filter sets used for imaging were DAPI: 380-405/410-480, FITC: 460-490/500-550, Cy3/TRITC: 540-570/580-640, and Cy5: 625-645/655-705. Laser scanning confocal imaging was performed using a Zeiss 710 34-channel Quasar LSC Microscope.

Sigh classification

Custom unsupervised methods were developed to distinguish between eupneic bursts and "sigh attempts" evoked by channelrhodopsin stimulation in *in vitro* recordings. First, bursts in the integrated pre-Bötzinger recording were detected such that the prominence of each peak was greater than 2.5 times the standard deviation of the integrated activity. The onset of the burst was defined as the time at which the trace reached 20% of the subsequent peak height. Bursts that were aberrantly large amplitude (~>75 times the mean amplitude) or very fast rising (reached peak amplitude in less than 150 ms) were discarded as noise. The burst shape for all bursts was extracted from the onset to 1.5 s after onset of the burst. Burst shapes were then decomposed into principal components. The first n components (where n is the number of components needed to explain 95% of the variance) of the spontaneous bursts (i.e., not evoked by optogenetic stimulation) were used as features to fit a robust covariance estimator (sci-kit learn MinCovDet). Since the spontaneous bursts were observed never to be putative sighs, this covariance represents the prior distribution of eupnea, that is, the expected eupneic shape. We calculate the Mahalnobis distance (D) of each burst to the mean eupneic shape. D quantifies how similar each burst is to the "average" eupnea. We then determine a threshold as:

$$D_{thresh} = \widetilde{D_{spontaneous}} + 4 * IQR\left(D_{spontaneous}\right) \quad \text{Eq.21}$$

All evoked bursts where $D_{evoked} > D_{thresh}$ were considered outliers. This outlier detection included many false positive bursts in which the burst shape was different from the average eupnea, but upon inspection was not typical of a sigh (often long slow bursts or large amplitude noise). We boost this outlier detection with an identical method using instead the intuitive features of burst amplitude, full width at half max (FWHM) and time to next burst (post-burst apnea) as features to the covariance estimator. A burst was considered a sigh attempt when it was determined to be an outlier in both the classifier fit on burst shape and on the intuitive features. We imposed a set of final criteria where a sigh attempt must be larger in amplitude than 90% of the spontaneous bursts. To classify sighs in *in vivo* recordings, diaphragm EMG was recorded, rectified, and integrated as described above. Bursts in the integrated diaphragm EMG were detected, and each burst shape was extracted. The area under the curve was computed for each burst. Bursts were labeled as "sighs" if both the area under the curve and the amplitude for a given sigh was >6x the median absolute deviation (MAD) of the 20 bursts preceding and following the given burst.

Statistical analysis

Analyses were performed using GraphPad Prism 9 software. Groups were compared using paired two-tailed t-tests or ordinary one-way or ANOVAs followed by Bonferonni's post hoc tests, if necessary. Statistical significance was set at $\alpha = 0.05$. Data are presented as means $\pm$ SE. Masking was not used during data collection or analysis.

Code availability

Source code is available at (https://github.com/nbush257/sighnet).

Data availability

The raw data presented in all figures of this manuscript is available upon request.

Caveats and limitations

The use of transverse preBötC slices as a model for respiratory rhythm generation is associated with significant caveats of which oxygenation (42), incomplete network, low temperature, elevated [K+] saline are the most obvious concerns, and have been discussed in most of our publications (2, 4, 42-44). Although transverse slices generate rhythmicity in 3 mM K^+ (45-47) rhythmicity is more reliable and consistently generated at 8 mM K^+. Thus, in the present study we consistently use the extracellular concentration of 8 mM K^+. To distinguish the fast-respiratory rhythm from the slow sigh rhythm, we refer to the fast-respiratory rhythm as "eupneic" activity throughout this study. However, we do not imply that this *in vitro* activity represents "eupnea" in the behavioral sense. Rather this activity characterizes primarily the inspiratory component of the respiratory activity generated within the preBötC(2, 48, 49). Furthermore, sighs were characterized based on their appearance in the in vivo preparation and were carefully distinguished using a novel pipeline aimed at reducing bias. However, in vivo recordings should involve increased diaphragm activity along with the characteristics observed of sighs, and thus in vitro work is limited in this sense. In our analysis, we did not consider doublets to be sighs. Despite these caveats and limitations, the comparisons between the experiments performed *in vitro* revealed many similarities to the testable predictions set forth by the computational model.

FIGURES

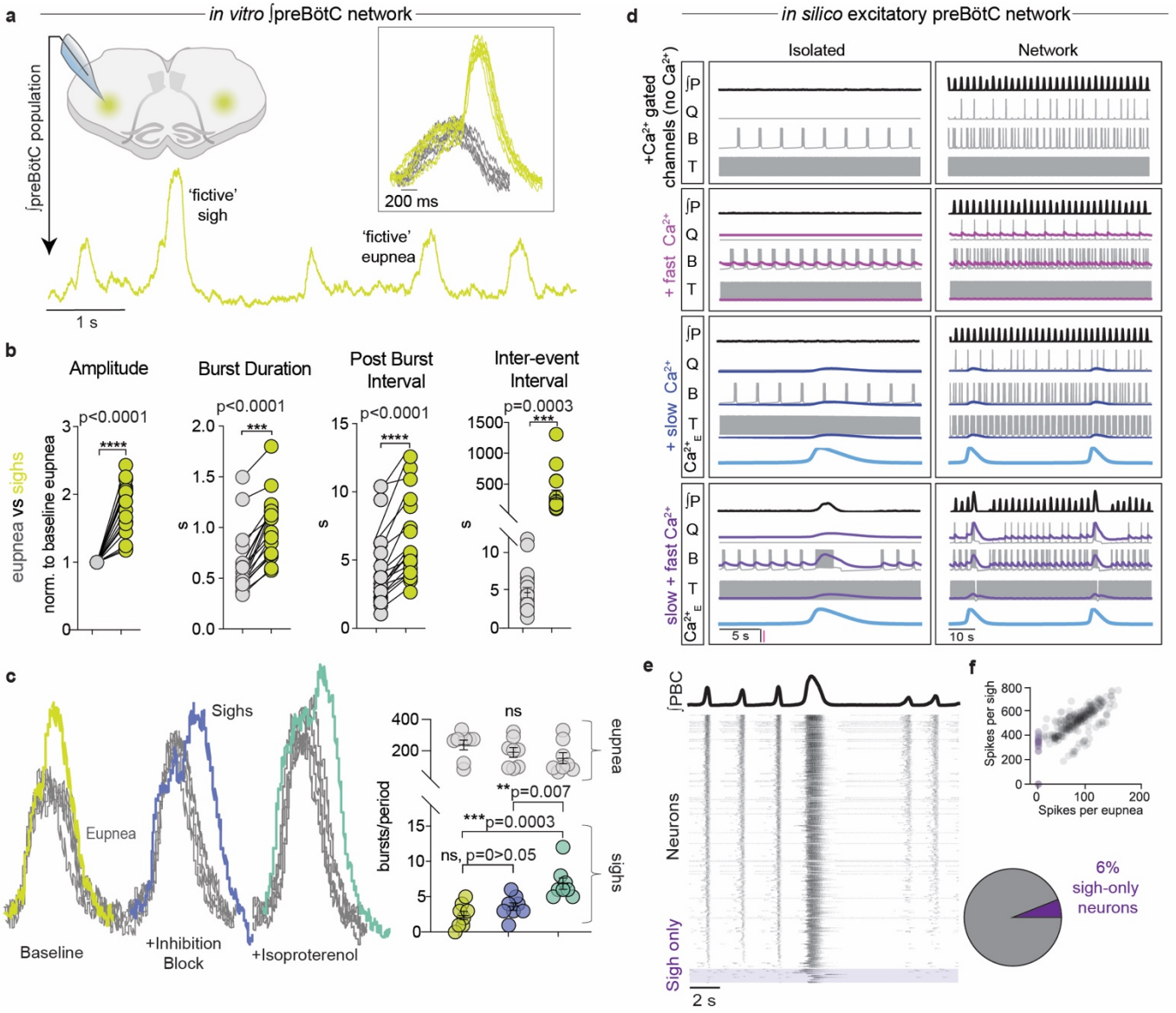

Figure 1. Sigh generation in the preBötC can be mimicked *in silico* by introducing fast and slow Ca^{2+} oscillations into an excitatory network model. (a) integrated population activity of eupnea and sighs recorded from the transverse slice preparation. Inset shows overlaid 'fictive' eupnea (gray) and sighs (green) for comparison. (b) Amplitude, burst duration, post burst interval, and inter-event interval of eupnea and sighs differ significantly (paired t-test). (c) Inhibition block (strychnine and gabazine) does not alter sigh frequency at baseline or with β-adrenergic agonist isoproterenol (ordinary one-way ANOVA). (d) *In silico* generation of 'fictive' sighs is altered by adjusting modeled fast (eupnea associated) and slow (extrinsically driven) Ca^{2+} transients. Inclusion of both Ca^{2+} sources resulted in sigh-like bursts. Integrated population rates ($\int P$), and quiescent, bursting, and tonic neuron voltages (Q,B,T) are shown isolated and in network for different Ca^{2+} inclusions. (e) Integrated population activity and spiking raster for 300 simulated neurons. Purple shading highlights 18 "sigh-only" neurons (f) Median number of spikes per eupnea is plotted against median number of spikes per sigh burst; each dot represents one neuron. Sigh only neurons are shown in purple. Proportion of sigh-only neurons is 6% (18/300).

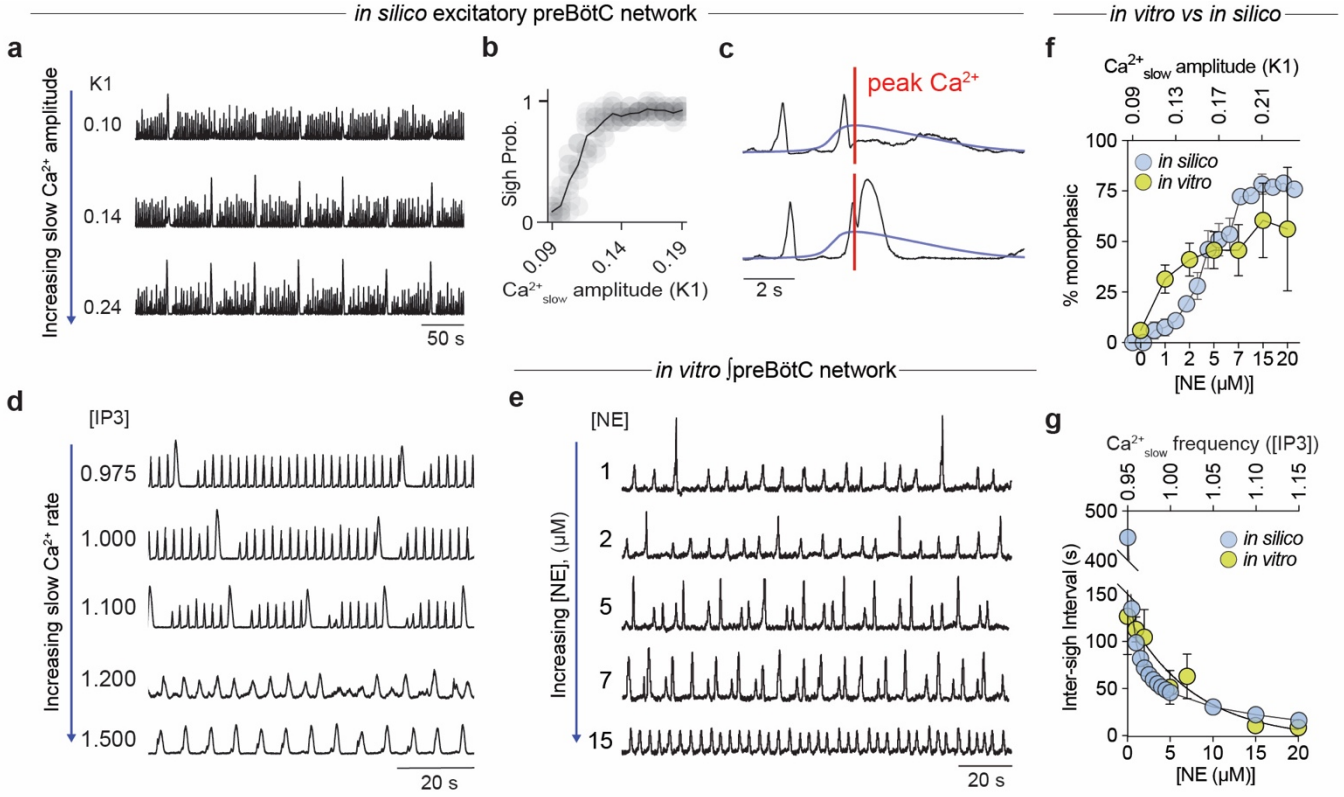

Figure 2. Sigh frequency and shape is similarly affected by manipulations of Ca^{2+} *in vitro* and *in silico*. (a) *In silico* population activity from simulations with increasing amplitude of Ca^{2+}_{slow} signals ($k1$). (b) Sigh probability during an extrinsic Ca^{2+} burst as a function of slow Ca^{2+} amplitude ($k1$) represented by independent simulations (gray circles) and average of 8 simulations (black line). (c) Population traces (black), extrinsic Ca^{2+} (blue), and peak extrinsic Ca^{2+} (red) for sigh failure and success. (d) Population firing rates of simulated networks with increasing frequency of extrinsic slow Ca^{2+} transients as governed by increases in $[IP3]$. (e) Representative traces of *in vitro* preBötC population activity; increasing [NE] increases number of sigh bursts. (f) Sighs are more likely to be monophasic as slow Ca^{2+} amplitude (blue) or [NE] (green) increases. (g) Average inter-sigh interval decreases for *in silico* simulations (blue) as function of extrinsic Ca^{2+} oscillation frequency ($[IP3]$) with fixed amplitude and *in vitro* recordings as a function of [NE] (green).

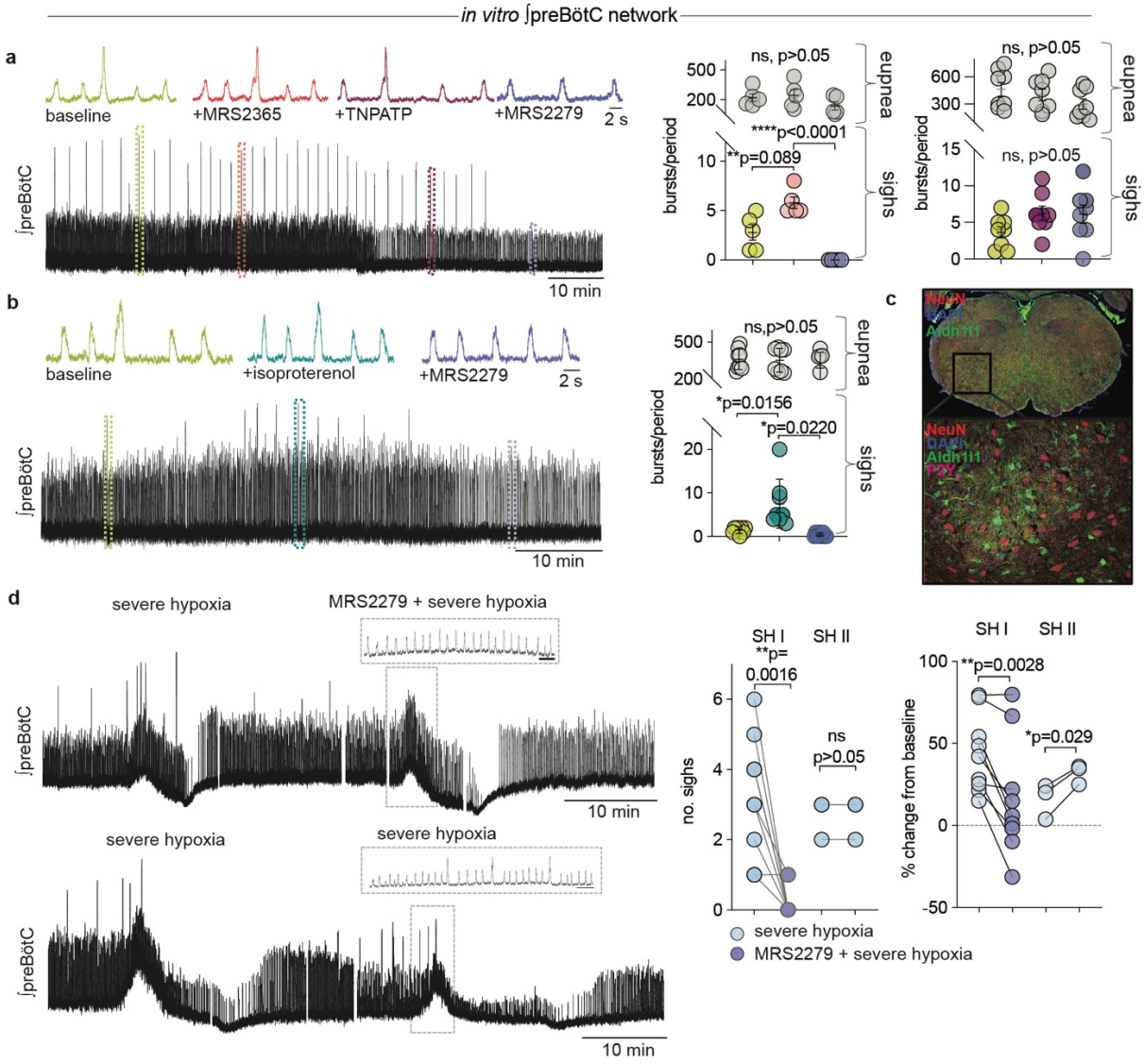

Figure 3. P2Y1$_R$ dependent signaling is necessary for spontaneous and hypoxia induced sigh generation in the preBötC. (a) Integrated preBötC activity depicting time course for P2Y1$_R$ manipulation. MRS2365 significantly increased the number of sighs from baseline while P2Y1$_R$ antagonist MRS2279 abolished all sighs. P2X$_R$ antagonist (TNP-ATP) did not significantly affect sigh frequency; no significant effect on eupneic frequency was observed with any drug additions. Analysis of sigh and eupnea burst number is reported as number of bursts/20 min period (one-way ANOVA). (b) P2Y1$_R$ antagonist MRS2279 eliminated the β-adrenergic agonist induced increase in sighs (one-way ANOVA). (c) PreBötC section immunostained with NeuN and EYFP (for Aldh1l1cre^{Rosa26eYFP}). Inset is 40x confocal image of PreBötC slice with additional immunostaining for the P2Y1$_R$. (d) P2Y1$_R$ inhibition blunts the augmented portion of the hypoxic response. Representative traces from transverse preBötC slices during initial bout of severe hypoxia (SH, 6mins), followed by a recovery period and second hypoxic challenge with MRS2279. Lower panel depicts control with two consecutive bouts of severe hypoxic challenge. Gaps in recordings were made to align control and experimental traces. Inset preBötC integrated traces have time scales of 10s. MRS2279 in addition of severe hypoxia significantly impaired the hypoxic response by eliminating sighs (left) and reducing the augmenting phase of the eupneic rhythm (right, both paired t-test).

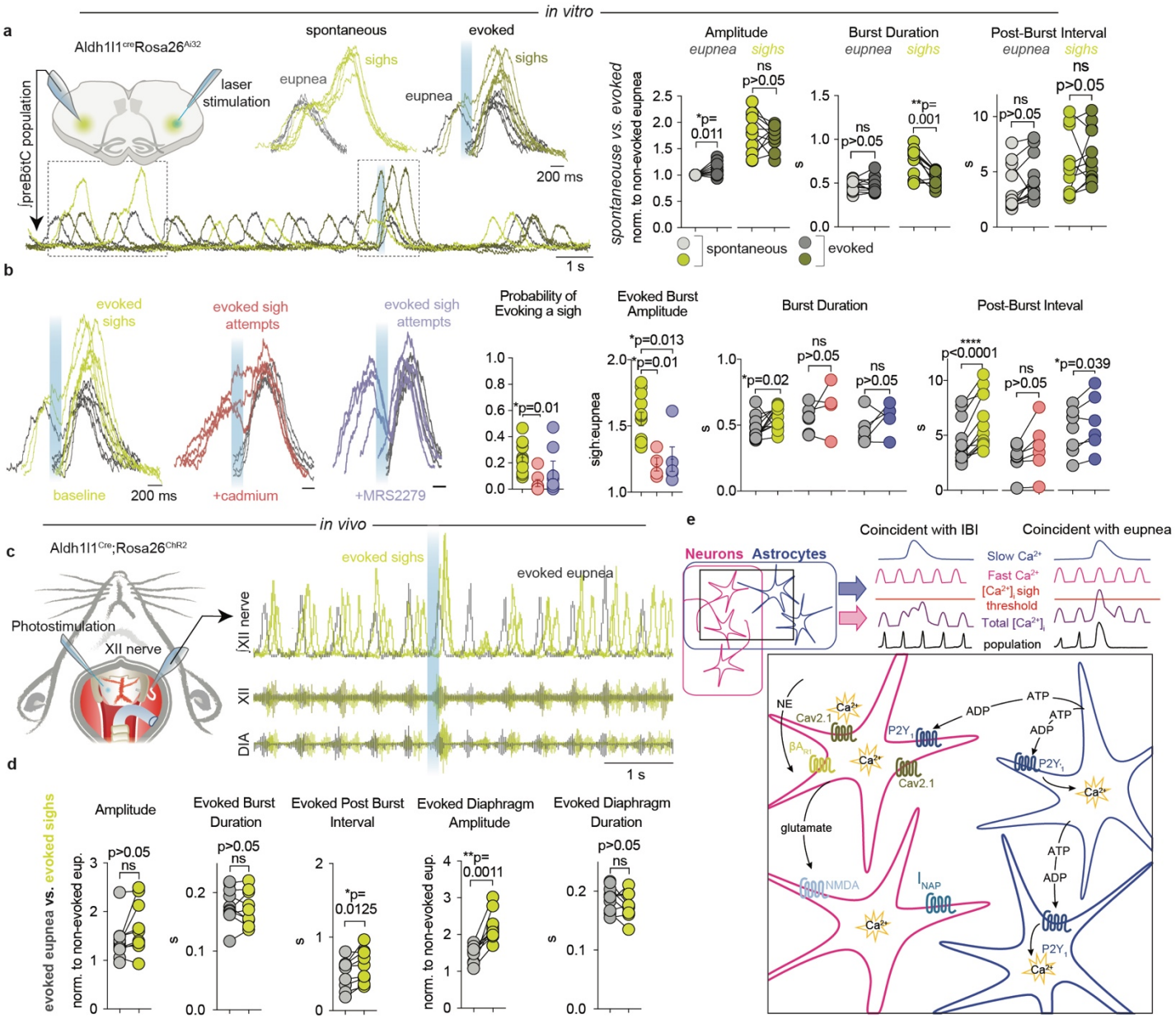
in vitro
a
Aldh1l1cre Rosa26Ai32
laser stimulation
∫preBötC population
spontaneous
evoked
eupnea
sighs
200 ms
1 s
Amplitude
Burst Duration
Post-Burst Interval
eupnea sighs
spontaneous
evoked
b
evoked sighs
evoked sigh attempts
baseline
+cadmium
+MRS2279
Probability of Evoking a sigh
Evoked Burst Amplitude
Burst Duration
Post-Burst Inteval
in vivo
c
Aldh1l1Cre;Rosa26ChR2
Photostimulation
XII nerve
∫XII nerve
XII
DIA
d
Amplitude
Evoked Burst Duration
Evoked Post Burst Interval
Evoked Diaphragm Amplitude
Evoked Diaphragm Duration
e
Neurons Astrocytes
Coincident with IBI
Coincident with eupnea
Slow Ca2+
Fast Ca2+
[Ca2+]i sigh threshold
Total [Ca2+]i
population
NE
Cav2.1
ADP
ATP
P2Y1
glutamate
NMDA
INAP

Figure 4. Activation of preBötC astrocytes drives sighing *in vitro* and *in vivo*. (a) PreBötC slice depicting electrode and laser placement and representative traces comparing spontaneous (light green, gray) and photo-evoked (dark green, dark gray) sighs and eupnea, with expanded view above. turquoise bar represents 200ms light pulse. Evoked sighs withheld the same characteristics as spontaneous sighs with a smaller duration given the larger number of evoked monophasic sighs. (b) Optogenetically evoked sighs are blocked by Cadmium (4μM) and MRS2279 (20μM). Representative traces depicting differences between baseline evoked sighs and 'sigh attempts' and eupnea in drug conditions. Cadmium, but not MRS2279 significantly reduced the probability of evoking a sigh. Sigh characteristics were absent from evoked bursts in cadmium and MRS2279 including a reduction in burst amplitude, burst duration, and post burst interval. Graphs show that 'sigh attempts' did not significantly differ from eupnea in most characteristics. Missing symbols in Cadmium or MRS2279 represent that no sigh attempts were evoked. (c) Schematic depicting *in vivo* anesthetized preparation and corresponding (shortened) evoked sweeps as recorded from the hypoglossal (XII) nerve. Evoked sighs *in vivo* were best distinguished by diaphragm amplitude and generally retained sigh characteristics that were significantly different from evoked eupnea, with the exception of burst duration and post burst interval. (d) Hypothesis of sigh rhythm generation. Changes in PO_2 levels increase intracellular Ca^{2+} in astrocytes, resulting in ATP release, which is converted to ADP. ADP binds to purinergic $P2Y1_R$'s leading to Ca^{2+} increase in astrocytes and neurons through g-protein signaling cascades. *In silico* data supports the hypothesis that the externally derived, astrocytic Ca^{2+}_{slow} increases intracellular Ca^{2+} in neurons; Ca^{2+}_{slow} coincides with Ca^{2+}_{fast} to enhance Ca^{2+}_{total}, generating an augmented burst. Based on *in vitro* and *in vivo* data, we postulate that the Ca^{2+}_{slow} oscillation in the modeled network is initiated through $P2Y1_R$ signaling. $P2Y1_R$ driven sighs *in vivo* can be overridden my neuromodulation from upstream pathways (e.g. Norepinephrine, neuromedin B, gastrin releasing peptide) to provide further sigh modulation depending on metabolic state.

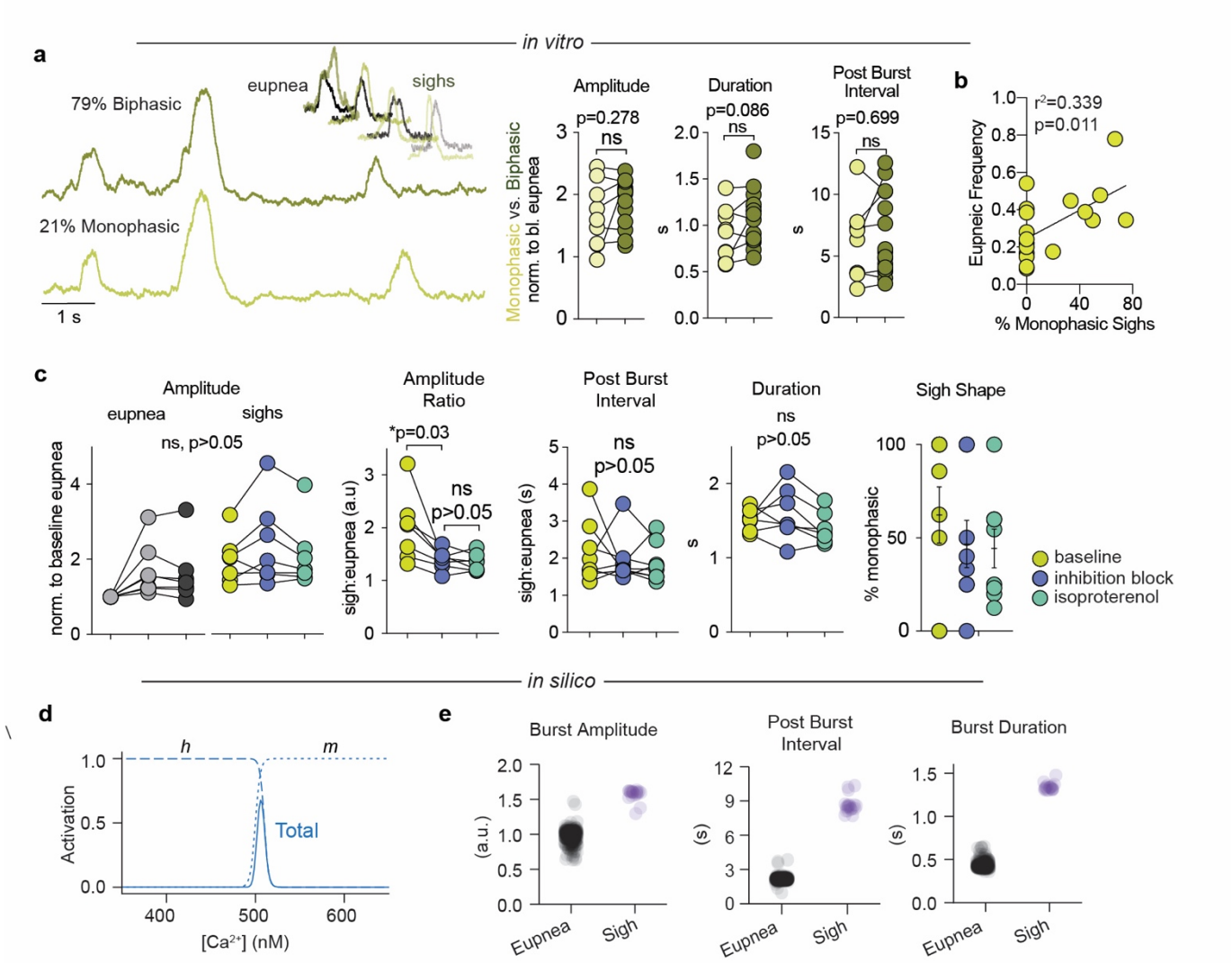

Extended Data Figure 1. (a) Sighs observed in the transverse preBötC slice preparation are commonly 'biphasic' or 'monophasic' but retain the same distinguishing sigh characteristics (paired t-tests). Inset shows overlayed eupnea (gray) and sighs (green) for comparison. (b) Higher eupneic frequencies were positively correlated with a larger number of monophasic sighs (simple linear regression). (c) Inhibition block does not alter sigh characteristics or frequency. No change in the amplitude of sighs was observed with inhibition block, however a significant increase in eupneic amplitude led to a decrease in the sigh:eupnea ratio. No change was observed in the sigh burst duration, sigh post burst interval, or sigh shape (ordinary one-way ANOVA). (d) Ca^{2+}-sensitive cation channel steady state activation curves. Steady state activation m_{Cas_∞}, inactivation (h_{Cas_∞}), and total activation ($m^2{}_{Cas_\infty} \cdot h_{Cas_\infty}$,) of the Ca^{2+} sensitive channels are shown as a function of intracellular Ca^{2+} concentration. Activation starts at zero for low $[Ca]_{in}$; inactivation starts at 1 for low $[Ca]_{in}$. These channels open only when the $Ca^{2+}{}_{in}$ levels fall in the center "activation window". The curves follow the expressions in equation 16; the onset and offset of the "activation window" are governed by the parameters $[Ca]_{m_{cas}}$ and $[Ca]_{h_{cas}}$, respectively. (e) *in silico* sigh burst amplitude, post-burst interval, and burst durations are larger than eupneic bursts, consistent with *in vitro* results (see Fig. 1a). Each dot represents one burst.

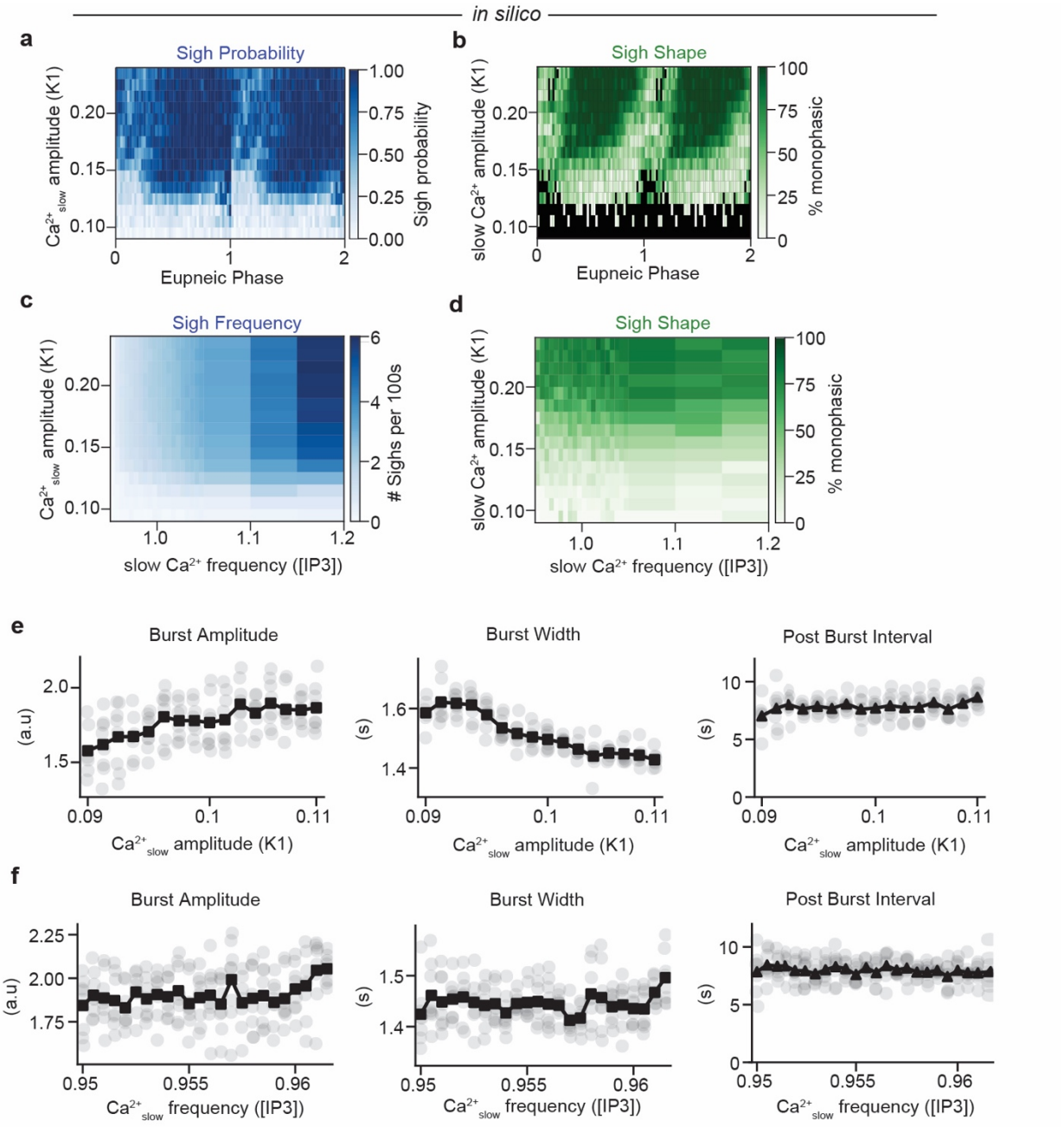

Extended Data Figure 2. (a-d) Varying rate and amplitude of Ca^{2+}_{slow} *in silico* modulates sigh frequency and shape. Heatmaps show sigh probability (a) and sigh shape (b) as a joint function of Ca^{2+}_{slow} amplitude and eupneic phase. Eupneic phase is shown for 2 cycles to visualize effects occurring near eupneic onset (phase = 0, 1, 2). Black regions denote bins where no sighs were evoked. Heatmaps show sigh frequency (c) and shape (d) as joint function of Ca^{2+}_{slow} frequency ($[\mathrm{IP3}]$) and amplitude ($k1$). Each heatmap bin represents average of 8 independent simulations. Burst shapes are weakly influenced by Ca^{2+}_{slow} amplitude, not frequency. (e) Sigh burst amplitude, width, and post burst interval as a function of extrinsic Ca^{2+}_{slow} amplitude. Each gray dot is the mean shape characteristic across a single 1000s simulation, and each connected black dot is the average of those simulation averages (n = 8). (g) Same as (f), but extrinsic Ca^{2+}_{slow} frequency is varied.

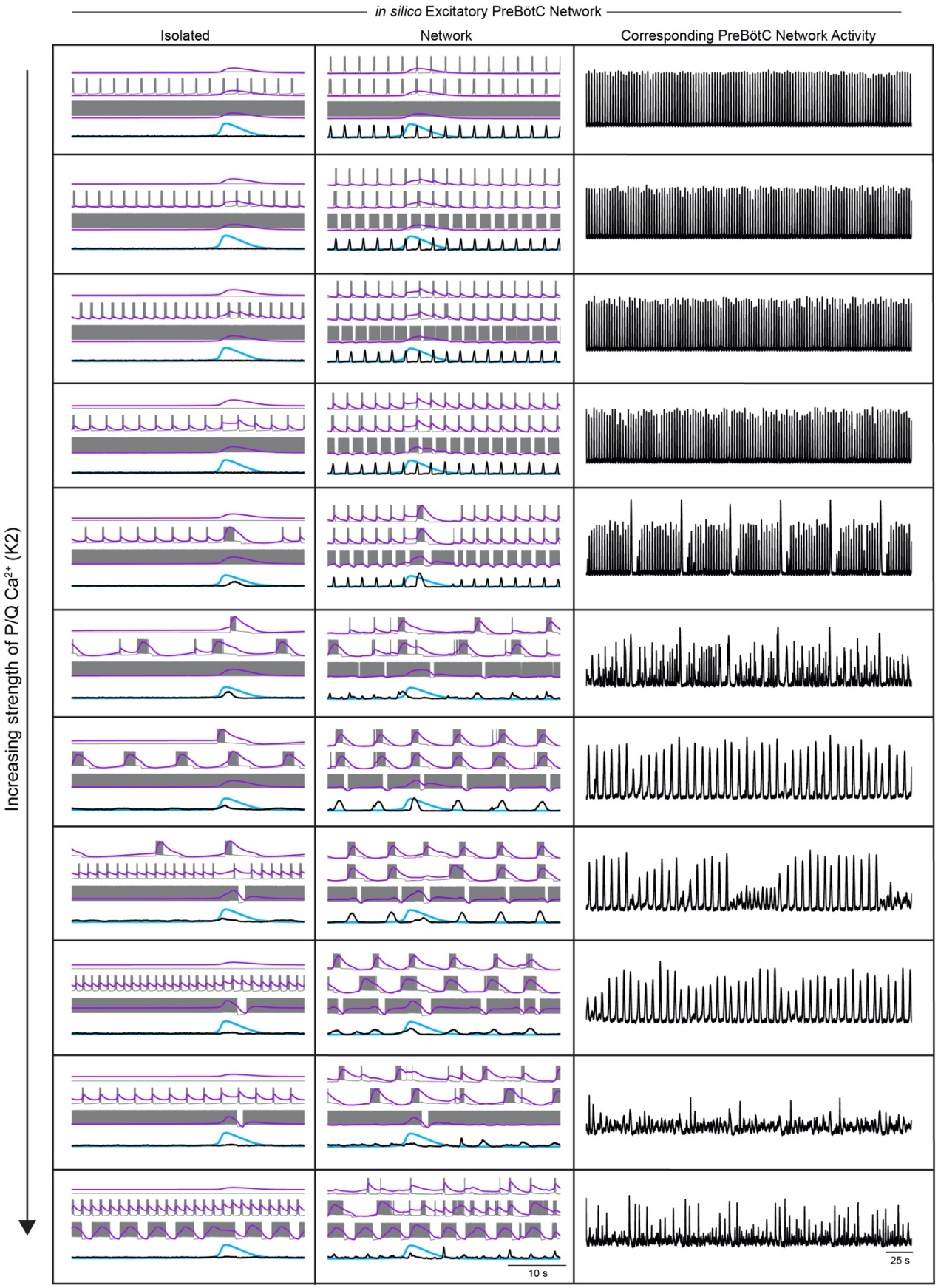
in silico Excitatory PreBötC Network
Isolated
Network
Corresponding PreBötC Network Activity
Increasing strength of P/Q Ca^{2+} (K2)
10 s
25 s

Extended Data Figure 3. Modulating P/Q-type calcium strength modulates network and sigh bursting behaviors. Example single neuron and population traces from networks while varying the strength of the P/Q type Ca^{2+} current (k_2). Each row shows voltage (gray) and $[Ca]_i$ (magenta) traces for 3 example neurons (quiescent, bursting, and tonic, top to bottom); the integrated population spiking activity (black); and the slow extrinsically generated Ca^{2+} signal (blue). Far left columns show the synaptically isolated neurons, middle column shows the synaptically connected network, and far right column shows the integrated population activity for the connected network over an expanded time frame.

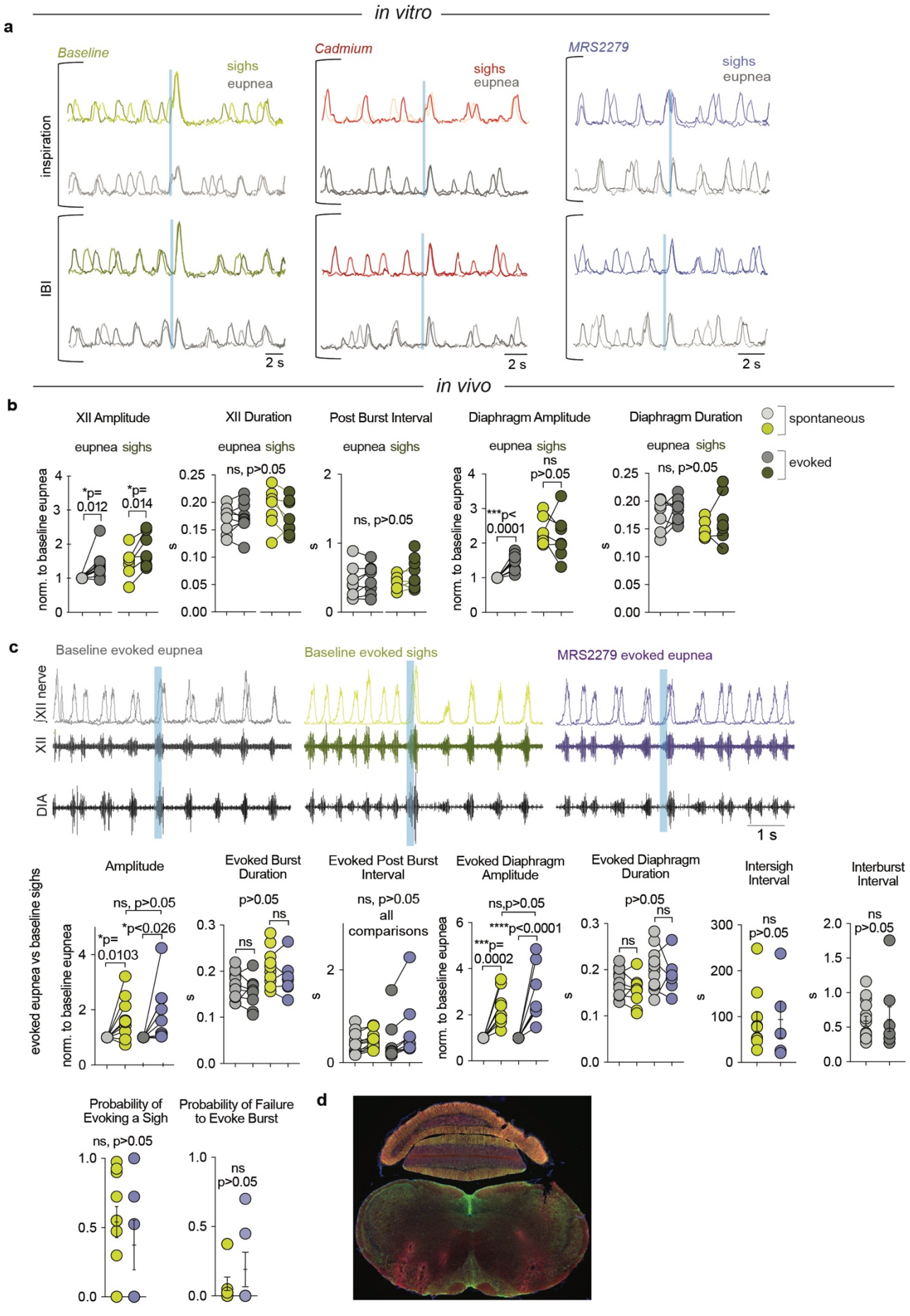
a
in vitro
Baseline
Cadmium
MRS2279
sighs
eupnea
inspiration
IBI
2 s
b
in vivo
XII Amplitude
XII Duration
Post Burst Interval
Diaphragm Amplitude
Diaphragm Duration
eupnea sighs
norm. to baseline eupnea
*p= 0.012
*p= 0.014
ns, p>0.05
***p< 0.0001
ns p>0.05
s
spontaneous
evoked
c
Baseline evoked eupnea
Baseline evoked sighs
MRS2279 evoked eupnea
∫XII nerve
XII
DIA
1 s
Amplitude
Evoked Burst Duration
Evoked Post Burst Interval
Evoked Diaphragm Amplitude
Evoked Diaphragm Duration
Intersigh Interval
Interburst Interval
evoked eupnea vs baseline sighs
norm. to baseline eupnea
*p= 0.0103
*p<0.026
p>0.05
ns, p>0.05 all comparisons
ns,p>0.05
****p<0.0001
***p= 0.0002
Probability of Evoking a Sigh
Probability of Failure to Evoke Burst
d

Extended Data Figure 4. (a). Representative population recordings from the preBötC *in vitro* showing eupnea (gray and black) and sighs/sigh attempts generated during inspiration and during the inter-burst interval (IBI). Blue line represents 200ms laser pulse. (b) Quantification of in vivo spontaneous vs. evoked eupnea and sighs. Diaphragm amplitude was most defining characteristic of sighs *in vivo*, as in XII nerve recordings evoked eupneic bursts had larger amplitudes than spontaneous eupneic bursts. (c) Evoked eupnea and sighs *in vivo* under baseline conditions and with application of MRS2279. MRS2279 was ineffective at blocking most sighs and limited the spontaneous and evoked response in a small number of experiments, regardless of injection location. (d) Representative MRS2279 injection sites located caudal to preBötC.

Table 1: Neuron and Calcium Parameters

Conductances	
C_m	$21pF$
g_{Na}	$28nS$
g_K	$11.2nS$
g_{NaP}	$3.3nS$
$g_{syn_{max}}$	$70nS$
g_{Cas}	$0.5nS$

Reversal Potentials	
E_{Na}	$50mV$
E_K	$-85mV$
E_{leak}	$-59mV$
E_{Cas}	$0mV$
E_{syn}	$0mV$

Calcium Dynamics	
f_i	$0.001pL^{-1}$
L	$0.37pL/s$
P	$31000pL/s$
k_I	$1\mu M$
k_a	$0.4\mu M$
C_t	$1.25\mu M$
σ	0.185
V_e	$400aMol/s$
k_e	$0.2\mu M$
A	$0.5\mu Ms^{-1}$
k_d	$0.4\mu M$
τ_{Ca}	$1s$

Gating and kinetics	
$\overline{\tau_n}$	$10ms$
$\overline{\tau_h}$	$10s$
$\overline{\tau_{m_{Cas}}}$	$134ms$
$\overline{\tau_{h_{Cas}}}$	$5.25s$
$\tau_{0_{m_{Cas}}}$	$2ms$
$\tau_{0_{h_{Cas}}}$	$50ms$
$[Ca]_{m_{Cas}}$	$500nM$
$[Ca]_{h_{Cas}}$	$510nM$
$\xi_{m_{Cas}}$	$-400\mu M^{-1}$
$\xi_{h_{Cas}}$	$-250\mu M^{-1}$
$\theta_{m_{Cas}}$	$-360\mu M^{-1}$
$\theta_{h_{Cas}}$	$420\mu M^{-1}$
V_m	$-34mV$
V_n	$-29mV$
V_{m_p}	$-40mV$
V_h	$-48mV$
σ_m	$-5mV$
σ_n	$-4mV$
σ_{m_p}	$-6mV$
σ_h	$5mV$
τ_{syn}	$15ms$
Q_s	$15mV$
σ_{syn}	$-3mV$

Table 1. Parameters of the computational model and cell specific and network parameters

References

1. Smith, J.C., et al., *Pre-Bötzinger Complex: A Brainstem Region That May Generate Respiratory Rhythm in Mammals.* Science, 1991. **254**(5032): p. 726-729.

2. Lieske, S., et al., *Reconfiguration of the neural network controlling multiple breathing patterns: eupnea, sighs and gasps.* Nature Neuroscience, 2000. **3**: p. 600-607.

3. Peña, F. and J.-M. Ramirez, *Endogenous activation of serotonin-2A receptors is required for respiratory rhythm generation in vitro.* The Journal of Neuroscience, 2002. **22**(24): p. 11055-11064.

4. Peña, F., et al., *Differential contribution of pacemaker properties to the generation of respiratory rhythms during normoxia and hypoxia.* Neuron, 2004. **43**(1): p. 105-17.

5. Tryba, A.K., et al., *Differential modulation of neural network and pacemaker activity underlying eupnea and sigh-breathing activities.* J Neurophysiol, 2008. **99**(5): p. 2114-25.

6. Viemari, J.-C., et al., *β-noradrenergic receptor activation specifically modulates the generation of sighs in vivo and in vitro.* Fontiers in Neural Circuits, 2013. **7**(179).

7. Li, P., et al., *The peptidergic control circuit for sighing.* Nature, 2016. **530**(7590): p. 293-7.

8. Koch, H., et al., *Stable respiratory activity requires both P/Q-type and N-type voltage-gated calcium channels.* Journal of neuroscience, 2013. **33**(8): p. 3633-3645.

9. Lieske, S. and J.M. Ramirez, *Pattern-specific synaptic mechanisms in a multifunctional network. II. Intrinsic modulation by metabotropic glutamate receptors.* Journal of Neurophysiology, 2006. **95**(3): p. 1334-1344.

10. Souza, G., et al., *Breathing regulation and blood gas homeostasis after near complete lesions of the retrotrapezoid nucleus in adult rats.* J Physiol, 2018. **596**(13): p. 2521-2545.

11. Chapuis, C., et al., *Emergence of sigh rhythmogenesis in the embryonic mouse.* J Physiol, 2014. **592**(10): p. 2169-81.

12. Borrus, D.S., et al., *Role of Synaptic Inhibition in the Coupling of the Respiratory Rhythms that Underlie Eupnea and Sigh Behaviors.* eNeuro, 2020. **7**(3).

13. Baertsch, N.A., et al., *A spatially dynamic network underlies the generation of inspiratory behaviors.* Proc Natl Acad Sci U S A, 2019. **116**(15): p. 7493-7502.

14. Butera, R.J., Jr., J. Rinzel, and J.C. Smith, *Models of respiratory rhythm generation in the pre-Botzinger complex. I. Bursting pacemaker neurons.* J Neurophysiol, 1999. **82**(1): p. 382-97.

15. Toporikova, N., M. Chevalier, and M. Thoby-Brisson, *Sigh and Eupnea Rhythmogenesis Involve Distinct Interconnected Subpopulations: A Combined Computational and Experimental Study(1,2,3).* eNeuro, 2015. **2**(2).

16. Li, Y.X. and J. Rinzel, *Equations for InsP3 receptor-mediated [Ca2+]i oscillations derived from a detailed kinetic model: a Hodgkin-Huxley like formalism.* J Theor Biol, 1994. **166**(4): p. 461-73.

17. Galaz-Montoya, M., et al., *beta2-Adrenergic receptor activation mobilizes intracellular calcium via a non-canonical cAMP-independent signaling pathway.* J Biol Chem, 2017. **292**(24): p. 9967-9974.

18. Viemari, J.-C. and J.-M. Ramirez, *Norepinheprine differentially modulates different types of respiratory pacemaker and nonpacemaker neurons.* Journal of Neurophysiology, 2006. **95**: p. 2070-2082.

19. Saez, J.C., A.P. Moreno, and D.C. Spray, *Norepinephrine induces Ca2+ release from intracellular stores in rat pinealocytes.* J Pineal Res, 1994. **16**(2): p. 57-64.

20. Angelova, P.R., et al., *Functional Oxygen Sensitivity of Astrocytes.* J Neurosci, 2015. **35**(29): p. 10460-73.

21. Funk, G.D., *Neuromodulation: purinergic signaling in respiratory control.* Compr Physiol, 2013. **3**(1): p. 331-63.

22. Ramirez, J.M., et al., *Advances in cellular and integrative control of oxygen homeostasis within the central nervous system.* J Physiol, 2018.

23. Rodrigues, R.J., J.M. Marques, and R.A. Cunha, *Purinergic signalling and brain development.* Semin Cell Dev Biol, 2019. **95**: p. 34-41.

24. Del Puerto, A., F. Wandosell, and J.J. Garrido, *Neuronal and glial purinergic receptors functions in neuron development and brain disease.* Front Cell Neurosci, 2013. **7**: p. 197.

25. Cotrina, M.L., et al., *Connexins regulate calcium signaling by controlling ATP release.* Proc Natl Acad Sci U S A, 1998. **95**(26): p. 15735-40.

26. Rajani, V., et al., *Release of ATP by preBotzinger complex astrocytes contributes to the hypoxic ventilatory response via a Ca2+ -dependent P2Y1 receptor mechanism.* J Physiol, 2017.

27. Chen, L., et al., *K(ATP) channels of parafacial respiratory group (pFRG) neurons are involved in H2S-mediated central inhibition of respiratory rhythm in medullary slices of neonatal rats.* Brain Res, 2013. **1527**: p. 141-8.

28. Rajani, V., et al., *The role of P2Y1 receptor signaling in central respiratory control.* Respiratory Physiology and Neurobiology, 2016. **226**: p. 3-10.

29. Lorier, A.R., et al., *P2Y1 Receptor Modulation of the Pre-Bötzinger Complex Inspiratory Rhythm Generating Network In Vitro.* The Journal of Neuroscience, 2007. **27**(5): p. 993-1005.

30. Huxtable, A.G., et al., *Glia contribute to the purinergic modulation of inspiratory rhythm-generating networks.* J Neurosci, 2010. **30**(11): p. 3947-58.

31. Tien, A.C., et al., *Regulated temporal-spatial astrocyte precursor cell proliferation involves BRAF signalling in mammalian spinal cord.* Development, 2012. **139**(14): p. 2477-87.

32. Srinivasan, R., et al., *New Transgenic Mouse Lines for Selectively Targeting Astrocytes and Studying Calcium Signals in Astrocyte Processes In Situ and In Vivo.* Neuron, 2016. **92**(6): p. 1181-1195.

33. Krause, K.L., et al., *Normal breathing pattern and arterial blood gases in awake and sleeping goats after near total destruction of the presumed pre-Botzinger complex and the surrounding region.* J Appl Physiol (1985), 2009. **106**(2): p. 605-19.

34. Doi, A. and J.M. Ramirez, *Neuromodulation and the orchestration of the respiratory rhythm.* Respir Physiol Neurobiol, 2008. **164**(1-2): p. 96-104.

35. Thoby-Brisson, M. and J.M. Ramirez, *Identification of two types of inspiratory pacemaker neurons in the isolated respiratory neural network of mice.* J Neurophysiol, 2001. **86**(1): p. 104-12.

36. Destexhe, A., *Oscillations, complex spatiotemporal behavior, and information transport in networks of excitatory and inhibitory neurons.* Phys Rev E Stat Phys Plasmas Fluids Relat Interdiscip Topics, 1994. **50**(2): p. 1594-1606.

37. Stimberg, M., R. Brette, and D.F. Goodman, *Brian 2, an intuitive and efficient neural simulator.* Elife, 2019. **8**.

38. Ramirez, J.M. and D.W. Richter, *The neuronal mechanisms of respiratory rhythm generation.* Curr Opin Neurobiol, 1996. **6**(6): p. 817-25.

39. Baertsch, N.A., H.C. Baertsch, and J.M. Ramirez, *The interdependence of excitation and inhibition for the control of dynamic breathing rhythms.* Nat Commun, 2018. **9**(1): p. 843.

40. Lemes, E.V., E. Colombari, and D.B. Zoccal, *Generation of active expiration by serotoninergic mechanisms of the ventral medulla of rats.* J Appl Physiol (1985), 2016. **121**(5): p. 1135-1144.

41. Baertsch, N.A. and J.M. Ramirez, *Insights into the dynamic control of breathing revealed through cell-type-specific responses to substance P.* Elife, 2019. **8**.

42. Hill, A.A., et al., *Graded Reductions in Oxygenation Evoke Graded Reconfiguration of the Isolated Respiratory Network.* Journal of Neurophysiology, 2011. **105**(2): p. 625-639.

43. Garcia, A.J., 3rd, et al., *Hydrogen peroxide differentially affects activity in the pre-Botzinger complex and hippocampus.* J Neurophysiol, 2011. **106**(6): p. 3045-55.

44. Zanella, S., et al., *When norepinephrine becomes a driver of breathing irregularities: how intermittent hypoxia fundamentally alters the modulatory response of the respiratory network.* J Neurosci, 2014. **34**(1): p. 36-50.

45. Ruangkittisakul, A., et al., *Generation of eupnea and sighs by a spatiochemically organized inspiratory network.* J Neurosci, 2008. **28**(10): p. 2447-58.

46. Ruangkittisakul, A., et al., *Identification of the pre-Botzinger complex inspiratory center in calibrated "sandwich" slices from newborn mice with fluorescent Dbx1 interneurons.* Physiol Rep, 2014. **2**(8).

47. Tryba, A.K., F. Pena, and J.M. Ramirez, *Stabilization of bursting in respiratory pacemaker neurons.* J Neurosci, 2003. **23**(8): p. 3538-46.

48. Carroll, M.S. and J.M. Ramirez, *Cycle-by-cycle assembly of respiratory network activity is dynamic and stochastic.* J Neurophysiol, 2013. **109**(2): p. 296-305.

49. Harris, K.D., et al., *Different roles for inhibition in the rhythm-generating respiratory network.* J Neurophysiol, 2017: p. jn 00174 2017.

A spatially dynamic network underlies the generation of inspiratory behaviors

Baertsch NA[1], Severs LJ[1], Anderson TM[1], Ramirez JM[1,2]

[1]Center for Integrative Brain Research; Seattle Children's Research Institute; Seattle, WA, USA

[2]Departments of Neurological Surgery and Pediatrics; University of Washington; Seattle, WA, USA

Corresponding Author and Lead Contacts:

Nathan Baertsch (nathan.baertsch@seattlechildrens.org) or Nino Ramirez (jan.ramirez@seattlechildrens.org)

Author Contributions: Conceptualization, N.A.B. and J.M.R.; Methodology, N.A.B., T.M.A. and J.M.R., Investigation, N.A.B., L.J.S, T.M.A.; Formal Analysis, N.A.B.; Writing–Original Draft, N.A.B.; Writing–Review & Editing, N.A.B., L.J.S., and J.M.R.; Funding Acquisition, N.A.B. and J.M.R.; Visualization, N.A.B.; Supervision, J.M.R.

Declarations of Interest: The authors declare no conflicts of interest

Published in PNAS, April 2019. Volume 116, Issue 15, pg. 7493-7502
Find the article here.

ABSTRACT

The ability of neuronal networks to reconfigure is a key property underlying behavioral flexibility. Networks with recurrent topology are particularly prone to reconfiguration through changes in synaptic and intrinsic properties. Here, we explore spatial reconfiguration in the reticular networks of the medulla that generate breathing. Combined results from in-vitro and in-vivo approaches demonstrate that the network architecture underlying generation of the inspiratory phase of breathing is not static but can be spatially redistributed by shifts in the balance of excitatory and inhibitory network influences. These shifts in excitation/inhibition allow the size of the active network to expand and contract along a rostrocaudal medullary column during behavioral or metabolic challenges to breathing, such as changes in sensory feedback, sighing, and gasping. We postulate that the ability of this rhythm-generating network to spatially reconfigure contributes to the remarkable robustness and flexibility of breathing.

KEYWORDS: preBötzinger complex, breathing, gasping, sighs, rhythmogenesis, reconfiguration, dynamic network, inhibition, flexibility, recruitment

SIGNIFICANCE

Breathing is a vital rhythmic behavior that originates from neural networks within the brainstem. It is hypothesized that the breathing rhythm is generated by spatially distinct networks localized to discrete kernels or compartments. Here, we provide evidence that the functional boundaries of these compartments expand and contract dynamically based on behavioral or physiological demands. The ability of these rhythmic networks to change in size may allow the breathing rhythm to be very reliable, yet flexible enough to accommodate the large repertoire of mammalian behaviors that must be integrated with breathing.

INTRODUCTION

From as early as the pioneering work of Ramón y Cajal, anatomical and electrophysiological investigations have sought to compartmentalize brain regions based on the properties of neurons contained within them (1). Testing functional hypotheses for a given brain region has been commonly achieved by implementing lesion and stimulation experiments to determine whether the region is necessary or sufficient for a given behavior (2-4). This approach has contributed greatly to our understanding of brain function, while supporting the general view that the brain is organized into discrete anatomical and functional modules that underlie distinct behaviors (5).

The introduction of modern genetic, imaging, and optogenetic tools has led to an exponential increase in our insights into the functional anatomy of defined neuronal regions in vertebrate(6-9) and invertebrate model systems (10-13). However, neuronal circuit functions are often dynamic, state-dependent (14-20), multifunctional (21-24), and task-dependent (25). Mechanisms of experience-dependent plasticity can shift the spatial distribution of a neuronal network over time (26), and the topology of active brain networks can also dynamically reconfigure on rapid time-scales (27, 28). In particular, networks with recurrent connectivity, such as motor cortex, appear to reconfigure by regulating the balance of excitation and inhibition to control the spread of neuronal activity through the network (26, 29, 30). However, while many mammalian studies are consistent with network reconfiguration, it is often difficult to define these dynamic changes at the cellular level.

The neuronal network controlling breathing offers a unique opportunity to characterize neural network dynamics in great detail (31). A series of studies identified the preBötzinger Complex (preBötC), a small “core” (32, 33) or “kernel” (34) network, which is critical for generating inspiration. Acute silencing of the preBötC causes apnea (4, 33), and when isolated in a thin medullary slice from neonatal rodents, it continues to produce a rhythm (35). Rostral to the preBötC, inhibitory neurons active during expiration were identified in the so-called Bötzinger Complex (BötC) (36), and caudal to the preBötC, a region referred to as the ventral respiratory group (VRG) was found to contain bulbospinal inspiratory and expiratory neurons thought to primarily serve premotor functions (37). These observations led to the respiratory network being described in terms of a series of discrete, rostrocaudally oriented “compartments”, the BötC, preBötC, and VRG (38-41).

Yet, there are no easily defined anatomical borders within the medullary respiratory network or between the hypothesized compartments. A rich array of recurrent connections (42), in particular among excitatory neurons derived from Dbx1-expressing progenitors (referred heretofore as “Dbx1 neurons”), is considered a critical property of the preBötC that gives rise to the inspiratory rhythm (33, 43). But, Dbx1 neurons extend far beyond the preBötC along the rostrocaudal axis of the VRC (43-45). Moreover, neuron types and spiking patterns are not homogeneous within each VRC compartment. Inhibitory neurons active during expiration, thought to characterize the BötC, are also found within the preBötC (43, 46, 47). Conversely, neurons active during inspiration are prevalent within the BötC, but also extend

rostrally (48, 49). This may explain why, in some cases, lesions of the preBötC have failed to eliminate all inspiratory behaviors (50-52). Thus, evidence suggests that neurons important for inspiratory rhythmogenesis may not be limited to a discrete preBötC kernel.

Using optogenetic and electrophysiological techniques, we investigate the generation of inspiration in the wider medullary network and test the hypothesis that the spatial extent of inspiratory activity generated by the preBötC can dynamically reconfigure. We find that inspiratory activity along a distributed column of excitatory neurons is regulated by inhibition and that this distribution expands rostrally from the preBötC during changes in sensory feedback or inspiratory behaviors such as sighs and gasps. We postulate that this dynamic network architecture allows the size of the active recurrent network to be adjusted on a cycle-to-cycle basis, endowing the breathing rhythm with remarkable robustness and flexibility during ever-changing behavioral, metabolic, and environmental demands.

RESULTS

Characterization of Inspiratory Activity in a Horizontal Medullary Slice

To explore inspiratory activity in the wider medullary network, we developed a horizontal brainstem slice preparation that encompasses the entire rostrocaudal extent of the ventral medulla (2) (Fig. S1A-D). Landmarks used to locate the preBötC in-vivo (43) are preserved on the ventral surface of horizontal slices and corresponded to a location ~1800μm caudal to the VII nerve (rostral edge of the slice) and ~950μm lateral from the midline. Horizontal slices prepared from male and female transgenic mice expressing fluorescent protein in cholinergic neurons confirmed that this location correlated with the known position of the preBötC relative to other neuronal landmarks such as the nucleus ambiguus (NA), facial nucleus (VII), and post-inspiratory complex (PiCo) (Fig. S1E). This region also contained Dbx1-derived neurons (Fig. S1F) known to be necessary and sufficient for generation of the inspiratory rhythm. However, as previously suggested (44, 45), these neurons extended along a rostrocaudal column, far beyond the preBötC. To further localize the preBötC in the horizontal slice, inspiratory modulated extracellular spiking activity was systematically mapped (Fig. S1G). Beginning at the anatomical coordinates corresponding the preBötC center, maximal integrated inspiratory activity was recorded in 100μm steps across the surface of horizontal slices. Inspiratory population activity spanned 1488±199μm in the medulla and could be recorded up to 625±106μm rostral of the preBötC center.

To determine how integration of the preBötC within the wider rostrocaudal medullary network influences rhythmogenesis, we compared preBötC inspiratory activity generated in horizontal slices with preBötC activity generated in conventional transverse brainstem slice preparations (32) (Fig. 1A, Fig. S1H). On average, horizontal slices (n=40) produced a slower inspiratory rhythm with longer duration bursts (TI), longer pauses between bursts (TE), and a longer time to reach peak burst amplitude (time to peak) compared to transverse slices from neonatal mice of a similar age (p7-10, n=41) (Fig. 1B, Fig. S1I). Although horizontal slices had a slightly more irregular period, horizontal slices exhibited much less

irregularity in burst amplitude and burst area than transverse slices (Fig. 1C, Fig. S1J), suggesting that horizontal slices produce a relatively robust and more synchronized rhythm compared to slices that isolate the preBötC. Because stronger synchronization within the preBötC leads to longer refractory periods following inspiratory bursts (43, 53), we compared the refractory period in horizontal (n=5) and transverse (n=4) slice preparations (Fig. 1D,E). Using $Dbx1^{CreERT2}$;$Rosa26^{ChR2\text{-}EYFP}$ mice, preBötC Dbx1 neurons were optogenetically stimulated contralateral to the extracellular electrode at random time-points during the inspiratory cycle. Shortly following spontaneous preBötC bursts, the probability of photoevoking a subsequent burst (200ms, 470nm, 0.5mW/mm^2) was low in both horizontal and transverse slice preparations, indicative of refractoriness (43, 54). The probability of evoking a burst increased with time but was more delayed in horizontal slices, with a >80% chance of evoking a burst at 1.25s and 2.75s in transverse and horizontal slices, respectively. Together, these results suggest that, when integrated within the wider medullary network, the preBötC generates a more robust rhythm associated with increased refractoriness.

A Distributed Heterogeneous Inspiratory Network

Next, we used the horizontal slice preparation to characterize the cellular determinants of the inspiratory rhythm along its rostrocaudal axis. Respiratory modulated neurons were selected for intracellular recording using the blind patch technique. The electrophysiological activity of each neuron was characterized in relation to preBötC population bursts, the anatomical location of each neuron was mapped using patch pipettes containing a fluorescent marker, and each neuron was classified as excitatory or inhibitory based on optogenetic stimulations (Fig. S2A,B). Electrophysiological activity patterns of respiratory neurons recorded in the horizontal slice fell into three main groups: inspiratory, expiratory, and postinspiratory. Locations of inspiratory and expiratory neurons and example spike raster plots of respiratory neurons during 30 consecutive inspiratory bursts are shown in Fig. 2. Respiratory neurons along the horizontal slice were primarily inspiratory, i.e. maximum firing rates occurred in phase with preBötC population activity (47/65 neurons). However, there was considerable heterogeneity among inspiratory neurons. In support of previous findings (43, 55), inspiratory neurons were almost evenly split between excitatory and inhibitory (22/47 were inhibitory). Interestingly, inhibitory inspiratory neurons generally exhibited a decrementing spiking pattern (neurons 4-6 in Fig. 2A), whereas the spiking pattern of excitatory inspiratory neurons was more variable. Some inspiratory neurons exhibited augmenting spiking activity or a “preinspiratory ramp” prior to preBötC population bursts, followed by high frequency spiking activity during bursts and were primarily excitatory (5/6 neurons). Inspiratory neurons that did not have an obvious pre-inspiratory ramp were generally silent between preBötC population bursts and varied from augmenting to decrementing and from weakly spiking to strongly spiking during bursts. Despite these general patterns, all inspiratory neurons exhibited considerable cycle-to-cycle stochasticity in spiking onset and activity (46, 56). Under control conditions, functionally

active inspiratory neurons were most commonly found near the preBötC center; however, consistent with our extracellular mapping results (see Fig. S1G), inspiratory neurons were found spanning 1.35mm in the rostrocaudal direction through the ventral medulla.

Neurons active out of phase with the preBötC population, were classified as either expiratory or postinspiratory (Fig. 2B). Similar to previous reports in the isolated preBötC (46), and as predicted by computational models (57), a minority of respiratory neurons along the horizontal slice were expiratory (12/65). These neurons exhibited moderate tonic activity between preBötC bursts, were silenced during bursts, and some had modest rebound activity following bursts. Our recordings failed to confirm a rostrocaudal segregation of expiratory and inspiratory neurons (Fig. 2C) as hypothesized by some respiratory models (38, 58). However, postinspiratory neurons were clustered significantly rostral to the preBötC in a region corresponding to the postinspiratory complex (PiCo) (2, 59). Neuromodulation, specifically a low concentration of norepinephrine (NE), is known to facilitate PiCo neurons such that they fire following every preBötC burst(2). However, the experiments described here were performed in the absence of NE, therefore PiCo neurons exhibited strong bursts of spiking activity immediately following some, but not all, preBötC bursts (2). PiCo neurons were mostly excitatory (2) although not exclusively (4/5); suggesting that, like the preBötC, the PiCo may be heterogeneous.

Collectively, these data support a network structure that departs from compartmental models of respiratory rhythm generation (58, 60). Inhibitory and excitatory respiratory neurons were not spatially separated into rostral and caudal compartments as often viewed as differentiating the preBötC from the BötC (39, 61). We also did not observe a spatial segregation between inspiratory and expiratory neurons, although postinspiratory neurons were located rostral to the preBötC. Thus, although the density of functionally active inspiratory neurons is likely highest near the preBötC center, we suggest that a distributed network of intermingled excitatory and inhibitory neurons with heterogenous spiking patterns underlies the inspiratory rhythm.

Inhibition Regulates the Extent of a Dynamic Inspiratory Column

To explore how the balance of excitatory and inhibitory mechanisms may influence the distribution of inspiratory activity, we performed paired recordings in horizontal slices during pharmacological suppression of fast synaptic inhibition. Integrated population activity was recorded at the preBötC and 534±40μm rostral (n=12) (Fig. 3A). Under baseline conditions, weak irregular inspiratory activity was observed in rostral recordings. However, following suppression of both glycinergic and GABAergic inhibition, integrated population activity in the rostral column increased by 129±24%, whereas preBötC burst amplitude only increased by 38±7% (Fig. 3B). The rise slope of inspiratory bursts at the preBötC center increased (75±15%), and changes in preBötC slope were proportional to changes in rostral burst amplitude (Fig. S3A) Blockade of inhibition reduced the irregularity of inspiratory bursts in the rostral column, but not at the preBötC center (Fig. S3B). When

glycinergic and GABAergic inhibition were blocked separately, effects on inspiratory burst amplitude were relatively modest (Fig. S3C). Moreover, effects on inspiratory burst amplitude were dependent on the dose of strychnine and gabazine when applied in combination (Fig. S3D), suggesting that changes in the rostral extent of inspiratory activity are dependent on the total amount of synaptic inhibition. Increased inspiratory activity along the column following suppression of synaptic inhibition was also associated with a decrease in burst frequency (-20+6%), likely due to greater synchronization within the network (57) and an increase in the refractory period (43).

Next, inspiratory population activity was systematically mapped in horizontal slices following suppression of synaptic inhibition (Fig. 3C). Heat maps of burst amplitude were constructed to visualize changes in the distribution of inspiratory activity in the presence and absence of synaptic inhibition. Differences in the distribution of inspiratory activity are displayed as a heat map of Bonferroni corrected p-values (Fig. 3C). In slices with synaptic inhibition blocked (n=4), inspiratory activity spanned 2625±232μm and was detectable up to 1575±93μm rostral of the preBötC, compared to 1488±199μm and 625±106μm, respectively, for control slices. Significant differences in integrated inspiratory burst amplitude were localized to the rostral column. Thus, these results indicate that synaptic inhibition within the respiratory network regulates the extent of inspiratory activity rostral to the preBötC.

To shed light on the cellular determinants underlying expansion of inspiratory activity, we tested the influence of synaptic inhibition on non-respiratory neurons rostral of the preBötC (Fig. 3D-F). Using blind patch-clamp recording, tonic or silent neurons (n=13) located ~500-600μm rostral of the preBötC center were selected for intracellular recording. Locations of recorded non-respiratory neurons are plotted in Fig. 3D and quantified in Fig. S4B. Following blockade of synaptic inhibition with strychnine and gabazine, excitatory neurons (7/9) began to discharge bursts of spikes during inspiration (Fig. 3E,F and Fig. S4A). In contrast, only 1/4 inhibitory neurons were weakly recruited to spike during inspiration (Fig. 3E,F), suggesting excitatory neurons are preferentially recruited rostral of the preBötC to expand the inspiratory column and that latent excitatory projections from the preBötC to more rostral neurons are revealed following suppression of synaptic inhibition.

Rhythmogenic Properties of the Inspiratory Column

Excitatory neurons derived from Dbx1-expressing precursors are a critical rhythmogenic element within the preBötC (33, 44, 45). Yet, Dbx1 neurons are distributed bilaterally throughout the rostrocaudal extent of the medulla (see Fig. S1F). Therefore, we explored the rhythmogenic properties of Dbx1 neurons along the rostrocaudal axis of the horizontal slice. In $Dbx1^{CreERT2}$;$Rosa26^{ChR2\text{-}EYFP}$ horizontal slices, a 100μm diameter optical fiber was used to stimulate Dbx1 neurons with light (200ms, 470nm, 0.5mW/mm^2) at six different locations between 1500μm rostral and 1000μm caudal of the preBötC center, while recording inspiratory activity from the contralateral preBötC. At each location, 50 light stimulations were performed at random time-points during the inspiratory cycle (Fig. 4A), and the

average probability of evoking a burst at each location was quantified (Fig. 4B). The highest probability of light-evoking contralateral inspiratory bursts was near the preBötC center (92±10%) and gradually declined as the fiber optic was moved farther rostral or caudal. However, even 1500μm rostral of the preBötC center, there was a 62±9% chance of evoking a burst. Differences in the probability of evoking bursts were dependent on the time of the stimulus relative to the preceding spontaneous burst (Fig. 4C), suggesting the refractory period of the inspiratory network is more difficult to overcome when activating Dbx1 neurons farther away from the preBötC center, perhaps because the network is more sparse (57). These data also suggest that the threshold for rhythmogenesis is lowest near the preBötC center.

Next, we began to explore the rhythmogenic properties of different regions of the inspiratory column in isolation. Beginning 100-200μm caudal to the VII nerves, four consecutive 550μm thick transverse slices were made from each animal (n=9), two rostral to the conventional preBötC slice and one caudal (Fig. 4D). Extracellular activity was recorded simultaneously from the caudal surface of all slices. The farthest rostral slices (R1) did not generate spontaneous bursts, whereas spontaneous bursting was generated in 4/9 R2 slices, 9/9 preBötC slices, and 8/9 caudal (C) slices. Spontaneous bursting in R2 and C slices was generally very slow and irregular with considerable variability between preparations. The shape of bursts generated by R2 slices resembled bursts generated by preBötC slices, whereas spontaneous bursts generated by C slices were weak with a pronounced decrementing pattern. To mimic excitatory input from the preBötC, we optogenetically stimulated Dbx1 neurons in rostral and caudal slices with light pulses triggered by preBötC bursts, i.e. yoked stimulations (Fig. 4E). When Dbx1 neurons were stimulated ipsilateral to the extracellular electrode, bursts were sometimes evoked in R1 slices (43±17% chance) and always evoked in R2 and C slices. When stimulations occurred contralateral to the extracellular electrode, bursts could not be evoked in R1 slices, were always evoked in R2 slices, and were sometimes evoked C slices (23±14% chance) (Fig. 4F). The influence of inhibition on each transverse slice was also tested (Fig. 4G,H). Blocking inhibition did not induce bursting in R1 slices (data not shown). However, in R2 slices that did not burst spontaneously, blocking synaptic inhibition revealed bursting in all slices (4/4); and in R2 slices that did burst spontaneously (n=4), blocking synaptic inhibition increased burst frequency (206±110%) but did not in preBötC (-38±6%, n=9) and C slices (-13±17%, n=9) (data not shown). Together, these results support the hypothesis that Dbx1 neurons along the rostrocaudal axis of the ventral medulla can contribute to rhythmogenesis and that synaptic inhibition restrains the rhythmogenic properties of the rostral column.

Sensory Feedback Regulates the Extent of an Inspiratory Column In-vivo

The vagal nerves (X) contain sensory afferents that relay lung stretch information to the respiratory network in the medulla. These afferents create a negative feedback loop that suppresses inspiratory activity via inhibitory mechanisms within the preBötC (43, 62), thereby preventing over inflation of the lungs (i.e the Breuer-Hering reflex). Eliminating this vagal-mediated feedback loop

reveals a slow, large amplitude breathing pattern (62, 63) and increased refractoriness indicative of a shift in the balance between excitation and inhibition within the preBötC network (43).

To begin to explore how the distribution of inspiratory activity may change in response to alterations in network states, we performed paired extracellular recordings to map multiunit spiking activity along the ventral medulla in spontaneously breathing urethane-anesthetized adult mice (p38-p416) (Fig. 5A). One electrode was inserted into the preBötC based on previously established landmarks (43). As expected, robust rhythmic population activity was recorded from this region. Another electrode was positioned rostral to the preBötC center (558±20μm). At this location, near the rostral "edge" of inspiratory activity, integrated population bursts were smaller and the amplitude was more irregular than at the preBötC center (Fig. 5B, Fig. S5A). After establishing baseline breathing activity in rostral, preBötC, and XII nerve recordings, mice were vagotomized bilaterally (n=6) (Fig. 5B). Similar to previous findings, a large increase in inspiratory motor output from the XII nerve was observed (278±93%) along with a corresponding decrease in frequency (-55±9%). Surprisingly, inspiratory activity at the preBötC center was only modestly increased (13±6%), whereas the amplitude of inspiratory bursts in the rostral region was increased by (138±29%), over 10 times that observed near the preBötC center (Fig. 5C). Although changes in preBötC burst amplitude were modest, burst rise slope was increased by 35±8%, suggesting network reconfiguration(64). Changes in the slope of the preBötC burst rise had a strong positive linear relationship with changes in rostral burst amplitude (Fig. S5B). Removal of vagal sensory feedback also reduced the irregularity in the amplitude of rostral bursts (-32±8%), however burst amplitude remained more irregular in the rostral column relative to the preBötC center (Fig. S5C).

These results suggested a shift in the distribution of inspiratory activity within the ventral medulla. To further characterize this change in distribution, inspiratory population activity was mapped in control (intact vagus) and vagotomized mice. Beginning at the preBötC center, maximal integrated inspiratory activity was mapped along the ventral medulla and differences between control and vagotomized mice were quantified (Fig. 5D). In control mice (n=5), a small amount of inspiratory activity could be recorded up to 960±60μm rostral of the preBötC center, whereas in vagotomized mice (n=7) inspiratory activity was detectable up to 1500±131μm rostral. Significant differences in integrated inspiratory burst amplitude were isolated to the rostral end of the column. Thus, similar to our observations following suppression of inhibition in-vitro, there was an anisotropic expansion of inspiratory activity rostral from the preBötC following removal of vagal-mediated sensory feedback in-vivo.

Gasping and Sighing Along the Inspiratory Column

We next sought to determine how inspiratory activity along the ventral medulla is regulated during different inspiratory behaviors with distinct physiological roles. Under control conditions, the preBötC periodically generates biphasic, large-amplitude, inspiratory bursts that correspond to sighs,

and during severe hypoxia, the network is reconfigured to generate bursts that correspond to gasps(65). Utilizing paired extracellular recordings as described above, integrated inspiratory activity was recorded at the preBötC center and 550±19μm rostral during a transient bout of anoxia in vagus-intact anesthetized mice (n=7) (Fig. 6A). As expected, eupneic activity transformed into gasping with large amplitude XII bursts (579±137%) and frequency depression (-62±7%). In the rostral column, inspiratory burst amplitude was increased by 179±37% during gasping, whereas at the preBötC center, gasping elicited relatively modest changes in inspiratory burst amplitude (40±7%) (Fig. 6B) and was associated with a change in burst shape from augmenting to decrementing (Fig S5D), as indicated by an increase in burst rise slope (117±24%). The increases in rostral amplitude were related to changes in preBötC burst rise slope (Fig. S5E). These experiments indicate that inspiratory activity expands rostrally from the preBötC during gasping in-vivo. However, a similar pattern was not observed during “fictive” gasping activity elicited in horizontal slices (n=10). Similar to other in-vitro preparations (48) the effects of severe hypoxia on respiratory output were suppressed relative to the in-vivo condition. During a transient 5min episode of anoxia, burst amplitudes during fictive gasping were reduced at both the preBötC center (-26±6%) and 540±64μm rostral of the preBötC (-15±8%; $p>0.05$). Frequency depression during fictive gasping (-24±7%) was also modest compared to gasping in-vivo, likely related to e.g. a lack of chemosensory drive from carotid bodies and/or excitatory neuromodulatory inputs that contribute to the hypoxic response in-vivo (66-68).

Large-amplitude biphasic inspiratory bursts called sighs occurred spontaneously under control conditions in vagus-intact anesthetized mice(69-71) (Fig. 6C,D). Sigh burst amplitude was quantified relative to normal inspiratory bursts or “eupnea” (%change from eupnea) at different rostrocaudal locations along the inspiratory column (n=29 sighs from n=6 animals). Sigh bursts were smaller near the preBötC center (44±6%) and increased in relative amplitude farther rostral along the inspiratory column (110±18% at 600μm) (Fig. 6E). In the horizontal slice, spontaneous sighs (n=9) were only observed in n=5 slices while performing paired extracellular recordings under control conditions. However, in support of our results in-vivo, sigh bursts 363±62μm rostral of the preBötC were significantly larger (68±11%) than at the preBötC center (39±3%, $p<0.05$; data not shown). Thus, the inspiratory column expands rostrally during sighs, suggesting the extent inspiratory activity rostral to the preBötC can change dynamically from cycle-to-cycle.

DISCUSSION

It is generally thought that breathing is generated by a strictly compartmentalized network within the medulla, with the preBötC being the best characterized compartment. However, Dbx1-derived inspiratory neurons, the necessary neuronal substrate underlying rhythm generation in the preBötC, are found along a column that extends rostrally through the BötC and beyond (43, 44). Here, we propose a distributed network structure in which the inspiratory rhythm arises from a dynamically regulated

rhythmogenic column with the preBötC defined as the subregion with the lowest threshold for rhythmogenesis. The degree to which the preBötC is the exclusive site for rhythmogenesis depends on the metabolic or behavioral context. The rhythmogenic column includes the rostrally located BötC a compartment thought to be involved in expiratory rhythmogenesis (38, 39, 60). Our finding is consistent with data from vagotomized cats, in which multielectrode recordings have revealed inspiratory and expiratory neurons with a rich complexity of firing patterns intermingled along the VRC (72-74). This distributed activity has also been observed in sagittal slice preparations from neonatal rodents(48). Here, we identified neurons rostral of the preBötC that are phenotypically and functionally similar to those contained within the conventional “boundaries” of the preBötC (32, 75). Neither inspiratory/expiratory neurons, nor excitatory/inhibitory neurons were rostrocaudally segregated between the BötC and preBötC (Fig. 2C), and optogenetic stimulation of excitatory Dbx1 neurons as far as 500-1500μm rostral to the preBötC was sufficient to evoke inspiratory bursts (Fig. 4A,B). In slices that did not contain the preBötC, bursts could also be evoked by optogenetic stimulations of Dbx1 neurons (Fig. 4E,F) or by blocking synaptic inhibition (Fig. 4G,H), suggesting neurons distributed outside of the preBötC can contribute to inspiratory rhythm generation.

Our data indicate that the spatial extent of inspiratory activity is dynamic. This is reminiscent of cortical networks (29, 30), where behaviors are not controlled by one kernel, but rather by distributed sensori-motor networks (76, 77). Furthermore, extensive horizontal connections allow neural activity to spread across the network (29, 30). The spread of activity is controlled by inhibition, and relatively small reductions in the strength of inhibition can result in large changes in the spatial distribution of activity (29). For the respiratory network, we show that inhibition plays a critical role in regulating the spatial extent of inspiratory activity within the network. Suppressing synaptic inhibition led to a large anisotropic expansion of inspiratory activity (Fig. 3). This spatial reconfiguration of activity was controlled by the strength of both GABAergic and glycinergic mechanisms, which may reflect co-expression of these transmitters in many preBötC neurons (78). Removal of sensory feedback inhibition mediated by vagal pulmonary stretch receptors revealed a similar expansion of inspiratory activity rostral to the preBötC (Fig. 5), in accordance with previous demonstrations this vagal-mediated reflex ultimately dependent upon inhibitory mechanisms in the ventral medulla (43, 62). We also found that burst-to-burst amplitudes were more irregular farther rostral along the inspiratory column than near the preBötC center, both in-vitro and in in-vivo (Fig. S3B, Fig. S5C), and suppressing inhibition reduced this irregularity. Because in-silico models of the preBötC have demonstrated that the regularity of the rhythm depends on the balance between network inhibition and network connectivity (57) we predict that the influence of synaptic inhibition is greater and/or the network is more sparsely connected near the “edges” of the inspiratory column (Fig. 7). Indeed, blocking synaptic inhibition revealed rhythmic bursting in rostral transverse slices (Fig. 4G,H), and recruited rostral excitatory neurons to fire during inspiratory bursts (Fig. 3F). Based on these results, we postulate that the number and spatial extent of neurons that

contribute to the inspiratory rhythm changes from cycle-to-cycle depending on a dynamic balance between excitation and inhibition.

The ability of neuronal networks to spatially reconfigure may be an important property that promotes behavioral flexibility (14, 76, 79). Aside from important neuromodulatory control (16) the flexibility of the breathing rhythm is also regulated by the balance of excitatory and inhibitory mechanisms (53, 56). In the preBötC, hyperactivity of excitatory neurons following blockade of inhibition or vagotomy produces a highly synchronized, slow rhythm with long refractory times and a limited dynamic range(43). Conversely, inhibitory mechanisms reduce the extent of the network and permit rapid breathing frequencies by limiting synchronization and refractory properties of excitatory neurons (43, 53, 57). Thus, we hypothesize that during eupneic breathing, inspiratory activity rostral to the preBötC is suppressed by inhibition to reduce the number of participating neurons and the amount of synchronization during each inspiratory burst (Fig.7). This mechanism limits the influence of refractory properties and ensures a large dynamic frequency range and increased flexibility.

By contrast, under severe hypoxia or asphyxia, e.g. during airway occlusion, a highly synchronized network may become advantageous as a last resort to promote airway clearance and reoxygenation. During hypoxia-induced gasping, inhibition is suppressed which reconfigures the network such that it produces a decrementing burst pattern (Fig. S5D) (14). Here we show that activity in the rostral column was greatly increased during gasping in-vivo (Fig 6A,B). These important network properties may counteract hypoxia-induced suppression of neuronal activity and/or facilitate intrinsic bursting (80-82) to increase synchronization and expand the size of the active network to produce a very robust rhythm in response to severe hypoxia. Recruitment of the rostral column during gasping may also provide an explanation for how, in some cases, gasping can be generated after the preBötC is lesioned and eupnea is abolished (50), a finding that is difficult to reconcile with the hypothesis that the preBötC compartment is the exclusive site for gasping(83). In contrast to our in vivo finding, we found a relatively blunted gasping response in-vitro (48), which suggests that descending input from the pons, excitatory drive from the carotid body, or neuromodulatory inputs(66, 84) play an important role in generating gasping in-vivo.

As mammals evolved, breathing became integrated with an increasing repertoire of behaviors from vocalization to suckling, sniffing, whisking, and chewing (40, 85, 86). As a result, the rhythm generating network underlying such a widely integrated and vital behavior must be robust, yet also flexible to dynamically adapt breathing to a myriad of state- metabolic- and behavioral-dependent demands (87, 88). While the identification of functionally dedicated microcircuits and necessity and sufficiency criterion have guided much of our efforts to understand the neuronal origins of breathing, this approach may miss important characteristics of the network that endow breathing with its remarkable robustness and flexibility. Our investigations of inspiratory rhythm generation in the intact VRC suggest that the preBötC and BötC form a distributed inspiratory column of excitatory and inhibitory neurons that

allows the size of the active network to be dynamically controlled. Working as one, the preBötC and BötC may overcome the trade-off between a region's specialization and its capacity for network reconfiguration (89), thereby permitting robust and flexible breathing. The ability of distributed neuronal networks to spatially reconfigure may be a general property that bestows animals with the ability to adapt behaviors to continuous and often rapid changes in their internal and external environment.

METHODS

All experiments and animal procedures were approved by the Seattle Children's Research Institute's Animal Care and Use Committee and conducted in accordance with the National Institutes of Health guidelines. Male and female mice were selected randomly based on litter distributions. Protocols for in-vitro (2, 43, 57, 64) and in-vivo (32, 43) preparations, as well as optogenetic, electrophysiological, and pharmacological manipulations (2, 43, 64, 65, 70, 82, 90, 91) were performed as described previously. Detailed descriptions of the methods and data analysis are provided in SI Appendix, and a summary of the statistical tests used is provided in Table S1.

Acknowledgments: We thank NIH grants RO1 HL126523, PO1 HL 090554 and F32 HL134207 for funding this project.

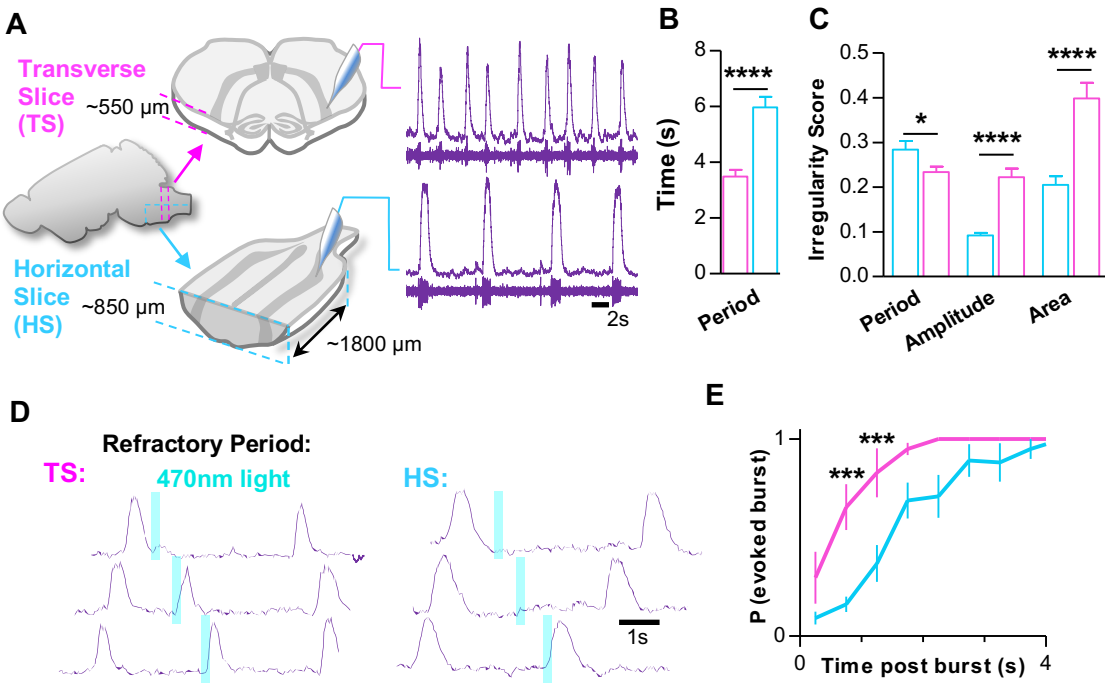

Figure 1: The intact ventral medullary column produces a more robust inspiratory rhythm than the isolated preBötC. A) Comparison of population spiking activity recorded from the preBötC in transverse (magenta) and horizontal (cyan) slice preparations. Example raw population spiking (below) and integrated (above) activity is shown for each slice preparation. B) Group data from n=40 transverse and n=41 horizontal slices comparing inspiratory period and C) burst-to-burst irregularity scores. D) Representative optogenetic stimulations in transverse and horizontal slice preparations from Dbx1^{CreERT2};Rosa26^{ChR2} mice showing differences in the refractory period. E) Quantified probability of photo-evoking an inspiratory burst relative to elapsed time following a spontaneous burst in n=4 transverse and n=5 horizontal slices. (*p>0.05, ***p>0.001, ****p>0.0001; means±SEM)

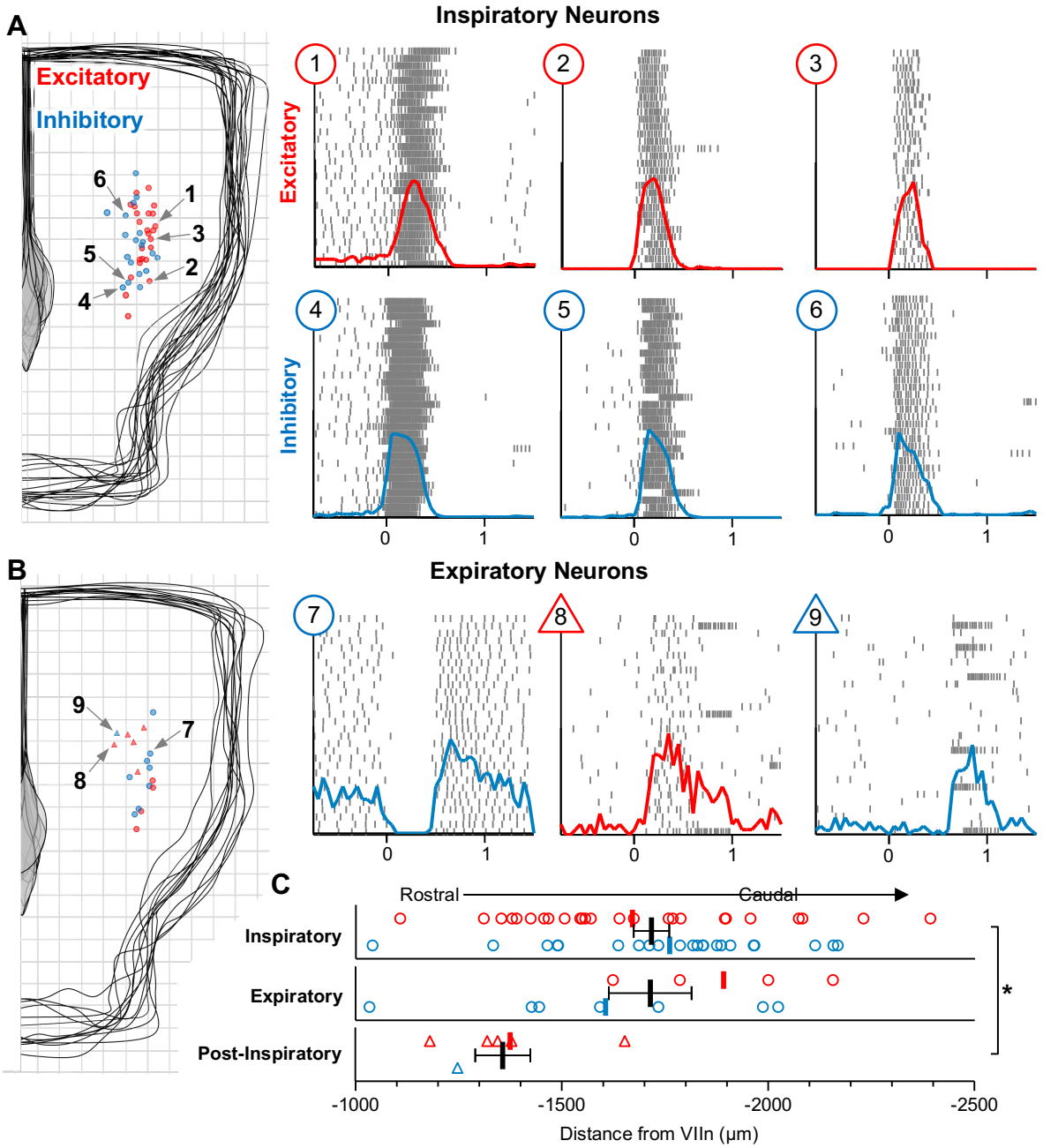

Figure 2: Spatial and functional characterization of respiratory neurons in the horizontal slice. A) Locations of 47 inspiratory neurons recorded from 12 horizontal slices (200µm grid), and three example excitatory (red, 1-3) and inhibitory (blue, 4-6) neurons. Raster plots show spiking activity over 30 consecutive inspiratory bursts; solid lines show integrated spiking activity (population burst onset at t=0). Note the decrementing spiking pattern of inhibitory neurons. B) Locations of 12 expiratory and 6 post-inspiratory neurons recorded from 6 horizontal slices. Raster plots (right) show a representative expiratory neuron with modest post-inhibitory rebound activity (7), an excitatory post-inspiratory neuron that is also active during inspiration (8), and an inhibitory post-inspiratory PiCo neuron. Note that strong post-inspiratory bursts only occur during some cycles in the absence of norepinephrine. C) Quantified rostrocaudal locations of excitatory (red) and inhibitory (blue) inspiratory, expiratory, and post-inspiratory neurons relative to the VII nerve. (*p<0.05; means±SEM)

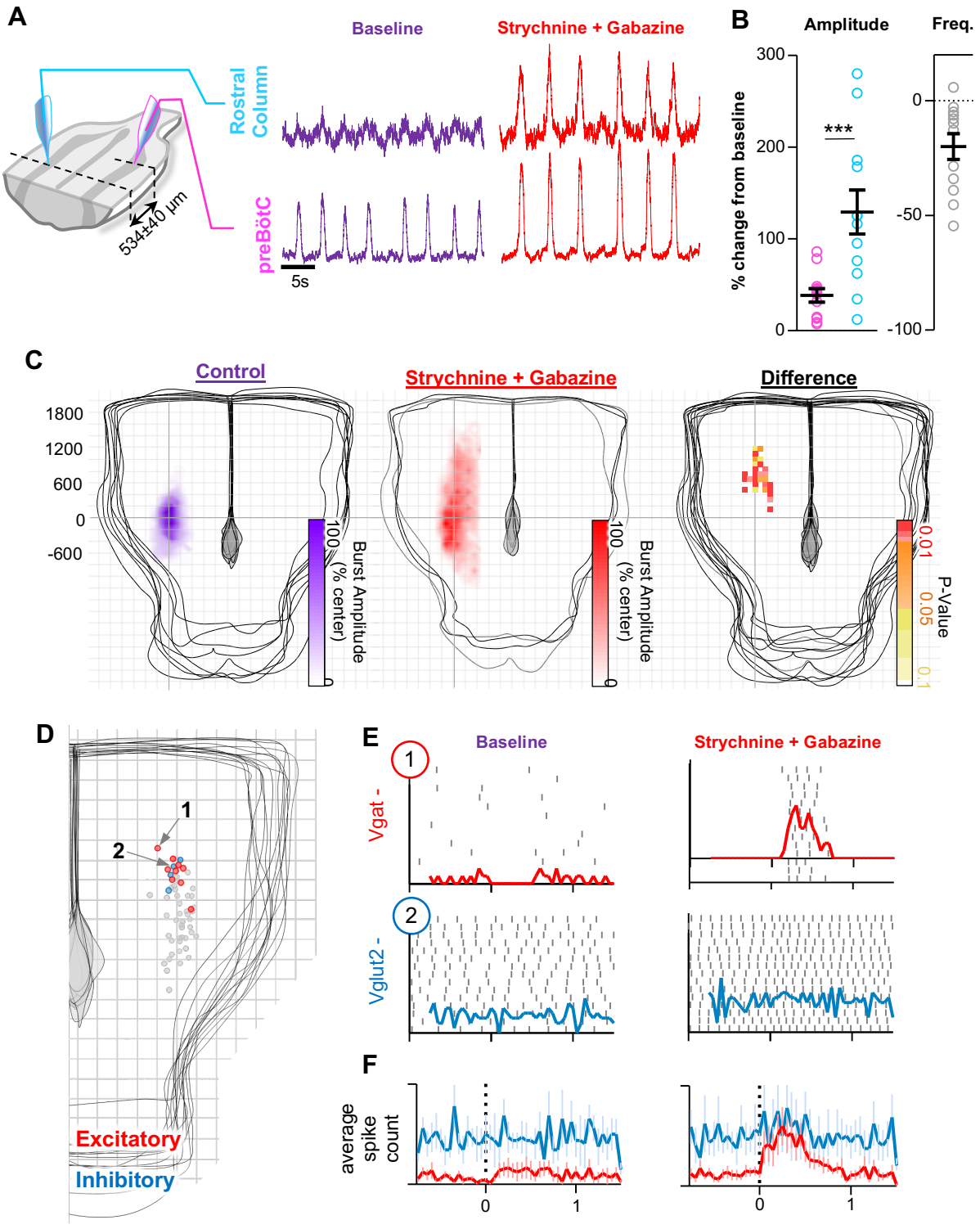
A
Baseline
Strychnine + Gabazine
Rostral Column
preBötC
534±40 µm
5s
B
Amplitude
Freq.
% change from baseline
300
200
100
0
***
0
-50
-100
C
Control
Strychnine + Gabazine
Difference
1800
1200
600
0
-600
100
(% center)
Burst Amplitude
0
0.01
0.05
0.1
P-Value
D
1
2
Excitatory
Inhibitory
E
Baseline
Strychnine + Gabazine
Vgat -
Vglut2 -
F
average spike count
0
1

Figure 3: Inhibitory mechanisms regulate spatial reconfiguration of the inspiratory network. A) Representative integrated population recordings from the preBötC center and 534±40μm rostral before (purple) and following suppression of GABAergic and glycinergic inhibition (red). B) Group data showing changes in burst amplitude and frequency (n=12). C) Heat maps (200μm grid) of inspiratory burst amplitude, across the horizontal slice under control conditions (n=8) and following suppression of synaptic inhibition with strychnine and gabazine (n=4). Differences rostral to the preBötC are shown as a map of Bonferoni-corrected p-values. D) Locations of silent or tonic spiking excitatory (red, n=9) or inhibitory (blue, n=4) neurons recorded rostral of the preBötC. Grey dots indicate the location of neurons with phasic inspiratory activity shown in Fig. 2A. E) Spike raster plots for example excitatory and inhibitory neurons during 15 consecutive inspiratory bursts at baseline and following co-application of strychnine and gabazine; solid lines show integrated spiking activity. F) Average spiking activity of excitatory (n=9) and inhibitory (n=4) neurons at baseline and following suppression of synaptic inhibition. (***p>0.001; means±SEM)

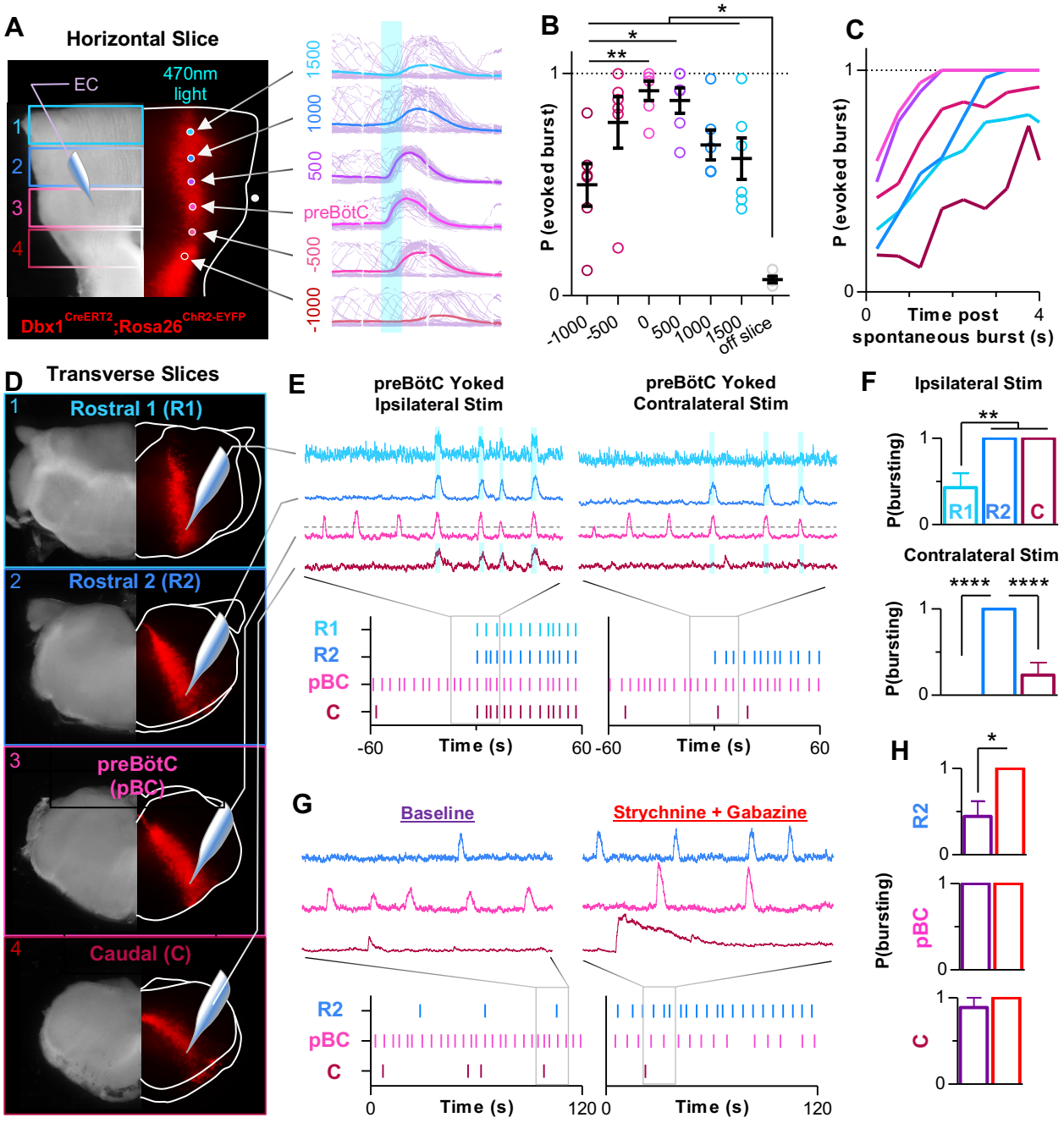
A
Horizontal Slice
EC
470nm light
1
2
3
4
Dbx1CreERT2;Rosa26ChR2-EYFP
1500
1000
500
preBötC
-500
-1000
B
P (evoked burst)
1
0
-1000
-500
0
500
1000
1500
off slice
C
P (evoked burst)
Time post spontaneous burst (s)
D
Transverse Slices
1 Rostral 1 (R1)
2 Rostral 2 (R2)
3 preBötC (pBC)
4 Caudal (C)
E
preBötC Yoked Ipsilateral Stim
preBötC Yoked Contralateral Stim
R1
R2
pBC
C
-60
Time (s)
60
F
Ipsilateral Stim
P(bursting)
R1
R2
C
Contralateral Stim
G
Baseline
Strychnine + Gabazine
R2
pBC
C
0
Time (s)
120
H
P(bursting)
R2
pBC
C

Figure 4: Rhythmogenic properties along the inspiratory column. A) Bright field (left) and EYFP fluorescence (right) images of a Dbx1^{CreERT2};Rosa26^{ChR2EYFP} horizontal slice showing optogenetic stimulation sites extending from 1500μm rostral to 1000μm caudal of the preBötC and representative integrated population activity (light purple) of the contralateral preBötC during 50 consecutive 200ms light stimulations (solid colored lines are averaged traces). B) Quantified probability of evoking a contralateral preBötC burst at each stimulus location, which was C) dependent on the elapsed time following a spontaneous preBötC burst (0.5s bins) (n=6 slices). D) Representative bright field and fluorescent images of consecutive transverse slices from a Dbx1^{CreERT2};Rosa26^{ChR2EYFP} mouse; two rostral (R1 and R2) to the preBötC (pBC) and one caudal (C). E) Representative integrated population activity and raster plots of bursting during ipsilateral (left) and contralateral (right) optogenetic stimulations yoked to preBötC bursting activity, and F) quantified probability of evoking bursts in each region (n=7 of each slice). G) Representative population activity and raster plots of spontaneous bursting in R2, pBC, and C slices and following suppression of synaptic inhibition with strychnine and gabazine (1μM each). H) Quantified probability of bursting under spontaneous conditions (purple) and following suppression of inhibition (red) in R2, pBC and C slices (n=9 of each slice). R1 slices did not burst spontaneously (EC: extracellular) (*p>0.05, ***p>0.001, ****p>0.0001; means±SEM)

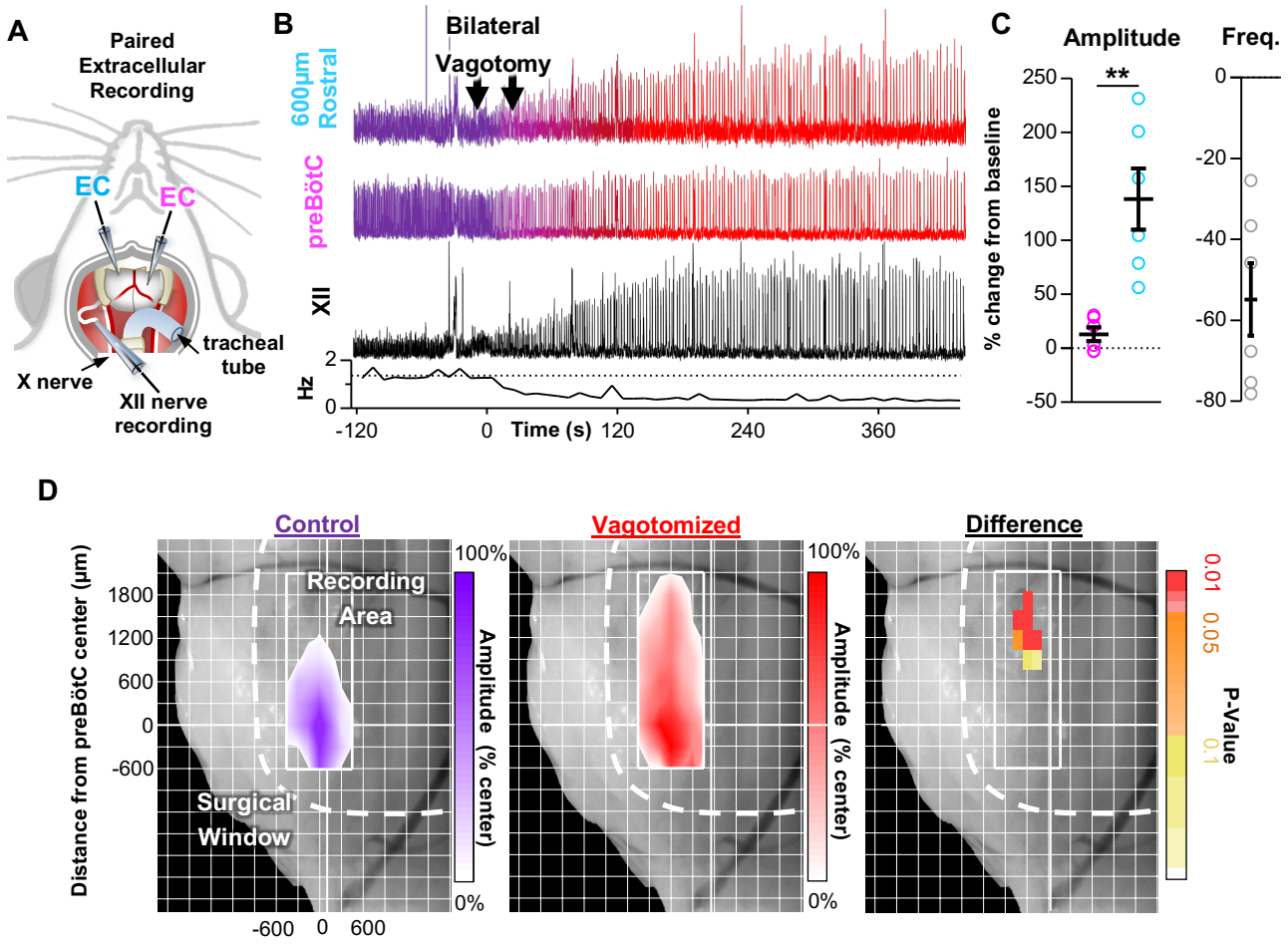

Figure 5: Vagal sensory feedback restricts inspiratory activity rostral of the preBötC. A) Schematic of the anesthetized in-vivo preparation used to perform paired recordings from the ventral medulla and motor output from the XII nerve. B) Representative experiment showing integrated population recordings of inspiratory activity from 600µm rostral to the preBötC (cyan), near the preBötC center (magenta), and from the hypoglossal (XII) nerve (black) under baseline conditions (purple) and following bilateral vagotomy (red). Breathing frequency is shown below (10s bins). C) Group data showing changes in burst amplitude and frequency (n=6). D) Heat maps of inspiratory activity, as a % of preBötC burst amplitude, across the ventral medulla under control conditions (n=5) and following vagotomy (n=7), and the difference shown as Bonferroni-corrected p-values. (*p>0.05; **p<0.01; ****p>0.0001; means±SEM)

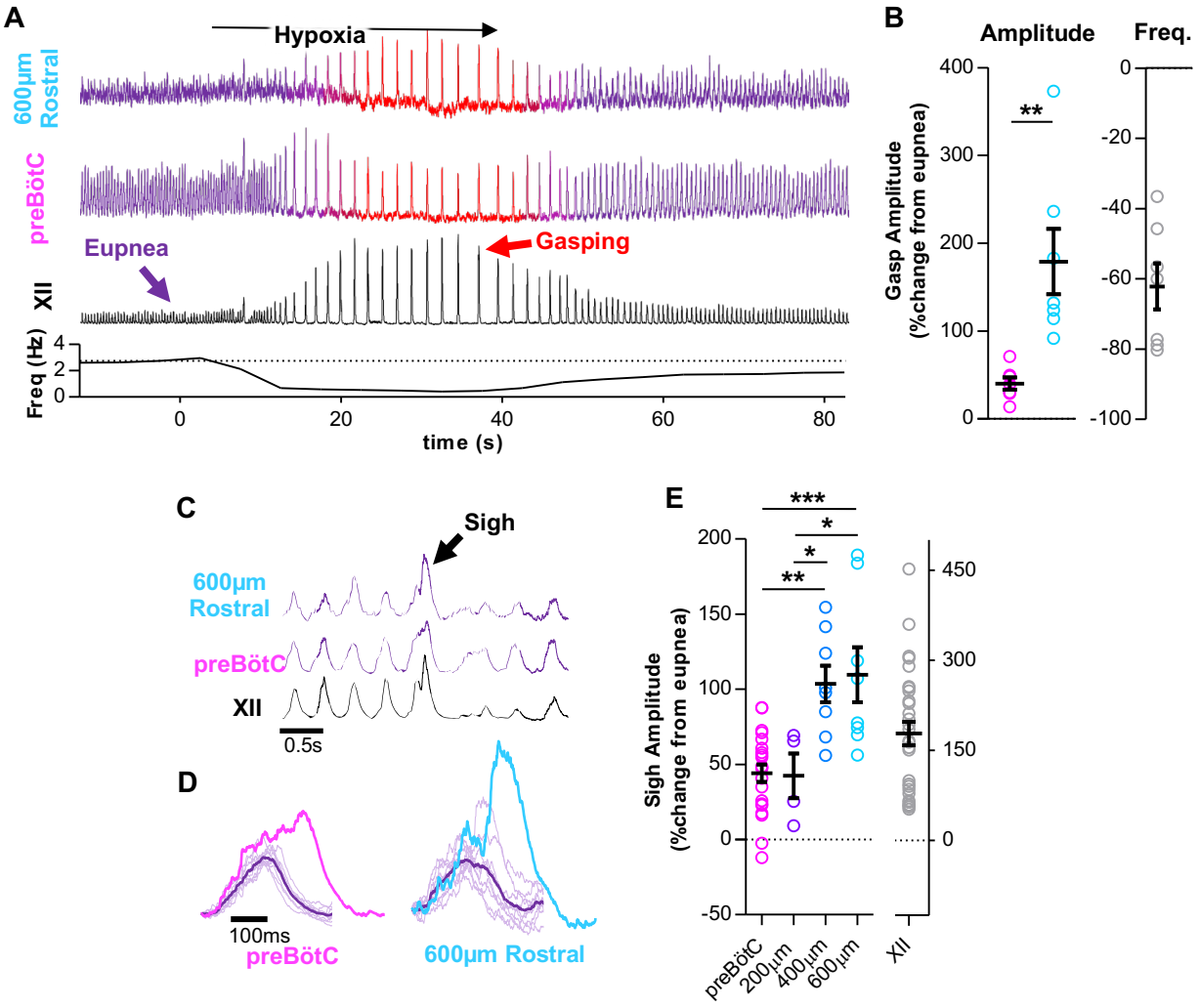

Figure 6: The spatial distribution of inspiratory activity expands during gasping and sighing in-vivo. A) Representative experiment showing integrated population recordings of inspiratory activity from 600µm rostral of the preBötC, near the preBötC center, and from the hypoglossal (XII) nerve during a brief bout of anoxia to evoke gasping. Breathing frequency is shown below (10s bins). B) Group data showing changes in burst amplitude and frequency (n=7). C) Representative eupnea and sigh recorded from the preBötC center, 600µm rostral, and the hypoglossal (XII) nerve, and D) overlaid eupneic bursts relative to the sigh at each location. E) Group data of sigh burst amplitude, as a percent of eupnea amplitude, recorded at the preBötC center and 200µm, 400µm, and 600µm rostral (*p>0.05, **p>0.01, ***p>0.001; means±SEM).

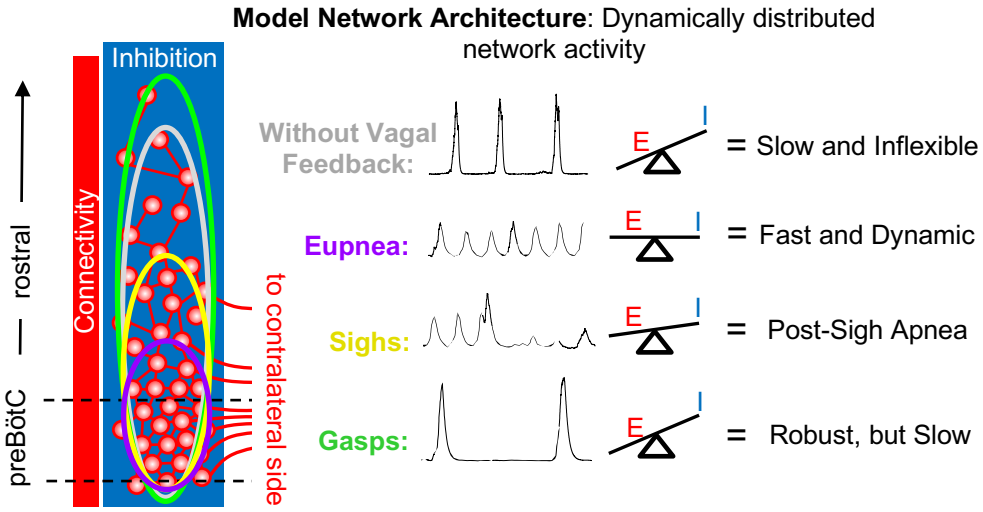

Figure 7: Hypothesized model for dynamic spatial reconfiguration of inspiratory activity based on a distributed network of excitatory and inhibitory neurons. Gradients of functional connectivity and inhibition determine the threshold for rhythmogenesis, which is lowest in the preBötC. During eupneic breathing (purple), a balance of excitation and inhibition restricts inspiratory activity and permits fast, dynamic rhythmic activity. Suppression of inhibition or removal of vagal sensory feedback (grey) leaves recurrent excitatory mechanisms unrestrained, leading to a rostral expansion of inspiratory activity, hyper synchronization of the network, and a slow inflexible rhythm. During sighs (yellow), a transient increase in excitation during the sigh burst expands the network rostrally resulting in a post-sigh apnea. During severe hypoxia or asphyxia, the network is reconfigured to produce gasping (green). Excitatory drive to the network increased and inhibition is suppressed leading to a large rostral expansion of inspiratory activity and a very robust, but slow, rhythm.

References

1. Swanson LW & Lichtman JW (2016) From Cajal to Connectome and Beyond. *Annual review of neuroscience* 39:197-216.

2. Anderson TM*, et al.* (2016) A novel excitatory network for the control of breathing. *Nature* 536(7614):76-80.

3. Eaton RC & DiDomenico R (1985) Command and the neural causation of behavior: a theoretical analysis of the necessity and sufficiency paradigm. *Brain Behav Evol* 27(2-4):132-164.

4. Tan W*, et al.* (2008) Silencing preBotzinger complex somatostatin-expressing neurons induces persistent apnea in awake rat. *Nat Neurosci* 11(5):538-540.

5. Young RM (1970) *Mind, brain and adaptation in the nineteenth century: Cerebral localization and its biological context from Gall to Ferrier* (Oxford University Press, New York, NY).

6. Seeman SC*, et al.* (2018) Sparse recurrent excitatory connectivity in the microcircuit of the adult mouse and human cortex. *Elife* 7.

7. Regev A*, et al.* (2017) The Human Cell Atlas. *Elife* 6.

8. Strange BA, Witter MP, Lein ES, & Moser EI (2014) Functional organization of the hippocampal longitudinal axis. *Nat Rev Neurosci* 15(10):655-669.

9. Ampatzis K, Song J, Ausborn J, & El Manira A (2014) Separate microcircuit modules of distinct v2a interneurons and motoneurons control the speed of locomotion. *Neuron* 83(4):934-943.

10. Gendrel M, Atlas EG, & Hobert O (2016) A cellular and regulatory map of the GABAergic nervous system of C. elegans. *Elife* 5.

11. Simpson JH & Looger LL (2018) Functional Imaging and Optogenetics in Drosophila. *Genetics* 208(4):1291-1309.

12. Diao F, Elliott AD, Diao F, Shah S, & White BH (2017) Neuromodulatory connectivity defines the structure of a behavioral neural network. *Elife* 6.

13. Aso Y*, et al.* (2014) The neuronal architecture of the mushroom body provides a logic for associative learning. *Elife* 3:e04577.

14. Peña-Ortega F (2017) Neural Network Reconfigurations: Changes of the Respiratory Network by Hypoxia as an Example. *Adv Exp Med Biol* 1015:217-237.

15. Weimann JM & Marder E (1994) Switching neurons are integral members of multiple oscillatory networks. *Curr Biol* 4(10):896-902.

16. Doi A & Ramirez JM (2008) Neuromodulation and the orchestration of the respiratory rhythm. *Respir Physiol Neurobiol* 164(1-2):96-104.

17. Ramirez JM*, et al.* (2012) The cellular building blocks of breathing. *Compr Physiol* 2(4):2683-2731.

18. Koch H, Garcia AJ, 3rd, & Ramirez JM (2011) Network reconfiguration and neuronal plasticity in rhythm-generating networks. *Integr Comp Biol* 51(6):856-868.

19. Getting PA (1989) Emerging principles governing the operation of neural networks. *Annual review of neuroscience* 12:185-204.

20. Kupfermann I & Weiss KR (2001) Motor program selection in simple model systems. *Curr Opin Neurobiol* 11(6):673-677.

21. Arnold A, Ekstrom AD, & Iaria G (2018) Dynamic Neural Network Reconfiguration During the Generation and Reinstatement of Mnemonic Representations. *Front Hum Neurosci* 12:292.

22. Berkowitz A, Roberts A, & Soffe SR (2010) Roles for multifunctional and specialized spinal interneurons during motor pattern generation in tadpoles, zebrafish larvae, and turtles. *Front Behav Neurosci* 4:36.

23. Bolser DC, Poliacek I, Jakus J, Fuller DD, & Davenport PW (2006) Neurogenesis of cough, other airway defensive behaviors and breathing: A holarchical system? *Respir Physiol Neurobiol* 152(3):255-265.

24. Kristan WB, Jr. & Shaw BK (1997) Population coding and behavioral choice. *Curr Opin Neurobiol* 7(6):826-831.

25. Kouchtir-Devanne N, Capaday C, Cassim F, Derambure P, & Devanne H (2012) Task-dependent changes of motor cortical network excitability during precision grip compared to isolated finger contraction. *J Neurophysiol* 107(5):1522-1529.

26. Sanes JN & Donoghue JP (2000) Plasticity and primary motor cortex. *Annual review of neuroscience* 23:393-415.

27. Morton DW & Chiel HJ (1994) Neural architectures for adaptive behavior. *Trends Neurosci* 17(10):413-420.

28. Braun U*, et al.* (2015) Dynamic reconfiguration of frontal brain networks during executive cognition in humans. *Proc Natl Acad Sci U S A* 112(37):11678-11683.

29. Capaday C, van Vreeswijk C, Ethier C, Ferkinghoff-Borg J, & Weber D (2011) Neural mechanism of activity spread in the cat motor cortex and its relation to the intrinsic connectivity. *J Physiol* 589(Pt 10):2515-2528.

30. Capaday C*, et al.* (2009) On the nature of the intrinsic connectivity of the cat motor cortex: evidence for a recurrent neural network topology. *J Neurophysiol* 102(4):2131-2141.

31. Feldman JL & Kam K (2015) Facing the challenge of mammalian neural microcircuits: taking a few breaths may help. *J Physiol* 593(1):3-23.

32. Ruangkittisakul A, Kottick A, Picardo MC, Ballanyi K, & Del Negro CA (2014) Identification of the pre-Botzinger complex inspiratory center in calibrated "sandwich" slices from newborn mice with fluorescent Dbx1 interneurons. *Physiol Rep* 2(8).

33. Wang X*, et al.* (2014) Laser ablation of Dbx1 neurons in the pre-Bötzinger complex stops inspiratory rhythm and impairs output in neonatal mice. *Elife* 3:e03427.

34. Koshiya N & Smith JC (1999) Neuronal pacemaker for breathing visualized in vitro. *Nature* 400(6742):360-363.

35. Smith JC, Ellenberger HH, Ballanyi K, Richter D, W. , & Feldman JL (1991) Pre-Bötzinger Complex: A Brainstem Region That May Generate Respiratory Rhythm in Mammals. *Science* 254(5032):726-729.

36. Ezure K, Tanaka I, & Kondo M (2003) Glycine is used as a transmitter by decrementing expiratory neurons of the ventrolateral medulla in the rat. *J Neurosci* 23(26):8941-8948.

37. Feldman JL, Loewy AD, & Speck DF (1985) Projections from the ventral respiratory group to phrenic and intercostal motoneurons in cat: an autoradiographic study. *J Neurosci* 5(8):1993-2000.

38. Smith JC, Abdala AP, Borgmann A, Rybak IA, & Paton JF (2013) Brainstem respiratory networks: building blocks and microcircuits. *Trends Neurosci* 36(3):152-162.

39. Smith JC, Abdala AP, Rybak IA, & Paton JF (2009) Structural and functional architecture of respiratory networks in the mammalian brainstem. *Philos Trans R Soc Lond B Biol Sci* 364(1529):2577-2587.

40. Ramirez JM, Dashevskiy T, Marlin IA, & Baertsch N (2016) Microcircuits in respiratory rhythm generation: commonalities with other rhythm generating networks and evolutionary perspectives. *Curr Opin Neurobiol* 41:53-61.

41. Del Negro CA, Funk GD, & Feldman JL (2018) Breathing matters. *Nat Rev Neurosci* 19(6):351-367.

42. Del Negro CA & Hayes JA (2008) A 'group pacemaker' mechanism for respiratory rhythm generation. *J Physiol* 586(9):2245-2246.

43. Baertsch NA, Baertsch HC, & Ramirez JM (2018) The interdependence of excitation and inhibition for the control of dynamic breathing rhythms. *Nat Commun* 9(1):843.

44. Bouvier J*, et al.* (2010) Hindbrain interneurons and axon guidance signaling critical for breathing. *Nat Neurosci* 13(9):1066-1074.

45. Gray PA*, et al.* (2010) Developmental origin of preBotzinger complex respiratory neurons. *J Neurosci* 30(44):14883-14895.

46. Carroll MS, Viemari JC, & Ramirez JM (2013) Patterns of inspiratory phase-dependent activity in the in vitro respiratory network. *J Neurophysiol* 109(2):285-295.

47. Lindsey BG, Segers LS, & Shannon R (1987) Functional associations among simultaneously monitored lateral medullary respiratory neurons in the cat. II. Evidence for inhibitory actions of expiratory neurons. *J Neurophysiol* 57(4):1101-1117.

48. Barnes BJ, Tuong CM, & Mellen NM (2007) Functional imaging reveals respiratory network activity during hypoxic and opioid challenge in the neonate rat tilted sagittal slab preparation. *J Neurophysiol* 97(3):2283-2292.

49. Zuperku EJ*, et al.* (2018) Inputs to medullary respiratory neurons from a pontine subregion that controls breathing frequency. *Respir Physiol Neurobiol*.

50. Ramirez JM, Schwarzacher SW, Pierrefiche O, Olivera BM, & Richter DW (1998b) Selective lesioning of the cat pre-Botzinger complex in vivo eliminates breathing but not gasping. *J Physiol* 507 (Pt 3):895-907.

51. Neumueller S*, et al.* (2011) Anatomic changes in multiple brainstem nuclei after incremental, near-complete neurotoxic destruction of the pre-Botzinger Complex in adult goats. *Respir Physiol Neurobiol* 175(1):1-11.

52. Krause KL*, et al.* (2009) Normal breathing pattern and arterial blood gases in awake and sleeping goats after near total destruction of the presumed pre-Botzinger complex and the surrounding region. *J Appl Physiol (1985)* 106(2):605-619.

53. Ramirez JM & Baertsch NA (2018a) The Dynamic Basis of Respiratory Rhythm Generation: One Breath at a Time. *Annual review of neuroscience* 41:475-499.

54. Kottick A & Del Negro CA (2015) Synaptic Depression Influences Inspiratory-Expiratory Phase Transition in Dbx1 Interneurons of the preBotzinger Complex in Neonatal Mice. *J Neurosci* 35(33):11606-11611.

55. Winter SM*, et al.* (2009) Glycinergic interneurons are functionally integrated into the inspiratory network of mouse medullary slices. *Pflugers Arch* 458(3):459-469.

56. Ramirez JM & Baertsch N (2018b) Defining the Rhythmogenic Elements of Mammalian Breathing. *Physiology (Bethesda)* 33(5):302-316.

57. Harris KD*, et al.* (2017) Different roles for inhibition in the rhythm-generating respiratory network. *J Neurophysiol*:jn 00174 02017.

58. Molkov YI, Rubin JE, Rybak IA, & Smith JC (2017) Computational models of the neural control of breathing. *Wiley Interdiscip Rev Syst Biol Med* 9(2).

59. Anderson T & Ramirez J (2017) Respiratory rhythm generation: triple oscillator hypothesis. *F1000Res* 6(139).

60. Rybak IA, Abdala AP, Markin SN, Paton JF, & Smith JC (2007) Spatial organization and state-dependent mechanisms for respiratory rhythm and pattern generation. *Prog Brain Res* 165:201-220.

61. Smith JC, Abdala AP, Koizumi H, Rybak IA, & Paton JF (2007) Spatial and functional architecture of the mammalian brain stem respiratory network: a hierarchy of three oscillatory mechanisms. *J Neurophysiol* 98(6):3370-3387.

62. Janczewski WA, Tashima A, Hsu P, Cui Y, & Feldman JL (2013) Role of inhibition in respiratory pattern generation. *J Neurosci* 33(13):5454-5465.

63. Clark FJ & von Euler C (1972) On the regulation of depth and rate of breathing. *J Physiol* 222(2):267-295.

64. Lieske S, Thoby-Brisson M, Telgkamp P, & Ramirez J (2000) Reconfiguration of the neural network controlling multiple breathing patterns: eupnea, sighs and gasps *Nature Neuroscience* 3:600-607.

65. Peña F, Parkis MA, Tryba AK, & Ramirez JM (2004) Differential contribution of pacemaker properties to the generation of respiratory rhythms during normoxia and hypoxia. *Neuron* 43(1):105-117.

66. Morris KF*, et al.* (2018) Carotid chemoreceptors tune breathing via multipath routing: reticular chain and loop operations supported by parallel spike train correlations. *J Neurophysiol* 119(2):700-722.

67. Rybak IA*, et al.* (2004) Modelling respiratory rhythmogenesis: focus on phase switching mechanisms. *Adv Exp Med Biol* 551:189-194.

68. Guyenet PG (2014) Regulation of breathing and autonomic outflows by chemoreceptors. *Compr Physiol* 4(4):1511-1562.

69. Ramirez JM (2014) The integrative role of the sigh in psychology, physiology, pathology, and neurobiology. *Prog Brain Res* 209:91-129.

70. Tryba AK*, et al.* (2008) Differential modulation of neural network and pacemaker activity underlying eupnea and sigh-breathing activities. *J Neurophysiol* 99(5):2114-2125.

71. Li P*, et al.* (2016) The peptidergic control circuit for sighing. *Nature* 530(7590):293-297.

72. Lindsey BG*, et al.* (1994) Distributed actions and dynamic associations in respiratory-related neuronal assemblies of the ventrolateral medulla and brain stem midline: evidence from spike train analysis. *J Neurophysiol* 72(4):1830-1851.

73. Abbott SB, Stornetta RL, Coates MB, & Guyenet PG (2011) Phox2b-expressing neurons of the parafacial region regulate breathing rate, inspiration, and expiration in conscious rats. *J Neurosci* 31(45):16410-16422.

74. Segers LS*, et al.* (2012) Discharge Identity of Medullary Inspiratory Neurons is Altered during Repetitive Fictive Cough. *Front Physiol* 3:223.

75. Ruangkittisakul A*, et al.* (2008) Generation of eupnea and sighs by a spatiochemically organized inspiratory network. *J Neurosci* 28(10):2447-2458.

76. Brovelli A*, et al.* (2017) Dynamic Reconfiguration of Visuomotor-Related Functional Connectivity Networks. *J Neurosci* 37(4):839-853.

77. Auffret M*, et al.* (2018) Optogenetic stimulation of cortex to map evoked whisker movements in awake head-restrained mice. *Neuroscience* 368:199-213.

78. Oke Y, Miwakeich F, Oku Y, Hirrlinger J, & Hulsmann S (2018) Cell Type-Dependent Activation Sequence During Rhythmic Bursting in the PreBotzinger Complex in Respiratory Rhythmic Slices From Mice. *Front Physiol* 9:1219.

79. Hearne LJ, Cocchi L, Zalesky A, & Mattingley JB (2017) Reconfiguration of Brain Network Architectures between Resting-State and Complexity-Dependent Cognitive Reasoning. *J Neurosci* 37(35):8399-8411.

80. Peña-Ortega F (2009) Neuronal network properties underlying the generation of gasping. *Clin Exp Pharmacol Physiol* 36(12):1218-1228.

81. Richter DW, Bischoff A, Anders K, Bellingham M, & Windhorst U (1991) Response of the medullary respiratory network of the cat to hypoxia. *J Physiol* 443:231-256.

82. Peña F & Ramirez JM (2004) Substance P-mediated modulation of pacemaker properties in the mammalian respiratory network. *J Neurosci* 24(34):7549-7556.

83. St John WM (2009) Noeud vital for breathing in the brainstem: gasping--yes, eupnoea--doubtful. *Philos Trans R Soc Lond B Biol Sci* 364(1529):2625-2633.

84. Izumizaki M, Pokorski M, & Homma I (2004) Role of the carotid bodies in chemosensory ventilatory responses in the anesthetized mouse. *Journal of Applied Physiology* 97(4):1401-1407.

85. Moore JD*, et al.* (2013) Hierarchy of orofacial rhythms revealed through whisking and breathing. *Nature* 497(7448):205-210.

86. Milsom WK (2010) Adaptive trends in respiratory control: a comparative perspective. *Am J Physiol Regul Integr Comp Physiol* 299(1):R1-10.

87. Mateika JH & Duffin J (1994) Coincidental changes in ventilation and electromyographic activity during consecutive incremental exercise tests. *Eur J Appl Physiol Occup Physiol* 68(1):54-61.

88. Ramirez J*, et al.* (2013) Central and peripheral factors contributing to obstructive sleep apneas. *Respiratory Physiology and Neurobiology* 189(2):344-353.

89. Chai LR, Mattar MG, Blank IA, Fedorenko E, & Bassett DS (2016) Functional Network Dynamics of the Language System. *Cereb Cortex* 26(11):4148-4159.

90. Vong L*, et al.* (2011) Leptin action on GABAergic neurons prevents obesity and reduces inhibitory tone to POMC neurons. *Neuron* 71(1):142-154.

91. Kottick A, Martin CA, & Del Negro CA (2017) Fate mapping neurons and glia derived from Dbx1-expressing progenitors in mouse preBotzinger complex. *Physiol Rep* 5(11).

CHAPTER 7

FUTURE DIRECTIONS

The sigh as a brain-wide reset and oxygen sensor

Sighing is a very interesting behavioral phenomenon in that it is both an autonomic function necessary for normal breathing and an emotional function that can be stimulated physiologically in times of stress and evoked purposefully during a variety of emotions. This logically points to the sigh being tightly linked to higher order brain regions, especially regions like the amygdala and somatosensory cortex. This concept stimulated the idea that sighs could be relayed from the brainstem networks to the cortex to communicate (1) oxygenation status/arousal state and (2) emotional responses. Given the implication of sighs in arousal, the sigh would be an appropriate link to the rest of the brain to stimulate oxygenation status when PO_2/PCO_2 rises above or below the normal physiological threshold. Furthermore, given the role of astrocytes in generating sighs in preBötC, a secondary question is if astrocytes could be a part of this relay.

Several experiments would allow interrogation of this circuity to determine if, and how, sighs are transmitted to other brain areas. Both provide significant challenges and the use of multiple techniques. The first experiment would involve making a craniotomy in a transgenic animal (either astrocyte or neuron specific) expressing a GECI, or to inject a Ca^{2+} dye or GCaMP virus into the amygdala/different somatosensory cortex areas. Ca^{2+} imaging would be performed while simultaneously monitoring breathing through a bipolar diaphragm electrode. In the case of dye injections into the amygdala, other cortical layers would most likely need to be aspirated to allow for this deep of imaging. Post hoc analysis would look for activity patterns that coincide with breathing in general or specifically sighing. Performing this experiment in awake mice is ideal to avoid anesthetic depression of the respiratory circuits but is an approach that would add significant challenges and a strong behavioral component to the study.

Alternatively, neuropixels (a multielectrode array of 300 channels which can be placed very deep in the brain) would be inserted into the coordinates for the amygdala. A corresponding optrode fiber would be placed into the preBötC of a transgenic mouse expressing channelrhodopsin driven by an astrocytic or neuronal (e.g., Vglut2) promoter. Evoked sighs at the level of the preBötC then be more tightly associated with sigh and eupnea related oscillatory activity within cortical or sub-cortical structures.

Methods:

Optic fiber cannulation

Optic fibers would first be implanted unilaterally into experimental mice. One unilateral 220mm or two 125mm bilateral fiber optic cables would be implanted targeting the preBötC using a 15° rostral to caudal sagittal angle. The following coordinates have been used previously by our lab to target the preBötC: 6.7mm caudal to bregma, 1.2mm lateral to the midline, and 4.8mm below the skull surface; and for RTN: 6.3mm caudal to bregma, 1.6mm lateral to the midline, and 5.2mm below the skull surface (1). After all surgical procedures, mice are treated with carprofen (5mg/kg/d for 2d) and allowed to recover for at least 10d before functional experiments are performed *(2)*.

Craniotomy

Craniotomies and thin skull windows would allow visualization of underlying cellular structures. Generally, full craniotomies are more difficult, given that any bleeding or swelling of the brain can alter cell activity and therefore, results and interpretation of data. Therefore, thin skull windows may be beneficial; they are much easier to perform while preventing damage of the anatomy but do prevent imaging at deeper brain structures. Cranial windows can be performed as an access point for imaging at the surface or subsurface regions of the brain. Performing craniotomies is much easier on the caudal portion of the skull- the frontal cortex in adult mice is much thicker and more difficult to produce a clean window without damaging brain tissue. An incision in the skin above the skull is made, exposing most of the skull between the ears, extending just behind the eyes and above neck muscles. Before beginning, coordinates should be approximately determined for craniotomy location. A small titanium head cap is glued to the skull using dental cement (C&B Metabond), making sure it is flat on top of the skull. It is important to lightly wet the surface of the skull in this area and observe the underlying brain vasculature. Areas of dense vascularity or with large blood vessels should be avoided in area in which the craniotomy will be performed. A dental drill (Osada) with vert fine drill tips (Fine scientific tools, 19007-05) is then used to very carefully create a small ‘volcano’ in the skull. The drill should not be kept constantly on, and instead used in small spurts to prevent overheating of the tissue, cells, and blood vessels underneath, which can result in aberrant cell activity. The skull can be intermittently cooled with cold PBS or ACSF. The drill is also kept at a slight angle, so that when the skull becomes very thin, a small gauge needle (I.e., 30G) can be delicately slipped under the cap within the ‘volcano’ and removed. This prevents the brain from swelling

drastically and also helps to prevent bleeding. Once the bone is removed from the cranial window, a small piece of dental sponge wet with PBS is placed over the exposed brain tissue. Immediately before applying a small glass coverslip over the window, the sponge is removed. There must not be any bleeding of tissue before placing the coverslip or the window will become clouded and unusable. If there is slight bleeding, gently pipette PBS in small pulses through the dental sponge until it subsides. The coverglass is then carefully glued to the skull using crazy glue added into a 1ml syringe, while pressing gently down in the center of the cover glass.

Thin skull window

To perform a thin skull window, instructions for craniotomy should be followed and the head holder affixed similarly. When drilling the thin skull window, gently shave off the entire area in the region of interest, moving the drill in a back-and-forth motion evenly over the area. As you progress deeper into the skull tissue, you will observe a change in the look of the skull- first blood vessels are apparent, then as you move through these cranial vessels, you will notice the bone takes on a white speckled appearance. Once you pass through this layer, be careful not to puncture through the skull. When an even layer of bone is removed glue a coverslip on top of the window, with a small drop of Loctite 401 glue underneath. Loctite 401 glue is important, as it is clear and will allow imaging through the window.

Viral/dye injections

Viral injections (with AAV) require approximately 2-3 weeks lead time before imaging. A small incision is made in the skin above the area of interest. Using the drill, make a very small hole in the skull, being careful to not break entirely through the skull. Once you are almost through, take a small gauge needle and flip up a piece of the skin skull, just large enough to fit a needle. Pull injection capillaries (Hirschmann ringcaps, REF 960 01 05) to be very thin, and pressure pull up a small amount of virus or dye (~100nL, fill needle to approx. 3μL). Very slowly using a stereotax, inject the needle containing dye/virus to the desired depth of anatomical target. Very slowly (<1μL/min) pressure inject a small amount of virus/dye. Wait several minutes for the dye to settle, then incrementally remove the needle.

Note: if using dye (e.g., Oregon Green Bapta-1), the dye should be diluted in the following proportion: 4μL pluronic F-127 in DMSO to facilitate cell uptake. Vigorously vortex dye and PF127, spin down, and add 72μL of buffer (e.g., PBS) and vortex again. Filter dye to remove any particulate using a small c-tube filter (costar, 0.22μm filter, 2mL).

Selective targeting of the P2Y1 receptor on astrocytes

Specifically targeting astrocytes is difficult, as they express many of the same receptors as neurons. Furthermore, many tools used for selective targeting such as inhibitory optogenetics and DREADDs were designed to be used with neurons and have been shown to be ineffective when used with astrocytes. Our preliminary experiments using inhibitory opsins in astrocytes *in vitro* did not show any effects. We have demonstrated that the purinergic P2Y1 receptor plays a significant role in sigh modulation (Ch. 5). Furthermore, histological analyses show a large amount of this receptor throughout the brainstem areas, and it is unclear if P2Y1 is expressed only on astrocytes or also on neurons. Therefore, an experiment that would allow for the interrogation specifically of the role of astrocytes in sigh generation would be to temporarily or permanently knock down purinergic receptors on astrocytes. This would answer several important questions: (1) Do P2Y1 receptors on neurons play a role in sighing? (2) how important are P2Y1 receptors to generating sighs? (3) Are there redundancies that would occur without them, or are they necessary for sighs at the level of the preBötC? and (4) does purinergic signaling through astrocytes and P2Y1 receptors also affect normal breathing significantly?

Several techniques would be useful in this type of knockdown experiment. Crispr/cas9 or siRNA knockdown are both commonly utilized techniques. With these methods, guide RNA's would be designed or purchased to the P2Y1 receptor, as well as 'scrambled' control RNA's. P2Y1R's would be expressed in HEK cell lines, then transfected with Crispr/cas9 or siRNA's to determine the efficacy of the constructs in eliminating the receptor. Then the constructs would be tested in cultured astrocytes isolated from the brainstem. Functional effects of the knockdown could be tested with Ca^{2+} imaging in cultured astrocytes, and more extensive experiments would apply the techniques *in vivo* followed by whole body plethysmography or the *in vivo* anesthetized preparation to determine the effects of P2Y1R knockdown in astrocytes on breathing.

Identifying subpopulations of astrocytes within the respiratory networks

It is known that astrocytes have distinct subpopulations- in injury, reactive astrocytes seal off the site of injury to form a barrier to the rest of the CNS. Astrocytes exhibit many different regional characteristics, such as modulation of the cerebrovasculature(3). However, there is still a large amount of information that we do not know about astrocyte lineages and subtypes. Specific to the preBötC is a population of neurons and astrocytes that developmentally express the transcription factor developing homeobox protein 1 at a specific time point in embryogenesis- day 9.5 to 11- and these cells become neurons and astrocytes

that make up the preBötC inspiratory column. A group of dbx1-expressing astrocytes are derived from the d11 timepoint in development. Given the importance to breathing that these neurons have in breathing, we also postulated that this population of astrocytes might have strong effects on breathing or chemosensitivity. Therefore, exploring RNAseq methods to discover more astrocytic markers for subtypes would drastically enhance our understanding of astrocytes.

A second experiment which would help to answer this question is the use of transgenic animals. Aldh1l1DTA transgenic mice express diphtheria toxin driven by the Aldh1l1 promoter, thereby specific to astrocytes. When exposed to cre, the DTA expressing cells are lesioned. Therefore, a cross with Aldh1l1^{DTA} with a Dbx1^{cre} mouse would specifically lesion astrocytes expressing Dbx1. However, depending on the severity and amount of Dbx1 expression in astrocytes throughout the brain, this approach could result in other detrimental effects outside of the respiratory networks. In order to more specifically target Dbx1 expressing astrocytes of the brainstem, an astrocyte specific, cre-expressing AAV could be targeted to the preBötC to more selectively lesion this population of cells.

Pharmacological experiments

ATP and ADP

ATP and its derivatives -ADP and ADO – are somewhat difficult to study, as they are very rapidly broken down by ectonucleotidases. Therefore, we attempted to perform experiments with caged compounds- ATP and ADP contained in a peptide construct, that when undergoing a conformational change as a result of UV spectrum light, are released into the medium. It is unclear why these experiments were ineffective; however, an important set of experiments would be to apply these drugs in a simple slice preparation (perhaps with ectonucleotidase inhibitors) to determine if ATP or ADP is what is resulting in the results that we observed in Ch 5. Furthermore, I predict that the extended post sigh apnea period is a result of ADO buildup. ATP is understood to be readily released by astrocytes; however little study as gone into understanding the effects of the breakdown into ADO on the network. Some papers have reported that ADO has inhibitory effects on the respiratory rhythm (4). The dynamics of the refractory period for the normal eupneic cycle fit the idea of the post sigh apnea, i.e., a burst of large magnitude results in depolarization block of the neuronal network, and the bigger the burst the longer the apnea. Indeed, experiments by our lab have demonstrated these dynamics (5). However, in optogenetic experiments when comparing Vglut2$^{cre/Ai32}$ optogenetic stimulation with

Aldh1l1$^{cre/Ai32}$, there are some observed differences that indicate the refractory dynamics alone do not explain the extended interval after sighs; in that a sigh burst evoked in Aldh1l1 has a longer post burst interval than a burst of 'equivalent size' in both Vglut2 and Aldh1l1. Thus, I suspect that ADO may build-up after the release of ATP from a sigh, and function to inhibit neuronal activity. This results in what we see as a 'sigh reset' (discussed below) which purportedly resets the respiratory rhythm.

Carbenoxolone

Many of the drugs that are used to target gap junctions are famously considered 'dirty drugs', i.e., they alter other cellular processes nonspecifically, thus making it difficult to tease out the precise roles of these different channels (6). Other drugs may have slightly more specific roles, but the use is still highly questioned. Several examples are mefloquine (more specific to Cx36)(6). However, the inavailability of better drugs for studying gap junctions does not provide many options when questioning their role. We hypothesized that gap junctions may play a role in sighing, given our data that astrocytes are involved in sigh generation. Lower concentrations than previously used in the breathing networks (50μM vs 100μM)(7) demonstrated that carbenoxolone is able to selectively block sighing. When applying published concentrations (100μM), carbenoxolone reduced or completely eliminated eupneic activity in transverse preBötC slices.

Is there a refractory period for the sigh?

In continuation of the ideas discussed above, the sigh must have a refractory period that prevents the onset of the next burst. Our modeled data from Ch. 5 suggests that it occurs with the coincidence of two overlapping Ca^{2+} signals. Furthermore, we have found neurons that exhibit slow wave spiking patterns that line up with the sigh but not the eupneic rhythm. Although evidence for these signals is still not abundant, our preliminary data points towards a slow wave signal that initiates the sigh when overlapping with the neuronal Ca^{2+} oscillation. Thus, there must be a limitation in the source of the slow wave signal. Future Ca^{2+} imaging experiments in slices isolated from Aldh1l1$^{cre/R26Lck}$ will hopefully help lead to this answer. Our hypothesis is that astrocytes will have slow fluctuations that have some jitter in relation to both eupnea and sigh activity.

What is a doublet?

Our colleagues characterize sighs as a ‘doublets’ in their publication by Li et al. in 2016 (8). Our observations *in vitro* and *in vivo* indicate that the doublet is a type of disordered breathing or orofacial behavior that doesn’t often occur during a stable slice or anesthetized preparation. Indeed, Li et al. primarily observe these in a slightly different slice preparation, where the preBötC signal is recorded from the hypoglossal nerve rootlets as opposed to population activity recorded directly form the preBötC. Therefore, in Ch. 5, we highlight the characteristics of sighs, and further compared sighs evoked with light stimulation and spontaneous sighs *in vitro* and *in vivo*. *In vitro*, it is sometimes difficult to distinguish sighs from eupnea when the rhythm is robust; monophasic sighs can be of similar amplitude with less obvious post burst interval. Doublets *in vitro* appear as two consecutive bursts of similar amplitude. *In vivo* sighs are more easily distinguished, as the diaphragm provides a clear difference between sighs and eupneic breaths, and doublets. *In vivo*, doublets often occur at the end of an experiment or if the brainstem is damaged during the surgical preparation, and do not have a consistent frequency. More commonly, doublets *in vivo* do not have diaphragm activation, and thus can be suggested to be a type of orofacial behavior, given that the diaphragm is not active during these bursts(9, 10). This could be explored in vitro by using a sagittal slice preparation where both hypoglossal nerve rootlet and ventral cervical spinal root C1-C2 can be recorded(10). Furthermore, diaphragm activation during doublets mimics that of two consecutive eupneic cycles and does not have an enhanced burst duration or amplitude as is observed during sighing. However, the physiological reason for these doublet breaths remains unclear.

Summary of primary findings

The experiments and discussion that are presented in this thesis describe a role for astrocytes in generating the sigh through purinergic mechanisms within the preBötzinger complex. The results presented are supported by a large breadth of existing literature which highlight previous and existing theories of sigh generation and the role of astrocytes in modulating respiratory rhythm generation. We have shown that sighs are generated by the coincidence of two calcium signals: one slow oscillation initiated outside of the neuronal network, and a fast oscillation generated by neural activity. The slow oscillation is translated to neural activity through purinergic signaling from astrocytes, which also contributes to generating the central hypoxic response. This thesis also presents a novel hypothesis for the organization of the respiratory networks. This hypothesis suggests that the preBötC in not a small kernel, but is a dynamic column composed of subsets of neurons which control breathing to meet metabolic demand. The major hypotheses presented here contribute to a better understanding of rhythm generation in two primary ways: ***(1) How rhythm generating networks can simultaneously generate and modulate multiple rhythms with different timing characteristics*****, and** ***(2) How rhythm generating networks can adjust depending on metabolic state.***

References

1. Franklin, K.B. and G. Paxinos, *The Mouse Brain in Stereotaxic Coordinates*. 2008, New York: Elsesvier.
2. Oliveira, L.M., et al., *Unraveling the Mechanisms Underlying Irregularities in Inspiratory Rhythm Generation in a Mouse Model of Parkinson's Disease.* J Neurosci, 2021. **41**(21): p. 4732-4747.
3. Marina, N., et al., *Astrocytes monitor cerebral perfusion and control systemic circulation to maintain brain blood flow.* Nat Commun, 2020. **11**(1): p. 131.
4. Reklow, R.J., et al., *The Purinome and the preBotzinger Complex - A Menage of Unexplored Mechanisms That May Modulate/Shape the Hypoxic Ventilatory Response.* Front Cell Neurosci, 2019. **13**: p. 365.
5. Baertsch, N.A., H.C. Baertsch, and J.M. Ramirez, *The interdependence of excitation and inhibition for the control of dynamic breathing rhythms.* Nat Commun, 2018. **9**(1): p. 843.
6. Connors, B.W., *Tales of a dirty drug: carbenoxolone, gap junctions, and seizures.* Epilepsy Curr, 2012. **12**(2): p. 66-8.
7. Gourine, A.V., et al., *Astrocytes control breathing through pH-dependent release of ATP.* Science, 2010. **329**(5991): p. 571-5.
8. Li, P., et al., *The peptidergic control circuit for sighing.* Nature, 2016. **530**(7590): p. 293-297.
9. Huff, A., et al., *Sex-specific vagal and spinal modulation of swallow and its coordination with breathing.* PLoS One, 2020. **15**(6): p. e0234194.
10. Pitts, T., et al., *Evidence of intermediate reticular formation involvement in swallow pattern generation, recorded optically in the neonate rat sagittally sectioned hindbrain.* J Neurophysiol, 2021. **125**(4): p. 993-1005.

APPENDIX I

DISSOCIATION AND CULTURE OF PRIMARY NEURONS AND ASTROCYTES FROM THE RHYTHM GENERATING NETWORKS

Protocol produced by Jane M. Sullivan and adapted by Liza J. Severs

Introduction

Cell culture is a valuable tool for studying cells in isolation. Specific to the respiratory field, there few papers which utilize cell culture to study network dynamics. Here, we introduce a preliminary protocol to successfully isolate, culture, and record from neurons and astrocytes of the ventral respiratory column. Neurons isolated specifically from the preBötC and piCo continue to exhibit bursting dynamics that mimic their activity in the slice. Astrocytes from these networks can be propagated for >1month in culture. Further electrophysiological experimentation and analysis is required to characterize cells isolated in these cultures; however, we have demonstrated that respiratory neurons expressing Dbx1, NK1R, and SST can be successfully maintained for at least 3 weeks *in vitro*. Given the lack of understanding of synaptic plasticity and individual cell dynamics in the respiratory centers, the use of culture cells provides a powerful method of studying the breathing networks when further isolated from the slice preparation.

Primary Isolation and culture of rhythmic brainstem neurons

Methods

Preparation

Purchase pre-coated PDL/laminin coverslips

OR coat in advance

Coverslip/plate coating:
Poly D Lysine in PBS- (25µg/mL) ~2hrs-overnight
Laminin in sterile water (2.5µg/mL) ~4hrs-overnight
-Rinse with sterile water before plating cells

Neuronal media (200mL):
164.75 mL MEM + Glutamax (5mL glutamax to 500mL MEM)
20 mL horse serum (10%)
5 mL 1M HEPES (25mM final conc.)
4 mL 1M Glucose in MEM (9g glucose in 50ml of MEM- sterile filter)
0.25 mL Pen/Strep
4 mL B-27

2 mL Sodium Pyruvate

Astrocyte media (200mL):
186 mL MEM + Glutamax (5mL Glutamax to 500mL MEM)
20 mL horse serum (10%)
4 mL 1M Glucose in MEM
0.25 mL Pen/Strep

Isolation Media:
50 mL HBSS+ calcium and magnesium (helps prevent clumping of tissue)
250 μL 10mM HEPES
250 μL D-Glucose (5mM)

Enzyme Solution:
10 mL HBSS
100 μL 1M HEPES (10mM)
80-100 μL Papain Stock (~20-25 U/ml)

Agar block preparation:

5% W/V solution should be used. Weigh agar and add to a clean beaker (make sure beaker is large-agar will be boiled and bubbles up). Add DI H20, and microwave until agarose begins to bubble up (~1 minute) remove and stir. Continue to stir and microwave agar in short intervals, being careful not to boil it over. When agar is clear, it can be poured into a sterile petri dish. Apply lid and allow to cool. Store inverted to prevent condensation and sealed in a plastic bag to prevent contamination.

Tools:

Sterile scalpel blade/razor blade
Scalpel handle
Curved Dumont forceps
Curved iridectomy scissors
Paintbrush
Large scissors
Vibratome

Preparation of dissection area and supplies:

i. Make all solutions described above.
ii. Prepare 4 small petri dishes with cold dissection media for washing steps. A fourth empty dish can be used for dissection- if preferred, dissections can be carried out on dissecting pads and pinned.
iii. place enzyme solution in incubator to warm before starting protocol.
iv. clean all tools thoroughly with soap and water, followed by wiping with EtOH, and allowing sprayed EtOH to dry.
v. Place coated coverslips into the wells of a 24-well plate. 5 whole brainstems typically produces enough cells for 5-10 coverslips. Place 1mL of neuronal media, making sure coverslips are submersed, and place in the incubator during isolation procedures.

Dissection procedure:

* If possible, dissection should be performed in a laminar flow hood to prevent tissue contamination. If this is not possible, ensure sterile environment by wiping down area and clean tools with EtOH followed by spraying and allowing it to thoroughly dry before beginning procedure).

1. Rapidly decapitate embryo/newborn mice (p0/1 is ideal, protocol can be successful with p2/3) just above the shoulder girdle to retain part of the spinal cord.
2. Use a scalpel blade to slice along the skin along the midline of the skull. Tear skin away from skull using forceps.
3. Use the scalpel blade to slice the skull along the midline up to the junction with the cerebellum. Tear away the skull tissue, exposing the brain and cerebellum. Continuously pipette small amounts of dissection solution onto the brain and brainstem throughout the dissection.
4. Using curved scissors, make a vertical incision on each side of the brain at the junction of the cortices and cerebellum to loosen the skull from the rest of the spinal column.
5. Gently, using curved forceps, pull the brain away from the bottom of the skull. Sever optic nerve to release the cortex.
6. With fine tipped forceps, delicately pull the remainder of the skull away from the brainstem and spinal cord. If the spinal cord encased in the spinal column is difficult to remove, small iridectomy scissors can be used to carefully cut laterally along the spinal column to release start of the spinal cord. Gently pull away the remainder of the bone.

7. Using a scalpel, cut the cortex away from the cerebellum and medulla but making a clean, vertical cut at the juncture of the cortex and cerebellum. Flip the brain onto the cut side (coronal) so that the spinal cord is facing upwards. Using a paintbrush, gently pull the cerebellum away from the medulla and use the scalpel to again make a vertical incision to separate the cerebellum at the more rostral point where it connects to the brain. Use the scalpel to slice away the pons and any excess spinal cord tissue.
8. Peel back the vascularized meninges from the medulla using curved forceps.
9. If isolating cells from whole brainstem, place dissected medullary tissue into cold dissection media on ice. Continue to dissect remaining mice, then proceed to step 11. If specific medullary regions are desired, proceed to next step.
10. For isolation of the preBötC, the medulla can be placed ventral side up on an agar block at a ~20-degree angle and sectioned on a vibratome. *EXTREME care must be taken in this case to prevent bacterial contamination of cell cultures. Wipe all equipment surrounding vibratome with 70% EtOH thoroughly, then spray again with EtOH allowing tools and equipment to dry properly. Special 5% agarose should made in a sterile petri dish and stored in a cell culture refrigerator in a bag to prevent contamination. Block can be sprayed with EtOH and immediately rinsed in dissection solution prior to use to prevent contamination.
    10a. Adjust the brainstem so it is oriented ventral side up, and make sure the rostral portion is as straight as possible, aligned with the bottom of the block on the slicing plate. Line the block with a thin strip of krazy glue, not touching the brainstem. Using a thin needle (~25G) pull the glue to each side of the brainstem and sweeping away excess- wipe excess glue away from needle and continue, making sure the brainstem is secured to the agar block but that excess glue does not remain. *Too much glue will result in the brainstem being ‘squished’ by the blade; not enough will prevent even slicing if the brainstem is not completely glued to the block.
    10b. Place agar block on slicing plate into vibratome and add dissection solution to cover the brainstem and block.
    10c. Make 200-300μm sections from the rostral aspect of the medulla, until reaching the facial nerve. From the facial nerve, the rostral edge where the preBötC will be made is ~1000μm from the facial nerve, depending on the age of the animal. Continue to slice, until you observe the shape of the medulla change from a half circle to having two ‘bumps’ (the pyramids) at the ventral aspect. This is where you will make the ~600μm cut for the preBötC slice.
    10d. Remove the slice, carefully cutting away the glue from the slice. Place into fresh dissection media and add the rest of the brainstem slices as they are made.
    10e. Slices containing piCo, or horizontal slices may also be produced to isolate the ventral respiratory column.

10f. For horizontal slices: proceed with the slicing protocol (step 10a) until reaching the facial nerve. When the facial nerve is visible, remove the agar block from the slicing plate and re-glue so the ventral surface of the spinal cord is facing up. Orient the slice in the vibratome so that the rostral portion of the slice is cut first. Make a `750-800μM slice to isolate the VRC. Err on the side of obtaining more tissue to ensure you isolate the appropriate cell types. Proceed to step 11.

11. Transfer tissue to dish with dissection media. Perform 3 consecutive washes of tissue.
12. In the final wash container, use a sterile scalpel blade to slice each brainstem/slice into 5-10 small pieces.
13. Transfer minced brainstem pieces using a serological pipette. Pull up all tissue in dissection media and allow tissue to settle to bottom of pipette. Transfer tissue to warmed enzyme solution, eliminating as much dissection media as possible to prevent dilution of enzyme solution (usually use 1-2 tubes of enzyme solution/litter of embryos depending on how many there are)
14. Incubate for 30 minutes in incubator, with gentle agitation (belly dancer placed in incubator on slowest setting or manually (gently avoiding bubbles) tip the tube back and forth to disperse tissue every 5-10 minutes).

Mechanical dissociation of cells from digested tissue:

15. Remove tissue from incubator and allow pieces to settle to the bottom of the tube-if needed minimally spin down cells at very low speed for 10-20sec.
16. Remove enzyme solution and wash pieces of tissue once with ~1mL neuronal media to neutralize remaining enzyme
17. Remove wash and add mL ~2-3mL neuronal culture media
18. Triturate tissue with 5mL falcon pipette avoiding bubbles until no large pieces of tissue remain. Place pipette tip flush with bottom of 15mL c-tube and pipette up and down slowly once or twice (4-6 cycles max-cells should be phase bright and have some processes attached)
19. Pass dissociated cell solution through a 70μm cell strainer into a new 50mL c-tube.
20. Perform cell count on hemacytometer, do not count gray/damaged cells
21. Plate cells at ~100,000 cells/well in 24 well plate.

Application of anti-mitotic agents and feeding

Apply FUDR 2-4 days after plating to inhibit glial cells from overrunning the culture. If astrocyte cultures are desired, do not add FUDR. If pure astrocytic cultures are desired, allow cells to settle for 1hr. after

isolation, then place well plate on belly dancer and allow to slowly rotate overnight. Glia should settle and fix to coverslips, while neurons will not and can be removed with media change next day.

FUDR Stock

10mg 5-fluoro-2'-deoxyruidine (2mM)

25mg Uridine (5mM)

-Mix. Sterile filter. Store in 1mL aliquots in -20.

i. Add 5μl FUDR stock to 2mL media (24 well), or 2.5μL stock to 1mL media (12-well).

ii. Replace 50% of media after first day to remove debris. Pull old media gently by tipping wells and slowly pulling off half. Adding fresh media should be done at the side of the well, and not directly onto coverslip.

iii. Feeding should be conservative. Only pipette about ½ to 1/3 of cell media after a week in culture.

iv. Replace with fresh neuronal warmed to 37deg.

Notes:

* Ideally, mice aged p0/1 are best, but protocol has been successful in p2/3 pups as well. See next note.

* The amount of brainstem tissue/ tube of enzyme solution is CRITICAL to the success of this protocol. Adding more than 5 brainstems to one tube will result in tissue 'stickiness' and low to no yield. For older animals, increasing the amount of papain to each tube of solution can increase yield by helping to break down myelinated tissue better.

* When purchasing serum, several of the same batch should be ordered at once. Serum has large batch-batch variability and changing batches can have large effects on cultures.

* PDL and laminin coverslips can be produced in house; we found most consistency with using pre-coated coverslips

* FUDR is optional but increases success of neuronal cultures. Do not add FUDR for astrocytic cultures.

* Use of Pen/strep is also optional but depends on the cleanliness of dissection area and sterile technique. Leaving it out can enhance cultures and time in culture, but risk of infection is much higher.

* Mechanical dissociation is also a critical step. Very gentle dissociation is required for successful cell survival; given the large number of myelinated fibers in the brainstem, extreme delicacy and preventing any bubbling will increase the success of the preparation. Typically a 5mL serological pipette placed gently at the bottom of a 15mL conical tube works well. Pulling ~1-3mL media before cells helps to prevent bubbles, which can shear the cell membranes. You will be able to tell when you have a successful prep best when you can observe cells under the hemacytometer which still have small processes attached.

Purchase Supplies List

PDL coated coverslips	Neuvitro co. GG-12-PDL
Papain	Worthington Biochemical LS03126
MEM	Gibco 51200-038, with Earle's salts, no L-Glutamine
Glutamax	Invitrogen 35050-061
Horse serum	Horse Serum Defined HYCLONE SH30074.03
1M HEPES	Gibco (100ml) 15630-080
Pen/Strep	Gibco 15070-063
B-27	Gibco 17504-044
Sodium Pyruvate	Gibco 11360-070
HBSS +Calcium and Magnesium	Gibco 24020117
5-fluoro-2'-deoxyruidine	Calbiochem 343333 (50mg)/Sigma F0503
Uridine	SIGMA U3003
Cell strainers	70 um tube filter (Falcon 2350) Fisher 08-771-2
Culture dishes	6 well (Costar 3516) Fisher 07-200-83, 12 well (Costar 3513) Fisher 07-200-82, 24 well (Costar 3524) Fisher 07-200-84
Filter units	SFCA Membrane 0.2□m pore (NUNC 157 0020) Fisher 0974025E (250ml); 500 mL Receivers 0974022K
Agar	type IIA Sigma A9918 (10g)

Appendix II

JOHN WILEY AND SONS LICENSE TERMS AND CONDITIONS

Dec 10, 2021

This Agreement between The University of Washington -- Liza Severs ("You") and John Wiley and Sons ("John Wiley and Sons") consists of your license details and the terms and conditions provided by John Wiley and Sons and Copyright Clearance Center.

License Number	5205080412268
License date	Dec 09, 2021
Licensed Content Publisher	John Wiley and Sons
Licensed Content Publication	Journal of Physiology
Licensed Content Title	Advances in cellular and integrative control of oxygen homeostasis within the central nervous system
Licensed Content Author	Ibis M. Agosto-Marlin, Sanja C. Ramirez, Liza J. Severs, et al
Licensed Content Date	Jun 28, 2018
Licensed Content Volume	596
Licensed Content Issue	15
Licensed Content Pages	23
Type of Use	Dissertation/Thesis
Requestor type	Author of this Wiley article
Format	Print and electronic
Portion	Full article
Will you be translating?	No
Title	The Mechanisms Underlying Sigh Generation in the PreBötzinger Complex are Dependent on Neuroglial Interactions
Institution name	University of Washington
Expected presentation date	Dec 2021
Order reference number	123
Requestor Location	The University of Washington 8017 Roosevelt Way NE Seattle, WA 98115 United States Attn: The University of Washington
Publisher Tax ID	EU826007151
Total	**0.00 USD**
Terms and Conditions	

TERMS AND CONDITIONS

This copyrighted material is owned by or exclusively licensed to John Wiley & Sons, Inc. or one of its group companies (each

a"Wiley Company") or handled on behalf of a society with which a Wiley Company has exclusive publishing rights in relation to a particular work (collectively "WILEY"). By clicking "accept" in connection with completing this licensing transaction, you agree that the following terms and conditions apply to this transaction (along with the billing and payment terms and conditions established by the Copyright Clearance Center Inc., ("CCC's Billing and Payment terms and conditions"), at the time that you opened your RightsLink account (these are available at any time at http://myaccount.copyright.com).

Terms and Conditions

- The materials you have requested permission to reproduce or reuse (the "Wiley Materials") are protected by copyright.

- You are hereby granted a personal, non-exclusive, non-sub licensable (on a stand-alone basis), non-transferable, worldwide, limited license to reproduce the Wiley Materials for the purpose specified in the licensing process. This license, **and any CONTENT (PDF or image file) purchased as part of your order,** is for a one-time use only and limited to any maximum distribution number specified in the license. The first instance of republication or reuse granted by this license must be completed within two years of the date of the grant of this license (although copies prepared before the end date may be distributed thereafter). The Wiley Materials shall not be used in any other manner or for any other purpose, beyond what is granted in the license. Permission is granted subject to an appropriate acknowledgement given to the author, title of the material/book/journal and the publisher. You shall also duplicate the copyright notice that appears in the Wiley publication in your use of the Wiley Material. Permission is also granted on the understanding that nowhere in the text is a previously published source acknowledged for all or part of this Wiley Material. Any third party content is expressly excluded from this permission.

- With respect to the Wiley Materials, all rights are reserved. Except as expressly granted by the terms of the license, no part of the Wiley Materials may be copied, modified, adapted (except for minor reformatting required by the new Publication), translated, reproduced, transferred or distributed, in any form or by any means, and no derivative works may be made based on the Wiley Materials without the prior permission of the respective copyright owner.**For STM Signatory Publishers clearing permission under the terms of the STM Permissions Guidelines only, the terms of the license are extended to include subsequent editions and for editions in other languages, provided such editions are for the work as a whole in situ and does not involve the separate exploitation of the permitted figures or extracts,** You may not alter, remove or suppress in any manner any copyright, trademark or other notices displayed by the Wiley Materials. You may not license, rent, sell, loan, lease, pledge, offer as security, transfer or assign the Wiley Materials on a stand-alone basis, or any of the rights granted to you hereunder to any other person.

- The Wiley Materials and all of the intellectual property rights therein shall at all times remain the exclusive property of John Wiley & Sons Inc, the Wiley Companies, or their respective licensors, and your interest therein is only that of having possession of and the right to reproduce the Wiley Materials pursuant to Section 2 herein during the continuance of this Agreement. You agree that you own no right, title or interest in or to the Wiley Materials or any of the intellectual property rights therein. You shall have no rights hereunder other than the license as provided for above in Section 2. No right, license or interest to any trademark, trade name, service mark or other branding ("Marks") of WILEY or its licensors is granted hereunder, and you agree that you shall not assert any such right, license or interest with respect thereto

- NEITHER WILEY NOR ITS LICENSORS MAKES ANY WARRANTY OR REPRESENTATION OF ANY KIND TO YOU OR ANY THIRD PARTY, EXPRESS, IMPLIED OR STATUTORY, WITH RESPECT TO THE MATERIALS OR THE ACCURACY OF ANY INFORMATION CONTAINED IN THE MATERIALS, INCLUDING, WITHOUT LIMITATION, ANY IMPLIED WARRANTY OF MERCHANTABILITY, ACCURACY, SATISFACTORY QUALITY, FITNESS FOR A PARTICULAR PURPOSE, USABILITY, INTEGRATION OR NON-INFRINGEMENT AND ALL SUCH WARRANTIES ARE HEREBY EXCLUDED BY WILEY AND ITS LICENSORS AND WAIVED BY YOU.

- WILEY shall have the right to terminate this Agreement immediately upon breach of this Agreement by you.

- You shall indemnify, defend and hold harmless WILEY, its Licensors and their respective directors, officers, agents and employees, from and against any actual or threatened claims, demands, causes of action or proceedings arising from any breach of this Agreement by you.

- IN NO EVENT SHALL WILEY OR ITS LICENSORS BE LIABLE TO YOU OR ANY OTHER PARTY OR ANY OTHER PERSON OR ENTITY FOR ANY SPECIAL, CONSEQUENTIAL, INCIDENTAL, INDIRECT, EXEMPLARY OR PUNITIVE DAMAGES, HOWEVER CAUSED, ARISING OUT OF OR IN CONNECTION WITH THE DOWNLOADING, PROVISIONING, VIEWING OR USE OF THE MATERIALS REGARDLESS OF THE FORM OF ACTION, WHETHER FOR BREACH OF CONTRACT, BREACH OF WARRANTY, TORT, NEGLIGENCE, INFRINGEMENT OR OTHERWISE (INCLUDING, WITHOUT LIMITATION, DAMAGES BASED ON LOSS OF PROFITS, DATA, FILES, USE, BUSINESS OPPORTUNITY OR CLAIMS OF THIRD PARTIES), AND WHETHER OR NOT THE PARTY HAS BEEN ADVISED OF THE POSSIBILITY OF SUCH DAMAGES. THIS LIMITATION SHALL APPLY NOTWITHSTANDING ANY FAILURE OF ESSENTIAL PURPOSE OF ANY LIMITED REMEDY PROVIDED HEREIN.

- Should any provision of this Agreement be held by a court of competent jurisdiction to be illegal, invalid, or unenforceable, that provision shall be deemed amended to achieve as nearly as possible the same economic effect as the original provision, and the legality, validity and enforceability of the remaining provisions of this Agreement shall not be affected or impaired thereby.

- The failure of either party to enforce any term or condition of this Agreement shall not constitute a waiver of either party's right to enforce each and every term and condition of this Agreement. No breach under this agreement shall be deemed waived or excused by either party unless such waiver or consent is in writing signed by the party granting such waiver or consent. The waiver by or consent of a party to a breach of any provision of this Agreement shall not operate or be construed as a waiver of or consent to any other or subsequent breach by such other party.

- This Agreement may not be assigned (including by operation of law or otherwise) by you without WILEY's prior written consent.

- Any fee required for this permission shall be non-refundable after thirty (30) days from receipt by the CCC.

- These terms and conditions together with CCC's Billing and Payment terms and conditions (which are incorporated herein) form the entire agreement between you and WILEY concerning this licensing transaction and (in the absence of fraud) supersedes all prior agreements and representations of the parties, oral or written. This Agreement may not be amended except in writing signed by both parties. This Agreement shall be binding upon and inure to the benefit of the parties' successors, legal representatives, and authorized assigns.

- In the event of any conflict between your obligations established by these terms and conditions and those established by CCC's Billing and Payment terms and conditions, these terms and conditions shall prevail.

- WILEY expressly reserves all rights not specifically granted in the combination of (i) the license details provided by you and accepted in the course of this licensing transaction, (ii) these terms and conditions and (iii) CCC's Billing and Payment terms and conditions.

- This Agreement will be void if the Type of Use, Format, Circulation, or Requestor Type was misrepresented during the licensing process.

- This Agreement shall be governed by and construed in accordance with the laws of the State of New York, USA, without regards to such state's conflict of law rules. Any legal action, suit or proceeding arising out of or relating to these Terms and Conditions or the breach thereof shall be instituted in a court of competent jurisdiction in New York County in the State of New York in the United States of America and each party hereby consents and submits to the personal jurisdiction of such court, waives any objection to venue in such court and consents to service of process by registered or certified mail, return receipt requested, at the last known address of such party.

WILEY OPEN ACCESS TERMS AND CONDITIONS

Wiley Publishes Open Access Articles in fully Open Access Journals and in Subscription journals offering Online Open. Although

most of the fully Open Access journals publish open access articles under the terms of the Creative Commons Attribution (CC BY) License only, the subscription journals and a few of the Open Access Journals offer a choice of Creative Commons Licenses. The license type is clearly identified on the article.

The Creative Commons Attribution License

The Creative Commons Attribution License (CC-BY) allows users to copy, distribute and transmit an article, adapt the article and make commercial use of the article. The CC-BY license permits commercial and non-

Creative Commons Attribution Non-Commercial License

The Creative Commons Attribution Non-Commercial (CC-BY-NC)License permits use, distribution and reproduction in any medium, provided the original work is properly cited and is not used for commercial purposes.(see below)

Creative Commons Attribution-Non-Commercial-NoDerivs License

The Creative Commons Attribution Non-Commercial-NoDerivs License (CC-BY-NC-ND) permits use, distribution and reproduction in any medium, provided the original work is properly cited, is not used for commercial purposes and no modifications or adaptations are made. (see below)

Use by commercial "for-profit" organizations

Use of Wiley Open Access articles for commercial, promotional, or marketing purposes requires further explicit permission from Wiley and will be subject to a fee.

Further details can be found on Wiley Online Library http://olabout.wiley.com/WileyCDA/Section/id-410895.html

Other Terms and Conditions:

v1.10 Last updated September 2015

Questions? customercare@copyright.com or +1-855-239-3415 (toll free in the US) or +1-978-646-2777.

THE AMERICAN PHYSIOLOGICAL SOCIETY ORDER DETAILS
Dec 13, 2021

This Agreement between Liza J Severs ("You") and The American Physiological Society ("The American Physiological Society") consists of your order details and the terms and conditions provided by The American Physiological Society and Copyright Clearance Center.

Order Number	501697249
Order date	Dec 10, 2021
Licensed Content Publisher	The American Physiological Society
Licensed Content Publication	Journal of Neurophysiology
Licensed Content Title	Neuron-astrocyte networking: astrocytes orchestrate and respond to changes in neuronal network activity across brain states and behaviors
Licensed Content Author	Marion R. Van Horn, Nicholas J. Benfey, Colleen Shikany, et al
Licensed Content Date	Aug 1, 2021
Licensed Content Volume	126
Licensed Content Issue	2
Type of Use	Thesis/Dissertation
Requestor type	author of original work
Format	print and electronic
Portion	full article
Will you be translating?	no
World Rights	no
Order reference number	456
Title	The Mechanisms Underlying Sigh Generation in the PreBötzinger Complex are Dependent on Neuroglial Interactions
Institution name	University of Washington

Expected presentation date	Dec 2021
Order reference number	456
Requestor Location	The University of Washington 8017 Roosevelt Way NE Seattle, WA 98115 United States Attn: The University of Washington
Billing Type	Invoice
Billing Address	The University of Washington 8017 Roosevelt Way NE Seattle, WA 98115 United States Attn: Liza J Severs
Total	0.00 USD

Terms and Conditions

Terms and Conditions:

The APS hereby grants to you a nonexclusive limited license to reuse published material as requested by you, provided you have disclosed complete and accurate details of your proposed reuse of articles, figures, tables, images, and /or data in new or derivative works. Licenses are for a one-time English language use with a maximum distribution equal to the number of copies identified by you in the licensing process, unless additional options for translations or World Rights were included in your request. Any form of print or electronic republication must be completed within three years from the date hereof. Copies prepared before then may be distributed thereafter

The following conditions are required for a License of Reuse:

Attribution: You must publish in your new or derivative work a citation to the original source of the material(s) being licensed herein, including publication name, author(s), volume, year, and page number prominently displayed in the article or within the figure/image legend.

Abstracts: APS Journal article abstracts may be reproduced or translated for noncommercial purposes without requesting permission, provided the citation to the original source of the materials is included as noted above ("Attribution"). Abstracts or portions of abstracts may not be used in advertisements or commercial promotions.

Non-profit/noncommercial reuse: APS grants permission for the free reuse of APS published material in new works published for educational purposes, provided there is no charge or fee for the new work and/or the work is not directly or indirectly commercially supported or sponsored. Neither original authors nor non-authors may reuse published material in new works that are commercially supported or sponsored including reuse in a work produced by a commercial publisher without seeking permission.

Video and photographs: Some material published in APS publications may belong to other copyright holders and cannot be republished without their permission. The copyright holder of photographs must be ascertained from the original source by the permission requestor. Videos and podcasts may not be rebroadcast without proper attribution and permission as requested here. For further inquiries on reuse of these types of materials, please contact cvillemez@the-aps.org

Figures/Tables/Images are available to the requestor from the APS journals website at http://www.the-aps.org/publications/journals/. The obtaining of content is a separate transaction and does not involve Rightslink or CCC, and is the responsibility of the permission seeker. Higher resolution images are available at additional charge from APS; please contact cvillemez@the-aps.org

Original Authors of Published Works: To see a full list of original authors rights concerning their own published work http://www.the-aps.org/publications/authorinfo/copyright.htm

Content reuse rights awarded by the APS may be exercised immediately upon issuance of this license, provided full disclosure and complete and accurate details of the proposed reuse have been made; no license is finally granted unless and until full payment is received either by the publisher or by CCC as provided in CCC's Billing and Payment Terms and Conditions. If full payment is not received on a timely basis, then any license preliminarily granted shall be deemed automatically revoked and shall be void as if never granted. Further, in the event that you breach any of these Terms and Conditions or any of CCC's Billing and Payment Terms and Conditions, the license is automatically revoked and shall be void as if never granted. Use of materials as described in a revoked license, as well as any use of the materials beyond the scope of the license, may constitute copyright infringement and the Publisher reserves the right to take action to protect its copyright of its materials.

The APS makes no representations or warranties with respect to the licensed material. You hereby indemnify and agree to hold harmless the publisher and CCC, and their respective officers, directors, employees and agents, from and against any and all claims arising out of your use of the licensed material other than as specifically authorized pursuant to this license.

This license is personal to you /your organization and may not be sublicensed, assigned, or transferred by you /your organization to another person /organization without the publisher's

permission.This license may not be amended except in writing signed by both parties, or in the case of the publisher, by CCC on the publisher's behalf.

The APS reserves all rights not specifically granted in the combination of (i) the license details provided by you and accepted in the course of this licensing transaction, (ii) these Terms and Conditions and (iii) CCC's Billing and Payment Terms and Conditions.

v1.0

APPENDIX I: List of Abbreviations

A

α1-AR	alpha-1 adrenergic receptor
α7nAChR	α7-nicotinic acetylcholine receptors
AAV	adeno-associated virus
ACSF	Artificial cerebrospinal fluid
ADO	adenosine
ADP	adenosine diphosphate
Aldh1L1	aldehyde dehydrogenase 1 family member L1
ATP	adenosine triphosphate

B

β-Ars	beta adrenergic receptors
BötC	Bötzinger complex

C

Ca^{2+}	Calcium
cAMP	cyclic adenosine monophosphate
$CaCl_2$	calcium chloride
CB	carotid bodies
Cd	cadmium
ChAt	choline acetyltransferase
CHR2	Channelrhodopsin 2
CIH	chronic intermittent hypoxia
CNS	Central nervous system
CO_2	Carbon Dioxide
CPG	central pattern generator
CVLM	caudal ventrolateral medulla
cVRG	caudal ventral respiratory groups

D

DIA	Diaphragm
Dbx1	developing homeobox protein 1
dnSNARE	dominant negative SNARE protein
DREADD	Designer Receptors Exclusively Activated by Designer Drugs
DRG	Dorsal respiratory group

E

EKG	electrocardiogram
ER	endoplasmic reticulum

	EYFP	enhanced yellow fluorescent protein
F		
	FWHM	full width at half max
G		
	GECI	Genetically encoded calcium indicator
	GFP	Green fluorescent protein
	GPCR	G protein-coupled receptor
	GIRK	G protein-coupled inwardly rectifying potassium channel
	GPR4	G protein-coupled receptor 4
	GRP	gastrin releasing peptide
H		
	H+	hydrogen ion
	HVR	hypoxic ventilatory response
I		
	I_{NAP}	persistent sodium current
	IP_3	inositol trisphosphate
	ITR	Intertrigeminal Region
	IX	Glossopharyngeal Nerve
K		
	K+	potassium
	KCl	potassium chloride
	KF	Kölliker-Fuse Nucleus
	K_{ir}	inward rectifying potassium channels
L		
	LC	Locus Coeruleus
	LPS	lipopolysaccharide
M		
	MAD	median absolute deviation
	$MgCl_2$	magnesium chloride
	mGluR	metabotropic glutamate receptor
	mm	millimeter
	mM	millimolar
	mRNA	messenger ribonucleic acid
	mW	milliwatt
N		
	Na+	sodium

NA	Nucleus Ambiguous
$NaHCO_3$	sodium bicarbonate
NaH_2PO_4	sodium phosphate
NaCl	sodium chloride
NE	norepinephrine
nm	nanometer
NMDAR	Anti-N-Methyl-D-Aspartate receptor
NMB	neuromedin B
NTS	Nucleus tractus solitarius

O

OIRD	opioid induced respiratory depression
OSA	obstructive sleep apnea
O_2	Oxygen

P

PBS	phosphate buffered saline
PCO2	partial pressure of carbon dioxide
PGE2	prostoglandin E2
PiCo	Postinspiratory Complex
PO_2	partial pressure of oxygen
preBötC	preBötzinger complex
P2Y	Purinergic receptor type 2Y

R

REM	rapid eye movement
ROS	reactive oxygen species
RSA	Respiratory Sinus Arrhythmia
RVLM	rostral ventrolateral medulla
rVRG	rostral ventral respiratory groups

S

SST	somatostatin
SIDS	Sudden infant death syndrome
SERCA	sarcoendoplasmic reticulum calcium transport ATPase

T

TASK	TWIK-related acid sensitive potassium channel
TeLC	light chain of tetanus toxin

U

um	micron

μM	micromolar

V

V	Trigeminal Nerve
Vglut2	vesicular glutamate transporter 2
VRC	ventral respiratory column
VRG	ventral respiratory groups

X

XII	Hypoglossal Nerve
X	Vagus Nerve